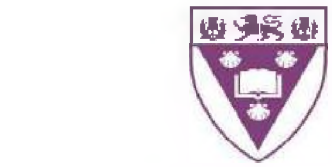

A RECONCILIATION STUDY OF DIFFERENT RESOURCE ESTIMATION METHODS AND DRILL HOLE SPACING AS APPLIED TO THE LANGER HEINRICH CALCRETE-HOSTED URANIUM DEPOSIT, NAMIBIA.

A thesis submitted in partial fulfilment of the requirements for the degree of

MASTER OF SCIENCE
(Economic Geology)

Geology Department
RHODES UNIVERSITY

By Sven Baufeldt

Supervisor: Professor R.E. Harmer (Rhodes University)

March 2018

STATUTORY DECLARATION

I, Sven Baufeldt, declare this thesis to be my own work. It is submitted in fulfilment of the Degree of Master of Science at Rhodes University. It has not been submitted before for any degree or examination in any other University or tertiary institution.

Signature of the candidate: ..... 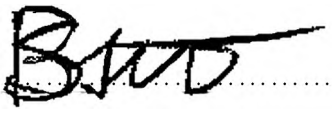

Date: 14/03/2018 .....

ACKNOWLEDGMENTS

My immense appreciation goes out to Professor R.E. Harmer for his help, advice, patience and constant support during this research. I would also like to thank Dave Princep for the help in setting up and contributing to my thesis. I have learnt so much throughout the last two years and have developed a passion in line with my research topic. I am thankful for the skills and knowledge that you have passed on.

I also would like to thank Mrs. Goddard for her kindness and help throughout this course, and thereby making the studies for all international geology students much easier. I would like to thank Guy Freemantle for his support and advice on the uranium industry. Carlene, I would like to thank you dearly for your love and support throughout this research.

I am also grateful for the research topic, financial support and data provided from the Langer Heinrich Uranium Mine.

ABSTRACT

The Langer Heinrich calcrete hosted uranium deposit is situated approximately 90 km to east of the coastal town of Swakopmund in Namibia. It is run by an Australian owned company, Paladin Energy Limited, along with China National Nuclear Corporation (CNNC) who maintain 25% of the shares. Production commenced in 2007 and has been ongoing. Carnotite is the primary and only ore mineral, and the nature of mineralisation within the Langer Heinrich palaeo channel dictates westward-directed continuous open pit mining. Smaller-scale [1]micro pits target near-surface, high-grade, lenses toward the east. The high variability in uranium grade over relatively short distances complicates the grade estimation process. This combined with a low uranium price, and a study aimed at optimising of mine production is one of the key drivers for the research presented in this thesis.

The efficacy of four resource estimation techniques, commonly used in the mining industry, are investigated by application to variable exploration, infill drilling and grade-control drill pattern spacing. The drill spacing includes regular grids of 50 m x 50 m, 25 m x 25 m and 12,5 m x 12,5 m exploration data. Also included is grade control drill data, drilled on a 4 m x 4 m spacing. The current selective mining unit (SMU) is 4mE x 4mN x 3mRl which is an indication of the minimum dimension whereby the loading equipment can separate ore from waste. The two datasets are processed by four estimation techniques: Inverse Distance Weighting (IDW, squared and cubed), Ordinary Kriging (OK), Multiple Indicator Kriging (MIK) and Conditional Simulation (CS).

The two datasets consisted of real-time mining data from pit G1 (micro-pit) in the eastern parts of the mining licence, and pit H1 (continuous larger open pit) in the western area of the palaeo channel. The reconciliation project aims to provide results suitable for devising optimised mining strategies, particularly in future targets where drill spacing can perhaps be improved to provide suitable data with a greater cost saving strategy. Along with the optimal drill spacing or combination thereof, a preferred estimation technique can be suggested and recommended for future operations that involve mining of surficial calcrete-hosted uranium deposits.

Results of this study show that 12,5 m x 12,5 m drill spacing provided estimation accuracies similar to that of the narrow 4 m x 4 m grade control spacing (blast hole drilling spacing). The 12,5 m x 12,5m spacing has potential for accurate grade estimations during mining, and could be supplemented by infill downhole radiometric logging on a 4 m x 4 m spacing when

[1] Micro pit: Small pits within palaeo channel usually targeted for their near surface high-grade ore

necessary. In general, Multiple Indicator Kriging (MIK) provided the most accurate and robust estimations on the wider spaced exploration data and conditional simulation (CS) proved more efficient on the narrow grade control data. These results correspond with current exploration practices for surficial uranium deposits world-wide. Deposit type, therefore complexity and hence SMU sizes play a pivotal role in drill hole planning and estimation accuracies.

TABLE OF CONTENTS

LIST OF FIGURES

LIST OF TABLES

LIST OF EQUATIONS

ABBREVIATIONS

ATV	All-Terrain Vehicle
CS	Conditional Simulation
CV	Coefficient of variation
DYL	Deep Yellow Limited
IAEA	International Atomic Energy Agency
IDW^2	Inverse Distance Weighting squared
IDW^3	Inverse Distance Weighting cubed
LHF	Langer Heinrich Formation
MIK	Multiple Indicator Kriging
ML	Mining licence
MM	Micromine
OK	Ordinary \kriging
QAQC	Quality Assurance Quality Control
RC	Reverse Circulation
ROM	Run of Mine
WF	Wireframe

cm^3	cubic metres
cps	counts per second
g	grams
m	metres
Mt	Million tonnes
ppm	parts per million or grams per ton
t	tonnes
USD	United States Dollars

W	Waste
LG	Low-grade
MG	Medium-grade
HG	High-grade

CHAPTER 1. INTRODUCTION

The Langer Heinrich uranium mine is situated approximately 90 km east of the coastal town of Swakopmund and 40 km south-east of the Rössing Uranium (Rio Tinto). The mine is situated in the north-eastern part of the Namib Naukluft National Park at co-ordinates 15°20´E and 22°49´S and is accessible via the C28 district road as indicated in Figure 1.

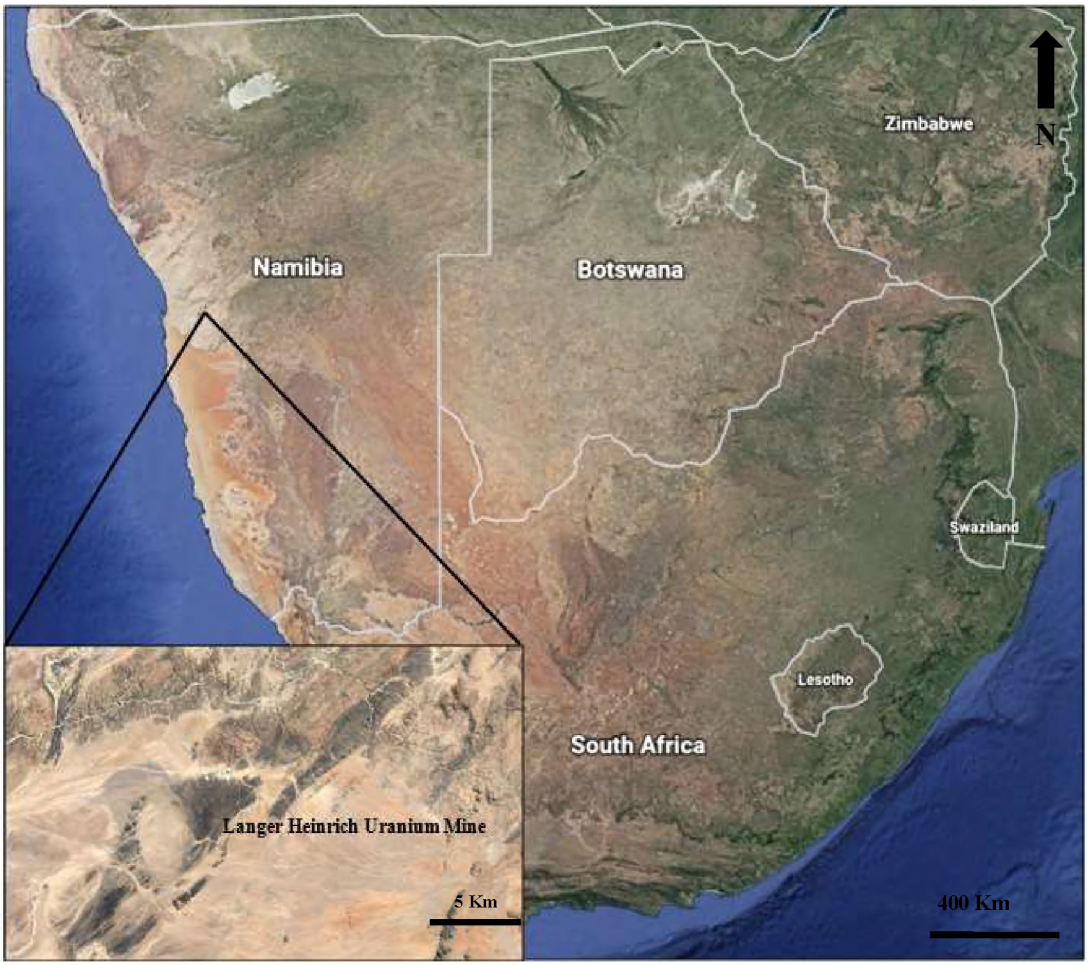

Figure 1: Locality map showing the Langer Heinrich deposit in Namibia (Google Earth, 2016)

The mine lease is situated between the Langer Heinrich Mountain in the north and the Schieferberg Mountains to the south. The mine is registered under the mining licence ML 140 and covers approximately 45 km^2. The surrounding environment is classified as hot desert climate and receives less than 100 mm of rain per year (Trittschack, 2008), of which a substantial amount is accumulated from the coastal fog. The Langer Heinrich uranium deposit is located within a palaeo channel deposit within the Gawib River, a tributary of the larger Swakop River that runs westwards into the Atlantic Ocean. The only uranium mineral mined is carnotite ($K_2(UO_2)_2V_2O_8.3H_2O$), which is a yellow potassium uranium vanadate mineral occurring in calcareous sediments.

1.1 Historical overview

Following the discovery of the Langer Heinrich anomaly in the 1970s, Gencor (General Mining Union Corporation Limited) did evaluation drilling on the uranium target. Gencor sold the project due to low uranium prices (<20 USD/pound) at that time to Acclaim Uranium NL. Further drilling by Acclaim Uranium, along with a prefeasibility study conducted between 1998 and 2000 provided additional data on the deposit. Acclaim Uranium NL sold the project in 2002 to Paladin Energy Ltd. The mine's construction was commenced during 2005-2006 with production starting in 2007-2008 (Paladin Energy PTY Ltd, 2015). Langer Heinrich Uranium (Pty) Ltd. underwent various stages of production improvements and was wholly owned by the Australian company Paladin Energy until 2014, when a 25 % share was sold to CNNC (China National Nuclear Corporation).

1.2 Langer Heinrich Mine: Production, infrastructure and processing facility

Production commenced in 2007 and a total product of 2.7 Mlb of U3O8 for the years 2008/2009 were achieved for the first stage. Expansion to Stage 2 increased production to 3.7 Mlb per year for 2010. Stage 3 expansion was accomplished during 2012 which saw an increase to a total of 5.2 Mlb per year. Stage 4 expansions are currently on hold due to depressed uranium prices, but are anticipated to push production to 8.7 Mlb per year. Research and experimentation is underway to improve the plant's efficiency to process decreased feed grades in the near future (Paladin Energy PTY Ltd, 2015). Table 1 and Table 2 provide details on the resources and reserves of the Langer Heinrich uranium deposit.

Table 1: Mineral resource estimate for the Langer Heinrich Mine as 30 June 2015 (Paladin Energy Annual report, 2015)

250 ppm cut-off	*Mt*	*Grade % U_3O_8*	*t U_3O_8*	*Mlb U_3O_8*
Measured	19.6	0.056	10 912	24.1
Indicated	62.9	0.054	34 051	75.1
Measured and Indicated	82.5	0.055	44 964	99.1
Stockpiles	32.1	0.040	12 867	28.4
Inferred	17.0	0.06	9 842	21.7

Table 2: Ore Reserve Estimate for the Langer Heinrich Mine as 30 June 2015 (250ppm U_3O_8 Cut-off)

250 ppm cut-off	*Mt*	*Grade % U_3O_8*	*t U_3O_8*	*Mlb U_3O_8*
Proved Ore Reserve	15.80	0.057	8 955	19.74
Probable Ore Reserve	52.83	0.055	29 273	64.54
Stockpiles	32.1	0.040	12 867	28.37
Total Ore Reserve	100.7	0.051	51 095	112.64

1.2.1 Exploration history, detection and removal of ore from host rock

Exploration was done by various companies before Paladin Energy acquired the project due to a lack in technological advances regarding drilling equipment, the elevated water table in the palaeo channel created penetrating issues. Percussion drilling during the initial stages of exploration had difficulties penetrating rock near the groundwater table at deeper depths. Early exploration phases from various exploration companies were drilled using a 100 m x 50 m grid. Paladin Energy took over in 2002 and improved exploration strategies using reverse circulation rigs (RC). Paladin Energy initiated infill drilling phases on the initial exploration drill spacing. During later stages of drilling the final grid spacing was a 12,5 m x 12,5 m during which about 20 000 m were drilled each month until 2016. This is also called ore delineation drilling/ infill drilling. All drilling was done vertically through the lateral calcareous sediments of the palaeo channel. The systematic drilling was done usually in north-south lines that would slowly progress across the east-west flowing palaeo channel.

The Langer Heinrich deposit's uranium has been classified to be in equilibrium with no abnormal concentrations of thorium and therefore gamma counts can be recorded using probes (Bowel et al, 2009). After drilling, a radiometrically calibrated probe containing a scintillometer is lowered into the drill hole to measure the gamma radioactivity and grade thereof. The probes use a K factor that ranges between 0,34 - 0,59 and due to the dry desert climate no water factor is needed. A casing factor is also calculate depending on the thickness of the drill rods used (Barrett, 2008). Daily sensitivity checks were done on the probe in order to identify if the probe needed to be recalibrated. Calibrations of probes were done on site in a concrete pad with known concentrations of uranium on a need be basis as there were numerous probes that could be utilised if a faulty probe was identified. The probe which contains a small detector crystal in the front of the cylinder measures radioactivity precisely of up to 50cm into the surrounding rock. The probe takes readings in counts per second (cps) for every 5 cm down the hole. This data is captured on a tough-book laptop and transferred to a computer in the offices. Here the data is de-convoluted to parts per million (ppm) at capture intervals of 1 m. The ratio from cps to ppm is approximately at 2:1. All the closely spaced drilling data is analysed in order to find preferable sites for future mining operations and to reduce excavation of unnecessary waste.

Blasting is a relatively low-cost operation (in comparison to hard rock uranium mines in the region), as the ore is found in softer host rocks. The cut-off grade at Langer Heinrich is 250 ppm, and production blast areas are marked out with colour markers according to prescribed grade bins (Table 3). Thereafter drilling and blasting is done after which the ore is transported by 90t haul trucks. Geo-technicians are responsible for grade control procedures after blasting

and guide the operations often using hand-held Radeye scintillometers. Mining operations focuses on 9 meter thick blast blocks that are mined on 3 meter [2]flitches at a time. Three large loading equipment (2 x Komatsu PC 2000 excavators, 1 x Caterpillar 993K loader) allows for mining on multiple blast blocks targeting sites of progressive waste stripping and ore mining simultaneously. Multiple pits can be mined simultaneously. The load and haul fleet comprises eighteen 90 tonne Komatsu haul trucks that are fed by two excavators and one articulated front end loader. The haul trucks pass through scanners (uranium ore discriminator) that do a reasonable measure (± 30 ppm) of the grade in the truck, after which the truck is sent to the correct destination on the Run of Mine pad (ROM).

Table 3: Colour associations with correlated uranium grade

Grade	*U3O8 ppm*	*Colour*
Waste	0-250	
Low-grade	250-400	
Medium-grade	400-650	
High-grade	650-900	
High-grade (concentrated high-grade)	>900	

1.2.2 Processing of uranium ore

On the ROM, smaller articulated dump trucks (ADT) and loaders feed the plant at 11 000 tons per day. The current feed grade is 680 ppm U_3O_8. The circuit is designed to meet the objective of producing 1 100 tons per annum U_3O_8. Ore is delivered by 40t ADT that run permanently back and forth from various stockpiles. They feed two tipping bins that are covered with a protective grizzly. The bin has been fitted with a 400 mm static grizzly to remove and reject rocks larger than 500 mm. Ore containing rock thereafter is progressed into two jaw crushers in series. During the initial stages, crushing reduces ore size to ±200 mm and thereafter to ±75 mm. The ore from the crushing section is transported to a scrubber where some of the uranium is removed by washing. The ore is transported through a series of rotating drums, which contain different sieve sizes used for screening. Ore is ultimately screened to a size of ±5 mm during these processes and washed with water that dissolves the soluble carnotite. In addition, most of the uranium oxide still entrained on the quartz pebble coatings is removed. The slurry product is thickened and conditioned by the addition of heat and reagents. The thickened slurry is pumped to the first of 9 cascading alkaline leach tanks installed in series. The leach product is dewatered in a series of 6 counter-current decantation thickeners, with the final pregnant solution being pumped to the ion exchange circuit. The thickened slimes are routed to a tailings disposal dump for final disposal in the tailings storage facility. The ion exchange circuit extracts the uranium from the solution through adsorption onto a resin and accounts for most of the uranium extraction in the plant.

[2] Flitch: Loading platform dependent on the reach of the loading equipment used

Uranium is precipitated from the eluate by the addition sulphuric acid, hydrogen peroxide and sodium hydroxide. This uranium saturated solution is then pumped to a thickener where the uranium precipitates under gravitation. The thickened product is pumped to a de-watering centrifuge, the recovered solution is recycled to the thickener and the centrifuge product discharged into a storage bin. The dewatered uranium cake is transferred to a calciner. Here, the water of the crystallised product is driven off to generate the final U_3O_8 product, which is then packed in sealed and labelled 40 gallon drums (S. Malan 2012, pers. comm.[3]).

1.2.3 Global uranium production

Kazakhstan, Canada and Australia are the leading producers of uranium, followed by Russia, Niger and Namibia. The USA, Brazil, South Africa and China do add some uranium production to the supply market, however this usually comes in the form of a by-product of other primary commodities such as gold (World-Nuclear Association, 2015). Most of the uranium produced is shipped to rapid developing countries such as China and India for electricity production. The largest producing mines are operated by Kazatomprom, Cameco and Areva. In the majority of these deposits, uranium ore is hosted in sandstone related deposits as well as unconformity related deposits. Most underground operations are mechanised and are operated remotely from the surface, due to the high radiation exposure. Good examples of extreme high-grade uranium deposits include Rabbit Lake, McArthur River and Cigar Lake in Canada. Deposits such as Cameco's Cigar Lake mine has uranium grades between 3-7 % U_3O_8 (CAMECO, 2015). With focus on surficial calcrete-hosted uranium deposits, the Langer Heinrich Uranium Mine is currently (2016) the only producing mine for the Company. The deposit itself produced 2-3 % of the total uranium production for the year 2015 (World-Nuclear Association, 2015) and is the only major surficial hosted uranium mine currently in operation.

[3] Sarel Malan: Presently Metallurgy Manager, Swakop Uranium Mine (Husab Project).

1.2.4 Global calcrete hosted uranium deposits

Table 4: Near-surface calcrete hosted uranium deposits and their exploration practices

Deposit	Company	Drill spacing used	Estimation methods used for resource estimation	Comments
Tubas deposit (Namibia)	Deep Yellow Limited, Australia	Early exploration drilling on 200m x 200m and 100m x 100m. Target drilling was drilled on 50m x 50m	[4]MIK was the preferred estimation method	On tighter drill spacings, both [5]OK and [6]CS were used as comparisons Uniform conditioning was another alternative that was suggested (Deep Yellow Limited, 2014)
Tumas deposit (Namibia)	Deep Yellow Limited, Australia	Mostly drilled on a 50m x 50m drill spacing with minor 12,5m x 12,5m drilling	MIK was the preferred estimation method	Both Tubas and Tumas deposits have cut-off grades of 100 ppm (Deep Yellow Limited, 2016)
Trekkopje deposit (Namibia)	Areva, France	Early stage drilling on 600m x 800m, followed by 200m x 400m drilling. Minor target drilling was done on a 50m x 50m drill grid	OK with various search neighbourhood analysis to improve estimations	Cut-off grade at 80 ppm (Uramin Inc., 2007)
Wiluna deposit (Australia)	Toro Energy, Australia	A mixture of 75m x 75m and 100m x 100m m drill spacings	OK was the preferred estimation method	Uniform conditioning was another alternative that was suggested (MEGA Uranium LTD, 2009) Cut-off grade of 200 ppm
Laguna Salada deposit (Argentina)	U3O8 Corporation, Canada	Trenching and pitting used to collect samples (no drilling)	OK was the preferred estimation method	Near surface calcrete-hosted deposit with trenches reaching maximum depths of 2,8m (U3O8 Corporation, 2011) Cut-off grade of 100 ppm

[4] MIK: Multiple Indicator Kriging
[5] OK: Ordinary Kriging
[6] CS: Sequential Gaussian Conditional Simulation

Surficial calcrete-hosted or valley fill deposits constitute only approximately 4,5 % of the global uranium deposit inventories (IAEA, 1984). Of the known 1 651 uranium deposits or prospects, 75 are surficial deposits; of these, 20 occur in Australia and 15 in Namibia (IAEA, 2016). Surficial deposits occur on almost all continents; however, their low-grades make them mostly uneconomic at present market prices ($27/ lb, as at June 2016). Namibia is among the leading producers of uranium in the world and is home to a variety of granite and surficial calcrete-hosted deposits. Surficial calcrete-hosted deposits such as the Langer Heinrich, Tumas, Tubas, Trekkopje and Marenica represent weathering products of uranium rich granites. The surficial calcrete-hosted uranium deposits discussed in Table 4 occur on almost all continents across the world and are therefore quite common in arid environments.

With regards to exploration or resource drilling as observed in Table 4 most of these projects have undergone somewhat extensive exploration phases through time. This is usually dependant on the spot price and resources available. Most of the deposits were drilled on grid spacings of up to 600 m x 800 m and later target drilling or infill drilling on a regular 50 m x 50 m drill spacing. The drilling techniques are usually factor of the geology and resources available. All of these deposits mentioned in Table 4 are near-surface deposits within calcrete-hosted rock. Reverse circulation (RC) drilling is the preferred method of drilling, whilst sonic drilling was preferred in deposits with a shallow ground table. The preferred estimation method is OK, however, in more recent years MIK seems to be more prominent.

1.3 Aims and objectives

The aim of this research was to assess the applicability of common industry-accepted geostatistical evaluation techniques within the context of drill grid spacing in the exploration and production environments. The four estimation techniques used during this research on the Langer Heinrich uranium deposit were tested in response to the characteristics of a sedimentary hosted uranium deposit.

This thesis presents results from applying various geostatistical resource estimation techniques at different drill spacing with the intention of determining which is optimally suited to a particular drilling application. The main research of this thesis focuses on two complete datasets from two mined out pits from the eastern and western sections of the palaeo channel. The estimation techniques used should be a realistic comparison to actual mined tonnages excavated from the different pits. The grade, tonnage, output, size, depth, and geology of both dataset are also taken into consideration. The comparative datasets gave a good indication how well the different geostatistical techniques manage variations in data size as well as other factors such as depth of deposition and grade variability. As both pits have been depleted of

ore, the actual mined figures are available and serve as the reality to which the estimation models can be compared. In these figures various forms of natural ore dilution have been incorporated, which occur in any normal mining operation.

Currently during mining operations, the 4 m x 4 m drill data is simulated using sequential Gaussian conditional simulation and serves as the current simulated form of reality on the mine. It is believed to be the most accurate form of estimation currently due to various characteristics in the nature of the secondary uranium deposit. The other three estimation techniques and various drill spacing were used as a comparison to both the actual mined figures and the conditionally simulated data. The results of these estimations have been described in chapter five and six. Chapter five provides the results on pit G1 which is situated in the eastern sections of the palaeo channel. Chapter six provides the results of pit H1 which is situated in the western section of the palaeo channel.

Furthermore, in chapter four, the infill drilling estimation results on 12,5 m x 12,5 m (ore delineation drill spacing) and 4 m x 4 m (grade control/ blast pattern) drill spacing will be tested in terms of estimation accuracy for future blasting of ore blocks. Although the 4 m x 4 m drill holes will be drilled due to blasting requirements, the time and resources needed to radiometrically log each of these holes could be reduced if the 12,5 m x 12,5 m estimations prove to be efficient. The impact of less data availability, a common known fact in geostatistical analyses, from various drill hole spacing was tested using various estimation techniques and compared to the mined figures.

Apart from finding the optimal estimation technique suitable for the deposit, various drilling phases and infill drilling were used prior to mining for more effective improvised pit designs. Currently ongoing pit delineation drilling or infill drilling at 12,5 m x 12,5 m is proving costly in light of low uranium prices. Thus, establishing estimation confidence on wider drill spacing (25 m x 25 m and 50 m x 50 m) or a combination thereof, backed by the findings of this comparative research project, could be beneficial for pit optimization design.

CHAPTER 2. GEOLOGICAL BACKGROUND

The Langer Heinrich uranium deposit is located within the NE-SW trending Southern Central Zone (sCZ) or Swakop Zone of the Damara Belt which, along with the Kaoko and Gariep Belts, forms the Pan African aged Damara Orogen. The three orogenic belts form part of the Damara Orogeny that was a result of the larger Pan African structural collisional event. The Damara Belt, along with the Kaoko and Gariep Belts, were formed by subsequent events of rifting, spreading and collision that lasted from 900 up to 460 Ma (Miller, 2008).

2.1 Regional Geology of the Southern Central Zone

As indicated in Figure 2 and 3, the southern Central Zone is dominated by 1 Ga metamorphic rocks, exposed as domes and inliers. These rocks comprise the Abbabis Metamorphic Complex (AMC) and are hereafter referred to as "the basement". The AMC is unconformably overlain by a heterogeneous Paleoproterozoic sedimentary package reflecting an evolution from rifting and fluviatile environments through to pelagic and flysch type sedimentation and diamictites. The AMC comprises a variety of high-grade metamorphic rocks and granites that form the basement of the Damara Orogeny. The lowermost rocks of the Damara Supergroup are the Nosib Group containing the Etusis and Khan formations that unconformably overlie the AMC basement. The Etusis formation is mostly made up of feldspathic quartzite that ranges in a variety of colours. The upper Nosib Group consists of fine clastic carbonates of the Khan formation, The Khan formation is thinner than the Etusis formation with a thickness of roughly 1 050 m, consisting of thick bedded clinopyroxene and hornblende bearing feldspathic quartzite (Miller, 2008). The Khan formation, along with the Etusis clastics, are the oldest sedimentary rocks within the Damara Supergroup (Wilkinson, 1991).

The Nosib Group is unconformably overlain by the Swakop Group which was deposited in half grabens. The Swakop formation forms the oldest formation within the regional area; however, the Chuos formation is the oldest formation in the area of Langer Heinrich. The Chuos formation is locally thicker and better developed than in other areas in Namibia. Thickness can vary from 600 m to as thin as 3 m, which indicates the heterogeneity of this formation. The rocks that make up the formation mainly consist of tillite and diamictite with dropstones (Miller, 2008). The Chuos formation consists mainly of calc-silicate layers that are interbedded with schist from the basal layer of the Kuiseb formation. The Schieferberg Mountains to the south of the deposit form part of the Tinkas formation and consist of interbedded near vertical calc-silicate schists. These calc-silicate schists form large parts of the basement (footwall) of the palaeo channel. The Kuiseb formation overlies the Karibib formation and is mainly comprised of schist that forms highly irregular shapes with numerous synforms that are filled

with Damara granites. The Kuiseb formation marks the top of the Swakop Group and the Damara Supergroup at this locality.

Intrusive rocks

Following the Pan African Orogeny, a number of post-tectonic 528 Ma granites intruded the metamorphosed sediments of the Damara Belt (Hambleton-Jones, 1976). In the Langer Heinrich vicinity, the contemporary Bloedkoppie Granites have been suggested as the most likely source of the uranium. These granites are exposed and cover large areas towards the east of the palaeo channel and hence up river. The Bloedkoppie Granite is a biotitic syenogranite, medium- to coarse-grained, and contains uranium grades of up to 10 ppm U (Miller, 2008). After the post tectonic 528 Ma granites, younger granites of post Karoo age (124 – 137 Ma) intruded and were followed by a number of granitic intrusions (80 – 130 Ma) such as the Spitzkoppe Mountain. These have been assumed to be the primary source for the Trekkopje Uranium deposit. These granites contain uranium grades of up to 30 ppm (Bowell, et al. 2009) that through weathering, could precipitate uranium under preferable conditions discussed in chapter 2.5.

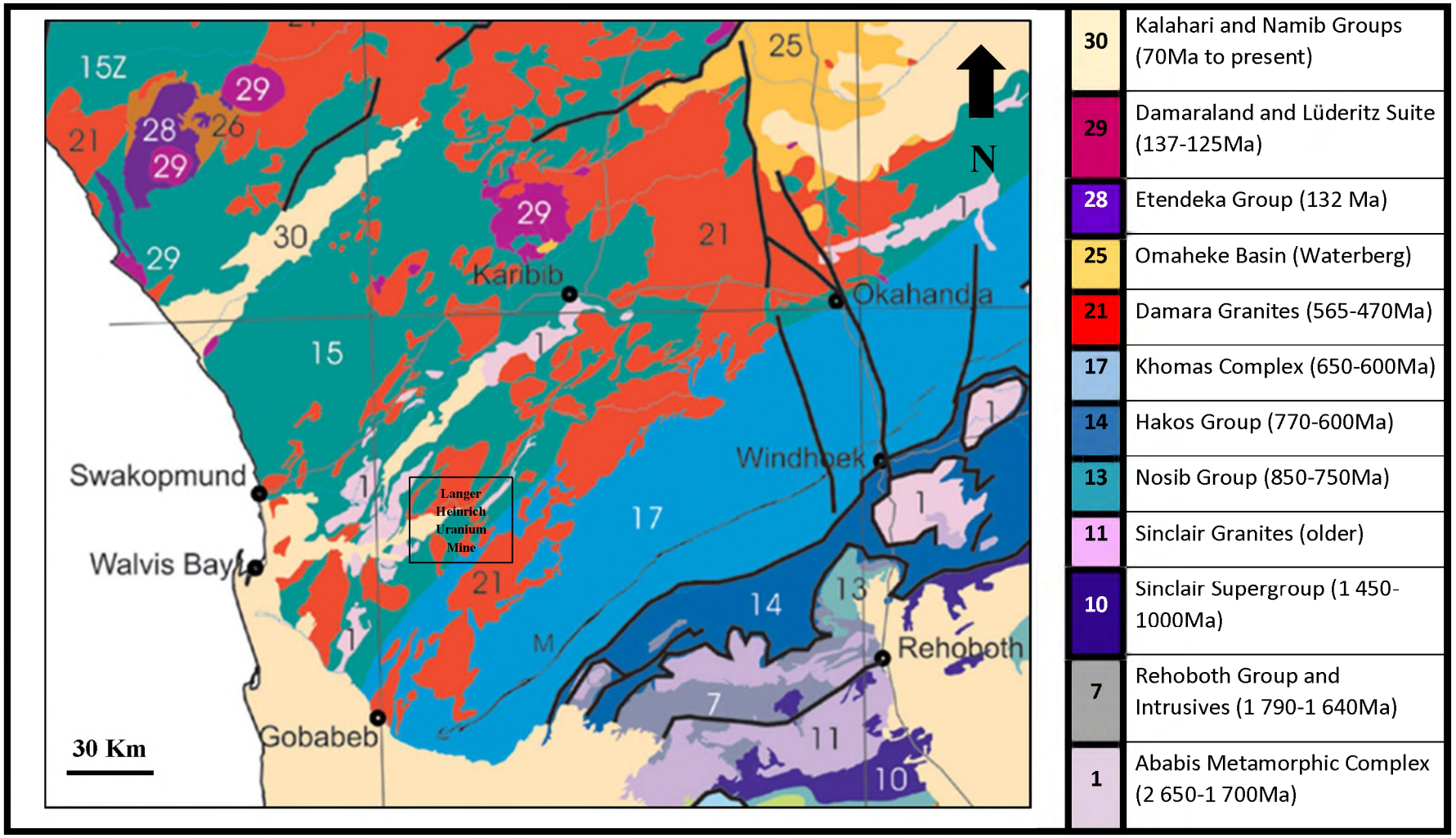

Figure 2: Geological map of Namibia modified after (Miller, 2008)

2.2 Local Geology

The Great Escarpment represents one of the most visible topographical features in Namibia and was formed by late Jurassic uplift and rifting, associated with the break-up of Gondwana. The Great Escarpment sets a divide between the higher lying Khomas Hochland Plateau and the Namib Desert. Over time, erosion of the Khomas Hochland Plateau provided an influx of sediments that produced numerous alluvial deposits towards the west. It is in these alluvial palaeo channel deposits that a number of calcrete uranium deposits have formed (Becker & Kärner, 2009). The subsequent deposition of eroded material resulted in the formation of the younger Namib Group on top of the much older Swakop Group as indicated in Figure 3. The Namib Group consists of successions of Cretaceous to Recent aged sediments that occur sporadically from the Orange River in the south, to the Kunene River Mouth in the north of Namibia (Miller, 2008). It is in these much younger sediments that the uranium ore mineral carnotite was deposited within the calcareous sediments (Gilchrist et al., 1994). The Tsondab Sandstone formation is the youngest formation found within the Gobabeb subgroup and consists of red-brown aeolian sandstone interbedded with fluviatile successions.

<table>
<tr><th></th><th>Group</th><th>Subgroup</th><th>Formation</th><th>Epoch</th></tr>
<tr><td rowspan="5"></td><td rowspan="3">Namib</td><td>Gawib</td><td>Sossus Sand
Bloedkoppie
(east)
Tumas (west)
Gemsbok</td><td rowspan="2">Recent to Pliocene</td></tr>
<tr><td colspan="2">Unconformity</td></tr>
<tr><td>Gobabeb</td><td>Langer
Heinrich
Tsondab</td><td rowspan="2">Miocene</td></tr>
<tr><td colspan="3">Unconformity</td></tr>
<tr><td rowspan="6">Damara
Sequence</td><td rowspan="3">Swakop</td><td>Khomas</td><td>Kuiseb
Karibib
Chuos</td><td rowspan="3">Late Precambrian</td></tr>
<tr><td colspan="2">Unconformity</td></tr>
<tr><td>Ugab</td><td>Rossing</td></tr>
<tr><td colspan="3">Unconformity</td><td rowspan="2">Precambrian</td></tr>
<tr><td rowspan="2">Nosib</td><td rowspan="2"></td><td rowspan="2">Khan
Etusis</td></tr>
<tr><td rowspan="2">Proterozoic</td></tr>
<tr><td colspan="4">Unconformity</td></tr>
<tr><td colspan="5">Abbabis Metamorphic Complex</td></tr>
</table>

Figure 3: Geological sequences with subdivisions and relative ages of the Central Damara Orogenic Belt in the area surrounding the Langer Heinrich Mine (modified after Hartleb, 1988)

2.2.1 Sediments of the Namib Group within ML 140

Langer Heinrich Mountain provides the name to the east-west striking palaeo channel and is the main site of deposition. The palaeo channel sediments vary in thickness from proximal upstream to downstream areas, but has an average thickness of 90 m (Hartleb, 1988). Increased drilling since then has provided an increased thickness of sediments in the ML140 mining licence that can vary between 4 m to 120 m. Throughout the palaeo channel the sedimentary successions are generally poorly sorted. The sediments often terminate abruptly throughout, which can be observed clearly in the conglomeritic horizons. This can be attributed to the natural braided form which the palaeo river created with varying influxes of water during rainy seasons. Alternating successions of calcrete bearing conglomerate, sandstone, grit and siltstone are observed, as described by Miller (2008). Carnotite is found as a secondary uranium mineral within the calcareous sediments.

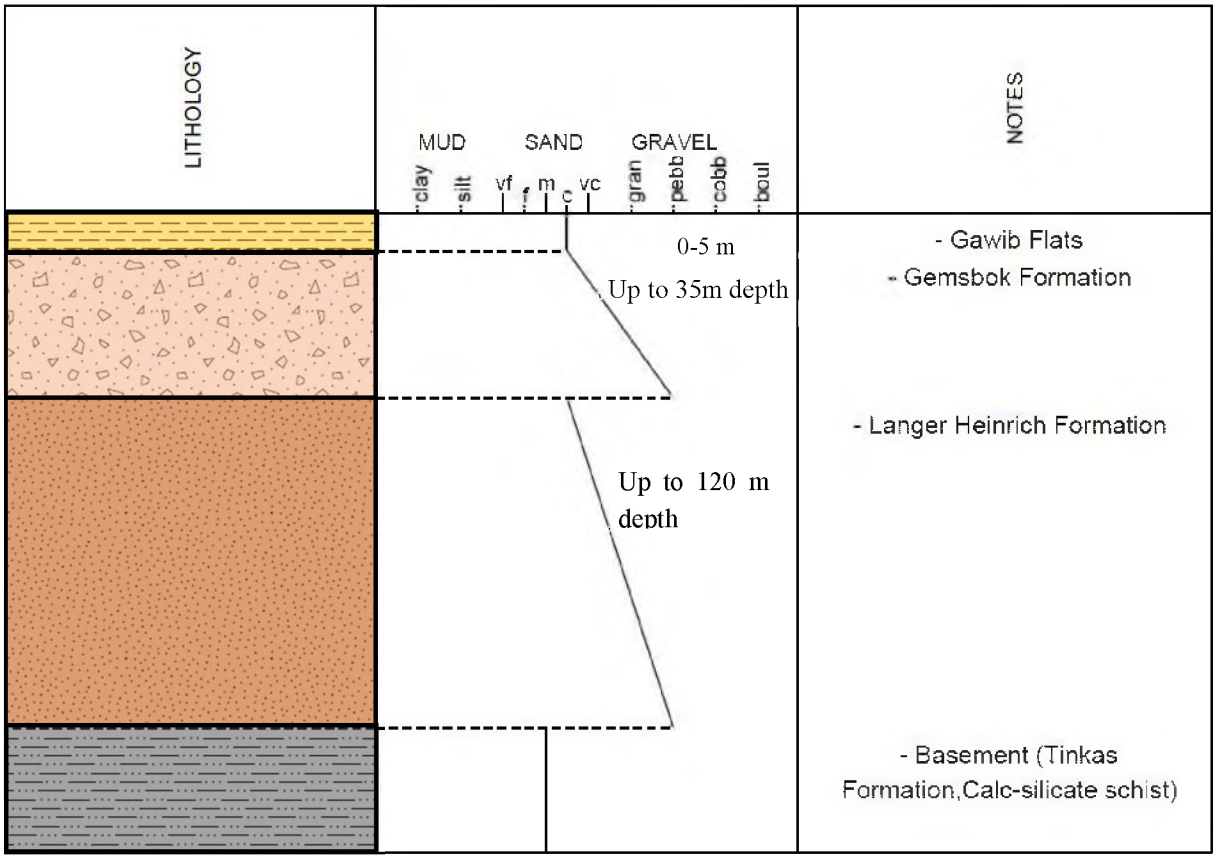

Figure 4: Stratigraphical profile of sediments in the western palaeo channel

Tinkas Formation

The Tinkas formation consists primarily of steeply dipping interbedded layers of calc-silicate and schist and these rocks form the basement within the mining licence. The biotite schists of the Tinkas formation are primarily fine-grained and interbedded with medium to coarse-grained calc-silicates. Granitic pegmatites or pegmatites associates with the granitic intrusions

within the area are common. It is believed that the unmineralised rocks of the Tinkas formation are the primary source of vanadium during carnotite mineralisation (Hartleb, 1988).

Langer Heinrich Formation

Mineralisation is predominantly confined to the Langer Heinrich formation (LHF). The LHF, as illustrated in Figure 4, forms the basal sedimentary succession that underlies the much older Tinkas formation. The LHF becomes systematically thicker from east to west, which is due to increased erosion in the eastern parts of the mining licence. The LHF consists of a variety of calcareous bearing sediments. Mineralogically defined, these calcretes consist of calcite, quartz, feldspar and minor amounts of micas as well as carnotite (Trittschack, 2008). The general fining-upward sedimentological sequence is visible over numerous cycles that are remnant products of annual floods. The calcareous sediments are classified according to their grain size fractions and their calcium carbonate. Lager grain sizes commonly visible in calcareous conglomerates are comprised of quartzites from the Etusis formation (Langer Heinrich Mountain) as well as calc-silicate schists from the Tinkas formation.

Gemsbok Formation and Gawib Flats

The upper and younger calcrete formations such as the Gemsbok formation that unconformably overlie the LHF are not mineralised and similarly increase in thickness towards the west. The Gemsbok formation illustrated in Figure 5 underlies the younger Gawib Flats that are clearly visible in the western area of ML 140. The contact between the underlying LHF and younger Gemsbok formation is not clearly visible. The Gemsbok formation consists of similar calcareous sediments compared to the Langer Heinrich formation. The Gawib Flats form the upper sediments of the palaeo channel and consist largely of unconsolidated material comprised of calc-silicate and quartzite from the surrounding basement outcrops.

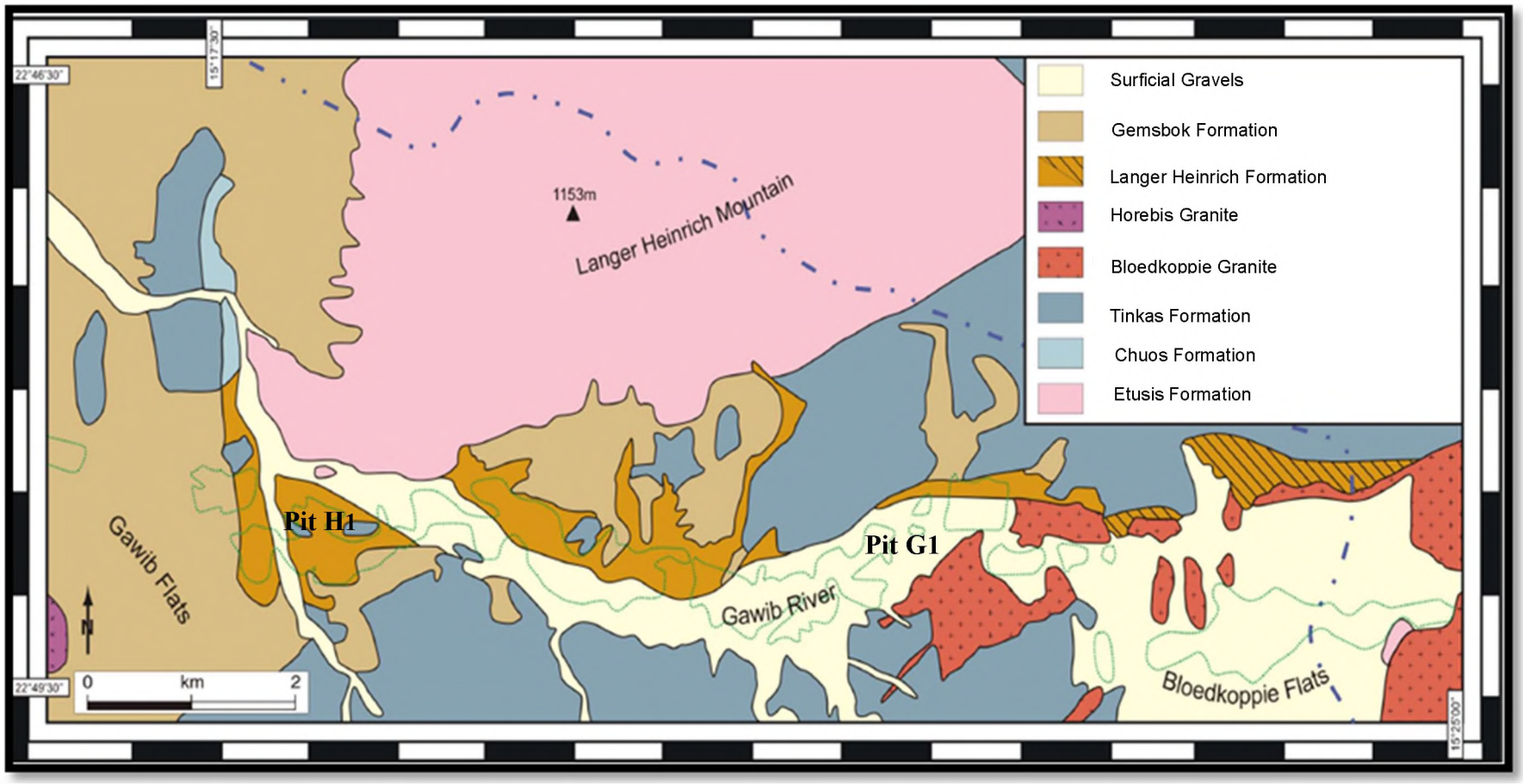

Figure 5: Local Geology of the Langer Heinrich Palaeo channel of the Langer Heinrich deposit (Trittschack, 2008)

2.3 Host rock: Calcrete characteristics and formation

The host rock in which carnotite predominantly mineralises is calcrete. Calcrete rocks are formed from a binding agent or cement that consists predominantly of calcium carbonate and occurs in near surface terrestrial environments (Wright & Tucker, 1991). The calcrete found at Langer Heinrich is a non-pedogenic calcrete that forms as a product of lateral transport of soluble ions to preferable deposition sites (Carlisle, 1980). Calcium carbonate acts as cement for detrital grains in sediments and weathered basement rock. The calcrete is thought to have been introduced after deposition of residual conglomerates, grits, sands and clays. Water, containing suspended calcium carbonate, had easy access through the porous sediments and, as $CaCO_3$ became progressively concentrated in the groundwaters, calcrete precipitated which acted as a binding agent between grains. The increase of $CaCO_3$ in groundwater was most likely due to periodic droughts when groundwater levels would drop. Calcrete is known to precipitate as a function of evaporation and evapotranspiration, as well as degassing of carbon dioxide (Wright et al., 1991). Carnotite is most frequently found, and has the highest grades, within the finer matrix of the calcareous sediments. Calcretes are known to occur in a variety of colours ranging from white, light-grey, grey, grey-brown, brown to darker variations. Carnotite at Langer Heinrich has been observed only as various shades of yellow.

Table 5: Classification of calcretes, structure and calcium carbonate contents (after Netterberg, 1976)

Nomenclature	Description	$CaCO_3$ Content
Calcareous soil	Weakly or non-cemented soil; usually with carbonate coatings around grains	1 to 10 %
Calcified soil	Weakly to moderately cemented soil	10 to 50 %
Powder calcrete (calcrete silt and sand)	High carbonate cemented soil and silt	±75 %
Nodular calcrete	Smooth to hard carbonate cemented unconsolidated soil; possible re-displacement of particles; occur usually as laminar coatings	75 % +
Honeycomb calcrete	Honeycomb weathering structures; lots of pore spaces filled with soil particles	75% +
Hardpan calcrete	Sheet-like; sharp upper surface and gradational lower surface	75% +
Laminar calcrete	Similar to hardpan calcrete caused by recurring cycles of solution and re-deposition	75% +
Calcrete boulders and cobbles	Eroded/weathered hardpan calcretes	75% +

Calcrete can occur in different forms as described in Table 5. The most common form observed at Langer Heinrich is hardpan calcrete. This calcrete is observed as long, laterally extensive beds or layers, ranging from 0.4 m to more than 10 m in thickness. Thicker homogenous beds of calcrete can be observed in Figure 6. Other forms of calcretes observed at Langer Heinrich include laminar calcretes, honeycomb calcretes and nodular calcretes. The higher carbonate containing calcrete layers in the palaeo channel, do have sharp contacts and are easily distinguishable from the other calcareous sediments in between the calcrete horizons.

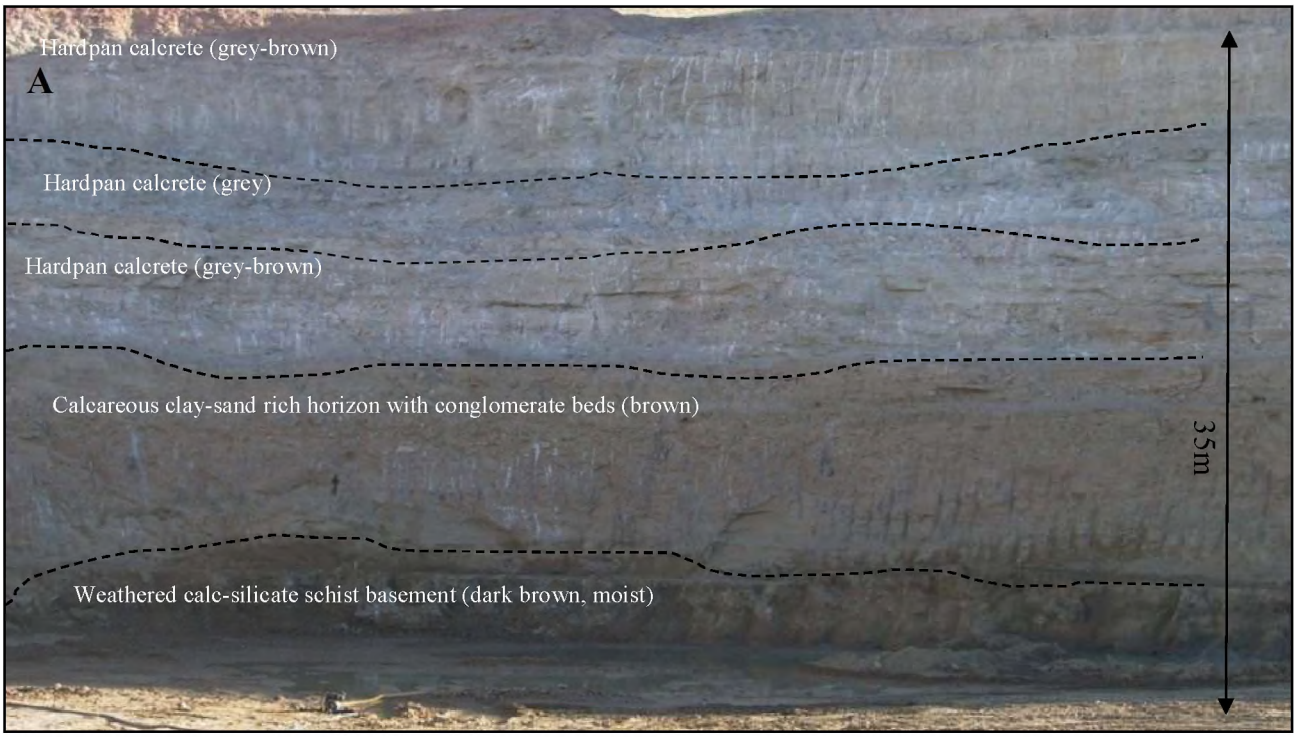
A
Hardpan calcrete (grey-brown)
Hardpan calcrete (grey)
Hardpan calcrete (grey-brown)
Calcareous clay-sand rich horizon with conglomerate beds (brown)
Weathered calc-silicate schist basement (dark brown, moist)
35m

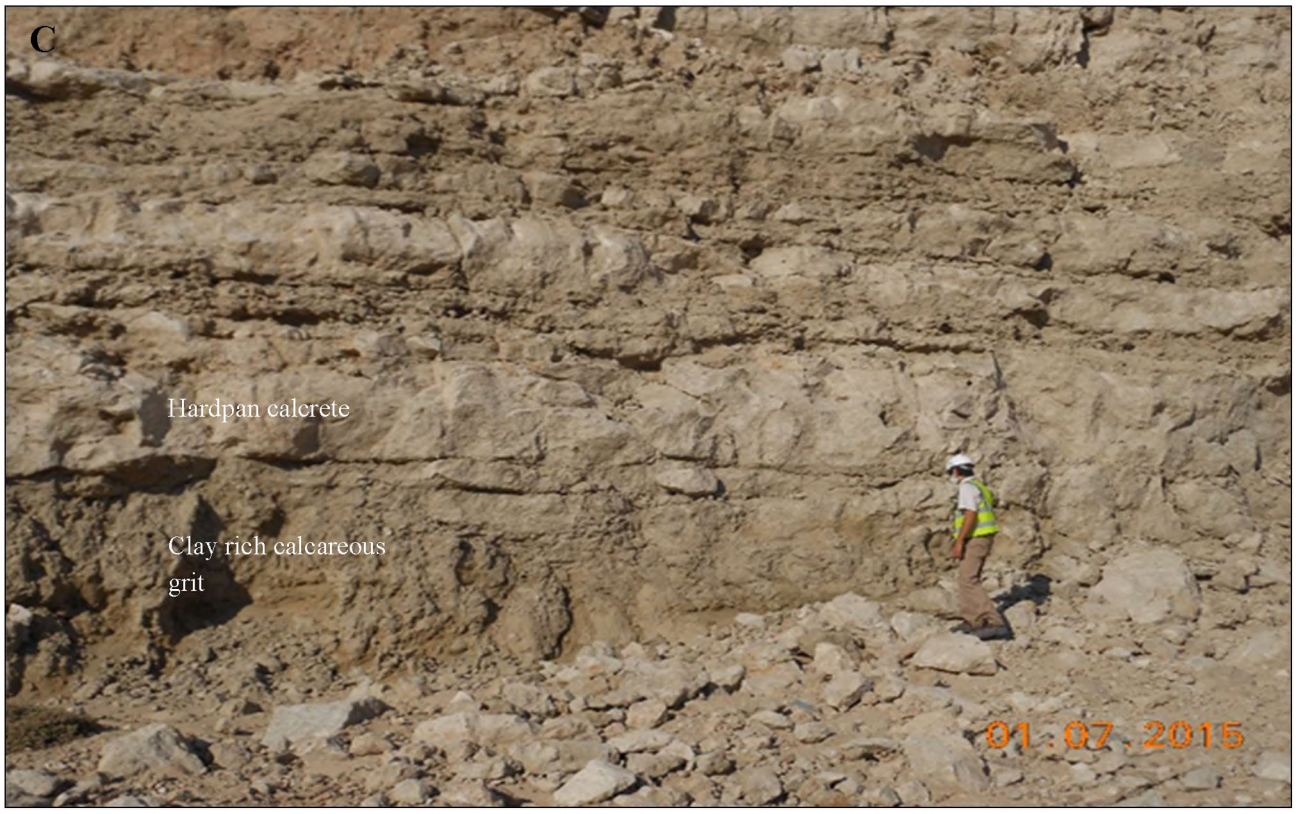
C
Hardpan calcrete
Clay rich calcareous grit
01.07.2015

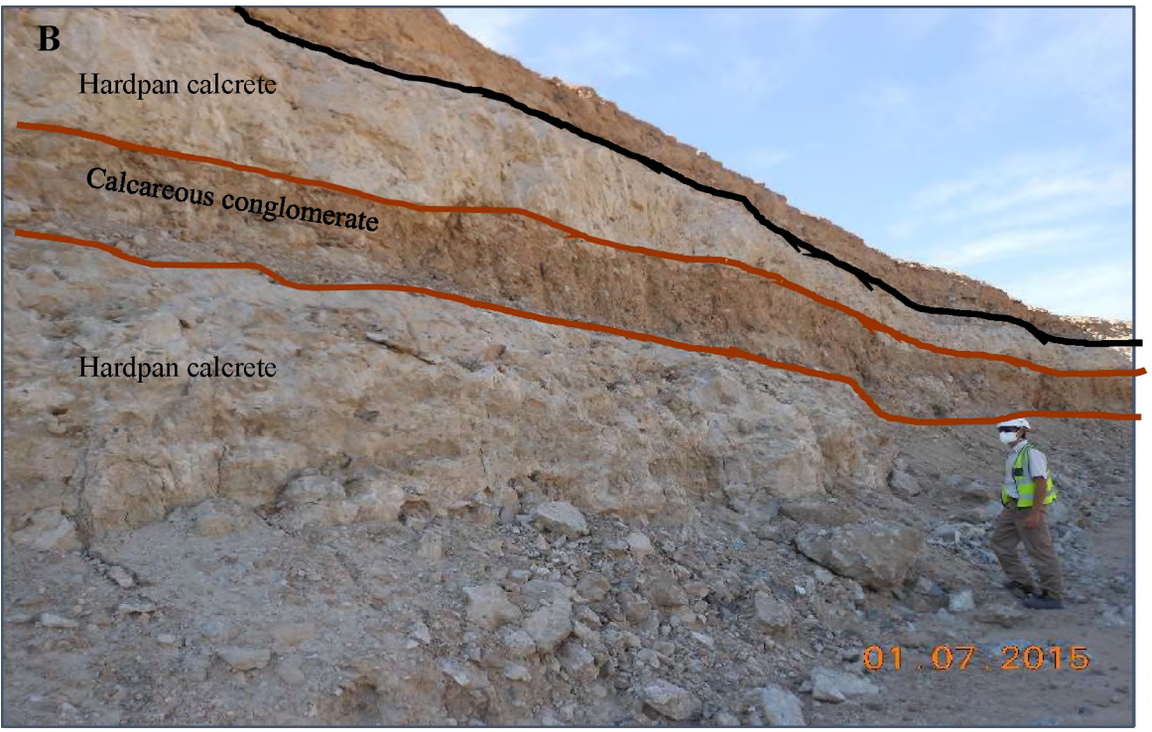

Figure 6: **A**: Pit H1- Hardpan calcrete layers indicated above with sharp upper contact towards the softer calcareous sediments near the bottom (after Baufeldt, 2012). **B**: Upper Pit G1- Sharp contacts between finer hardpan calcrete and coarser calcareous conglomerates. **C**: Lower Pit G1- Alternating beds of hardpan calcrete and calcareous grit (sands and clays)

2.4 Ore mineralogy

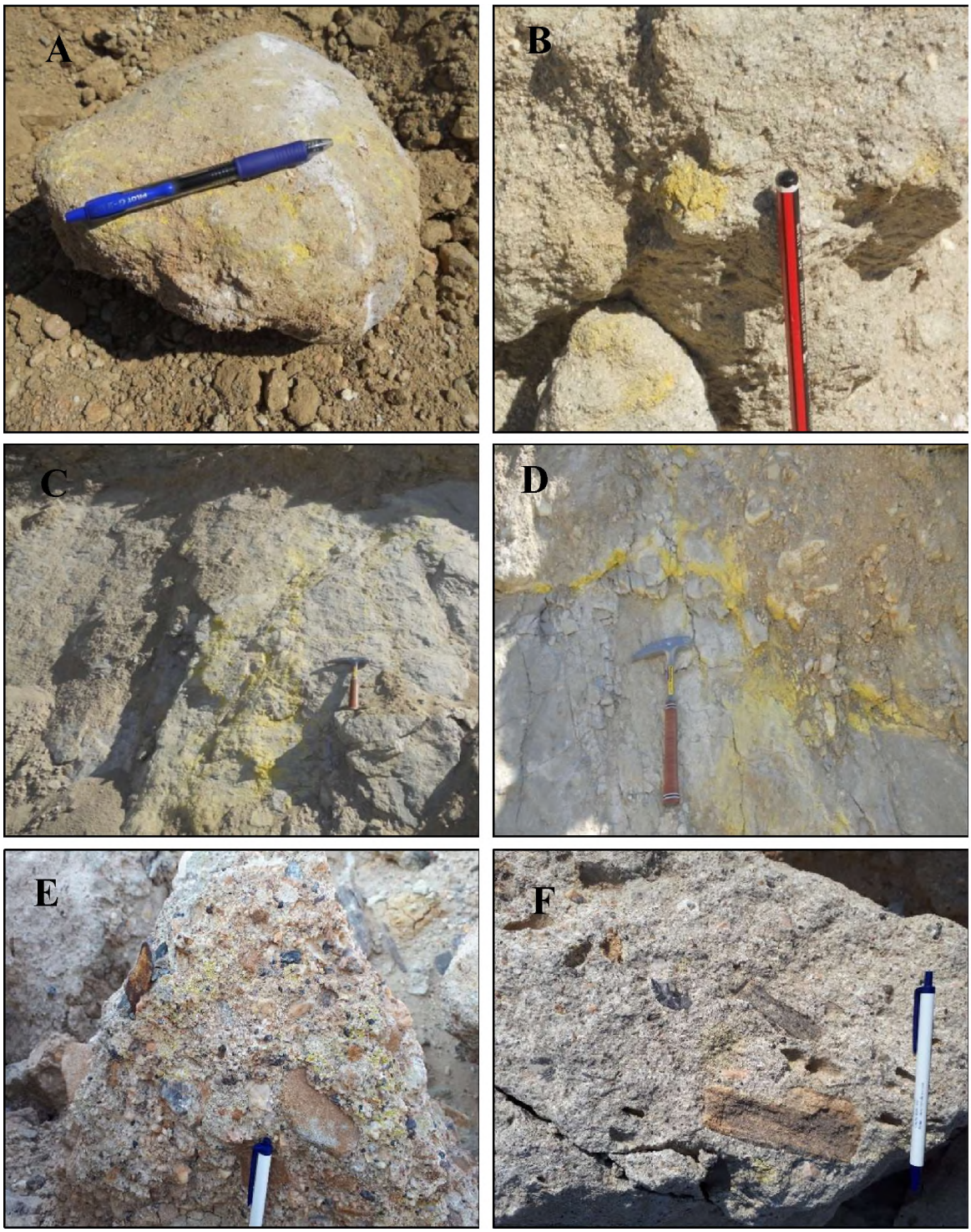

Figure 7: Mineralisation forms of carnotite (yellow) **A**: Clast coatings; **B**: In matrix of calcareous grit; **C** and **D**: On impermeable basement, probably due to ponding of groundwater (Baufeldt, 2012); **E** and **F**: Disseminated carnotite in calcareous conglomerate

To date, the only uranium ore mineral identified in the palaeo channel is carnotite ($K_2(UO_2)_2V_2O_8.3H_2O$) which is readily identified by its yellow colour. Carnotite occurs in a variety of colours, which should not be mistaken for weathered calc-silicate that makes up the underlying interbedded schistose basement rock. The colour differences in carnotite have been attributed to changes in the oxidation state from vanadium (V) to vanadium (VI) (Hambleton-Jones, 1984). Mineralisation as observed in Figure 7 is generally variable over short distances. Mineralisation has been described as being lenticular, forming pods and lenses, veins, coatings around pebbles and as stains or disseminations in the gritty calcareous matrix (Hambleton-Jones, 1984). It is also visible as concentrated coatings on the more impermeable underlying bedrock. This supports the theory of saturated groundwater ponding above the basement rock (Figure 7 C and D). Carnotite is known to replace voids and any openings in the calcrete matrix (Mann & Horwitz, 1979). Uranium mineralisation is continuous throughout the palaeo channel, but irregular in grade distribution over short intervals.

2.5 Genesis of carnotite deposition

Carnotite is well known for its solubility in water and therefore forms predominantly as secondary deposits in arid climates (Mann & Horwitz, 1979). The transport of uranium from the primary granitic source rock (Bloedkoppie Granites) involves an initial leaching process during weathering, where the uranium is dissolved and transported in mildly oxidised groundwater (Otton, 1984). Uranium (U^{6+}) is then transported as a uranyl carbonate or bicarbonate complexes at a shallow gradient downstream and precipitates when suitable conditions are met. These geochemical conditions have pH ranges between 6 and 8 and Eh ranges between 0 and 1, which are currently observed in Namibian groundwaters (Bowel et al., 2009). Vanadium found in carnotite is thought to have been added from the surrounding Tinkas formation bedrock that consist of calc-silicate schists. These conditions are summarised in point form below. A schematic representation is illustrated in Figure 8 from the Yeelirrie deposit in Australia. This is a prolonged event as the granitic sources often only contain low concentrations of primary uranium.

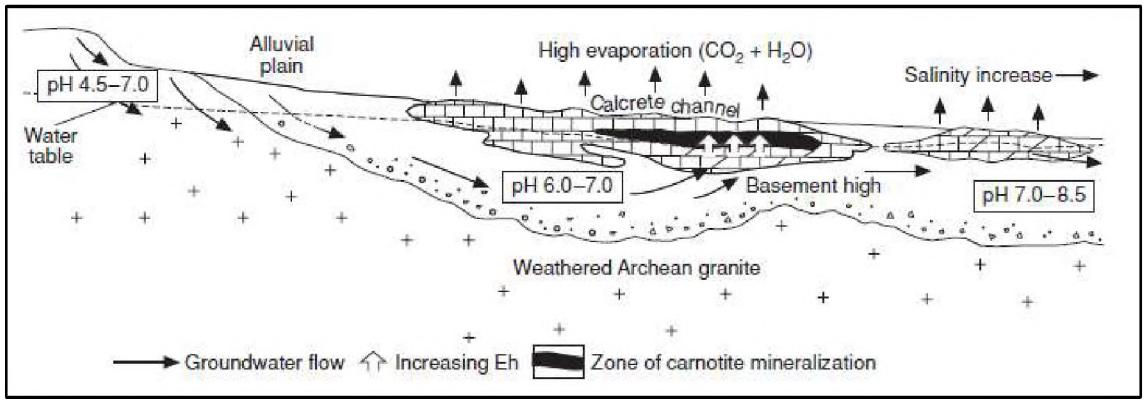

Figure 8: Geological setting proposed for the Yeelirrie calcrete deposit (Robb, 2005)

Carnotite precipitation is a very complex process and most likely involves a number of chemical processes. Boyle (1984) proposed that carnotite precipitation would be enhanced by: dissociation of uranyl complexes; changes in the redox states of the contributing components; pH fluctuation; sorption onto iron hydroxides, oxyhydroxides and/or clay; enrichment in source; evaporation of groundwaters near, or at, surface; colloidal precipitation; change in partial pressure of the dissolved carbon dioxide. Boyle (1984) also suggested that mixing of two or more different groundwaters could induce precipitation. At Langer Heinrich, blending of groundwaters from the Tinkas schists enriched in Vanadium and groundwaters from the Bloedkoppie Granites enriched in uranium, would provide optimal conditions for carnotite formation.

It is thought that the major process aiding carnotite formation at Langer Heinrich is evaporation of circulating groundwater: this removes carbon dioxide from the aqueous solution promoting carnotite precipitation as per the reaction in Equation 1. During precipitation of carnotite, hydrogen ions are produced which increases the acidity (lowers pH) in the fluid. Lowered pH promotes the solubility of calcite which in turn favours the solubility of carnotite (Robb, 2005). This provides an explanation why secondary uranium deposits are often in a state of remobilisation: surficial carnotite ores are rarely economic; the few sub-economic deposits are located in countries with arid environments such as Namibia, Australia and Argentina.

Carnotite precipitation occurs as described in the following equation:

Equation 1: Reaction explaining the precipitation of Carnotite formation from aqueous solution (Robb, 2005)

$$2UO_2^{2+} + 2H_2VO_4^- + 2K^+ + 3H_2O \leftrightarrow K_2(UO_2)_2(V_2O_8).3H_2O + 4H^+$$

CHAPTER 3. METHODOLOGY

3.1 Available datasets on study area

3.1.1 Previous work and research

The most recent work on the geological setting of the Langer Heinrich deposit has been done by Becker and Kärner (2009). Previous work has been done on the general deposit itself by Hambleton-Jones (1976 and 1984) and Hartleb (1988), which resembles that of the most recent publication by Becker and Kärner (2009). These articles focus on the general geology of the deposit and that surrounding the deposit. The unpublished Master's thesis by Trittschack (2008) focuses on the mineralogical aspects along with geological identification of the palaeo surface in and around the Langer Heinrich deposit.

Technical reports on the deposit and study have been done by D. Princep, who is the current Principal Resource Geologist of Paladin Energy Ltd. as well as A. Hudson (previous Paladin Energy Mine Manager), but have not been published.

3.1.2 The Langer Heinrich Mine dataset

The Pit G1 dataset

The dataset used for this research consisted of over 3 058 exploration and ore delineation drill holes at drill spacing that was scaled down from a 50 m x 50 m grid to a 12,5 m x 12,5 m grid. A further 60 922 grade control holes were drilled at a spacing of 4 m x 4 m to a maximum depth of 15 m. In the dataset are 3 143 drill holes at an interval of 12,5 m x 12,5 m, 799 drill holes at 25 m x 25 m and 208 drill holes at 50 m x 50 m. All drill holes are vertical and data is reported as one metre composites that are generated from five centimetre intervals of raw data collected from radiometric probes attached to Rhino ATVs. Pit G1 is located in the eastern section of the mine which mostly has calc-silicate, biotite schist and granite basement rocks. The channel is about 56 m deep in the deepest parts in this part of the palaeo channel and consists of calcareous grit with coarser beds of angular conglomerates. This pit was mined as a micro pit due to high-grade mineralisation that is close to the surface and requires a much lower ore to waste stripping ratio. The carnotite is concentrated in higher-grade lenses here and is therefore extracted from smaller pits. This exercise where small near-surface high-grade ore bodies are targeted is a result of cost reduction operations following the decrease in uranium prices post Fukushima. The blocks mined can consist of various size and shapes, but typically have a surface area of about 6 000 m^2. The block is usually mined in 3 m flitches with final bench heights of 9 m.

Pit G1 as seen in Figure 9 is about 980 m long and 550 m at its widest and covers an area of about 407 273 m^2. The pit was mined from an elevation of 695 m to a minimum elevation of 659 m above sea level and was therefore 35 to 40 m deep. The pit was started in the beginning of 2013 and was mined out by June 2014. Back filling and rehabilitation of pit G1 is currently in process and the area might be used in the future for stockpiling mined material.

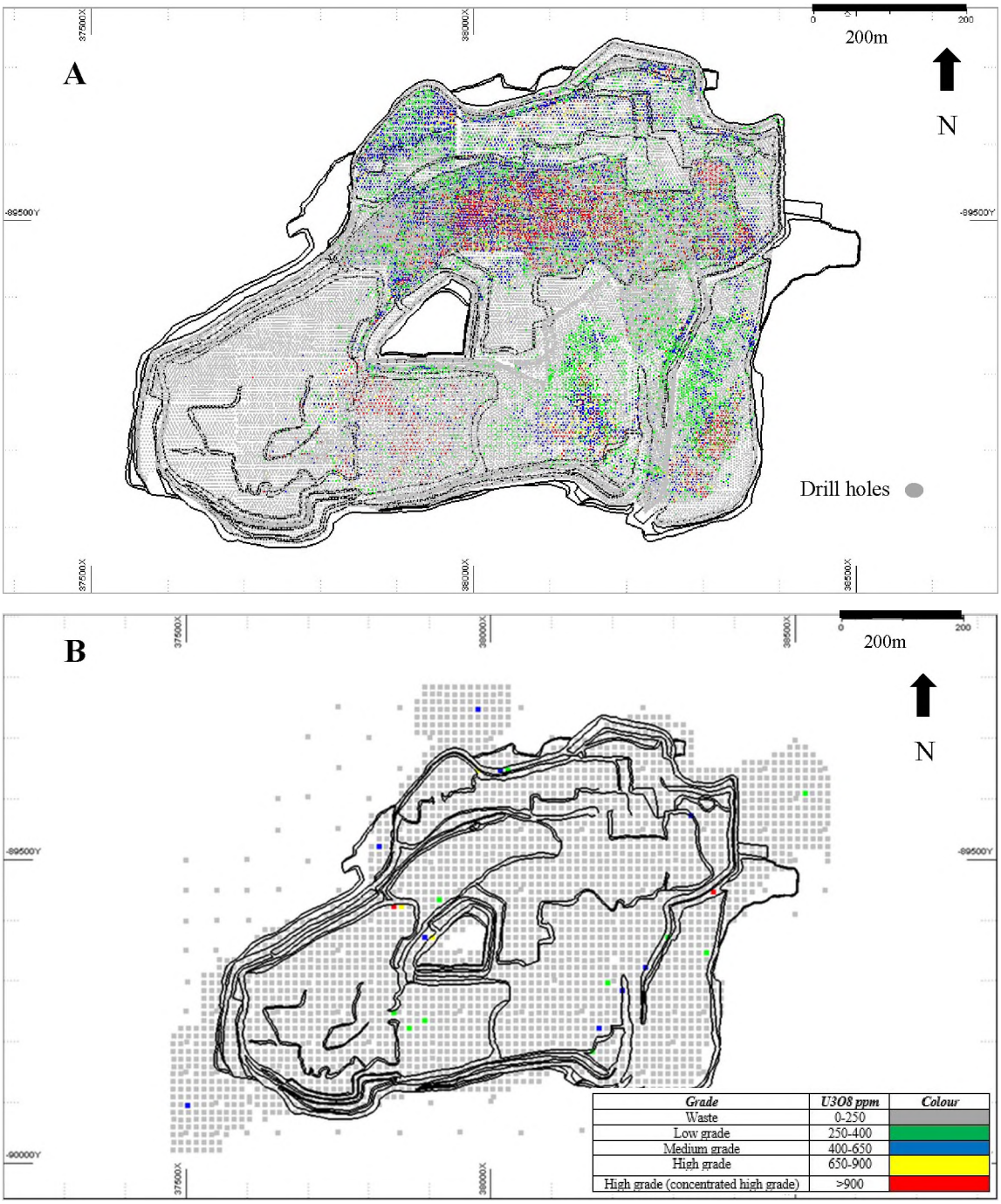

Figure 9: **A**: Grade control drilling in pit G1 on a 4 m x 4 m grid spacing. Various colours indicate different grade cut-offs. **B:** Grade control drilling in pit G1 on a 12,5 m x 12,5 m grid spacing

The Pit H1 dataset

The basic pit design with infill drill holes can be observed in Figure 10. The pit H1 dataset is somewhat smaller than the pit G1 dataset and will be a good comparison to the larger dataset. It is situated about 7 km downstream of pit G1 and is mined in the main palaeo channel and is therefore a continuously growing pit. The geology is somewhat different in terms of the sedimentological and chemical characteristics. Here, as in pit G, the same drill spacing was applied. A total of 22 950 drill holes were drilled during grade control at a spacing of about 4 m x 4 m. A further 1 308 holes were drilled at a spacing of 12,5 m x 12,5 m, 352 holes at 25 m x 25 m and 89 holes at 50 m x 50 m. The pit has a surface area of 217 487 m² and reaches a maximum depth of 70 m, dropping from an elevation of 615 to 545m above sea level. It is 390 m long and roughly 310 m wide. Estimations were done from an elevation of about 600 m, which is due to some discrepancies in the data. This upper rock is waste and subsequently not all the blasting blast block[7] were radiometrically logged. Furthermore, the pit was mined in the same way as pit G and will be used as a tailings storage facility (TSF) in the near future

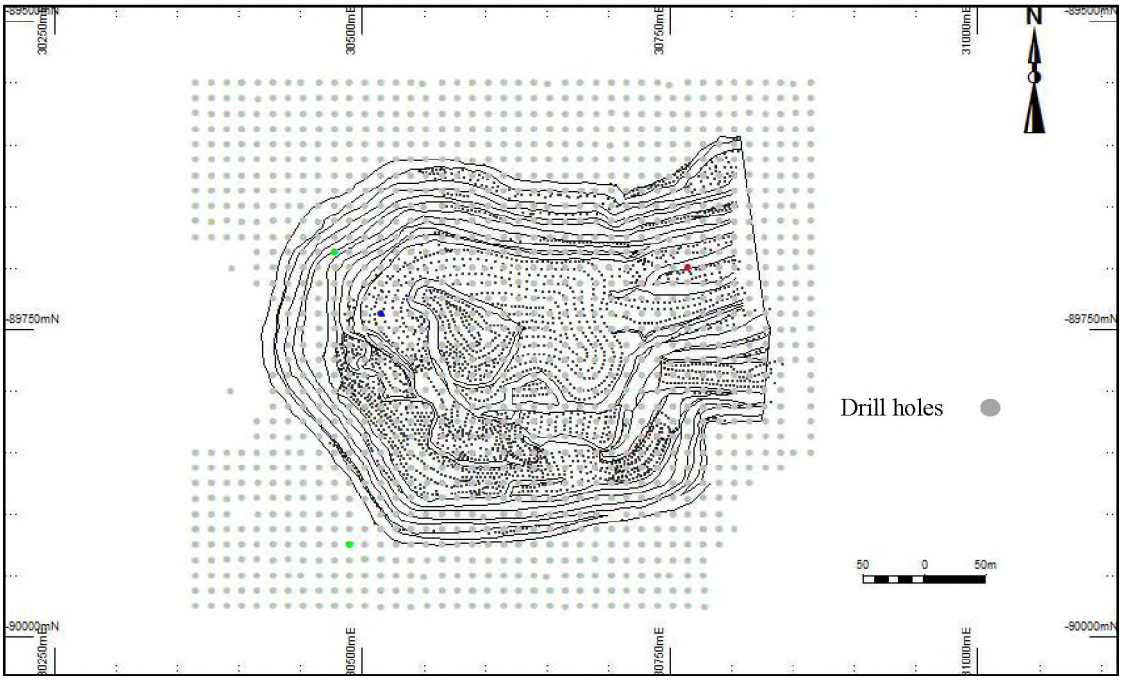

Figure 10: Ore delineation drilling in pit H1 on 12,5 m x 12,5 m grid spacing

[7] Blast block- Consists of a number of smaller ore blocks that are subdivided and mined according to their grades.

3.2 Software used for grade control modelling

The MPR grade control software used to perform ordinary kriging, multiple indicator kriging and conditional simulations was developed by Neil Schoefield more than 23 years ago. MPR is the only software used at Langer Heinrich to perform conditional simulation on blast blocks during each blast. It is a comprehensive software package which optimizes in-user friendliness and provides the essential tools for short term production strategies and ore optimization. MPR and its subsidiary module GS3 was used to create the block models for ordinary kriging, multiple indicator kriging as well as conditional simulation, with only multiple indicator kriging being calculated using the GS3 software.

The programme Micromine 2014 (MM) is the only programme used presently at the mine for exploration drilling, mining and blasting. Like other types of this software, e.g. Datamine, Vulcan etc., MM allows the user to import raw data and make it presentable for reporting. MM was used for the IDW estimation techniques. All the resulting block models from the different estimation/simulation techniques were plotted using MM. All estimates regarding these block models were also done using MM.

Centric mining systems is a relational database used currently at Langer Heinrich, which allows storing of vast amounts of data for record keeping. It allows multiple users from different departments on the mine to store large amounts of data daily. All data from pit G1 and H1 was entered over more than one year. The truck loads and grades can be exported into excel for analysis.

3.3 Variography

Variography was used in OK, CS and extensively in MIK. Variography used for OK and CS was basic and straight forward, while the MIK Variography is more tedious and time consuming. Variograms were constructed using the software MPR Grade Control System, whilst MIK used both MPR and GS3 during the estimation process. It should be noted that throughout the variogram construction, different drill spacing were used (4 m x 4 m, 12,5 m x 12,5 m, 25 m x 25 m and 50 m x 50 m) and therefore different parameters were used as well to create appropriate estimations. Variograms play a vital role in the estimation results and therefore different deposits have different criteria or distinct characteristics with regards to ore deposition. It must be said that variogram construction does have relative subjectivity incorporated into its modelling which should be acknowledged (Rossi & Deutsch, 2014).

For the construction of variograms for OK and CS, the gamma ray data for the different drill spacing was firstly run through a normal score transformation function which transforms the data to have a mean of 0 and variance of 1. The histogram therefore will be transformed from being highly positively skewed to the classic bell shape. Thereafter the transformed data of the different drill spacing is prepared for variography one dataset at a time. Holes drilled at Langer Heinrich are all drilled as close to vertical (90°) as possible as the sediments and ore are found in almost horizontal beddings. For the variogram setup, the lag tolerance chosen was always half the drill spacing. The number of lags used in the parameter setup would range between one and four, usually decreasing with wider drill spacing. The search radii used was always double to one and half the times the drill spacing. Direct experimental variograms were used for both OK and CS, whilst experimental indicator variograms were used during MIK. During MIK a total of 14 variograms were constructed in MP3. Each variogram as mentioned before is modelled in an X, Y and downhole (Z) dimension. These 14 variograms are then imported into the programme GS3 where the final changes are made before block model construction or display.

Data stationarity is described as common consistency of a spatial variability across the complete domain of the dataset as a whole. This is often the case in Sequential Gaussian Simulation as well as kriging where data can be either de-trended or transformed (Babish, 2006). They emphasise the importance of the distance between sample points irrespectively of the distance between them and also the mean, co-variance and variance across the entire domain remains more or less consistent (Larrondo & Deutsch, 2004). The use of a search radius or neighbourhood was also assumed to be at least twice the drill spacing in most cases. Although this relates to the believe that there is a trend in grade distribution, this is usually only the case over short distances and therefore the need for 12,5 m x 12,5 m drilling. In this research the data was transformed to provide a Gaussian distribution with a typical bell-shaped histogram.

3.4 Geostatistical modelling methods

3.3.1 Ordinary kriging (linear estimation method)

Equation 2: Ordinary kriging equation (Armstrong, 1988)

$$Z^*_{OK}(X_0) = \sum_i \lambda_{OK\,i}\, Z(x_i)$$

Z*= Estimated value

Xi= sample points at any given point

Kriging originated during the gold rush in the 1950s of the Witwatersrand goldfields in South Africa through the work of Danie Krige (Babish, 2006). Kriging is an estimation method that aims to produce accurate unbiased linear estimates and is frequently used in block models. Kriging techniques try to produce a minimum variance estimate (Armstrong & Boufassa, 1988). Factors that influence the accuracies of estimations are dependent on the number of samples, usually more samples result in higher confidence estimations. The quality of data is dependent on the assay accuracy and precision. Also relevant is the position of the sampling points in relation to the deposit and the distance between the sample points.

Ordinary kriging (OK) is a form of kriging often used in resource estimations. Other kinds of kriging include simple kriging, indicator kriging and universal kriging. OK is a typical example of linear kriging and is probably the most well-known and widely used form of kriging in the industry. It is now accepted that OK is reasonably unbiased and has been accepted in the geological society. OK is distinguishable from many other linear techniques by focusing on both distance between sample points and declustering of clustered samples (Isaaks & Srivastava, 1989). OK, unlike simple kriging, is an estimation method where the mean is unknown. This is due to the fact that the sum of the weights is limited to 1 and 0. When using OK the use of a probability model is acquired whereby both the error variance and bias can be distinguished. Assignment of weights to nearby samples is evaluated to provide an average error for the model to be 0 and also minimize the error variance. OK can be slightly more time consuming than other estimation techniques by making use of a variogram. The variogram, although a bit more tedious, makes the estimation technique more flexible and accurate than other estimation methods. The shape of the variogram used is a critical factor in determining the estimated results. Factors such as the nugget effect, range and sill amongst others play a role in the final results. The conditional bias sometimes created by OK is a sacrifice to obtain a decent estimate of the local mean (Yunsel, 2012). Smoothing of various degrees can be expected during OK and is a consequence of drill spacing or data availability, block size parameters and variogram construction (De Vitry et al., 2007).

During OK in this research, the software MPR Grade Control System was used for estimations and Micromine was used to display the results. These two software systems are also the current integrating and analyzing systems used in mining. The pit G1 and H1 data used during OK was the 4 m x 4 m, 12,5 m x 12,5 m, 25 m x 25 m and 50 m x 50 m drill spacing. During the procedure of each of the individual drill spacing datasets, all the data's univariate properties were calculated as well the normal scores transformed in order to create the various variograms for each dataset. The variogram created was used in the final step of the estimation. The block sizes used would be the same as the drill spacing, therefore 4 m x 4 m x 3 m, 12,5 m x 12,5 m x 3 m, 25 m x 25 m x 3 m and 50 m x 50 m x 3 m. The search radii used was twice the drill spacing. Discrete points used for both eastings and northings was 5 and for the level 2.

The 4 m x 4 m x 3 m drill data from pit G1 was collected from grade control drilling for blasting. The dataset contained too much data to be processed at once in MPR. It was therefore split into five sections, each roughly carrying the same amount of data and was then treated separately. The five estimated datasets were later compiled into one solid estimated dataset. Due to the extreme grades observed, various cut off values (capping grades) were used which have been provided in Table 6.

Table 6: Cut-off values for eliminating outliers used during OK estimation

Drill data	Cut-off grade/ capping (ppm)
4 m x 4 m x 3 m	13 000, 19 000, 20 000, 9 000, 6 000 (east to west)
12,5 m x 12,5 m x 3 m	15 000
25 m x 25 m x 3 m	7 000
50 m x 50 m x 3 m	3 500

3.3.2 Inverse Distance Weighted (Linear estimation method)

The inverse distance weighted (IDW) interpolation is probably one of the oldest and most well-known linear estimation technique around. The weights assigned to each point are inversely proportional to the distance at which the known point is located. Therefore, points that are situated further away from the unknown point carry less weight in determining the value at the unknown point. The IDW method can be manipulated by alternating the constant power which has an effect on the distance weighting relationship (Wong & Lu, 2008). As with OK, IDW provides a smoothed version of reality. IDW uses an unbiased method whereby all weights used sum up to 1, thereby reducing the bias. In most cases where IDW is applied, the constant used will either be squared or cubed (IDW^2 and IDW^3). IDW^2 is generally used in cases where the attributes are regularly characterized without too much variation. The IDW^3 is used in cases where the closest nearby known point gains the most weighting to determine the unknown point. This method has been favoured in deposits where grade variation is extreme in close proximities (Rossi & Deutsch, 2014) and therefore of interest in this research. During this research a constant of 2 and 3 was proposed and used as a comparison. MM was used for the estimation procedure. A search radius of twice the drill spacing was used during the IDW procedure, which is especially important on the broader drill spacing where there is less data availability. Different discretisations were used depending on the drill spacing. Discretisations are integer values that reflect the number of sub-blocks within the main block that is estimated. These sub-block grades are later averaged to represent a final block grade within the block model.

Equation 3: Inverse Distance Weighting equation (Rossi & Deutsch, 2014)

$$Z^* = \frac{\sum_{i=1}^{N} W_i \times Z_i}{\sum_{i=1}^{N} W_i}$$

Z^*= Estimated value

Z^i=correspondinf composite value

W_i= Weights assigned to each composite

IDW has been used in a variety of different studies, however, it is often less promoted in reporting resources and reserves which is most likely attributed to the absence of variography. OK uses the same linear attributes as IDW and is differentiated because it assumes minimum error variance. IDW is less time consuming and follows a less complex preparation process. One of the major drawbacks to IDW is that the decay constant chosen is applied to the entire dataset, not taking into consideration the drill spacing (Wong et al., 2008). Various cut off grades had to be incorporated that are represent in Table 7 and Table 8.

Table 7: Cut-off values for eliminating outliers used during IDW^2 estimation

Drill data	Cut-off (ppm)
4 m x 4 m x 3 m	6 000
12,5 m x 12,5 m x 3 m	3 400
25 m x 25 m x 3 m	2 100
50 m x 50 m x 3 m	1 100

Table 8: Cut-off values for eliminating outliers used during IDW^3 estimation

Drill data	Cut-off (ppm)
4 m x 4 m x 3 m	7 000
12,5 m x 12,5 m x 3 m	4 000
25 m x 25 m x 3 m	2 100
50 m x 50 m x 3 m	1 040

3.3.3 Multiple Indicator Kriging (Non-linear estimation method)

Equation 4: Multiple Indicator Kriging equation (Yi et al., 2014)

$$Z_{IK}^*(x) = \sum_{i=1}^{n(h_1)} \lambda_{IK}(x_i) Z^*(i; X_i)$$

Multiple Indicator Kriging (MIK) is a non-linear estimation technique which has gained a wide acceptance in the mining industries over the last years. Indicator kriging's introduction by Journal in 1983 has provided a fundamental research base on which many have expanded and

improvised. MIK forms part of indicator geostatistics which uses OK as a basic estimation technique, where indicator variograms are used to manipulate data. The results of indicator kriging are categorised between 1 and 0, whereby the kriged data below the cut-off has a value of 0 and data above the cut-off receives a value of 1 (Vann et al., 2000). This approach allows this method to handle a wide range of data with a large variation in grade and therefore decreases the effect of outliers (Babish, 2006). It has been noted that Indicator Kriging in general can deal with highly skewed data by making use of the multiple thresholds and treating and incorporating higher-grades therefore more efficiently (Glacken & Blackney, 1998). MIK allows for different thresholds or cut off values to be selected. This is typical of gold and uranium mines and therefore a viable option at the Langer Heinrich deposit to be used for resource estimation.

Variography undertaken on each of the thresholds is somewhat time consuming. In most cases MIK allows for a lower degree of smoothing of estimated data compared to the linear techniques and therefore is less prone to overestimation. It is a non-parametric estimation technique and therefore does not operate by using prior observations and assumptions (Lipton et al., 1998). A notable downfall of Indicator Kriging is the grouping system of 0 and 1 for cut-off grades. Although this assumption does have its benefits, the grouping of data below or above the cut-off within a certain threshold will be equal and therefore much higher values might be equal to much lower values. This is also known as rank correlation variances.

MPR was used for the MIK procedure to perform most of the variography. MM was only used to display the final block models. During this research 14 thresholds or cut-off values were used and therefore 14 indicator variograms were modelled for each of the drill spacing. The 14 thresholds used were a function of the grades within the dataset. The number of thresholds used correlated to the grades. These indicator variograms were constructed from data that was rank transformed first. One extra direct variogram was constructed using the whole dataset for each drill spacing without any transformations (no back transformation). Each of the variograms was fitted with precision and observed in an X and Y direction, as well as the down hole. Variography was observed and adjusted where necessary. The programme GS3 (extra subsidiary package of GS3) was used in the final steps of the MIK method which is not available on site at the moment.

3.3.4 Conditional Simulation (Sequential Gaussian Simulation)

Sequential Gaussian Simulation is one of the most common forms of conditional simulations (CS) has gained wide acceptance over geostatisticians in providing decent figures in resource estimation (Shi et al., 2000). It was introduced in the 1990s as an alternative to older linear

estimations methods such as kriging. The advantages and disadvantages of CS along with the other methods are summarised in Table 9. CS is a stochastic method known to produce optimal results from data that is closely spaced such as blast holes, which is the case in this study (Ravenscroft, 1994). CS and MIK have in recent years dominated the mining industry and are praised for the increased precision over linear methods. CS is a simulation method that creates numerous simulations, each representing a true but equally probable reality. During the initial stages of the simulation all the data has to be transformed into standard normal scores and post simulation the data is transformed back from Gaussian into data that is presentable. Declustering of the original data, although common, was not necessary as the data used was drilled on regular intervals. Simple kriging is usually used to obtain the mean and variance (Rossi & Deutsch, 2014). Due to the presence of variogram modelling during the simulation setup, the integrity and originality of the data or sample point is maintained. Spatial continuity is also maintained and data is not smoothed as in the linear methods. CS and similarly MIK are based on point estimates whilst OK and IDW are block estimates and are therefore sometimes less preferred. There was no need to decluster the data, although preferred, due to a regular drilling grid (no preferential drilling). Due to the fact that multiple forms of reality present themselves at the end of these simulations, an accurate form of reality can be obtained with improved accuracy over other alternative estimation techniques (Lipton et al., 1998).

During CS in this research, 50 simulations were run on the Pit G1 and H1 dataset. Although 100 simulations are often preferred, the large size of the two datasets and computer capabilities resulted in the use of 50 simulations. CS was only used on the 4 m x 4 m grid spacing from the grade control data. It is known in the literature that CS performs optimal in smaller grids as sufficient nodes can be incorporated and produce accurate results (Rossi & Deutsch, 2014). The results of these simulations were used as a form of alternative "reality" to which the other estimation techniques could be compared. CS is also the current estimation technique used at the Langer Heinrich Mine for the blast blocks using the grid spacing of 4 m x 4 m. MP3 was used during the setup and production of the conditional simulated model, while MM was only used to display the data and produce necessary calculations. During the initial steps in MP3, the dataset was run through the normal score transformation option. The transformed data was used to set up the direct variogram and was adjusted in the normal X and Y direction as well as down-hole.

3.3.5 Summary of geostatistical methods

Table 9: Advantages and disadvantages of various estimation methods used

Geostatistical method	Advantages	Disadvantages
Inverse Distance Weighted	- Fast and computationally simple - Similar to the nearest neighbour principal and therefore flexible and adaptive	- Smoothing data - Outliers or extreme values can create biasness - Exponent chosen provides subjectivity - No variography used
Ordinary Kriging	- Measure of uncertainty can be quantified - Widely used over a range of commodities - Variogram allows for reduced biasness - Flexible and more accurate	- Computationally more intensive - Smoothing data - Time consuming - In depth understanding of process (experience needed)
Multiple Indicator kriging	- Less smoothing of data - Robust method - Improved estimations over other kriging methods in deposits where grade distributions are erratic - Emphasis on variography throughout	- Time consuming - Computationally extensive - Experienced user - Potential smoothing
Conditional Simulation (Sequential Gaussian)	- Less smoothing of data - Multiple simulations of realistic scenarios - Variogram allows for reduced biasness - Improved representation of local variability often lost during kriging. Robust technique and degree of repeatability - Less smoothing than kriging - Honours spatial variability - Simpler and faster yet more restrictive than indicator based simulations	- Time consuming - Computationally extensive - Number of simulations could have an influence on estimation results - Increased simulations are time consuming and can create large amounts of data - Sensitive to extreme values - Restricted to larger data sets with short sampling intervals (Complications in wide spaced drill data)

CHAPTER 4. ADDITIONAL RECONCILIATION RESEARCH ON GRADE ESTIMATION EFFICIENCY AND MINING OPERATIONS ON INDIVIDUAL ORE BLOCKS

This chapter is an additional study that focuses on the difference between various drill spacing and estimation techniques by comparing the results to actual data collected from mining operations. The large-scale reconciliation project explained in chapter five and six, does not factor in small-scale practices that are focused on precision and mining efficiency. Therefore, a small-scale study using 12,5 m x 12,5 m and 4 m x 4 m drill spacing data was used to predict if the 4 m x 4 m drill hole needs to be radiometrically logged or not. The down-hole logging of 4 m x 4 m drill holes is the current operational standard at the Langer Heinrich Mine and should realistically yield the most accurate estimation results due to the closer drill spacing. However, the logging procedure of the 4 m x 4 m drill spacing is a cost and time-consuming operation. The extra costs can be related to well-trained staff, ATVs and maintenance thereof. Recently with the decline in uranium spot price, Langer Heinrich mining operations have initiated a procedure where grade control estimations were done on the drill data of the pit delineation drilling (12,5 m x 12,5 m). The theory of increased data availability on estimation and mining accuracy will be tested using mined data that was estimated using the 12,5 m x 12,5 m drill data. These blast blocks can therefore be modelled in advanced after pit optimisation drilling has been completed. The theory was tested using 10 blast blocks that were mined using both 4 m x 4 m and 12,5 m x 12,5 m drill data respectively. Should the hypothesis yield conclusive results in favour of 12,5 m x 12,5 m drill data, this operating procedure could save costs and will be less time consuming.

This small-scale research focused on ore blocks that on average have volumes of about 45 000m³ or 108 000 t. This is dependent on the ore block sizes which can vary from 24 000 to 260 000 t and is dependent mostly on ore selectivity that tries to minimise ore dilution. The blast blocks were drilled by Panthera 1500 rotary percussion rigs that drill on a 4 m x 4 m regular drill spacing. Hole diameters vary between 90 and 127 mm depending on the material mined (ore or waste), rig used as well as relative hardness of calcareous sediments and required fragmentation. The explosives used were high energy bulk emulsion explosives (HEF 100), which is a dense black emulsion consisting of recycled oil and alternative fuel (BME, 2016). Ore was hauled by 90 t Komatsu dump trucks and scanned for 45 seconds by radiometric truck scanners before hauling loads to designated stockpiles.

A total of 10 ore containing blast blocks were used that were radiometrically logged on a 12,5 m x 12,5 m and 4 m x 4 m drill spacing. These were selected from different elevations and

locations (pits) within the palaeo channel. The blast blocks were selected on the condition of containing more ore than waste. Waste and sometimes low-grade are usually not directed through the truck scanner to save on operational costs involved. The blast blocks were selected from both pit H1 and G1 as well as F1 pits. Their geology consists of both upper more competent calcrete blast blocks and lower less competent calcareous sediments like sands and clays. This is due to the nature and difficulty of mining various calcareous lithologies that require different drill spacing, variations in High Energy Fuel (HEF) usage and result in different fragmentation sizes. These factors make the more competent calcrete lithologies more difficult to mine compared to lower calcareous sand/clay that require less explosives and a wider drill spacing. It has to be noted that the 4 m x 4 m drill data was modelled using only conditional simulation, which is the conventional method used on the Langer Heinrich mine. The 12,5 m x 12,5 m drill data from the blast blocks were estimated using ordinary kriging in this study.

Statistical evaluations on the estimated and actual mined tonnages as well as grades is somewhat controversial. The decision to categorise an oreblock as being over or undermined was based on a 20% and 30% cut off in terms of tonnages. The 20 – 30 % cut off used in Table 10 with regards to differences in tonnage estimated versus mined was used because individual ore blocks within the larger blast blocks tend to be relatively small. It is easy to over or under mine these smaller ore blocks with large loading equipment and therefore the differences observed are usually more than 10%. The 20% would symbolise relatively good mined out ore block, whilst anything above 30% would be severely over mined (mined more ore from an ore block than expected). Estimated and mined grade classifications are somewhat more difficult to categorise as grade categories have a large grade variation. This can range between 150 to 250 ppm between different grade categories. Down or upgrading into a different grade category is of special concern and analysed more precisely; however, comments are also proposed on other unusual grade differences, usually more than 100 ppm.

4.1 Selected blast blocks estimated and mined using 4 m x 4 m drill data

Tonnage and grade comparison

In total 10 ore containing blast blocks were selected, five from each respective pit of interest. These 10 blast blocks contained 107 different ore blocks that varied in size, grade and tonnage. The blast blocks selected did contain some bias in the selection process as blast blocks with medium-grade (MG) and high-grade (HG) were preferred during selection. These are mined with the highest measure of precision and should therefore provide more confidence. The blast blocks selected from pit G1 were mined at an elevation of 680 m up to 659 m. The blast blocks from pit H1, which is situated downstream and westwards, were mined from an elevation of

572 m up to 548 m. The elevations used contained reasonable ore grades and were therefore selected. Mining at the Langer Heinrich Mine is done on nine metre [8]benches, at three metre mining flitches (depth intervals) at a time. Most of these blast blocks contained at least two to three flitches of three metres each.

From Table 10, various cut-offs were used to determine whether an ore block was under or over mined. This is somewhat a subjective matter and therefore both a 30 % and 20 % cut off in terms of mined versus estimated tonnages was used. From the 107 ore blocks mined, a total of 14 ore blocks were over mined and 17 ore blocks under mined (mined less from an ore block tan expected) in the 30 % cut off category. A total of 20 ore blocks were over mined and 26 ore blocks were under mined i.e. above 20 % difference. It can be seen that most ore blocks that were over or under mined were mined from specific blast blocks as well as flitch elevations. Larger blast blocks tend to have less precision in terms of mining efficiency of individual ore blocks.

From the 107 ore blocks available, 46 (43%) ore blocks in total were affected in terms of variations to their predicted grade category. This resulted in either a downgrade or upgrade of the estimated grade category. A total of 13 ore blocks were downgraded in their grade categories and 21 ore blocks were upgraded. Downgrading of ore block grade categories is not easy to assess. Reasons for downgrading and upgrading of ore blocks are often related to under and over mining, which is one of the main causes of ore dilution. From the 13 downgraded ore blocks, 9 ore blocks (64%) were either under or over mined. The other ore blocks are assumed to have been over estimated. A total of 23 ore blocks have been upgraded in their predetermined grade categories. From these 23 ore blocks, 10 ore blocks (48%) have been either affected by under or over mining. Upgrading of the remaining 13 ore blocks is possibly a result of under estimation by the conditional simulation process. From the above data it is clear that over or under mining has had a significant impact on downgrading ore into lower categories and therefore enhancing dilution. Although over and under mining has some influence on upgrading ore into higher-grade categories, this is less significant than losses. A total of 10 other ore blocks were identified where the grade category has remained unchanged, but the grades therein varied by more than 100 ppm between the estimated and mined grade. From the 10 ore blocks, 8 were thought to have been overestimated of which 7 ore blocks are estimated grades above 1 000 ppm (super high-grade). They have all resulted in mined grades that are significantly lower.

[8] Bench- A ledge or horizontal platform on which mining takes. The larger benches can be subdivide into smaller flitches depending on loading equipment used

Table 10: Mined and estimated grades and tonnages of data drilled from a 4 m x 4 m drill spacing

Pit	Blast block name	Oreblock	Design Tonnes (t)	Mined Tonnes (t)	Balance (t)	Difference (%)	30 % cut off	Difference (%)	20 % cut off	Design U308 (ppm)	Mined U308 (ppm)	Difference (%)	Comment
G	G-671-002	LG2	2 059.2	3 026.0	-966.8	-47.0	Overmined	-47.0	Overmined	370	487	-31.5	Upgraded due to overmining
		MG5	4 370.4	5 909.0	-1 538.6	-35.2	Overmined	-35.2	Overmined	504	383	24.1	Downgraded due to overmining
		MG6	2 109.6	2 576.0	-466.4	-22.1		-22.1	Overmined	480	434	9.6	
		MG8	14 968.8	15 498.0	-529.2	-3.5		-3.5		491	414	15.6	
		W6	3 348.0	3 797.0	-449.0	-13.4		-13.4		232	203	12.5	
		MG7	2 469.6	2 545.0	-75.4	-3.1		-3.1		433	448	-3.4	
		W7	2 282.4	1 581.0	701.4	30.7	Undermined	30.7	Undermined	240	220	8.5	
		HG4	27 763.2	28 695.0	-931.8	-3.4		-3.4		1127	976	13.4	Overestimated
		HG3	20 923.2	20 713.0	210.2	1.0		1.0		1043	830	20.4	Overestimated
		W5	7 005.6	6 583.0	422.6	6.0		6.0		244	264	-8.2	
		MG3	5 581.9	6 448.0	-866.1	-15.5		-15.5		481	485	-0.9	
		LG3	4 203.8	2 005.0	2 198.8	52.3	Undermined	52.3	Undermined	363	173	52.3	Downgraded due to undermining
		HG2	74 945.3	91 600.0	-16 690.7	-22.2		-22.3	Overmined	1108	822	25.8	Downgraded due to overmining
G	G-671-003	W1	1 368.0	1 369.0	-1.0	-0.1		-0.1		213	216	-1.4	
		LG4	11 476.8	5 976.0	5 500.8	47.9	Undermined	47.9	Undermined	342	385	-12.5	
		MG5	6 969.6	3 447.0	3 522.6	50.5	Undermined	50.5	Undermined	539	610	-13.2	
		HG1	14 529.6	9 654.0	4 875.6	33.6	Undermined	33.6	Undermined	746	574	23.0	Downgraded due to undermining
		MG6	12 679.2	5 816.0	6 863.2	54.1	Undermined	54.1	Undermined	499	445	10.9	
		HG5	13 852.8	43 112.0	-29 259.2	-211.2	Overmined	-211.2	Overmined	739	399	46.0	Downgraded due to overmining
		MG11	1 526.4	4 136.0	-2 609.6	-171.0	Overmined	-171.0	Overmined	438	361	17.5	Downgraded due to overmining
		LG11	2 880.0	2 314.0	566.0	19.7		19.7		347	315	9.3	
		LG10	921.6	1 031.0	-109.4	-11.9		-11.9		357	246	31.1	Downgraded due to overestimation
		MG10	31 708.8	28 187.0	3 521.8	11.1		11.1		492	283	42.5	Downgraded due to overestimation
		HG8	28 728.0	27 639.0	1 089.0	3.8		3.8		1032	772	25.2	Overestimated
		LG14	4 024.8	3 309.0	715.8	17.8		17.8		399	495	-24.0	Upgraded due to underestimation and undermining
		MG12	22 161.6	21 785.0	376.6	1.7		1.7		501	445	11.3	
		LG13	21 765.6	16 797.0	4 968.6	22.8		22.8		327	318	2.8	
		HG5	19 252.1	25 737.0	-6 484.9	-33.7	Overmined	-33.7	Overmined	897	833	7.2	
		MG8	1 568.2	1 002.0	566.2	36.1	Undermined	36.1	Undermined	469	469	-0.1	

Pit	Blast block name	Oreblock	Design Tonnes (t)	Mined Tonnes (t)	Balance (t)	Difference (%)	30 % cut off	Difference (%)	20 % cut off	Design U308 (ppm)	Mined U308 (ppm)	Difference (%)	Comment
		MG7	2 870.6	3 146.0	-275.4	-9.6		-9.6		483	621	-28.5	Underestimated
		LG8	2 190.2	2 846.0	-655.8	-29.9		-29.9	Overmined	313	388	-24.1	
		LG7	1 594.1	1 564.0	30.1	1.9		1.9		322	254	21.0	
		W6	37 512.7	31 458.0	6 054.7	16.1		16.1		85	89	-5.2	
G	G-671-004	MG1	16 488.0	8 540.0	7 948.0	48.2	Undermined	48.2	Undermined	580	520	10.4	
		LG1	7 329.6	1 463.0	5 866.6	80.0	Undermined	80.0	Undermined	351	351	-	
		LG2	5 644.8	4 174.0	1 470.8	26.1		26.1	Undermined	366	313	14.5	
		MG1	1 900.8	609.0	1 291.8	68.0	Undermined	68.0	Undermined	478	901	-88.6	Upgraded due to underestimation and undermined
		HG2	11 858.4	12 042.0	-183.6	-1.5		-1.5		680	632	7.1	
		MG4	5 176.8	5 588.0	-411.2	-7.9		-7.9		641	781	-21.8	Upgraded due to underestimation
		LG3	12 002.4	11 761.0	241.4	2.0		2.0		376	402	-6.8	
		MG2	5 356.8	5 375.0	-18.2	-0.3		-0.3		523	651	-24.5	Upgraded due to underestimation
		W1	9 475.2	8 729.0	746.2	7.9		7.9		249	359	-44.3	Upgraded due to underestimation
		HG1	14 522.4	14 372.0	150.4	1.0		1.0		733	537	26.7	Downgraded due to overestimation
		LG1	3 477.6	1 301.0	2 176.6	62.6	Undermined	62.6	Undermined	380	141	62.8	Downgraded due to undermining
		MG3	5 961.6	6 506.0	-544.4	-9.1		-9.1		445	282	36.7	Downgraded due to overestimation
		HG5	60 501.6	65 146.0	-4 644.4	-7.7		-7.7		1101	787	28.5	Overestimated
		MG9	5 306.4	4 448.0	858.4	16.2		16.2		553	537	2.9	
		LG3	9 568.8	10 313.0	-744.2	-7.8		-7.8		283	283	-0.1	
		HG3	14 541.1	16 748.0	-2 206.9	-15.2		-15.2		773	731	5.5	
		MG4	4 885.9	7 587.0	-2 701.1	-55.3	Overmined	-55.3	Overmined	510	849	-66.5	Upgraded due to overmining
		MG5	7 029.6	8 939.0	-1 909.4	-27.2		-27.2	Overmined	490	711	-45.1	Upgraded due to overmining
		LG4	10 537.4	15 273.0	-4 735.6	-44.9	Overmined	-44.9	Overmined	361	704	-94.9	Upgraded due to overmining
		LG5	2 672.6	4 091.0	-1 418.4	-53.1	Overmined	-53.1	Overmined	363	603	-66.0	Upgraded due to overmining
		W1	29 905.2	40 384.0	-10 478.8	-35.0	Overmined	-35.0	Overmined	110	338	-207.2	Upgraded due to overmining
G	G-671-012	MG15	23 444.4	17 680.0	5 764.4	24.6		24.6	Undermined	499	518	-3.8	
		LG13	4 542.2	2 298.0	2 244.2	49.4	Undermined	49.4	Undermined	360	353	1.8	
		MG15	24 709.4	19 262.0	5 447.4	22.0		22.0	Undermined	527	530	-0.6	
		LG19	7 974.8	9 226.0	-1 251.2	-15.7		-15.7		333	334	-0.3	

Pit	Blast block name	Oreblock	Design Tonnes (t)	Mined Tonnes (t)	Balance (t)	Difference (%)	30 % cut off	Difference (%)	20 % cut off	Design U308 (ppm)	Mined U308 (ppm)	Difference (%)	Comment
		MG10	3 448.1	1 127.0	2 321.1	67.3	Undermined	67.3	Undermined	490	385	21.4	Downgraded due to undermining
		LG9	15 766.2	23 086.0	-7 319.8	-46.4	Overmined	-46.4	Overmined	322	342	-6.2	
		W10	20 278.4	21 924.0	-1 645.6	-8.1		-8.1		103	103	-0.7	
G	G-680-024	W35	2 755.2	667.0	2 088.2	75.8	Undermined	75.8	Undermined	220	317	-43.9	Upgraded due to undermining
		MG36	4 399.2	3 068.0	1 331.2	30.3	Undermined	30.3	Undermined	588	503	14.5	
		LG41	18 453.6	14 363.0	4 090.6	22.2		22.2	Undermined	399	387	2.9	
		HG19	41 392.8	40 234.0	1 158.8	2.8		2.8		1081	1029	4.8	
		MG33	31 327.2	34 954.0	-3 626.8	-11.6		-11.6		565	528	6.6	
		LG35	32 925.6	28 929.0	3 996.6	12.1		12.1		347	342	1.5	
		MG31	19 474.6	14 335.0	5 139.6	26.4		26.4	Undermined	512	392	23.5	Downgraded due to undermining
		LG42	37 732.8	54 256.0	-16 523.2	-43.8	Overmined	-43.8	Overmined	361	356	1.4	
H	H-554-001	LG2	8 172.0	7 220.0	952.0	11.6		11.6		373	573	-53.7	Upgraded due to underestimation
		HG2	10 008.0	15 950.0	-5 942.0	-59.4	Overmined	-59.4	Overmined	789	910	-15.3	Overmined
		MG2	13 024.8	9 419.0	3 605.8	27.7		27.7	Undermined	486	505	-3.9	
		W4	2 628.0	2 373.0	255.0	9.7		9.7		197	605	-207.0	Upgraded due to underestimation
		W5	7 171.2	4 116.0	3 055.2	42.6	Undermined	42.6	Undermined	106	253	-138.8	Upgraded due to undermining
		MG2	29 836.8	33 124.0	-3 287.2	-11.0		-11.0		568	568	-0.0	
		LG1	3 501.1	757.0	2 744.1	78.4	Undermined	78.4	Undermined	399	426	-6.9	
		W4	4 912.3	13 894.0	-8 981.7	-182.8	Overmined	-182.8	Overmined	172	172	-	
H	H-554-002	HG1	10 310.4	7 239.0	3 071.4	29.8		29.8	Undermined	783	788	-0.7	
		MG1	9 648.0	10 591.0	-943.0	-9.8		-9.8		491	672	-36.8	Upgraded due to underestimation
		W1	12 988.8	11 663.0	1 325.8	10.2		10.2		158	304	-92.7	Upgraded due to underestimation
		HG1	21 448.8	26 256.0	-4 807.2	-22.4		-22.4	Overmined	2227	2225	0.1	
		W1	11 491.2	9 393.0	2 098.2	18.3		18.3		249	279	-12.0	
		W1	2 808.0	2 406.0	402.0	14.3		14.3		120	386	-221.6	Upgraded due to underestimation
		LG1	4 521.6	4 427.0	94.6	2.1		2.1		350	437	-24.9	Upgraded due to underestimation
		HG5	20 577.6	20 062.0	515.6	2.5		2.5		807	703	12.8	
		MG2	13 442.4	13 502.0	-59.6	-0.4		-0.4		551	499	9.5	
		MG4	2 671.2	2 803.0	-131.8	-4.9		-4.9		456	791	-73.5	Upgraded due to underestimation
		MG3	25 099.2	26 443.0	-1 343.8	-5.4		-5.4		643	527	18.1	

Pit	Blast block name	Oreblock	Design Tonnes (t)	Mined Tonnes (t)	Balance (t)	Difference (%)	30 % cut off	Difference (%)	20 % cut off	Design U308 (ppm)	Mined U308 (ppm)	Difference (%)	Comment
		HG4	9 576.0	10 117.0	-541.0	-5.6		-5.6		789	771	2.3	
		HG3	3 996.0	4 410.0	-414.0	-10.4		-10.4		813	765	5.9	
		HG3	38 593.0	39 020.0	-427.0	-1.1		-1.1		835	902	-8.1	
H	H-563-003	HG1	39 477.6	38 865.0	612.6	1.6		1.6		1346	1126	16.3	Overestimated
		HG1	21 859.2	22 499.0	-639.8	-2.9		-2.9		1072	683	36.3	Overestimated
		MG1	9 518.4	9 698.0	-179.6	-1.9		-1.9		748	731	2.3	
		LG1	8 100.0	8 054.0	46.0	0.6		0.6		399	302	24.2	
		HG1	28 473.4	32 267.0	-3 793.6	-13.3		-13.3		1206	1000	17.0	Overestimated
		W1	9 688.3	10 121.0	-432.7	-4.5		-4.5		236	254	-7.7	
H	H-572-005	MG1	15 256.8	16 267.0	-1 010.2	-6.6		-6.6		612	648	-5.8	
		LG1	9 972.0	10 072.0	-100.0	-1.0		-1.0		399	447	-12.1	
		HG3	21 412.8	27 831.0	-6 418.2	-30.0		-30.0	Overmined	786	776	1.2	
		W3	4 161.6	5 872.0	-1 710.4	-41.1	Overmined	-41.1	Overmined	87	195	-123.7	
		LG1	6 285.6	6 616.0	-330.4	-5.3		-5.3		342	569	-66.3	Upgraded due to underestimation
		MG3	29 908.8	28 190.0	1 718.8	5.7		5.7		708	911	-28.7	Underestimated
		W4	14 443.2	10 973.0	3 470.2	24.0		24.0	Undermined	183	297	-62.0	
		W3	3 636.0	2 923.0	713.0	19.6		19.6		92	311	-237.8	
		LG3	30 394.3	29 907.0	487.3	1.6		1.6		307	480	-56.5	Upgraded Underestimated
		W3	22 063.2	21 689.0	374.2	1.7		1.7		120	379	-215.4	Upgraded Underestimated

Grade category comparison

Table 11: Ore block classification status summary with regards to mined tonnages of 4 m x 4 m mined data

(Estimated vs. mined tonnages)	Ore block status	Number of ore blocks W	Number of ore blocks LG	Number of ore blocks MG	Number of ore blocks HG	Number of ore blocks Total
30 % cut off	**Overmined**	3	5	3	3	14
	Undermined	3	5	7	2	17
Total		6	10	10	5	31
20 % cut off	**Overmined**	3	6	5	6	20
	Undermined	4	8	11	2	25
Total		7	15	16	8	45

From the grade category comparison in Table 11 it can be seen that 31 ore blocks from the 107 were either over or under mined with regards to the 30 % tonnage cut off. It can be observed that more ore blocks were under mined compared to ore blocks that were over mined. Medium-grade blocks contained the highest number of under mined ore blocks followed by low-grade blocks. As predicted the 20 % cut off resulted in an increase in over and underestimated ore blocks. A total of 45 out of 107 ore blocks were allocated to fall out of the 20 % cut off. As previously mentioned, more ore blocks were under mined compared to over mined ore blocks. Again, medium-grade contained the highest number of ore blocks, followed by low-grade blocks.

To draw a conclusive summary, 1 485 457 t were designed or estimated to be mined from the given ore blocks. A total of 1 527 164 t have been mined which is 2,8 % higher than expected and is most likely due to minor over mining along the blast block boundaries. Larger ore blocks tend to be over mined, most which most likely due to their increased volumes. Most of the ore blocks were not over mined by more than 6 000 t or 67 truckloads which is acceptable. In one situation a flitch containing mostly high-grade was over mined by 16 500 t and subsequently the predicted grade dropped from 1 100 ppm down to 820 ppm. The average grade estimated from the 10 selected blast blocks was 511 ppm and an average of 520 ppm was mined, which is a difference of only 1,8 %.

4.2 Selected blast blocks estimated and mined using 12,5 m x 12,5 m drill data

A total of 10 blast blocks were selected from both pit H1 and F1 using 12,5 m x 12,5 m drill data for estimations. Pit F1 drill data was used because pit G1, which is of interest in this study, has been mined and estimated using only 4 m x 4 m drill data. The 12,5 m x 12,5 m drill data used for estimation was only introduced into the operation from early 2016 due to the low uranium spot price. This was suggested in efforts to reduce money spending on mining operations. The five blast blocks selected from pit F1 were mined at elevations of 653 m and 626 m. The five blast blocks selected from pit H1 were mined at 572 m and 563 m elevations respectively. A total of 69 ore blocks were mined from the 10 blast blocks.

Tonnage and grade comparison

From the 69 ore blocks available in Table 13, 31 (45%) ore blocks in total were affected in terms of variations to their predicted grade category. From the 31 ore blocks, 14 ore blocks were downgraded in comparison to their predicted grade. Five from the 13 ore blocks were downgraded or indicated a decrease in mined grade due to under mining. The remaining eight ore blocks were downgraded in their suggested grade categories due to over mining. Nine out of the total 31 ore blocks affected, indicated an upgrade in their estimated grade category. From the nine upgraded ore blocks, there are indications of both under and over mining. A further seven ore blocks have been unaffected in terms of their suggested grade categories, however grade variations of more than 100 ppm are observed. Among those ore blocks observed, varied grade differences are predominantly due to under and over mining, as well as under and overestimation in some cases.

Grade category comparison

Table 12: Ore block classification status summary with regards to mined tonnages of 12,5 m x 12,5 m mined data

(Estimated vs. mined tonnages)	Ore block status	Number of ore blocks W	Number of ore blocks LG	Number of ore blocks MG	Number of ore blocks HG	Number of ore blocks Total
30% cut off	Overmined	7	5	7	3	22
	Undermined	8	1	3	3	15
Total		15	6	10	6	37
20% cut off	Overmined	7	6	8	3	24
	Undermined	10	4	3	3	20
Total		17	10	11	6	44

Table 13: Mined and estimated grades and tonnages of data drilled from a 12,5 m x 12,5 m drill spacing

Pit	Blast block name	Ore block	Mined Tonnes (t)	Balance (t)	Difference (%)	30% cut off	Difference (%)	20% cut off	Design U308 (ppm)	Mined U308 (ppm)	Difference (%)	Comments: Grade variation between design vs. mined
F	F-626-009	W14	3 150.0	3 035	49.1	Undermined	49.1	Undermined	200	441	-120.7	Upgraded due to undermining and underestimation
		HG25	7 800.0	1 848	19.2		19.2		788	503	36.1	Downgraded due to undermining
		LG18	5 338.0	710	11.7		11.7		318	393	-23.6	
		MG33	11 702.0	-2 313	-24.6		-24.6	Overmined	560	517	7.7	
		HG13	28 641.0	2 542	8.2		8.2		949	862	9.2	
F	F-626-010	HG26	2 720.0	671	19.8		19.8		1099	1089	0.9	
		HG27	2 250.0	1 724	43.4	Undermined	43.4	Undermined	991	1419	-43.2	Undermined
		MG34	6 783.0	4 276	38.7	Undermined	38.7	Undermined	583	693	-18.9	Upgraded due to undermining
		LG19	4 944.0	-1 574	-46.7	Overmined	-46.7	Overmined	375	710	-89.4	Upgraded due to overmining
		HG14	24 750.0	4 206	14.5		14.5		1603	925	42.3	Overestimated and undermined
		MG17	7 568.0	-200	-2.7		-2.7		541	536	1.0	
F	F-626-011	HG28	9 677.0	-749	-8.4		-8.4		1100	1239	-12.6	Underestimated
		MG35	14 661.0	-5 099	-53.3	Overmined	-53.3	Overmined	620	823	-32.8	Upgraded due to overmining
		HG15	16 295.0	2 195	11.9		11.9		1759	1503	14.5	Overestimated
		HG4	3 569.0	3 913	52.3	Undermined	52.3	Undermined	720	668	7.2	
		MG16	8 658.0	1 712	16.5		16.5		550	658	-19.7	Upgraded due to undermining
F	F-626-012	HG29	50 951.0	-36 393	-250.0	Overmined	-250.0	Overmined	901	852	5.4	
		MG36	10 449.0	-427	-4.3		-4.3		500	550	-10.1	
		W15	20 107.0	-5 210	-35.0	Overmined	-35.0	Overmined	98	206	-110.7	
		MG18	25 671.0	-9 723	-61.0	Overmined	-61.0	Overmined	626	507	18.9	Overmined
		LG26	8 413.0	1 379	14.1		14.1		364	251	31.0	Undermined
		W29	10 710.0	3 035	22.1		22.1	Undermined	111	131	-18.4	
F	F-653-001	HG1	28 062.0	-16 038	-133.4	Overmined	-133.4	Overmined	887	422	52.4	Downgraded due to overmining
		MG6	7 909.0	882	10.0		10.0		485	302	37.6	Downgraded due to undermining
		W12	3 455.0	4 940	58.8	Undermined	58.8	Undermined	153	279	-82.4	Upgraded due to undermining
		W11	8 554.0	-526	-6.6		-6.6		167	237	-42.2	
		LG9	29 892.0	-11 237	-60.2	Overmined	-60.2	Overmined	334	317	5.0	
		W13	2 430.0	6 700	73.4	Undermined	73.4	Undermined	218	247	-13.4	
		W12	9 072.0	389	4.1		4.1		149	173	-16.3	
		W6	40 551.0	16 559	29.0		29.0	Undermined	119	166	-39.3	
H	H-563-031	MG24	18 626.0	-2 592	-16.2		-16.2		488	477	2.4	
		LG25	2 790.0	947	25.3		25.3	Undermined	321	336	-4.6	
		W49	3 880.0	1 916	33.1	Undermined	33.1	Undermined	148	265	-78.9	Upgraded due to undermining
		W48	2 250.0	1 048	31.8	Undermined	31.8	Undermined	58	227	-290.6	
H	H-563-032	LG14	16 474.0	8 992	35.3	Undermined	35.3	Undermined	280	279	0.4	
		MG25	16 878.0	-1 967	-13.2		-13.2		509	409	19.6	Overmined
		MG24	9 294.0	-5 564	-149.2	Overmined	-149.2	Overmined	417	384	7.9	Downgraded due to overmining
		LG17	12 404.0	-5 578	-81.7	Overmined	-81.7	Overmined	394	340	13.6	

Pit	Blast block name	Ore block	Mined Tonnes (t)	Balance (t)	Difference (%)	30% cut off	Difference (%)	20% cut off	Design U308 (ppm)	Mined U308 (ppm)	Difference (%)	Comments: Grade variation between design vs. mined
		HG14	20 483.0	-7 833	-61.9	Overmined	-61.9	Overmined	734	591	19.5	Downgraded due to overmining
		MG22	17 681.0	-11 467	-184.6	Overmined	-184.6	Overmined	473	326	31.1	Downgraded due to overmining
		LG24	8 522.0	-1 920	-29.1		-29.1	Overmined	391	407	-4.2	Upgraded due to overmining
H	H-563-035	LG20	2 520.0	914	26.6		26.6	Undermined	319	298	6.6	
		MG15	9 090.0	6 426	41.4	Undermined	41.4	Undermined	414	376	9.3	Downgraded due to undermining
		LG19	17 412.0	358	2.0		2.0		312	297	4.7	
		W30	2 430.0	4 201	63.4	Undermined	63.4	Undermined	60	60	0.0	
		MG26	32 802.0	3 011	8.4		8.4		556	497	10.6	
		W44	1 890.0	-479	-33.9	Overmined	-33.9	Overmined	200	258	-28.9	Upgraded due to overmining
		W42	9 141.0	-4 958	-118.5	Overmined	-118.5	Overmined	96	206	-114.1	
		W43	2 970.0	-947	-46.8	Overmined	-46.8	Overmined	240	231	3.7	
		MG23	19 226.0	15 183	44.1	Undermined	44.1	Undermined	403	449	-11.4	
H	H-572-042	MG34	3 240.0	194	5.7		5.7		529	528	0.2	
		LG27	2 160.0	-310	-16.7		-16.7		297	232	21.8	Downgraded due to overmining
		LG26	13 691.0	-4 561	-50.0	Overmined	-50.0	Overmined	357	342	4.1	
		W51	13 216.0	-90	-0.7		-0.7		123	122	0.6	
		LG25	4 264.0	-2 414	-130.4	Overmined	-130.4	Overmined	280	212	24.2	Downgraded due to overmining
		W69	17 537.0	8 145	31.7	Undermined	31.7	Undermined	144	164	-13.7	
		MG29	13 157.0	854	6.1		6.1		501	387	22.7	Downgraded due to undermining
		W63	1 324.0	2 722	67.3	Undermined	67.3	Undermined	112	194	-73.0	
		W62	13 521.0	-4 039	-42.6	Overmined	-42.6	Overmined	124	199	-60.2	
H	H-572-044	W53	14 130.0	-9 522	-206.6	Overmined	-206.6	Overmined	195	200	-2.7	
		HG20	20 901.0	-1 288	-6.6		-6.6		852	585	31.4	Downgraded and overestimated
		LG28	5 680.0	-1 475	-35.1	Overmined	-35.1	Overmined	400	534	-33.4	Overmined
		W52	8 925.0	-1 185	-15.3		-15.3		136	162	-18.8	
		MG30	5 946.0	-1 568	-35.8	Overmined	-35.8	Overmined	432	318	26.5	Downgraded due to overmining
		LG26	4 353.0	1 177	21.3		21.3	Undermined	396	341	13.8	
		W70	27 086.0	-9 585	-54.8	Overmined	-54.8	Overmined	172	229	-32.9	
		HG16	2 519.0	21 587	89.6	Undermined	89.6	Undermined	968	349	64.0	Downgraded due to undermining
		LG36	4 866.0	-1 136	-30.5	Overmined	-30.5	Overmined	400	251	37.2	Downgraded due to overmining
		W64	19 845.0	-2 176	-12.3		-12.3		95	110	-16.3	

The same cut off procedures were used here in both tonnages and grade variance compared to the 4 m x 4 m drill data. From Table 12 and Table 13 it can be seen that from the 69 total ore blocks, 22 (30%) ore blocks have been over mined by more than 30 %. From the 69 ore blocks a total of 24 (35%) ore blocks were over mined by more than 20 %. In addition, 15 (22%) ore blocks were under mined from the 30 % cut off category and 20 (29%) ore blocks in the 20 % cut off category. In the 30 % cut off category, waste was mined with the highest number of ore blocks that were classified as under or over mined. Waste was followed by medium-grade and low-grade ore, with high-grade ore displaying the lowest number of under and over mined ore blocks. The same trend is visible in the 20 % cut off category; however, the high-grade performed better than the low-grade and therefore indicates more accuracy is associated when mining it.

In total, from the 10 selected ore containing blast blocks, a predicted 804 104t of ore should have been mined, whilst in reality a total of 837 856 t were mined. This gives a discrepancy of about 4 % only or approximately 375 truckloads. Therefore, each blast block was over mined by about 37 truckloads. In general, the selected 10 blast blocks drilled on a 12,5 m x 12,5 m drill spacing contained 38 less ore blocks in comparison to the selected 4 m x 4 m blast blocks. One blast block was over mined by about 46 000 t and two others by about 24 000 t. This is most likely due to the fact that the blast blocks are situated near the bottom of the mineralised ore body in the palaeo channel and therefore extended strip mining is common to remove the last ore pockets. High-grade ore blocks near the bottom of the palaeo channel are often mined by rip and doze methods of less competent clays. From the 69 ore blocks an estimated grade of 452 ppm has been calculated and an average grade of 432 ppm has been mined. This gives a difference between estimated and mined grade of -4,4 %. This is somewhat lower than the data of the 4 m x 4 m drill data and could be a result of ore dilution during mining or perhaps a consequence of data limitations during the estimation process.

CHAPTER 5. RESULTS AND DATA ANALYSIS OF PIT G1

The results presented in chapters 5 and 6 are the results of the main topic of this thesis in which the different drill spacing and estimation techniques are compared to pit G1 and H1 that have been mined out. The two mined out pits from which the data has been extracted are explained in Chapter 3.

The block models that follow below were created from grade control and exploration drilling. These spacings include a drilling grid of 50 m x 50 m, 25 m x 25 m, 12,5 m x 12,5 m and of 4 m x 4 m. The size of the drill spacing represents the size of the blocks in the block model as well as a Z dimension of 3 m. It is evident from the northern sections along the pit that there is still in situ ore in the ground, but not of significant grades to benefit production during current market conditions. Pit G1 is an example of the so called smaller "rat hole mining[9]" operation that target lenses of higher-grades in the eastern parts of the mining license. These operations have become the only way to sustain the mine at the current low uranium prices. Numerous other small pits have since been mined to expose shallow high-grade ore that can be mined easily and efficiently with limited dilution. These smaller pits like pit G1 are usually not deeper than 40 m and are left open or backfilled to free new digging areas in the future. It should be mentioned that these smaller pits are often connected with areas of lower grades and are left in situ to be mined during times when the uranium price is higher.

Two different pit elevations were selected to illustrate the ore distribution in pit G1. The first selected elevation is situated at 678,5 m, which should give an indication of the ore distribution towards to the eastern side of the pit (higher elevation). Here the ore is situated closer to the surface. The next elevation will be illustrated at 669,5 m, which should illustrate ore distribution in the deeper part of the pit towards the west. The black line surrounding the pit resembles the pit boundary. Throughout the block model descriptions, visual aspects of the block models themselves were analysed and observed. The most visual diagnostic aspect that can be observed is the distribution of grades. The high-grade and super high-grade lenses in particular are the most obvious to observe and are sought after. These high-grade lenses, indicated in red and yellow, are often used as markers throughout the descriptions. General observations to note are the ore to waste ratio, the shape of distribution and ore grade changes. The overall shape, number and appearance of medium, low-grade and waste can also be observed.

[9] Rat hole mining: A mining operation that targets smaller near surface high grade ore lenses.

5.1 Conditional Simulation block models at 4 m x 4 m x 3 m and resulting Coefficient of Variation (CV) model

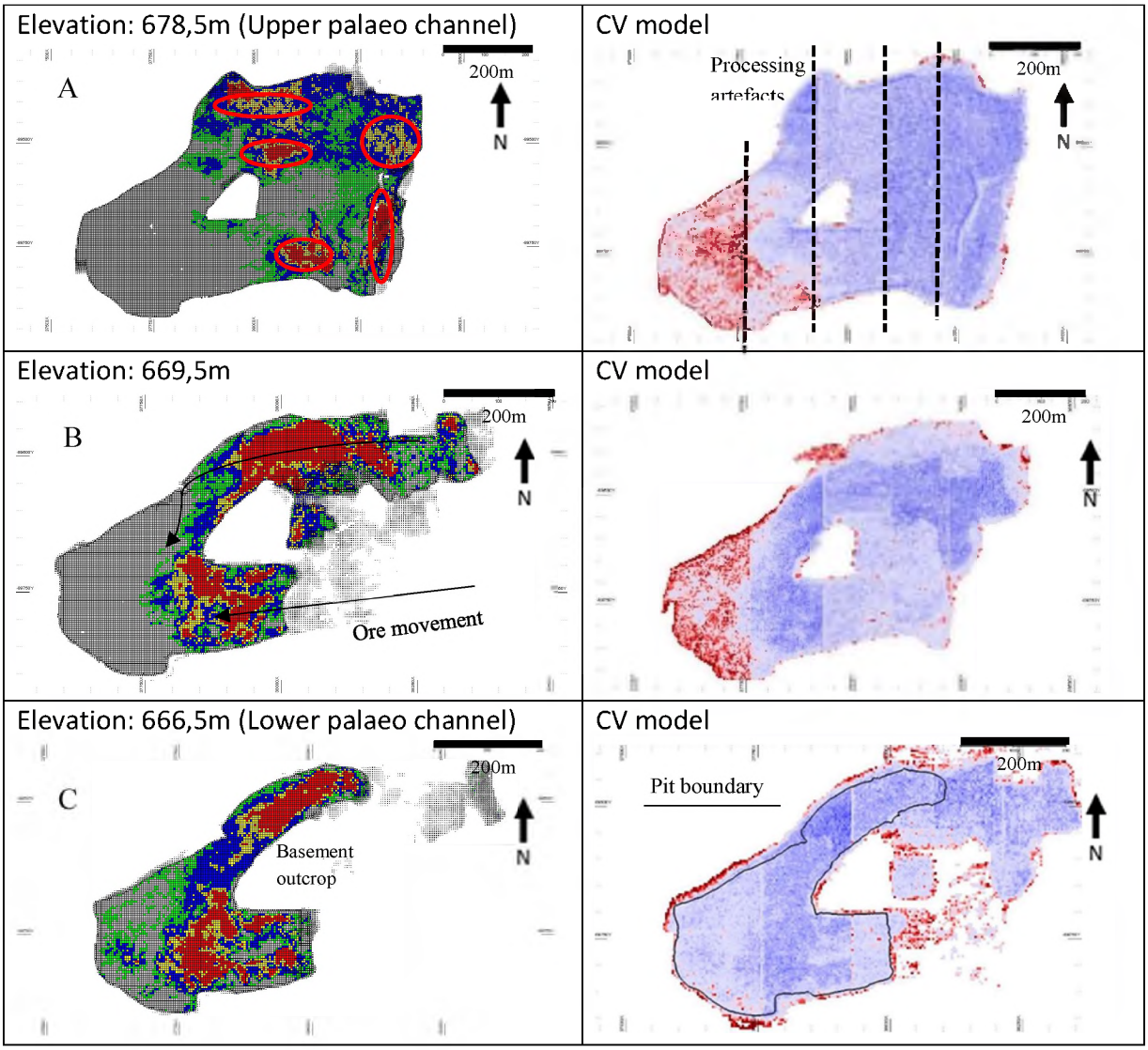

Figure 11: CS and resultant CV model of three selected elevations to illustrate ore distribution in pit G1

Table 14: Grades and associated colour representation on block models and colours of various coefficient of variation of the CV models (right)

Grade (ppm)	Colour	
Waste 0-250		
Low-grade 250-400		
Medium-grade 400-650		
High-grade 650-900		
Super high-grade 900+		

Value		Label
		< -0.11
-0.11		-0.11 to 0.14
0.14		0.14 to 0.22
0.22		0.22 to 0.30
0.30		0.30 to 0.45
0.45		0.45 to 0.62
0.62		0.62 to 0.70
0.70		0.70 to 0.86
0.86		0.86 to 0.93
0.93		0.93 to 1.02
1.02		1.02 to 1.22
1.22		1.22 to 1.34
1.34		>= 1.34

The block models in Figure 11 represent the conditional simulation model and their related CV models at three chosen elevations. Three elevations were chosen from the CS model as it was only used on the 4 m x 4 m drill data and provides a good representation of ore distribution. During mining the CS model at a 4 m x 4 m grid should reflect the most accurate estimation when compared to reality. This is, therefore, why the CS models displayed above are displayed separately from the rest of the other modeling methods followed below. From these models it is visible how fine the detail of the 4 m x 4 m x 3 m blocks are and how the mineralisation presents itself. With emphasis on the super high-grade lenses displayed in a red colour as indicated in Table 14, one can visualize how the ore migrates downstream or westwards. In the centre of pit G1 is a basement high or basement outcrop. This is made up of steeply dipping highly weathered calc-silicate schist of the Tinkas formation. This basement high contains no mineralisation and was therefore not mined. It is indicated in all block models as a white polygon. From the block models it is visible how the ore almost flows around the island, indicating the effect of groundwater movement on ore deposition. The ore distribution can be subdivided predominantly into a northern and southern subsection where the main super high-grade ore lenses occur.

At the 678,5 m (A) elevation it can be seen that in the northern part of the pit there are three smaller high-grade lenses. These mostly consist of a super high-grade nucleus and are surrounded by normal high-grade indicated in yellow. In the southern section of the pit another two high-grade lenses can be observed. These are somewhat larger than the northern counterparts and more concentrated. It should be mentioned throughout the block models that ore gradually fades from high-grade to waste and vice versa.

At the 669,5 m (B) elevation, roughly 9 m downwards, changes in the ore pattern can be noticed. The northern ore body has now fused into one large unit of super high-grade. It is surrounded by high-grade along the edges, however at lower numbers than the super high-grade. Towards the north eastern part of the pit, the ore blocks look much more erratic without any real distribution pattern. The two high-grade lenses in the southern section of the pit have disappeared and have migrated downstream or westwards. They fused together to form a larger irregularly shaped lens of super high-grade. This lens too is surrounded by a rim of high-grade.

At the elevation 666,5 m (C), ore presents itself in a downstream movement. The northern high-grade lens retained its size and shape but seems more homogenous. It can also be observed how the ore almost pivots in a flow motion around the unmineralised basement island at the centre of

the pit. The southern high-grade lens has migrated downstream as well and has retained its irregular shape. It seems to have created a split at its centre with lower grades.

The coefficient of variation (CV) models were interpolated from the CS models. These models were constructed to serve as a measure of data certainty and resulting distribution. From this model the 5 sections used to separate the large dataset are clearly visible by vague north-south trending white lines. These are known as processing artefacts and are the result of datasets that overlap. Areas indicated in lighter shades of blue, indicate areas with relative low data certainty whilst darker areas indicate areas of high certainty. These are usually areas of higher importance at that elevation and indicate areas of obtainable ore. The areas indicated in red, as seen at elevations 678,5m and 669,5m, towards the western end of pit G1 are the results of waste in that area at that elevation. The waste is never radiometrically logged and therefore show up in the bright red colour. The perimeter of the pit and indicate areas of low importance and data certainty and are therefore also classified as areas of high data variability.

5.2 Block models of other estimation methods at elevation 678,5 m

5.2.1 4 m x 4 m x 3 m block models

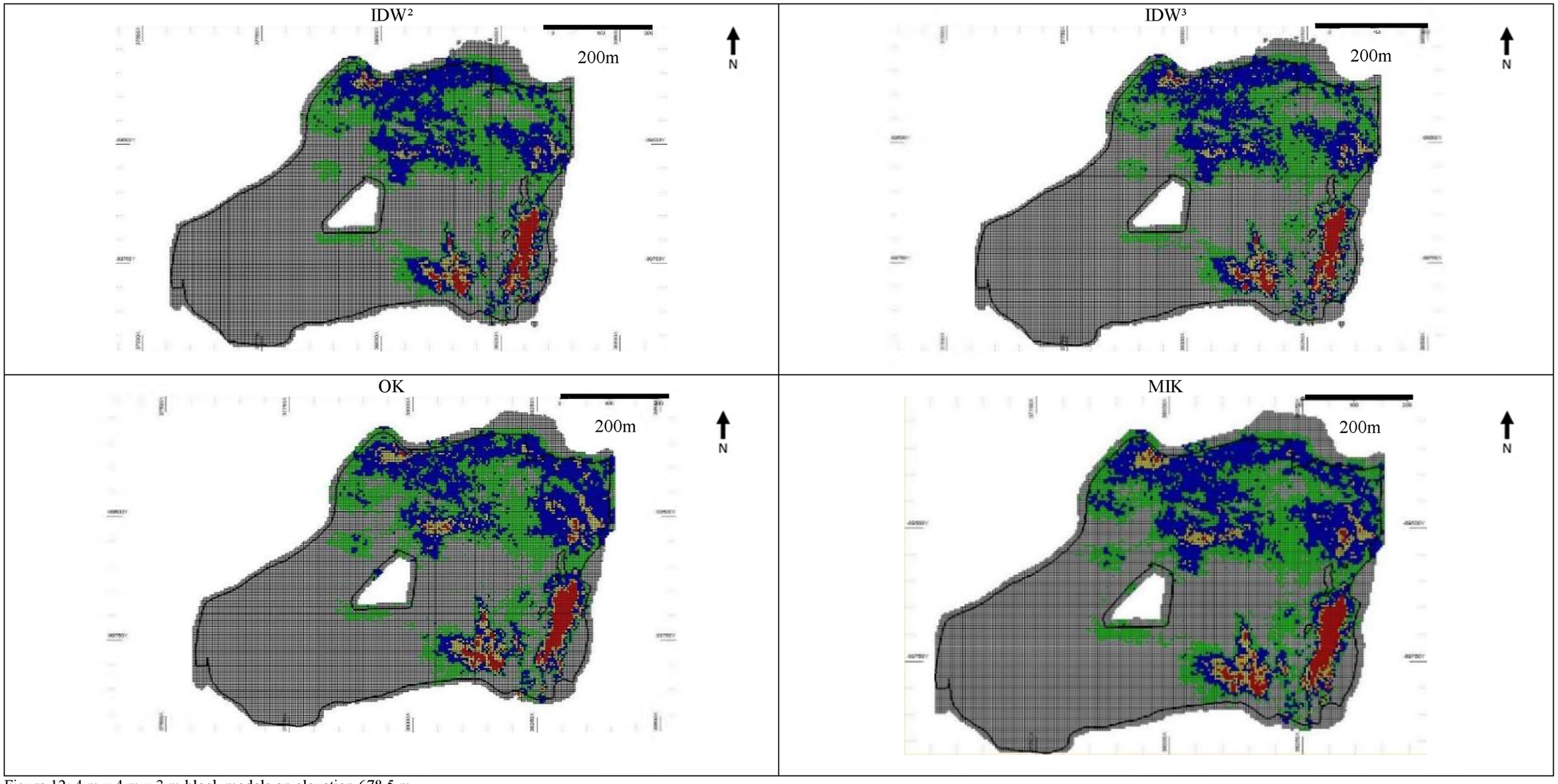

Figure 12: 4 m x 4 m x 3 m block models on elevation 678,5 m

Grade (ppm)	Colour
Waste 0-250	
Low-grade 250-400	
Medium-grade 400-650	
High-grade 650-900	
Super high-grade 900+	

General observations

The most important markers observed in Figure 12 at this elevation are three small high-grade lenses in the northern parts of the pit, surrounded mostly by medium and low-grade lenses. In the southern section of the pit two distinct super high-grade lenses can be seen surrounded by minor high, medium and low-grade ore. Towards the west, no significant ore occurrences can be observed.

Block model observations

With regards to individual block models and their estimation methods at this elevation, the inverse distance weighted technique with different power factors did not show significant visible differences. The northern and north-eastern section of the block models consist mostly of medium-grade, which is surrounded by low-grade ore. The higher-grades in the northern and central parts of the pit all occur in nucleated pockets, which is typical of this deposit. Not much super high-grades (>900 ppm) illustrated as red blocks in Figure 12 could be picked up in these sections using the IDW estimation technique. It is only in the southern section of the pit that larger high-grade pockets were identified in an elongated structure and another smaller pocket towards the west. From the two IDW block models, the observation of gradual grade progression is visible. The high-grade pockets are surrounded by lower grades that fade gradually into waste.

The OK model presented a slightly different picture than the IDW. In the northern sections of the pit there is an increase in size of the high-grade lens. This is also observed in the MIK model. A number of smaller pockets of high-grades have been established in the OK and MIK models. In the southern sections of pit G1 the higher-grade pockets have increased in both size and grade. This is visible by the increased number of red blocks in that section. From the four models only subtle differences of ore pocket size and grade distribution can be noticed. No major character changes are observed between the four methods.

5.2.2 12,5 m x 12,5 m x 3 m block models

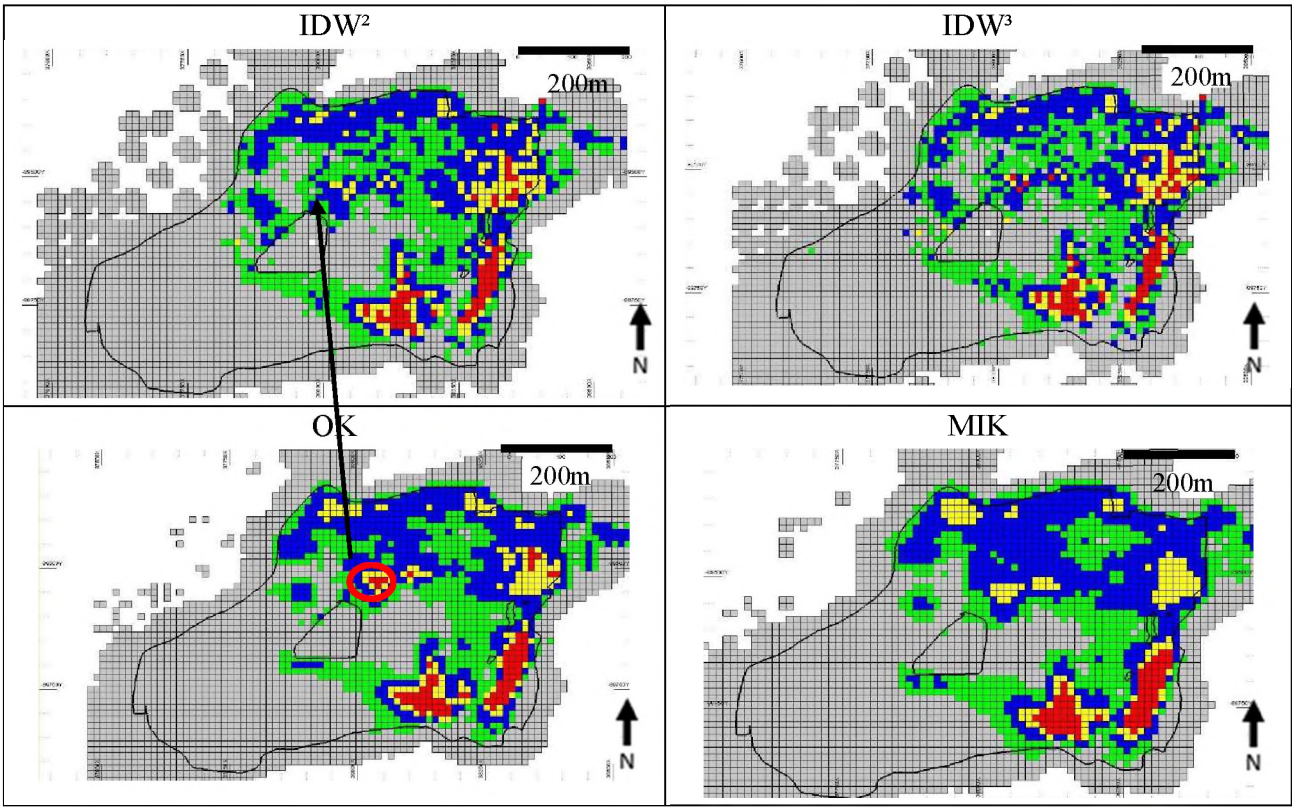

Figure 13: 12,5 m x 12,5 m x 3 m block models on elevation 678,5 m

The block models created on a 12,5 m x 12,5 m x 3 m dimension in Figure 13 represent the result of less data availability. Not too much in the general structure and grade distribution has changed, which is favourable but subtle differences have been noted. This is the result of volume variance as a function of less data availability. From the block models presented, the level of accuracy has decreased due to the bigger block sizes. Compared to each other, the IDW block models do not differ much. The northern section of the block models are still fairly similar to the 4 m x 4 m x 3 m block models, however they have become noisier. This can be expected from a larger drill spacing grid and less data availability. Waste sections in the northeast section have also decreased. Ore in the southeast section remains similar in appearance. Increased blocks of low-grade are visible as is the case in the northeast section of the pit.

The OK block model, as the IDW block models, does not have significant differences in the northern as well as the southern section of the pit. Medium-grades have increased slightly in numbers throughout. The only reasonable difference would be the increase in low-grades

throughout the eastern section of the pit. The MIK and OK block model shows a significant increase in medium-grades as well as high-grade blocks especially in the north and northeast section of the pit. Lower grades as with all 12,5 m x 12,5 m x 3 m block models have increased in number throughout the pit. It is curious to note the number of super high-grades have been removed in the north-eastern section of the pit. The ore blocks in this block model are profoundly different especially compared to the IDW block models. The grade distribution seems more gradual and much less noisy, with the OK model being a transition block model between the two.

5.2.3 25 m x 25 m x 3 m block models

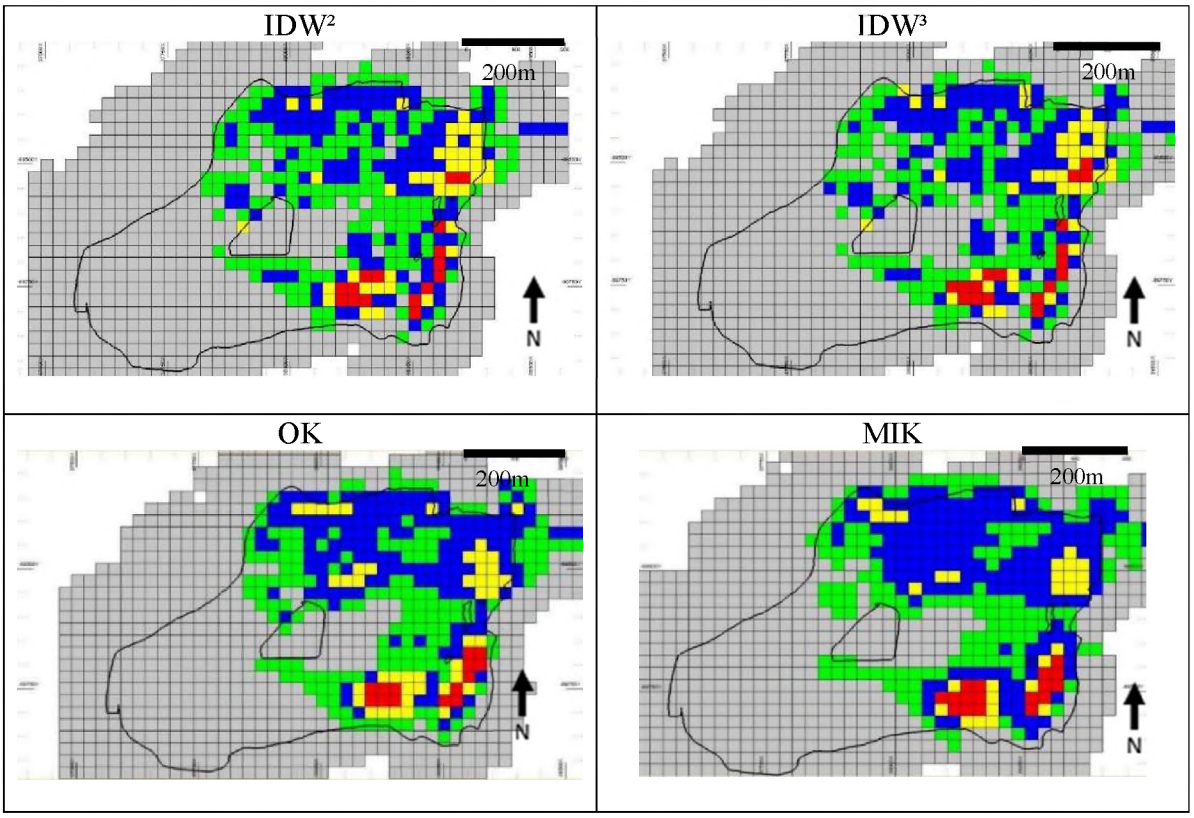

Figure 14: 25 m x 25 m x 3 m block models on elevation 678,5 m

The 25 m x 25 m x 3 m block models in Figure 14 show major differences to their smaller sized block models. Their total fluency in grade distribution has decreased and grade changes are more abrupt. The IDW block models have become more irregular and erratic with their grade distributions. In the north-eastern section of the pit, the high-grade lenses have almost totally disappeared with only one larger high-grade lens still visible all the way in the east. With regards to low and medium-grades the distribution has not changed that much in their general distribution and position. Clearly visible are the super high-grade blocks in the north-eastern section of the pit. These have already fallen out in the previous drill spacing using the MIK method. The two high-

grade lenses that have so far been easily visible in the south-eastern sections of the pit have now been diluted with some medium-grade blocks.

As in the previous drill spacing, the OK block model represents an intermediate between the IDW and MIK models. It is less erratic than the IDW block models but less fluent or smoothed than the MIK block model. No super high-grade is present in the north-eastern section of the pit, however high-grades are more visible compared to the IDW block models. The high-grade lenses observed in the northeast of the 4 m x 4 m x 3 m block models are visible in the OK block model, although less prominent. The high-grade lenses in the southeast section of the pit are clearly distinctive unlike in the IDW block models. As in the previous MIK model, the fluency of ore is visible especially in the north-eastern section of the pit. This is present especially with regards to the medium-grades. There is no super high-grade in the northeast section of the pit which is also observed in the OK model. The two high-grade lenses in the southern part of the pit are still clearly visible as in the MIK block model. These have been replaced in the IDW block models.

5.2.4 50 m x 50 m x 3 m block models

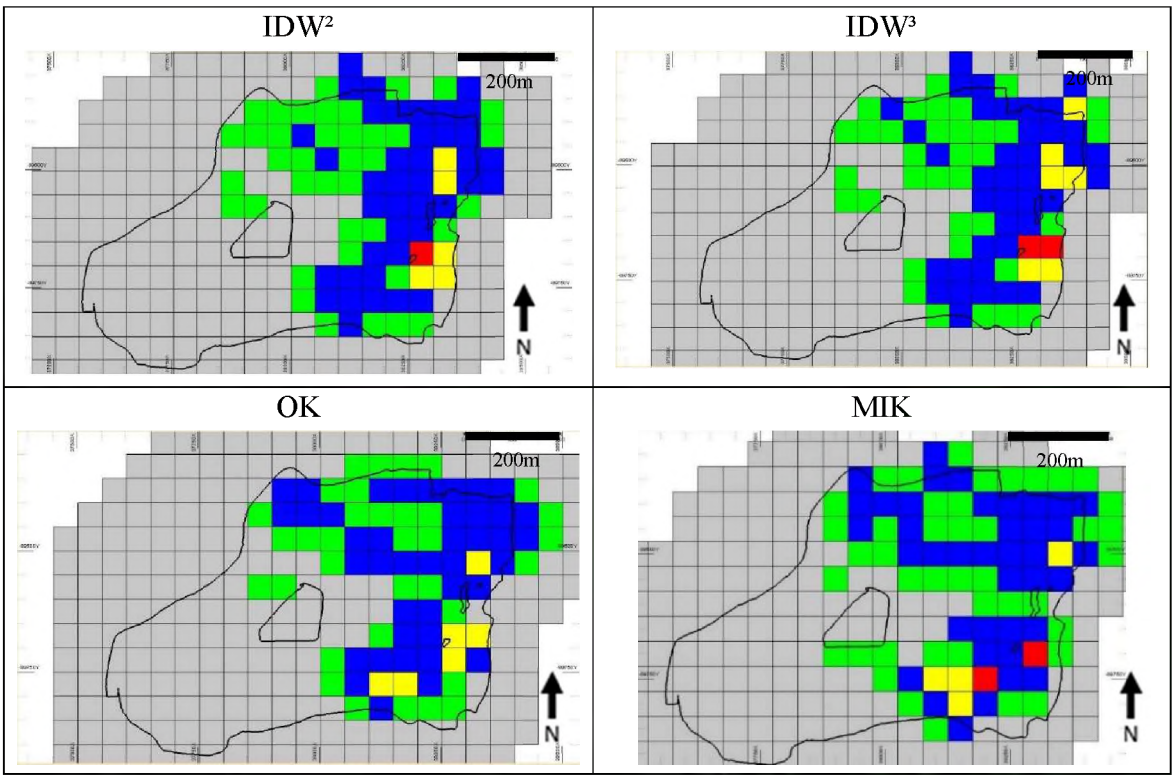

Figure 15: 50 m x 50 m x 3 m block models on elevation 678,5 m

On the exploration drill spacing of 50 m x 50 m represented in Figure 15, the expected block models created will be presumably less accurate than the smaller drill spacing block models. This is clearly evident from the block models presented above which should be expected. Some of the block models show a variety of differences between the various estimation techniques. Clearly visible in the IDW block models is the reduction of medium-grade blocks in the north-eastern section of the pit. The high-grade lenses have been replaced by lower grades in the northern part of the pit and only one block is present in both IDW^2 and IDW^3 towards the eastern part of the pit. The total low-grade blocks have increased compared to higher-grades. The south-eastern section of the pit has lost one of the two high-grade lenses that was still present in the 25 m x 25 m x 3 m block models. The presence of the high and super high-grade lens in the southeast is still visible. The two high-grade lenses that could always be observed previously as two different entities in this section of the pit have now fused into one high-grade lens. This high-grade lens has become smaller and decreased the grade concentration therein.

The OK block model has almost totally lost the presence of the high-grade lenses in the northern section of the pit. The previous high-grade lenses in the west have been transformed into medium-grade, whilst only one high-grade block can be observed in the east. The remaining block grade distribution of the previous smaller sized block models is only vaguely visible. The southern section of the pit still has two lenses of high-grade which are not visible in the IDW block models anymore. The two high-grade lenses are clearly separated from each other. Low-grade blocks have also decreased in number in the central and southern sections of the pit. It seems as if some of the low-grade blocks have been replaced by either waste or medium-grade blocks.

The MIK block model has a similar appearance as the OK block model. The northern section of the pit has lost the high-grade lenses in the western part and has only retained one high-grade block in the east. Some of the medium-grade blocks have been replaced by low-grade. From the four block models created, the MIK block model at these dimensions is the only model that shows evidence of super high-grade, which is present only in the southern section of the pit. The two high-grade lenses in the southern section are easily distinguishable from each other. The medium-grade blocks have also increased in number and area covered when compared to the previous model.

5.3 Block models of other estimation methods at an elevation of 669,5 m

5.3.1 4 m x 4 m x 3 m block models

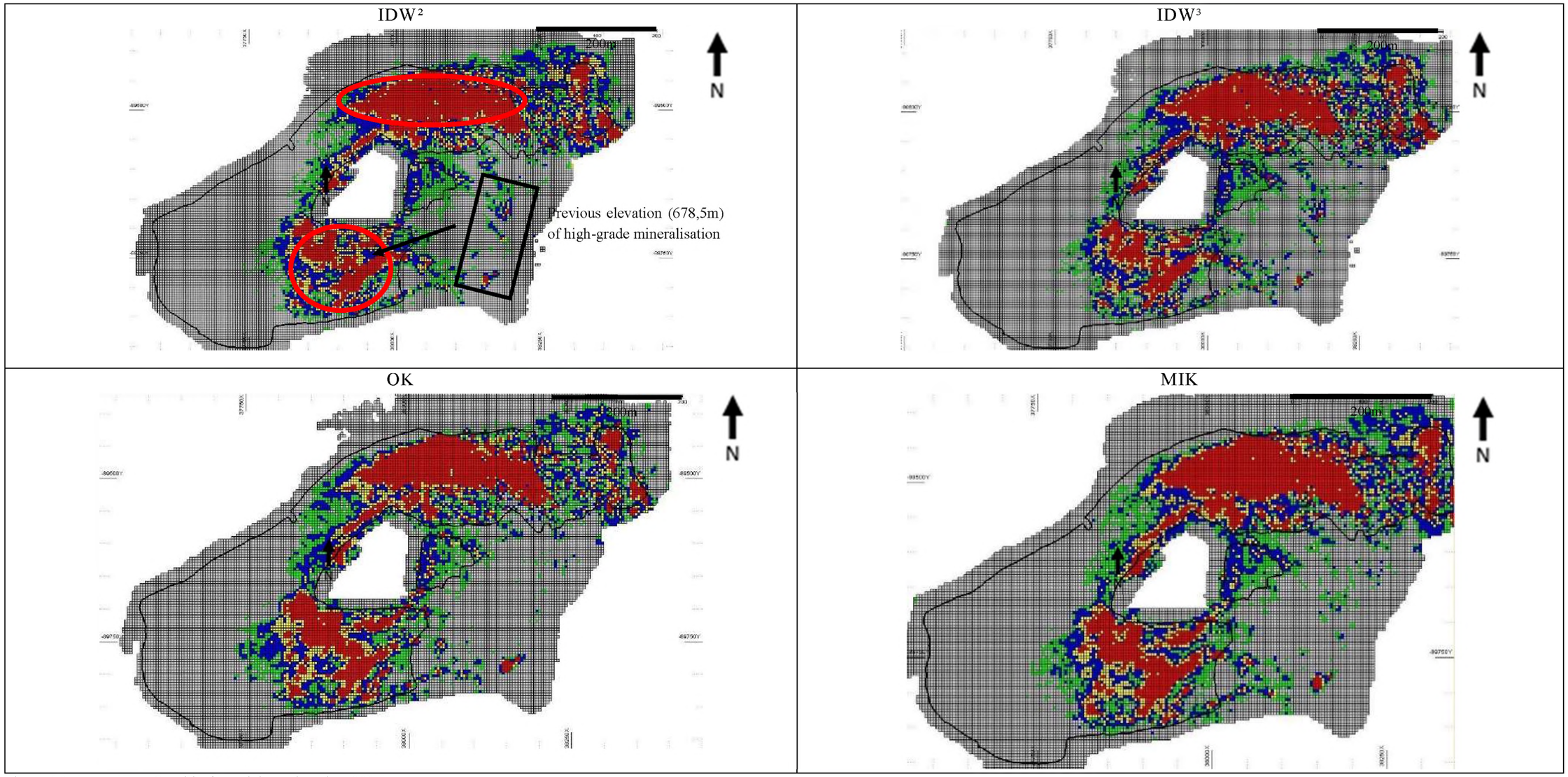

Figure 16: 4 m x 4 m x 3 m block models at elevation 669,5 m

Grade (ppm)	Colour
Waste 0-250	
Low-grade 250-400	
Medium-grade 400-650	
High-grade 650-900	
Super high-grade 900+	

General observations

In Figure 16 it is clear that ore has migrated downstream or westwards and is concentrated around the unmineralised basement island in the middle of the pit. The most obvious markers would be a large irregular shaped super high-grade lens indicated in red in the northern part of the pit. The other marker would be the super high-grade lens in the southern part of the pit. This high-grade as indicated in the IDW ^{2} model has migrated west wards when compared to the 678,5 m elevation models. The southern high grade lens is patchy in grade and distribution.

Block model observations

From the two IDW models it is clearly visible that there is a big concentration of higher-grades in the northern section of the pit. This depositional site of the high-grade is continuous and grades are more or less homogenous. The high-grade lens slowly fades into medium-grades and then into low-grade, followed by waste. In the northeast section of the pit the deposition of grades is very erratic. High-grade lenses can be distinguished from each other, however, they change abruptly into lower grades. It is also evident from the models that concentrations of uranium around the central island occur in a flow shape around the island. In the southern section of the pit the high-grade lens in the previous elevation has also migrated westwards. The high-grade lens can be easily observed, although more erratic than in the northern part of the pit. Low-grades and medium-grades comparatively occupy roughly the same area in the southern section of the pit.

The OK block model resembles the IDW models in terms of grade distribution. Not much can be said in terms of differences of the grade distribution, unlike that in the previous elevation. The high-grades in the northern section of the pit seem to have increased. Some of the medium-grades that were present in the IDW block models have been classified as high-grade in the OK block model, especially in the north-western areas. Some of the super high-grades have been downgraded into high-grade. The northeast section of the pit remains erratic and mineralisation is irregular. In the southern section of the pit the super high-grades have increased in size as well the high-grade in general. The same overall pattern of ore does resemble that of the IDW and MIK block models. From the OK model it can observed that especially low-grade and medium-grades have increased in number especially around the high-grade lenses.

The MIK block model as noted in the previous elevation shows more homogenisation in grade distribution. The high-grade lens in the northern section of the pit has increased in size compared to the previous models. Super high-grade has been displaced in some places by normal high-grade. Medium-grade is replaced by high-grade in some areas. Towards the north-eastern section of the

pit, the irregularity in grade distribution as in the previous block models is observed, but to a lesser extent. The high-grade lenses are more obvious to recognise. They fade abruptly into lower grades. In the southern section of the pit, the high-grade lens has also increased to super high-grade compared to the other previous models.

5.3.2 12,5 m x 12,5 m x 3 m block models

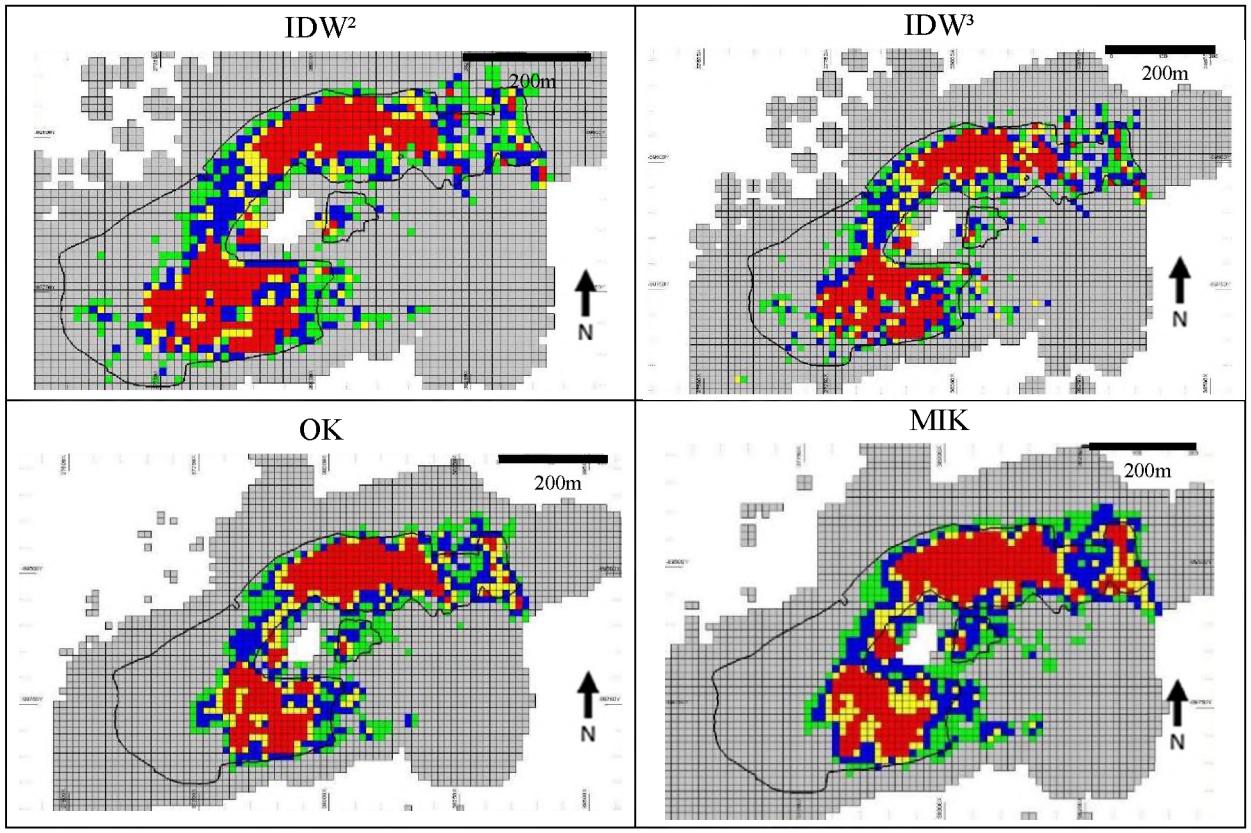

Figure 17: 12,5 m x 12,5 m x 3 m block models on elevation 669,5 m

The IDW block models in Figure 17 show a similar grade distribution as their previous drill spacing. The larger high-grade lens in the north of the pit is still visible and is composed mainly of super high-grade and surrounded by lesser high-grade. The high-grade is situated predominantly around the edges of the super high-grade lens. The high-grade fades abruptly into medium-grade and low-grade. In the north-eastern section of the pit the high-grade lenses have lost their previous definitive shape. This section seems much more erratic in its depositional pattern with no visible grade structure and distribution. An increased grade concentration of low-grade in this area is also visible. In the southern section of the pit, the high-grade lens has changed in shape and size, becoming more rounded and larger. It does, however, now contain isolated lower grade (yellow blocks) areas within the high-grade lens. This was not present before and is most likely small

blocks that were downgraded to normal high-grade as their prior grade model (4 m x 4 m) was relatively low super high-grade. The super high-grade itself in the southern section has also increased at the expense of high-grade. Abrupt grade changes are visible in these areas where high-grades diminish into low-grade and even waste. Ore previously classified as waste in the western section of the pit has now been classified as low-grade and even medium-grade in some instances. In general, it is observed that IDW^2 contains slightly more medium-grade than the IDW^3 block model.

The OK block model maintained its original structure from the previous block models. In the northern section of the pit the super high-grade lens is still clearly visible, surrounded by lesser high-grade. In the north-eastern section of the pit the smaller high-grade lenses have fused into one larger high-grade lens at the expense of some super high-grades. Towards the southern section of the pit the dominant high-grade lens has increased slightly in super high-grade concentrations towards the west. It is interesting to note grade changes among medium and low-grade blocks around the central basement island. Some of the low-grade blocks have been converted to medium-grade blocks and vice versa.

The MIK block as previously mentioned shows more homogenisation in grade distributions with little abrupt changes in grades. The dominant high-grade lens in the north is composed solely of super high-grades, surrounded by high-grade and fading into lower grades. The northeast section of the pit contains a more visible high-grade lens connected to the dominant lens by medium-grade. This adds to the overall continuity. The presence of more super high-grade is also visible in the north-eastern section, which was not the case in the other techniques used. More super high-grade is also present along the western edges of the central island, as well as more medium-grade on the eastern edge. The dominant high-grade lens in the southern section of the pit remains clear. Again, the fluency can be noted of high-grades fading slowly into waste without abrupt changes. More medium-grade is also observed along the eastern edge of the large high-grade body.

5.3.3 25 m x 25 m x 3 m block models

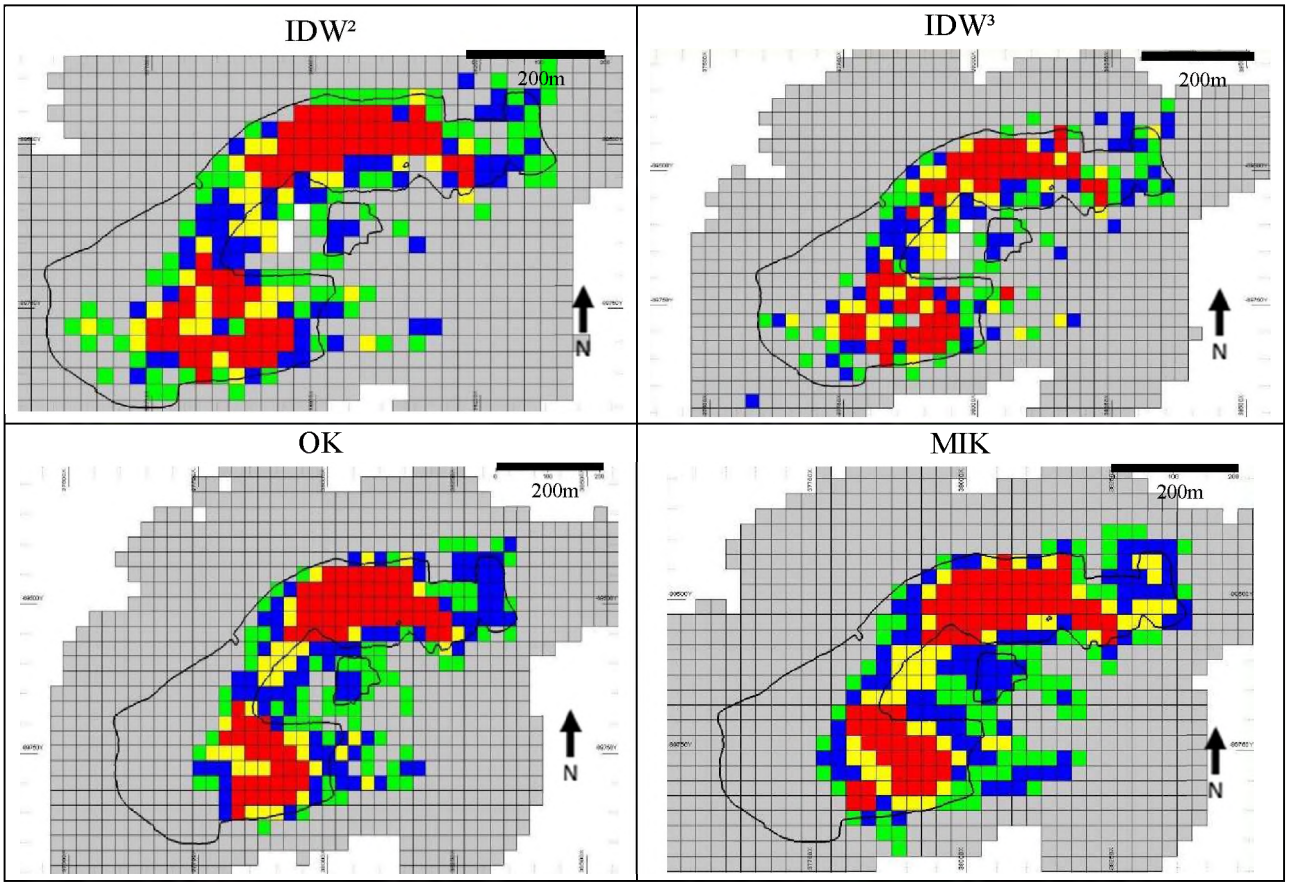

Figure 18: 25 m x 25 m x 3 m block model on elevation 669,5 m

The IDW block model as indicated in Figure 18 at these block parameters - still maintains the general shape and grade distribution as before. There are now larger differences between the two IDW techniques observed. In the northern section of the pit, the IDW² contains more super high-grade compared to IDW³. On the 25 m x 25 m parameters it is also visible that abrupt grade changes are also more frequent and make the entire model more erratic. The high-grade lens in the north-eastern section of the pit has also completely disappeared in both block models. These have been replaced by low-grade and minor medium-grades. Ore blocks around the eastern borders of the central island have also disappeared, whilst the western boundary has received more ore blocks. In the southern section of the pit the high-grade lens is still visible but contains more ore blocks of normal high-grade. These have displaced super high-grade blocks. The IDW³ block model generally contains increased lower grade blocks than the IDW².

The OK block model in the northern section retains its shape and grade distribution. The dominant high-grade lens is still as prominent as before. Towards the north-eastern section of the pit, the

high-grade lens has disappeared completely and has been displaced by medium-grade which has fused with the large high-grade lens towards the west. The high-grade lens in the southern section of the pit has become smaller and has lost some of its super high-grade. The super high-grade has been replaced by some high-grades and medium-grades.

The MIK block model at this elevation contains the dominant high-grade lens in the north. It has become somewhat constrained in terms of its super high-grade. The high-grade lens in the north-eastern section of the pit has not decreased in size compared to the other models. More medium-grade has been identified in this area at the expense of low-grade and minor high-grade. Towards the centre of the pit, waste has been replaced by low-grade and medium-grade in some cases. The high-grade lens in the southern section of the pit has shrunk in size and more high-grade is now present that has replaced the super high-grade. In general, the MIK model at these block parameters contain more ore blocks than any of the other methods at this elevation.

5.3.4 50 m x 50 m x 3 m block models

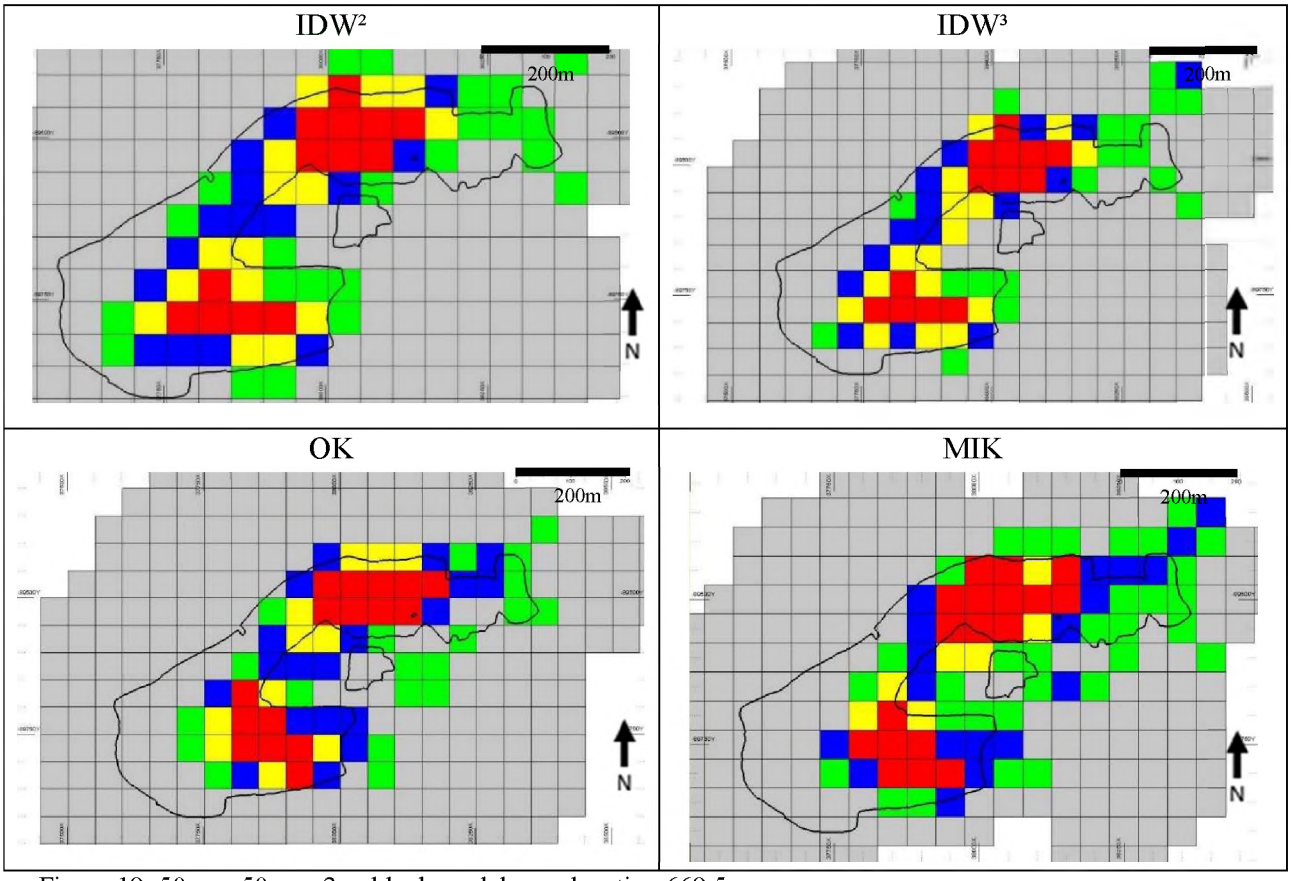

Figure 19: 50 m x 50 m x 3 m block models on elevation 669,5 m

The 50 m x 50 m x 3 m block models in Figure 19 have obvious differences in terms of prediction accuracy due to limited data and large blocks created that will smooth out smaller lenses. This can also be seen from the block models created above. In the northern and southern section of the pit the dominant high-grade lenses are still visible, and surrounded by lower grades.

In the northeast section of the pit there is no evidence of the small high-grade lenses that have been there in the finer spaced models. These areas are now classified as predominantly low-grade. High-grade along the edges of the super high-grade lens have been transformed into medium-grade in the northern parts. The IDW² model shows a general increased number in ore blocks compared to the IDW³ model in the northern parts of the pit. The eastern area around the central part of the pit has no more ore blocks, yet the western part still retains some ore blocks. The southern section of the pit retains the dominant high-grade lens. Although smaller and more erratic in shape, the high-

grade lens is still clearly visible. The IDW^2 block model contains increased high-grade in this area compared to the IDW^3 block model which shows more medium-grade.

The OK block model at this elevation retains its dominant super high-grade lens in the north of the pit. The northern part of the super high-grade has a line of high-grade which has replaced some of the super high-grade. In the northeast section of the pit the high-grade lens has disappeared, which was observed in the IDW block models as well. The high-grade has been replaced by low-grade and some medium-grade. Around the centre of the pit more ore blocks are present than in the IDW block models, especially along the eastern side. In the southern section of the pit the dominant high-grade lens is still present. Some of the medium-grade has replaced the high-grade along the outer edges of the lens.

The MIK block model presents the rectangular high-grade lens in northern part of the pit. More super high-grade is visible than normal high-grade in this area. Towards the northeast section of the pit, the high-grade lens still present in the 25 m x 25 m x 3 m block model has been replaced by mostly low-grade and some medium-grade. More ore blocks are observed, though, in the general area than in any of the other models at the 50 m x 50 m x 3 m dimensions. This is also visible in the central section of the pit. The additional ore blocks are mostly low-grade and in some cases some lower grades have been upgraded to higher-grades. The same is visible in the southern section of the pit. The high-grade lens is still clearly recognizable. Lesser high-grade is visible which has been replaced by medium-grade.

5.4 Block model setup, variography and statistical representation

5.4.1 Inverse Distance Weighted data preparation

IDW is probably the most simplistic method used during this research in terms of time used, methodology and software needed. It is nonetheless an established and accepted method. IDW was setup using Micromine only. No variography was needed, as Micromine does not offer this option using IDW, and was therefore relatively simple and fast. A search ellipsoid was used as a search radius style. A search radius one and half times the drill spacing was used and preferred over twice the drill spacing.

5.4.2 Conditional simulation data preparation

It has to be noted that identical block model parameters used in the modelling process were applied for both pit G1 and H1 respectively. This applies to all four geostatistical methods used in this

study. During construction of the variograms in conditional simulation a scale factor of 1,5 was usually used with only minor occurrences where the value was changed to a number between one and two. This was mainly due to the small scale spacing between adjacent drill holes or data points. Data first had to go through normal score transformation. Variograms were constructed in three different directions. The first was seen in an X direction which is modelled across strike. The second analysis is seen in a Y direction which is along strike and the third is seen downhole (Z). The resulting variograms have all been illustrated in Figure 21to Figure 25 for the four metre drill spacing using conditional simulation. Due to the extensive number of drill holes the data had to be split into five sections as mentioned earlier ranging from the eastern part of the pit to the west. The block models below illustrate ore distribution in different grade cut-offs, with the grades above 650 ppm being the most sought after. No elevation cut-off was provided in Figure 20. It can be observed that lower grades such as waste and low-grade are mostly observed in the upper elevations of pit G1, though in the south-eastern parts of the pit medium and high-grade can be observed close to the surface. The grade distribution is important and can be seen in the various variograms of the different sections illustrated below.

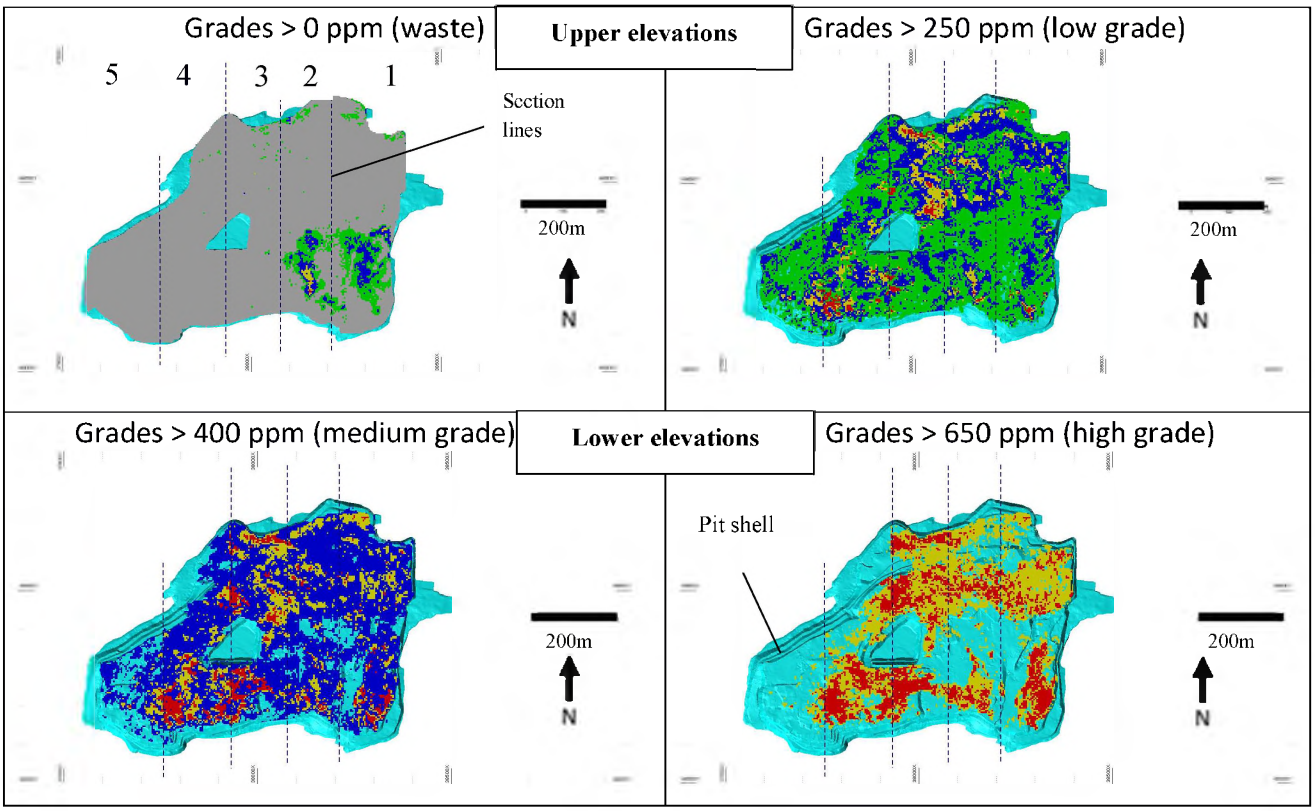

Figure 20: Five east to west sections of pit G1 and various grades within pit boundary

In Figure 21 the cumulative histograms are used to evaluate the cut-off used before the simulation process. This a standard procedure as outliers do play a pivotal role in some deposits. At Langer Heinrich the carnotite deposition is erratic where high-grades can be followed in close proximities by waste or lower grades. Super high-grades are therefore sometimes regarded as extreme outliers and removed as they can affect the final estimation results. The final result of the simulations have also been plotted in a Q-Q plot to illustrate the results of the simulation against the actual data.

The resulting variograms from the conditional simulations mostly indicated zonal anisotropy. This is indicative as the variograms do not flatten out and would probably do so outside the calculated variograms margins. This is observed on most of the variograms along strike and across strike variograms. These variograms consist of two dominant structures which have a short and steep start, followed by a longer and gradual finish. A relatively low nugget effect (>0,1) is observed in most of the variograms. Flattening or reduced gradients are observed to occur from a lag distance of 4 upwards and at a nugget effect of about 0,6. The down-the-hole variograms indicate signs of geometric variography. The Q-Q plots created from the original versus the simulated data was used as an estimation indication. This is an important reconciliation step which can be observed if the resultant estimation is over or under estimated. If all the data points fall in line with the X-Y line running diagonally, the data would be in perfect coherence. If the data points fall below the X-Y line, the resulting simulation data would be conservative and therefore underestimating. If the data fell above the X-Y line, the estimated data points would be overestimated. The CV and mean value are also good indicators and should ideally reflect each other. The further they are off, the more likely it is that your estimation is inconsistent. The first dataset, the east to west one, seems to be slightly underestimated as the original data is higher than the simulation data. The dataset east to west two seems to be on target, indicated by the X-Y line as well as the CV values which are closely correlated. A slight overestimation can be noted among the high-grades, especially in the simulation run for the datasets east to west, three to five.

Dataset east to west section 1

Across-strike Variogram

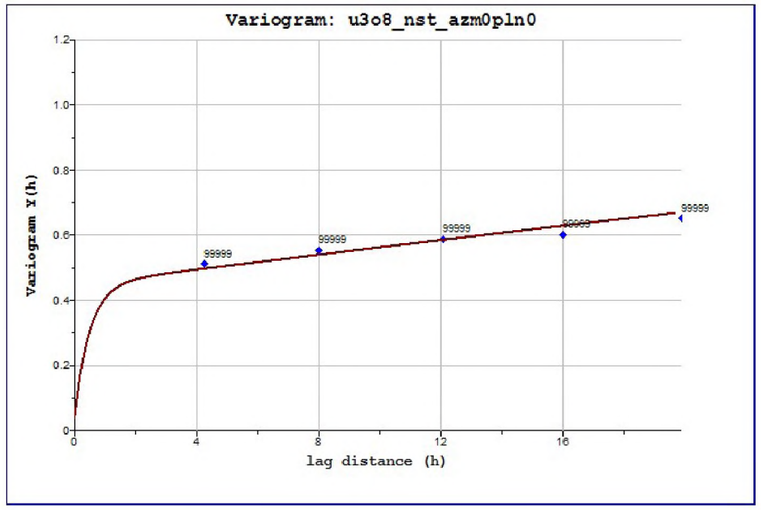

Along-strike Variogram

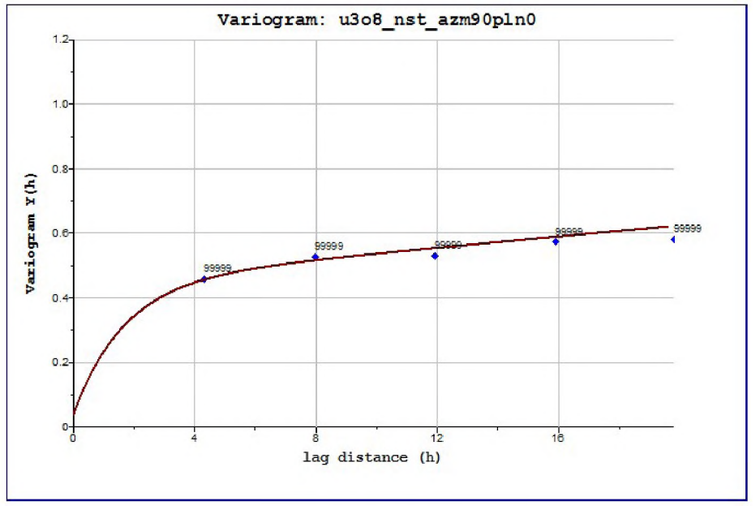

Down-hole variogram

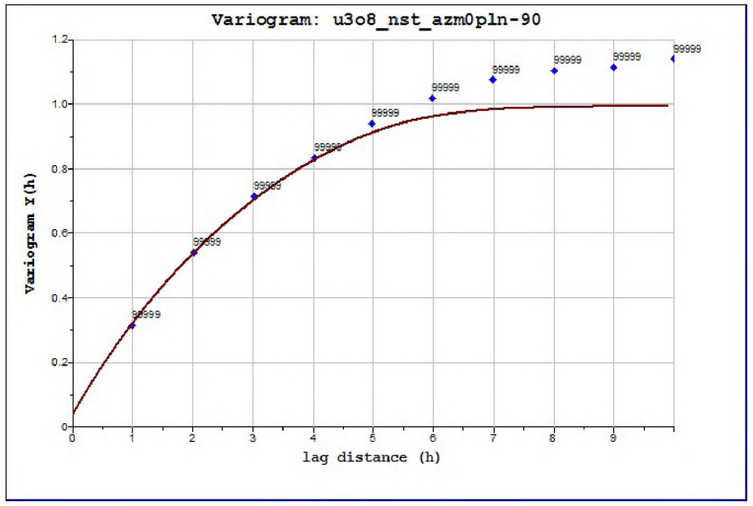

Variogram map

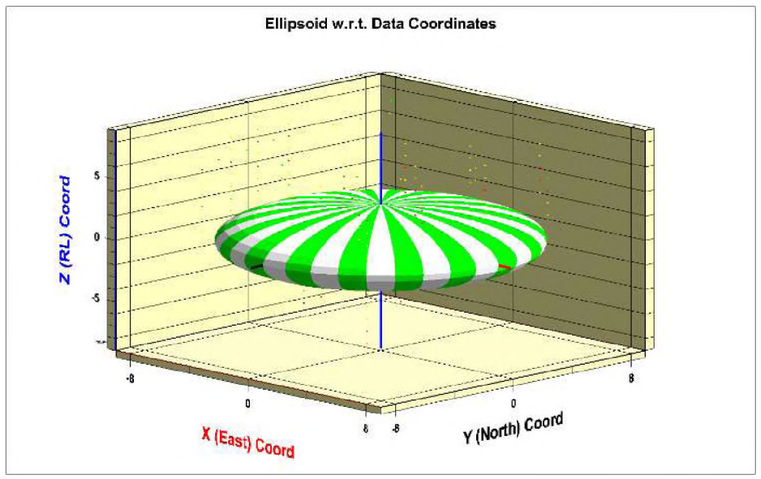

Cumulative frequency graph

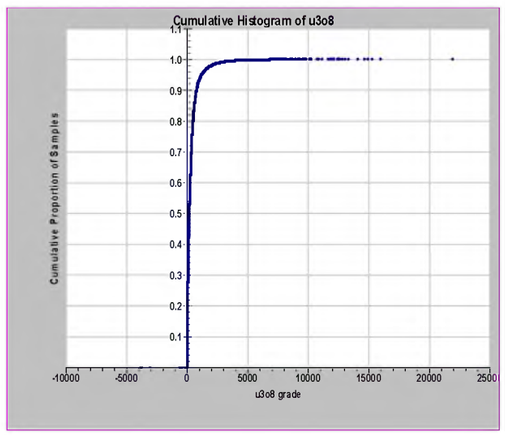

Univariate Statistics

Variable:	u3o8
Weighted by:	no weight
Mean:	329.203
Variance:	336577.844
CV:	1.762
Minimum:	-3841.008
Q1:	40.269
Median:	163.039
Q3:	390.877
Maximum:	21931.918
IQR:	350.608
No. Data:	146693

(Data set at full limits)

Q-Q plot Simulation vs. actual data

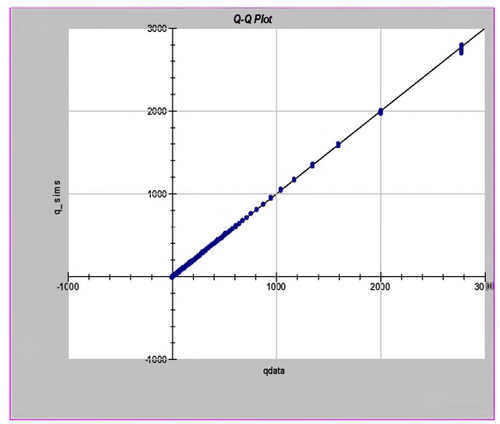

Data Statistics

Variable:	qdata	q_sims
Weight by:	--	--
Mean:	305.116	305.604
Variance:	185604.984	184902.953
CV:	1.412	1.407
Minimum:	-6.613	-5.986
Q1:	40.334	39.051
Median:	163.143	162.819
Q3:	391.044	394.062
Maximum:	2771.791	2796.555
IQR:	350.710	355.011
Covariance:	185245.844	
Pearson:	1.000	
Spearman:	1.000	
No. of Data:	4950	

(Data set at full limits)

Figure 21: Variograms, cumulative frequency graph and Q-Q plot of section 1 in pit G1

Dataset east to west section 2

Across-strike Variogram

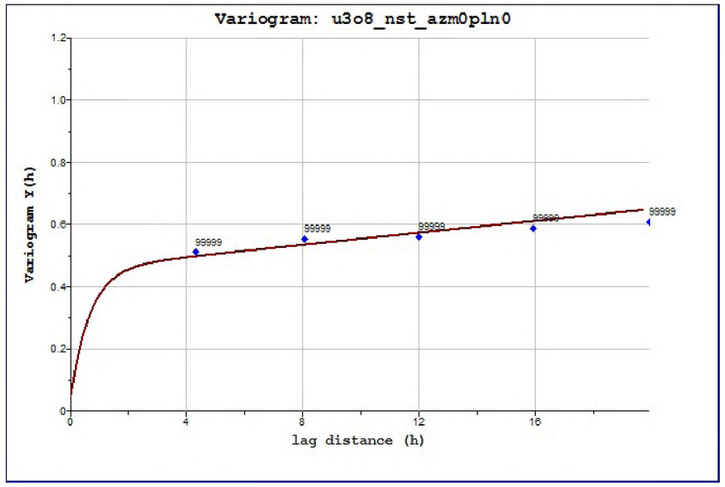

Along-strike Variogram

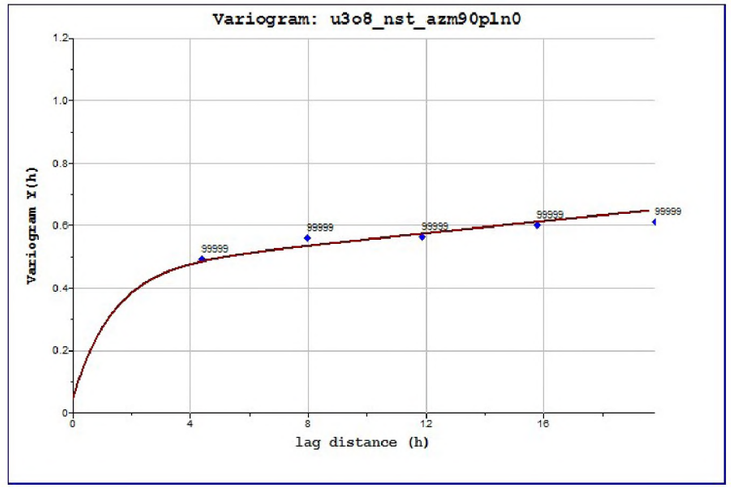

Down-hole variogram

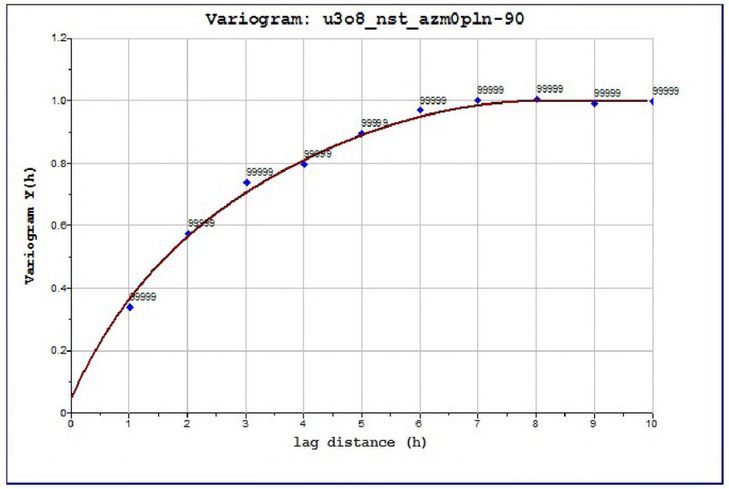

Variogram map

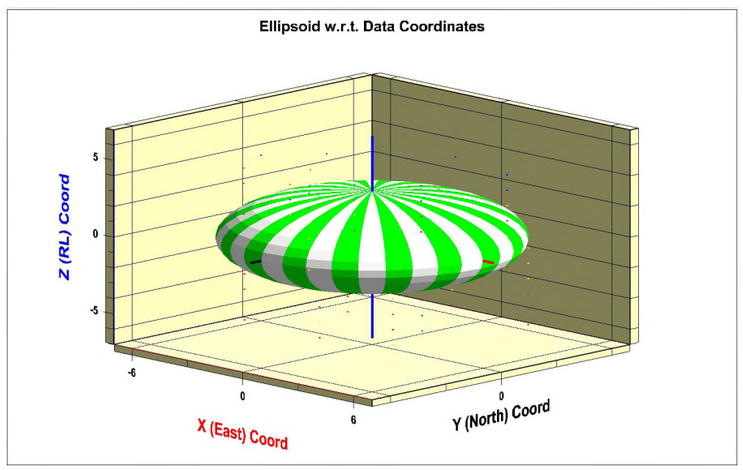

Cumulative frequency graph

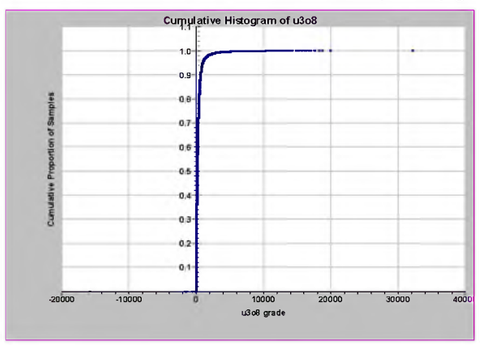

Univariate Statistics

Variable:	u3o8
Weighted by:	no weight
Mean:	323.576
Variance:	478802.969
CV:	2.138
Minimum:	-15752.089
Q1:	41.210
Median:	176.690
Q3:	370.204
Maximum:	32146.213
IQR:	328.994
No. Data:	144112

(Data set at full limits)

Q-Q plot Simulation vs. actual data

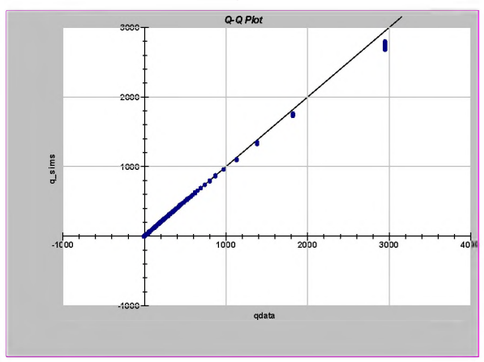

Data Statistics

Variable:	qdata	q_sims
Weight by:	--	--
Mean:	287.704	284.939
Variance:	165110.609	150235.453
CV:	1.412	1.360
Minimum:	-6.578	-6.290
Q1:	41.238	39.822
Median:	176.712	178.868
Q3:	370.252	374.978
Maximum:	2945.588	2795.319
IQR:	329.014	335.156
Covariance:	157397.922	
Pearson:	0.999	
Spearman:	1.000	
No. of Data:	4950	

(Data set at full limits)

Figure 22: Variograms, cumulative frequency graph and Q-Q plot of section 2 in pit G1

Dataset east to west section 3

Across-strike Variogram

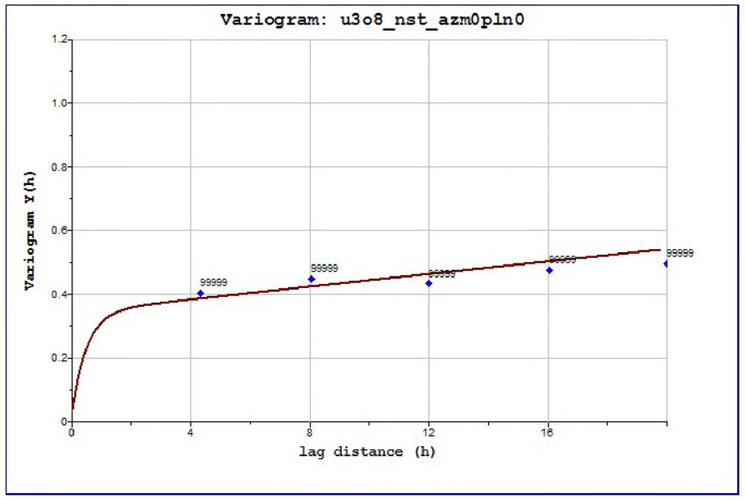

Along-strike Variogram

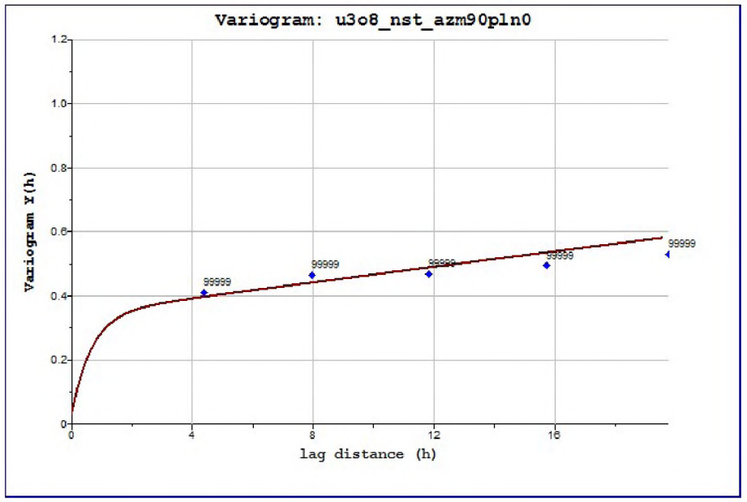

Down-hole variogram

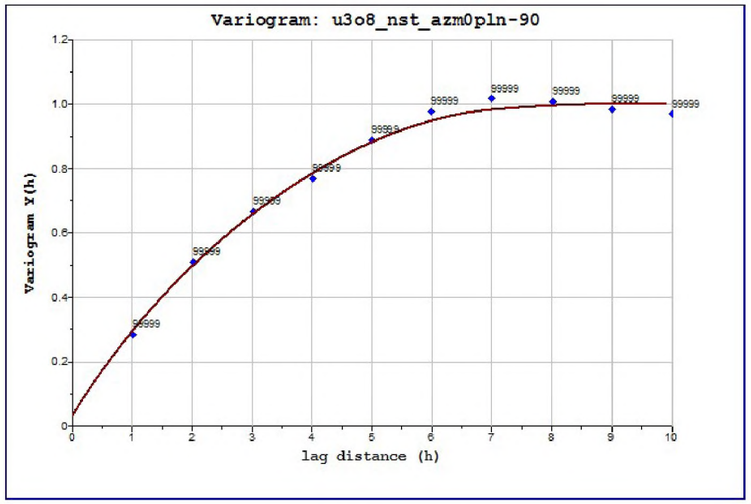

Variogram map

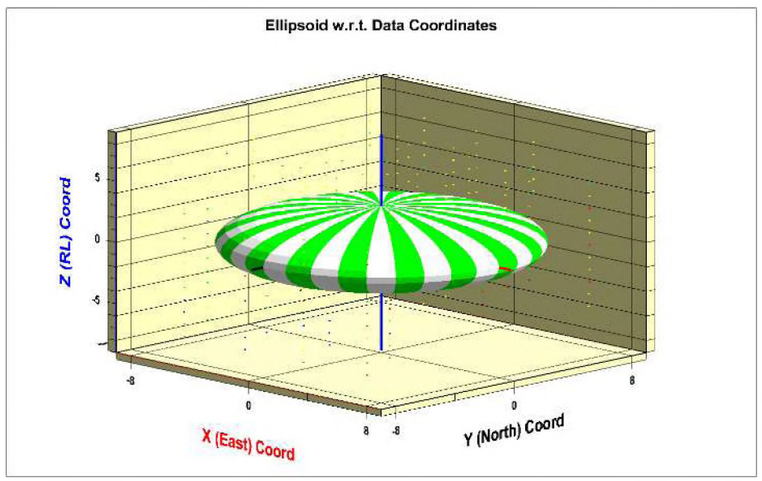

Cumulative frequency graph

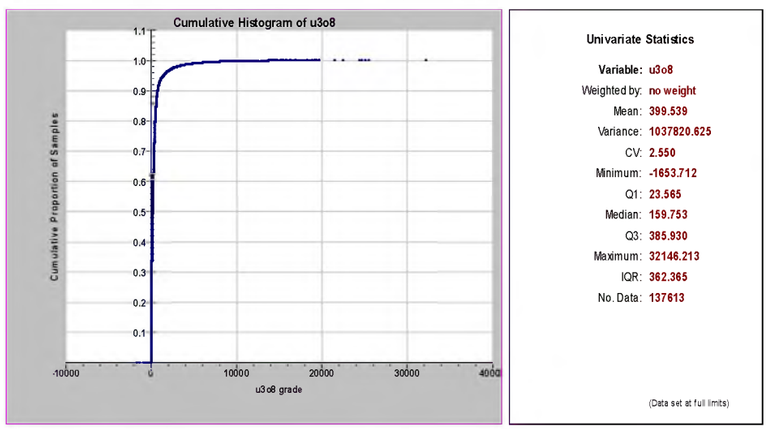

Univariate Statistics

Variable:	u3o8
Weighted by:	no weight
Mean:	399.539
Variance:	1037820.625
CV:	2.550
Minimum:	-1653.712
Q1:	23.565
Median:	159.753
Q3:	385.930
Maximum:	32146.213
IQR:	362.365
No. Data:	137613

(Data set at full limits)

Q-Q plot Simulation vs. actual data

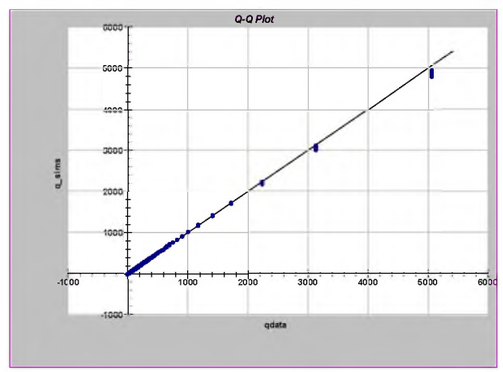

Data Statistics

Variable:	qdata	q_sims
Weight by:	--	--
Mean:	348.356	347.098
Variance:	441174.594	421220.125
CV:	1.907	1.870
Minimum:	-4.504	-3.640
Q1:	23.608	22.022
Median:	159.802	159.466
Q3:	385.977	390.842
Maximum:	5055.587	4951.586
IQR:	362.369	368.820
Covariance:	430999.969	
Pearson:	1.000	
Spearman:	1.000	
No. of Data:	4950	

(Data set at full limits)

Figure 23: Variograms, cumulative frequency graph and Q-Q plot of section 3 in pit G1

Dataset east to west section 4

Across-strike Variogram

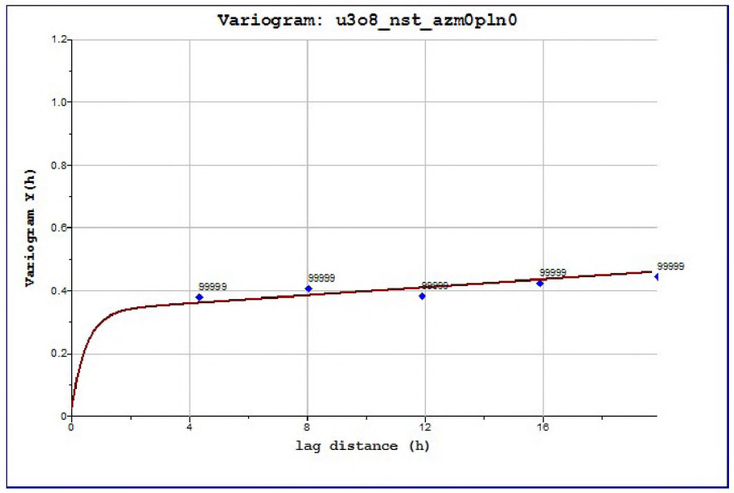

Along-strike Variogram

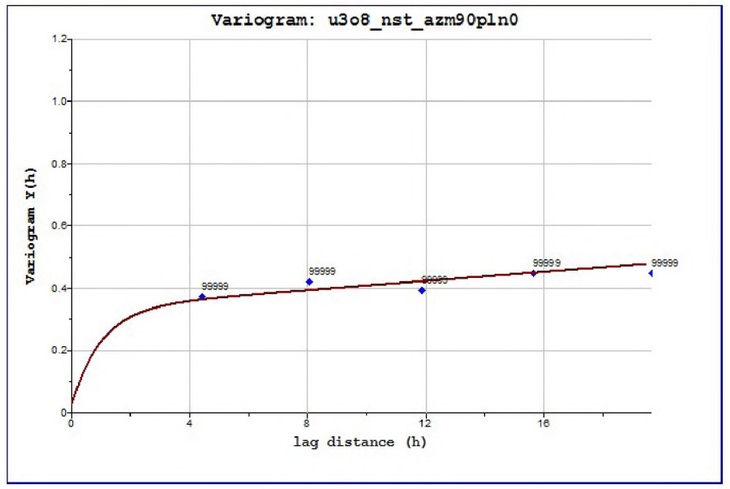

Down-hole variogram

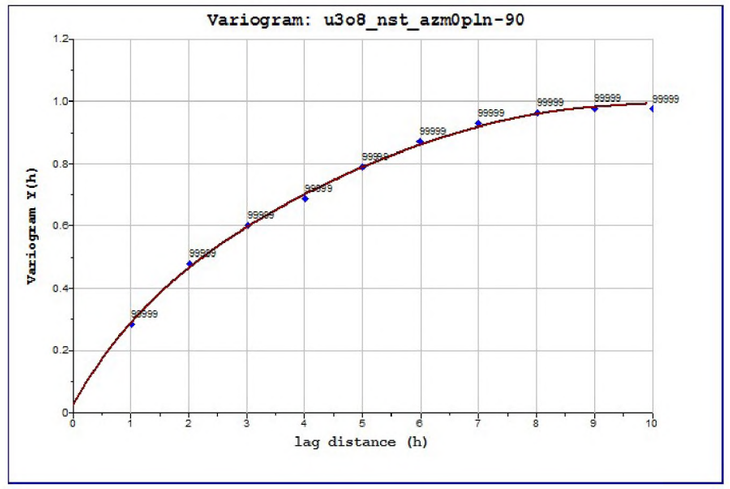

Variogram map

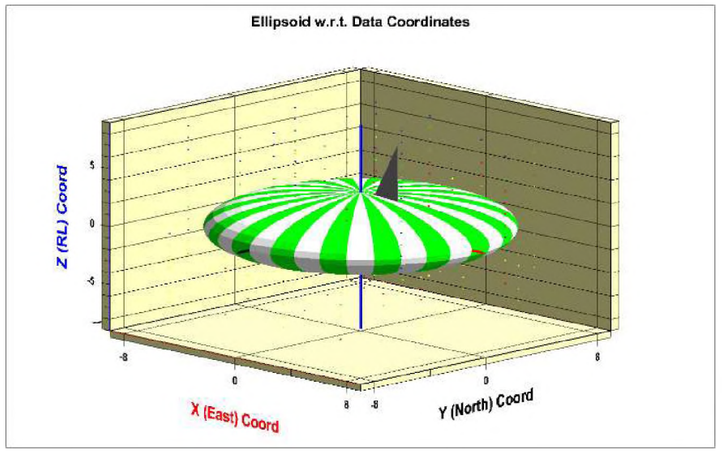

Cumulative frequency graph

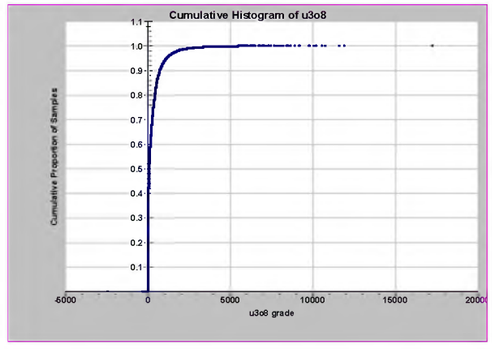

Univariate Statistics

Variable:	u3o8
Weighted by:	no weight
Mean:	265.804
Variance:	262714.094
CV:	1.928
Minimum:	-2461.102
Q1:	5.901
Median:	64.106
Q3:	330.516
Maximum:	17248.889
IQR:	324.615
No. Data:	134089

(Data set at full limits)

Q-Q plot Simulation vs. actual data

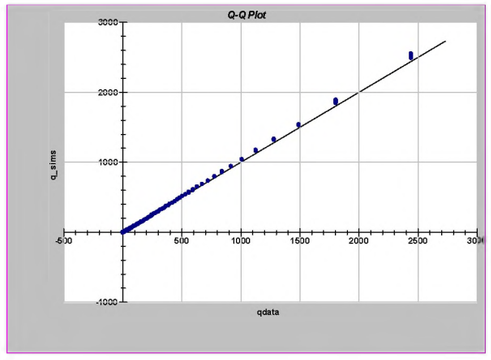

Data Statistics

Variable:	qdata	q_sims
Weight by:	--	--
Mean:	245.817	250.749
Variance:	165265.672	177643.609
CV:	1.654	1.681
Minimum:	-3.979	-2.602
Q1:	5.907	5.569
Median:	64.185	59.023
Q3:	330.652	334.336
Maximum:	2435.046	2552.843
IQR:	324.745	328.767
Covariance:	171334.609	
Pearson:	1.000	
Spearman:	1.000	
No. of Data:	4950	

(Data set at full limits)

Figure 24: Variograms, cumulative frequency graph and Q-Q plot of section 4 in pit G1

Dataset east to west section 5

Across-strike Variogram

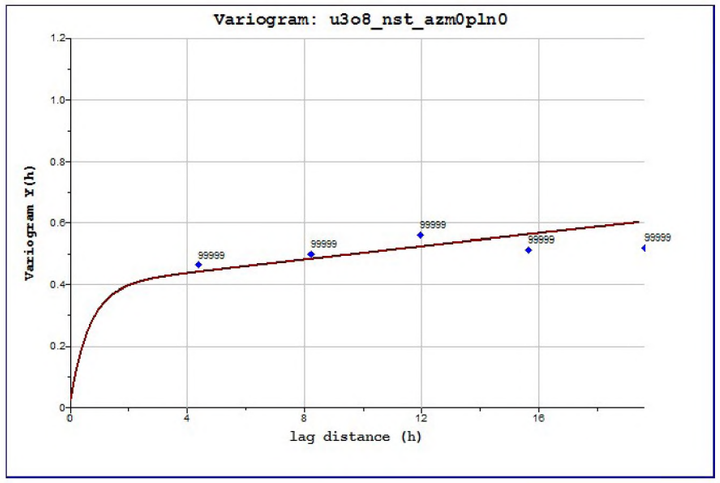

Along-strike Variogram

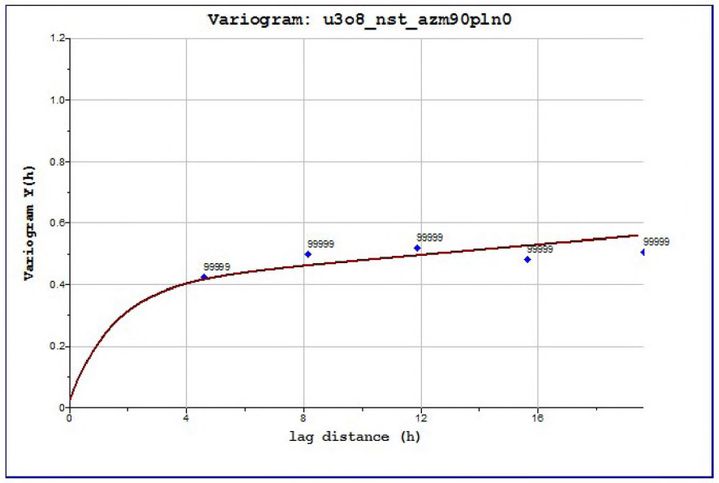

Down-hole variogram

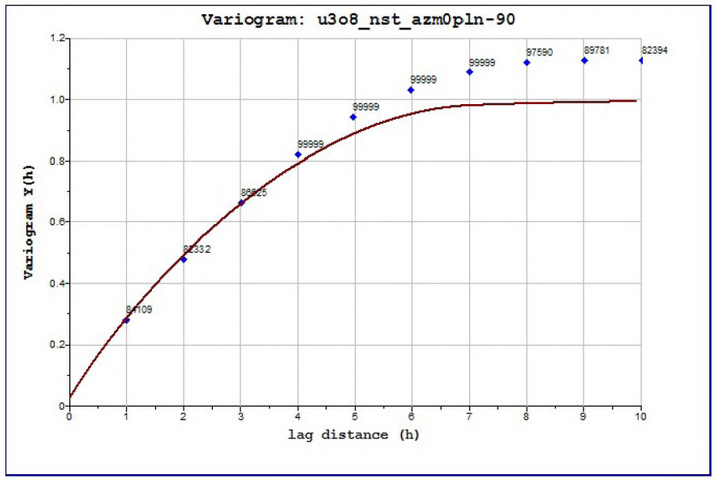

Variogram map

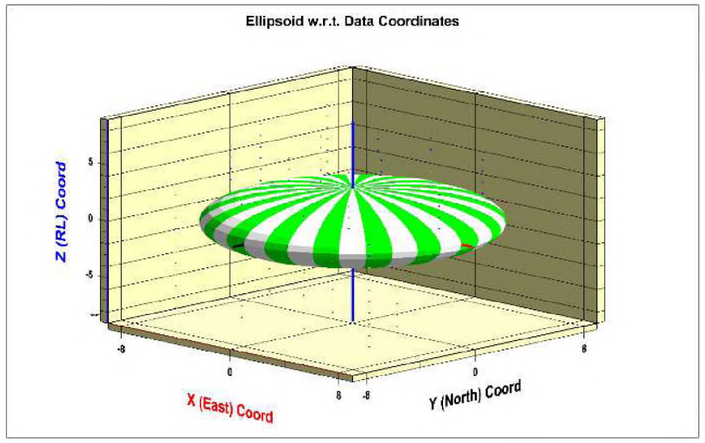

Cumulative frequency graph

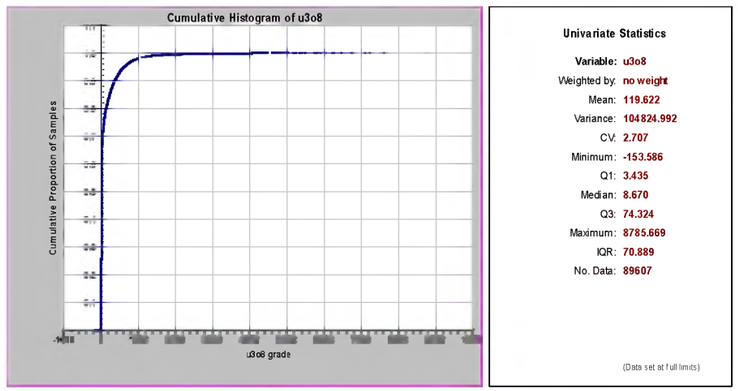

Univariate Statistics

Variable:	u3o8
Weighted by:	no weight
Mean:	119.622
Variance:	104824.992
CV:	2.707
Minimum:	-153.586
Q1:	3.435
Median:	8.670
Q3:	74.324
Maximum:	8785.669
IQR:	70.889
No. Data:	89607

(Data set at full limits)

Q-Q plot Simulation vs. actual data

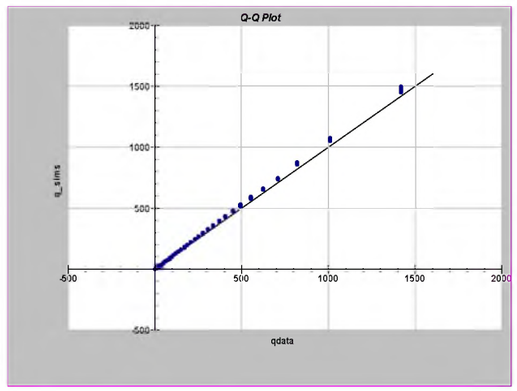

Data Statistics

Variable:	qdata	q_sims
Weight by:	--	--
Mean:	104.408	109.268
Variance:	52316.441	57551.320
CV:	2.191	2.196
Minimum:	-1.756	-1.173
Q1:	3.436	3.313
Median:	8.673	8.233
Q3:	74.329	76.419
Maximum:	1414.301	1494.771
IQR:	70.893	73.106
Covariance:	54868.941	
Pearson:	1.000	
Spearman:	1.000	
No. of Data:	4950	

(Data set at full limits)

Figure 25: Variograms, cumulative frequency graph and Q-Q plot of section 4 in pit G1

5.4.3 Ordinary Kriging data preparation

4 m x 4 m x 3 m data setup

Across-strike variogram

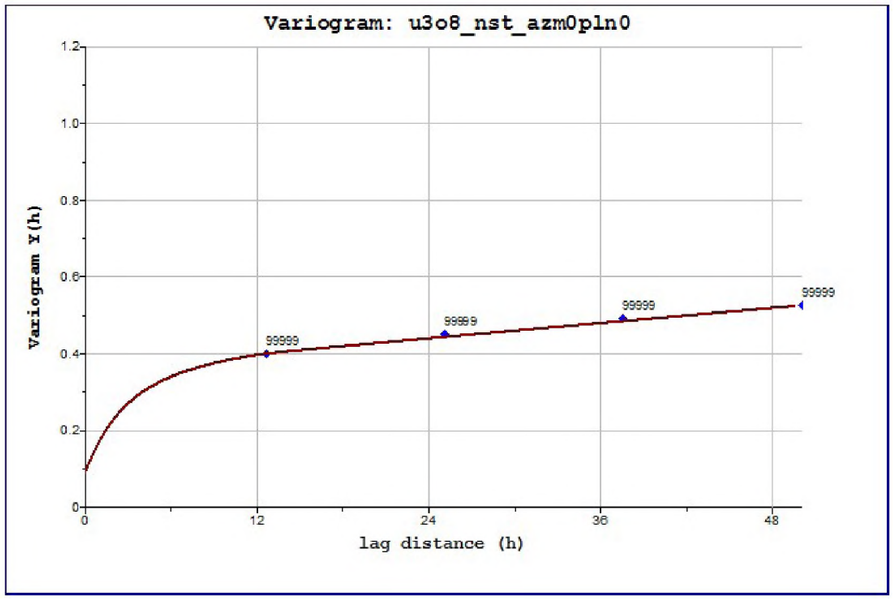

Along-strike variogram

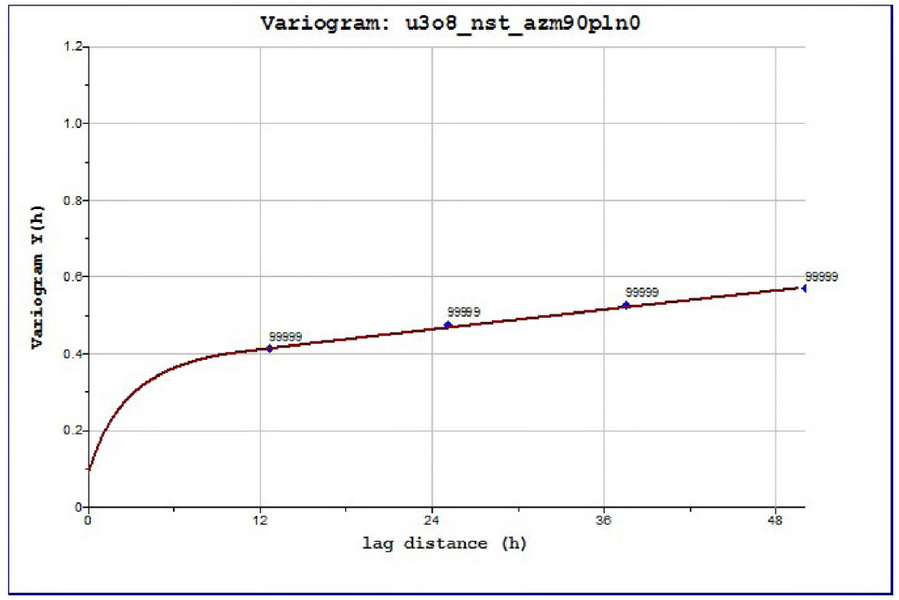

Downhole variogram

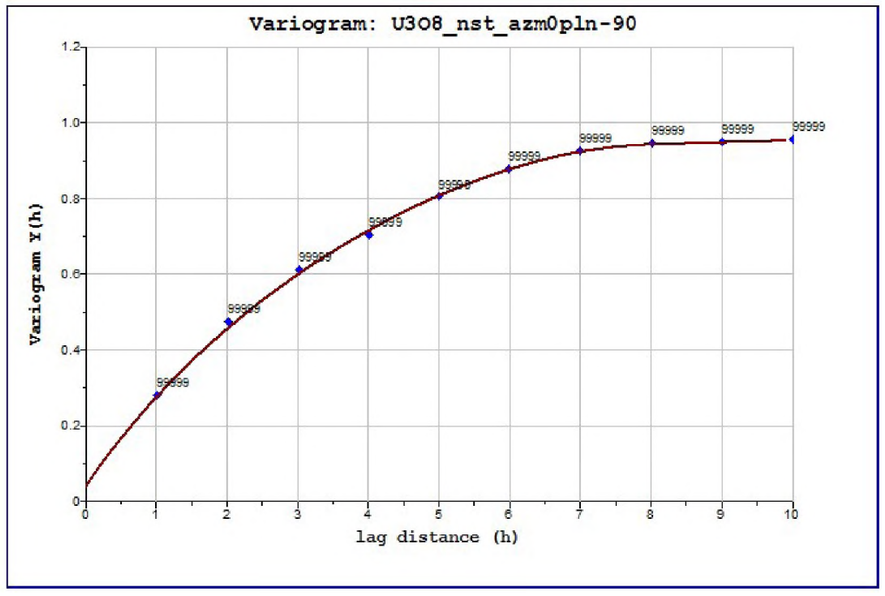

Variogram map

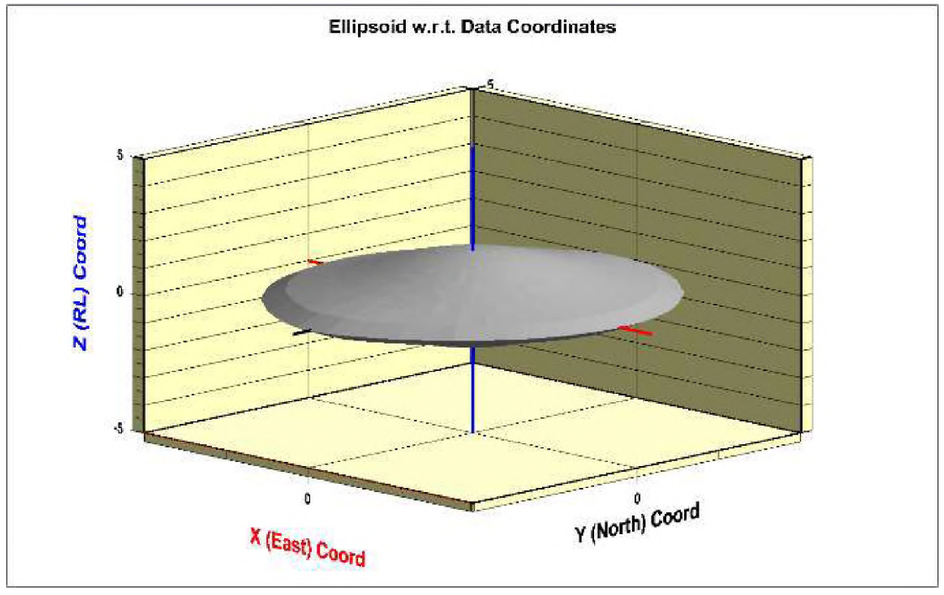

Figure 26: Variography of OK of 4 m x 4 m x 3 m block model.

12,5 m x 12,5 m x 3 m data setup

Across-strike variogram

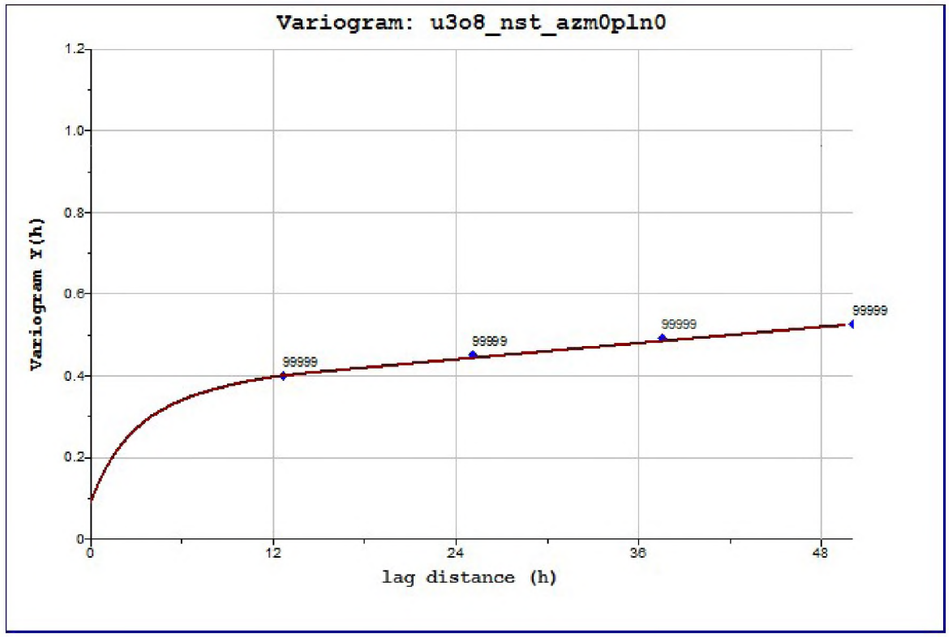

Across-strike variogram

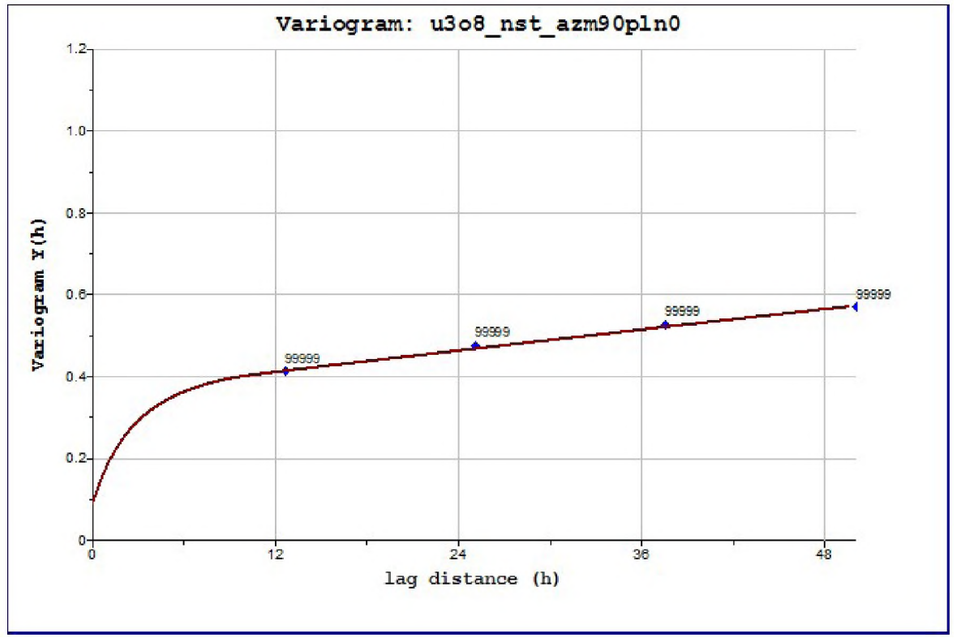

Downhole variogram

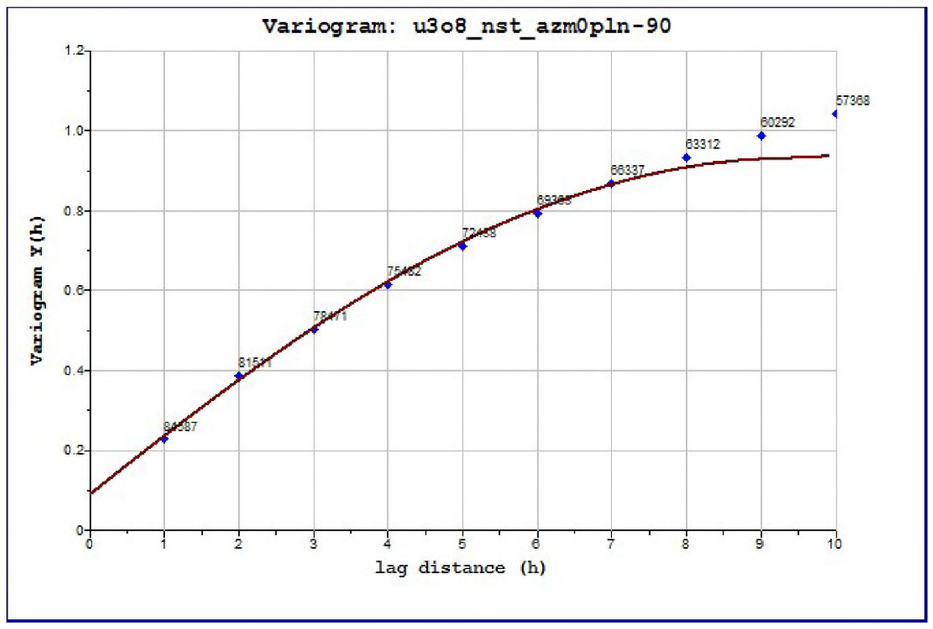

Variogram map

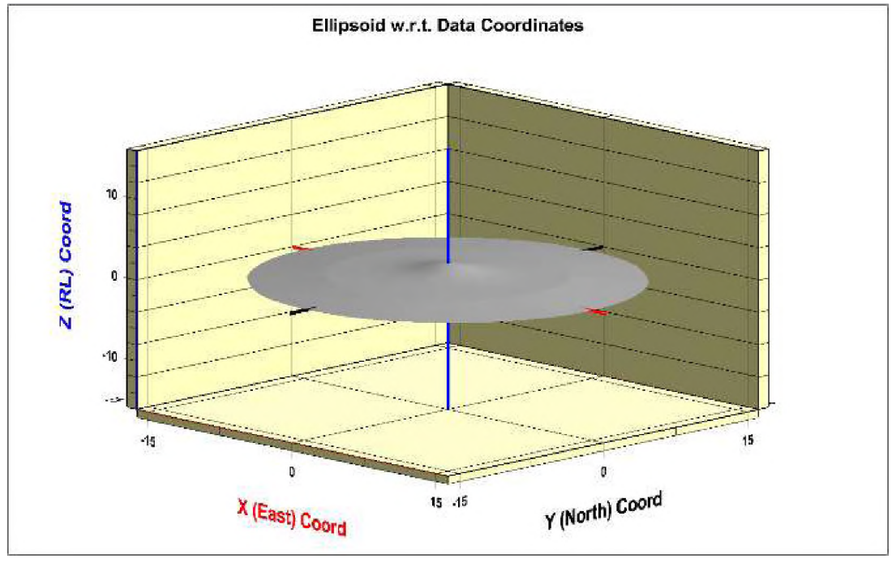

Figure 27: Variography of OK of 12,5 m x 12,5 m x 3 m block model

25 m x 25 m x 3 m data setup

Across-strike variogram

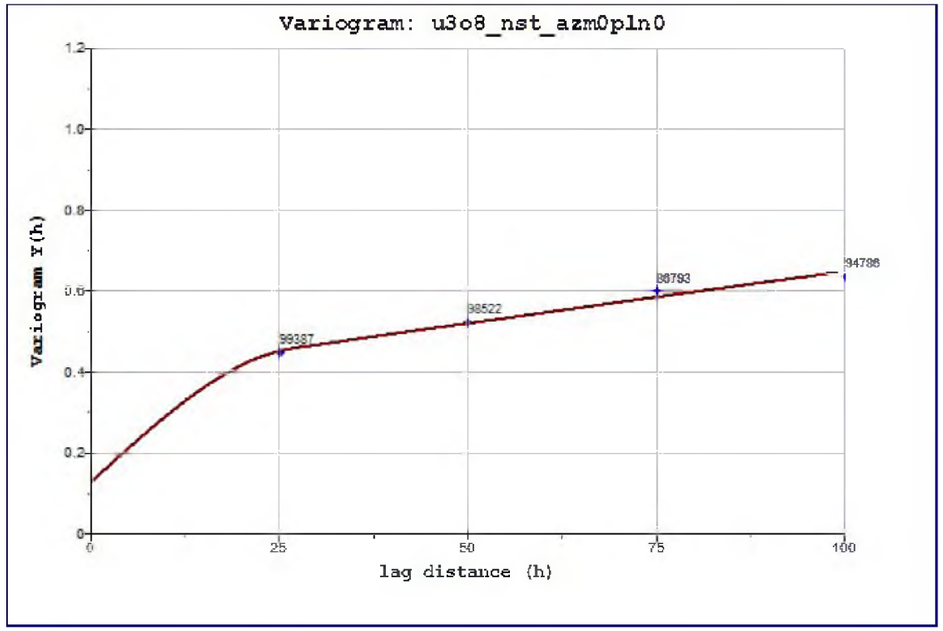

Across-strike variogram

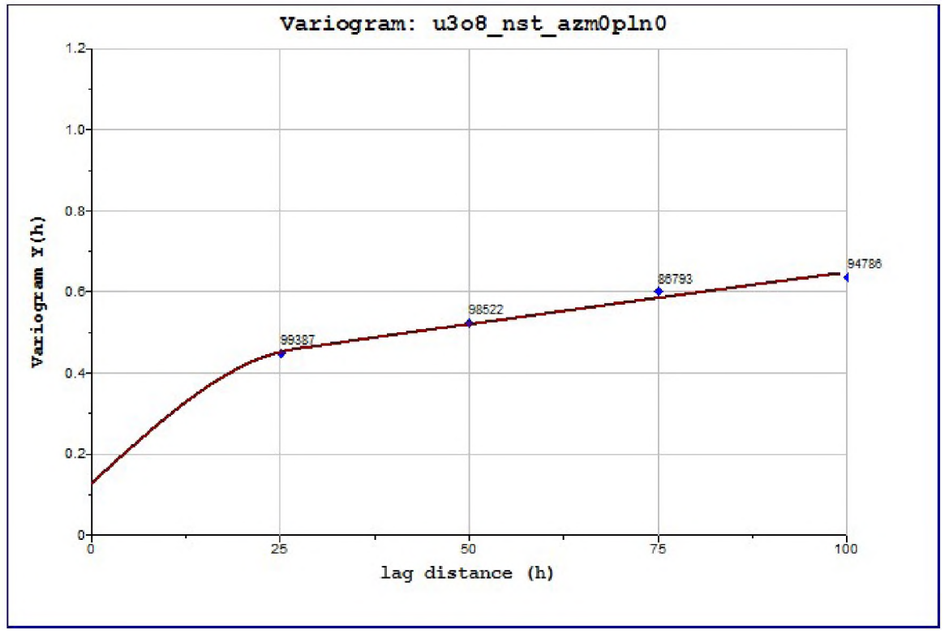

Downhole variogram

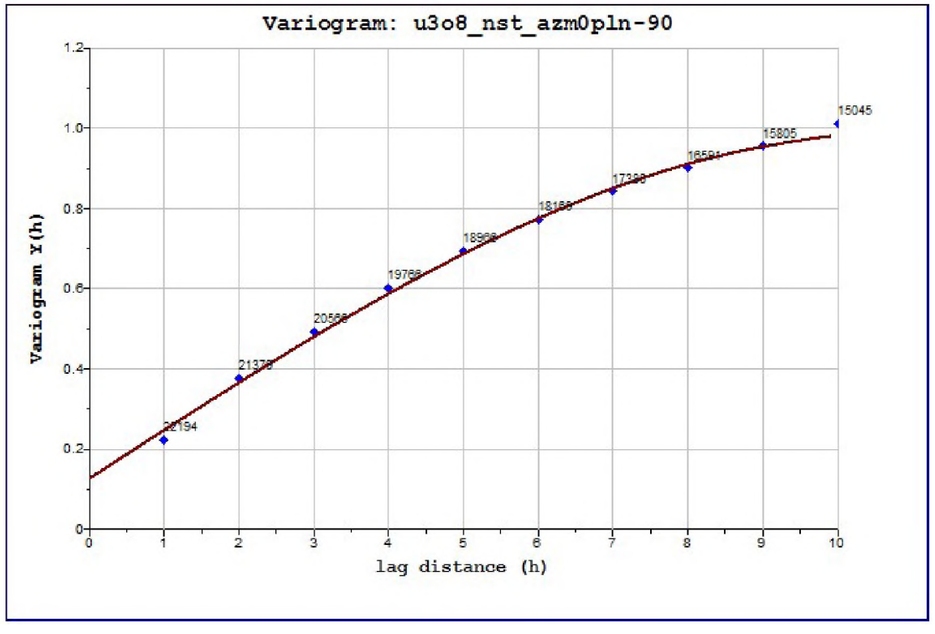

Variogram map

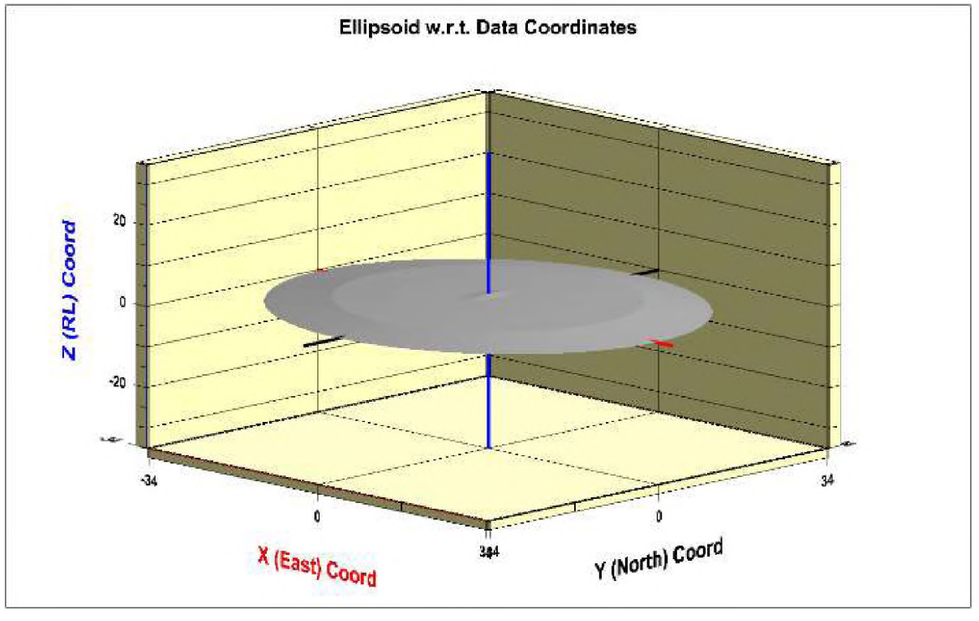

Figure 28: Variography of OK of 25 m x 25 m x 3 m block model

50 m x 50 m x 3 m data setup

Across-strike variogram

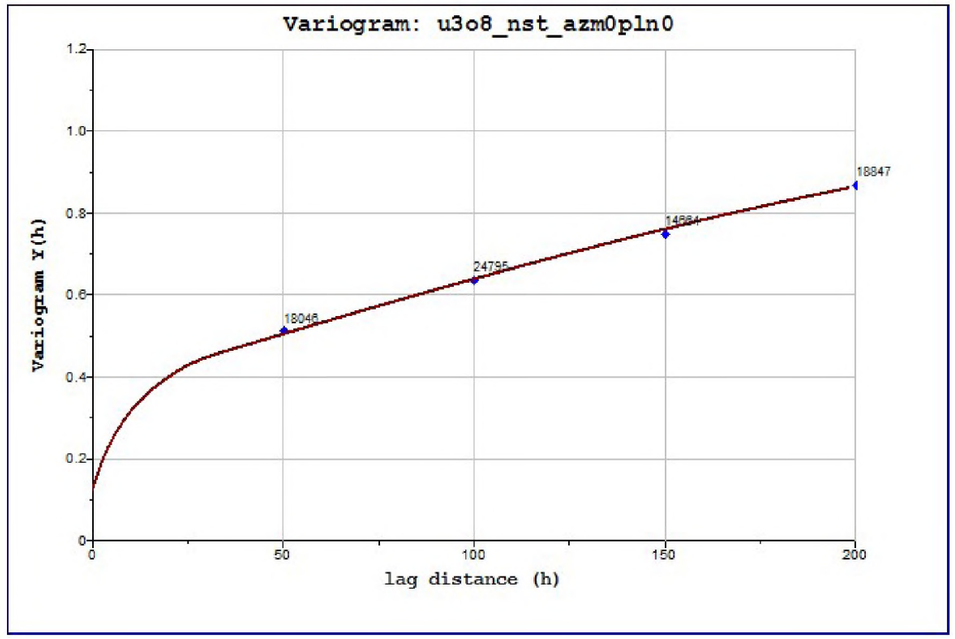

Across-strike variogram

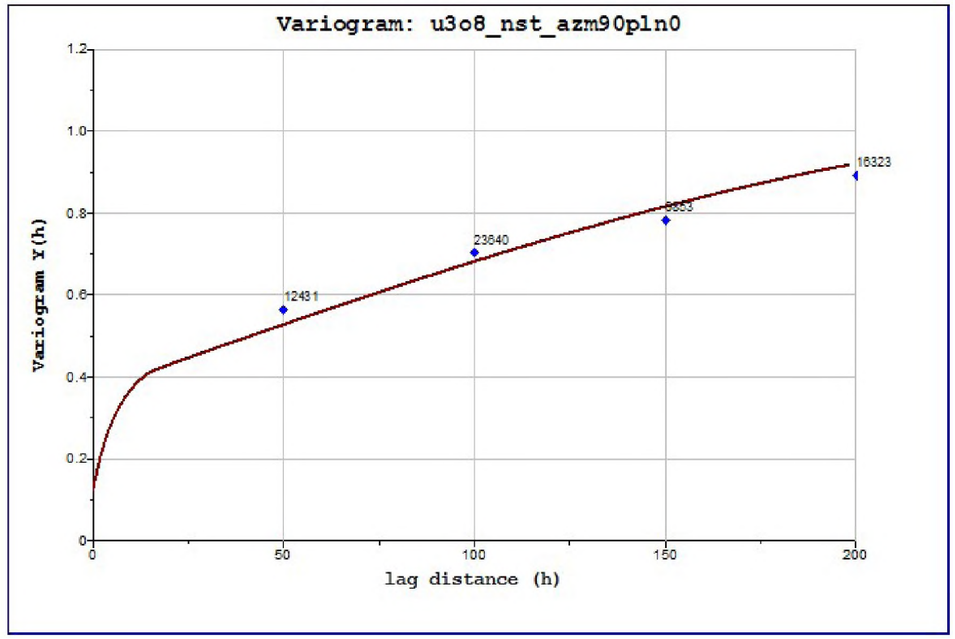

Downhole variogram

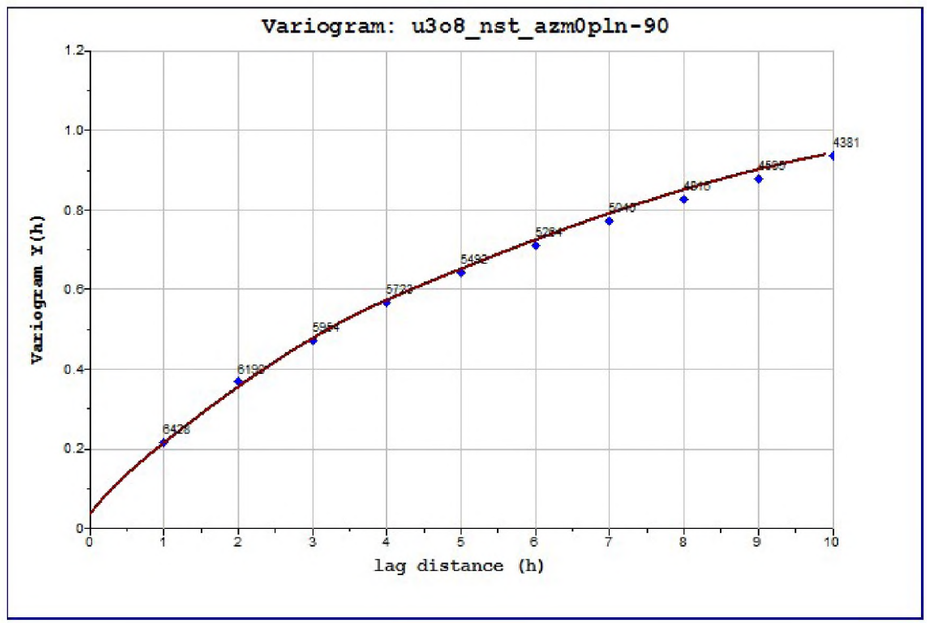

Variogram map

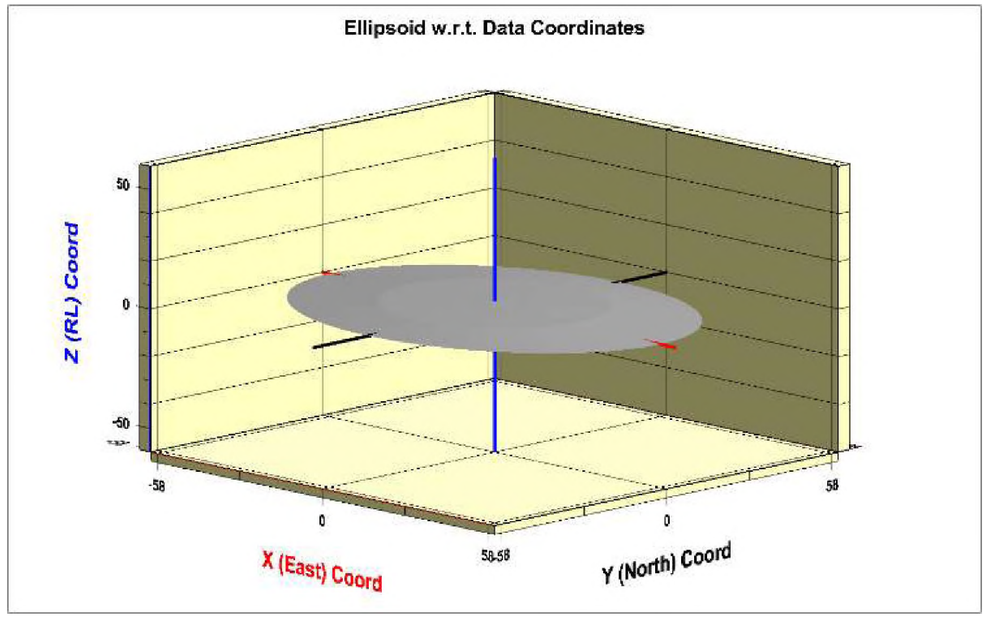

Figure 29: Variography of OK of 50 m x 50 m x 3 m block model

Variograms in OK were created along and across strike as well as downhole. Most variograms observed in Figure 26 to Figure 29 as mentioned previously indicated zonal isotropy along and across strike, whilst the downhole variograms showed more geometrical isotropy with regards to its shape. The zonal isotropy is caused when the sill value is never reached or reaches the expected value (Rossi & Deutsch, 2014). It should be noted that the small number above the points in the variograms represent the number of samples used for the construction of that section within the variogram. The search radius used was mostly less than twice the drill spacing. It is interesting to note, similarly to the CS variography, that the variograms constructed downhole match much easier with the sample points. The across and along strike variograms often result in a variogram of best fit. Variograms usually exhibit a low nugget effect between 0,1 and 0,2. A short and long structure in the along and across strike variograms are visible. The gradient of the long structures is steeper in the larger drill spacing compared to the smaller spaced drill grids.

5.4.4 Multiple indicator kriging data preparation

MIK is a long and extensive method that requires various steps of data processing throughout to be done correctly. These are MP3 and GS3 respectively in which all the variography and analysis is done. 14 different variograms were constructed on each of the various drill spacing. The probability threshold included 0.1, 0.2, 0.3, 0.4, 0.5, 0.6, 0.7, 0.75, 0.8, 0.85, 0.9, 0.95, 0.97 and 0.99. A total of 14 cut-off values were therefore created. These were 0, 100, 150, 200, 250, 300, 350, 400, 450, 500, 550, 600, 650 and 900 ppm for which a variogram of each cut off was constructed. It is therefore clear that a total of 42 (14 across and 14 along strike, 14 downhole) variograms were constructed for each drill spacing and therefore a total of 168 were constructed. The variograms presented in Figure 30 are the variograms modelled downhole for the 4 m x 4 m drill spacing. The variograms have an average nugget effect of around 0,08 to 0,38 and increase slightly with higher-grades. The variograms flatten out at a sill of 1,0 and displayed zonal anisotropy with an exponential model. This is observed in the variograms along and across strike as well, but due to the decrease in data availability these variograms show less continuity. The variograms consist of a short steep first structure followed by a longer gentle structure. These variograms in general have a less steep gradient compared to those of pit H1, hence the range is longer. This a common feature in directional variograms that indicate geometric anisotropy where the sill is more or less the same, however, the ranges differ (Rossi & Deutsch, 2014).

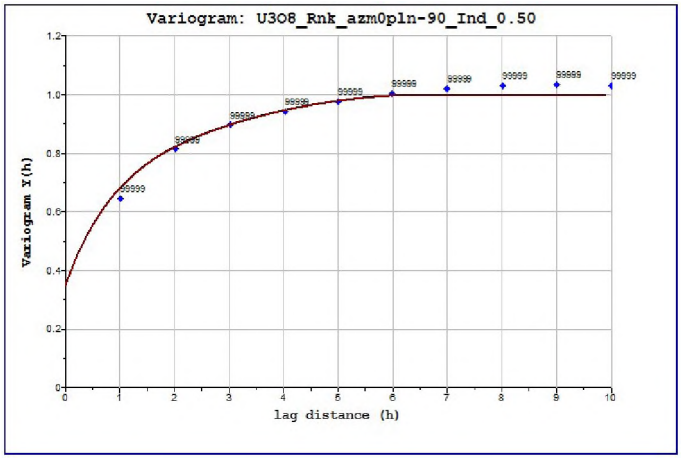
Variogram: U3O8_Rnk_azm0pln-90_Ind_0.50
Variogram Y(h)
lag distance (h)

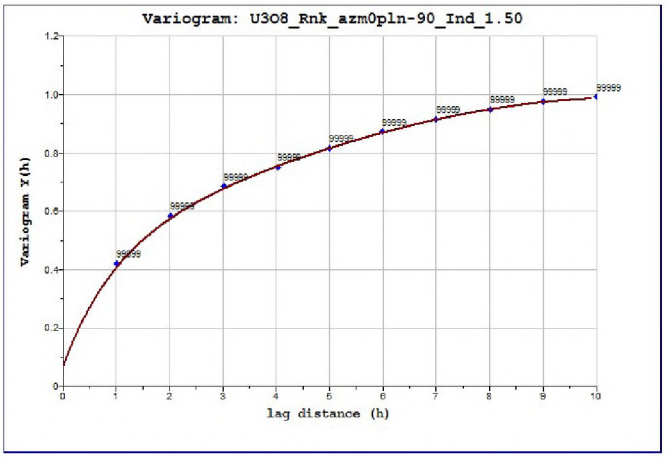
Variogram: U3O8_Rnk_azm0pln-90_Ind_1.50
Variogram Y(h)
lag distance (h)

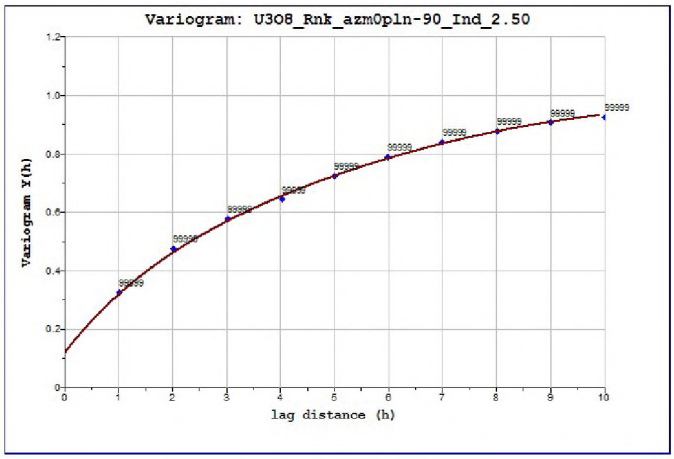
Variogram: U3O8_Rnk_azm0pln-90_Ind_2.50
Variogram Y(h)
lag distance (h)

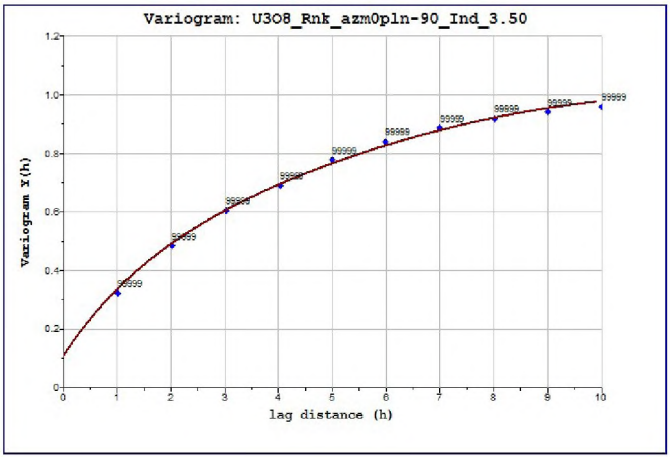
Variogram: U3O8_Rnk_azm0pln-90_Ind_3.50
Variogram Y(h)
lag distance (h)

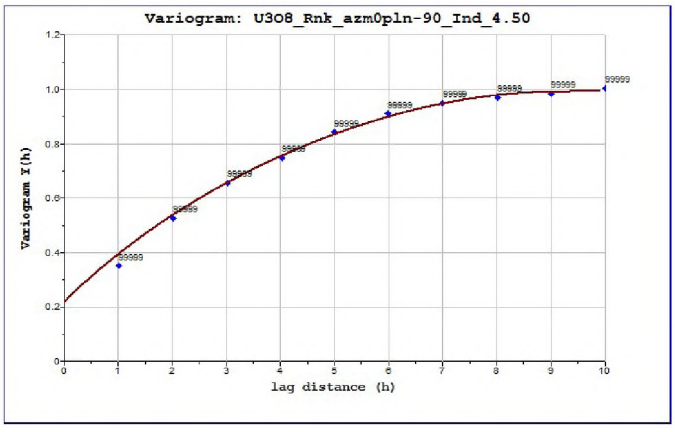
Variogram: U3O8_Rnk_azm0pln-90_Ind_4.50
Variogram Y(h)
lag distance (h)

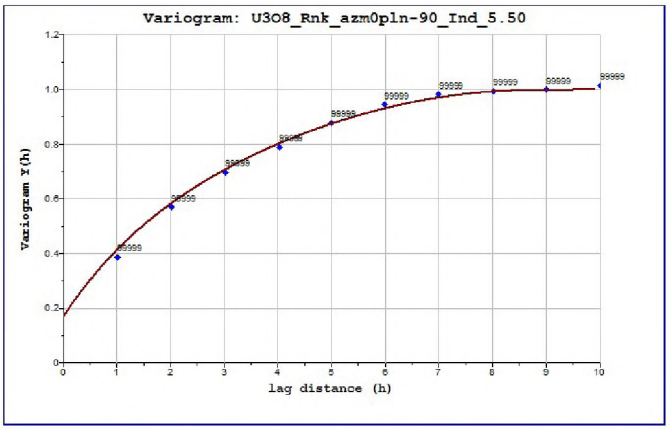
Variogram: U3O8_Rnk_azm0pln-90_Ind_5.50
Variogram Y(h)
lag distance (h)

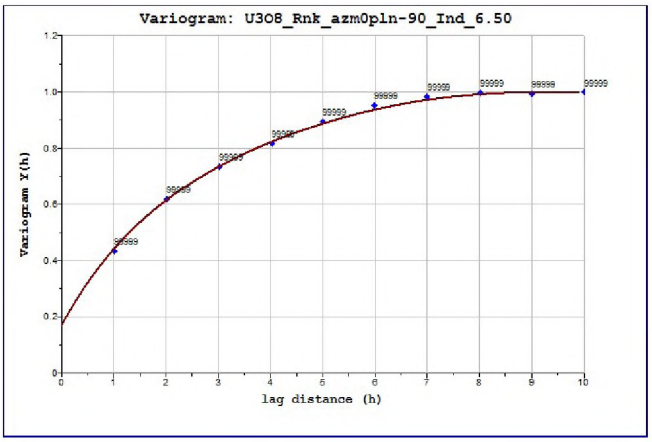
Variogram: U3O8_Rnk_azm0pln-90_Ind_6.50
Variogram Y(h)
lag distance (h)

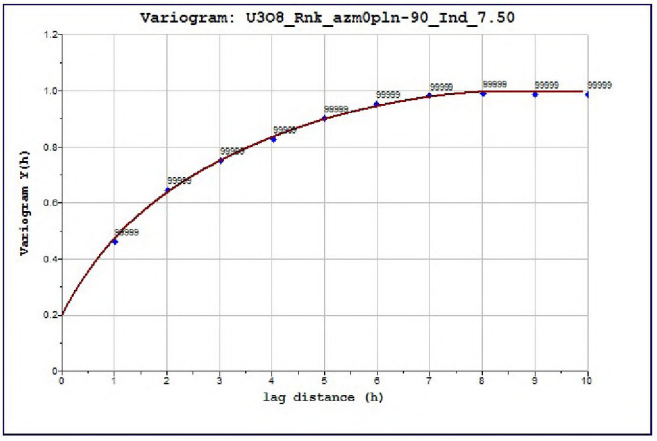
Variogram: U3O8_Rnk_azm0pln-90_Ind_7.50
Variogram Y(h)
lag distance (h)

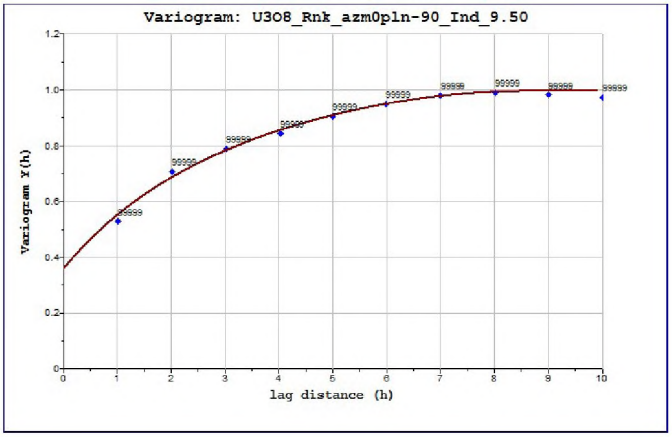
Variogram: U3O8_Rnk_azm0pln-90_Ind_9.50
Variogram Y(h)
lag distance (h)

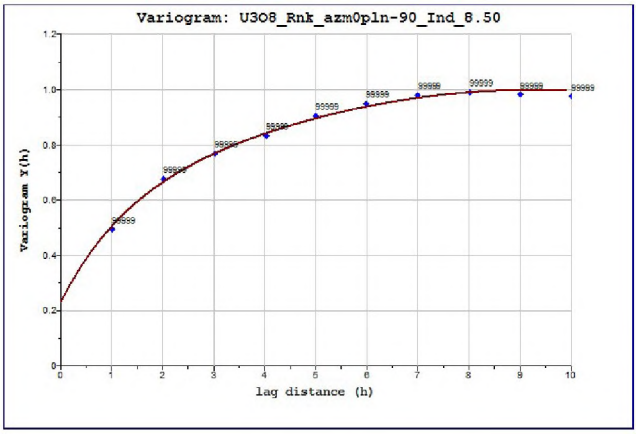
Variogram: U3O8_Rnk_azm0pln-90_Ind_8.50
Variogram Y(h)
lag distance (h)

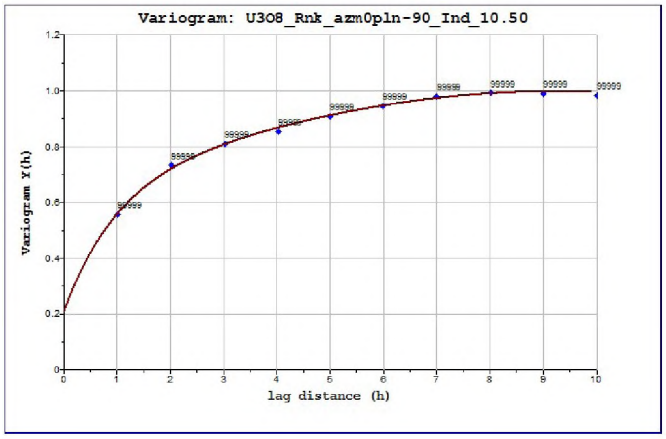
Variogram: U3O8_Rnk_azm0pln-90_Ind_10.50
Variogram Y(h)
lag distance (h)

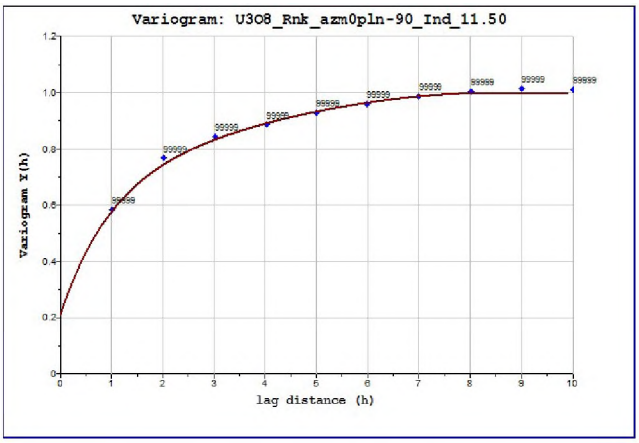
Variogram: U3O8_Rnk_azm0pln-90_Ind_11.50
Variogram Y(h)
lag distance (h)

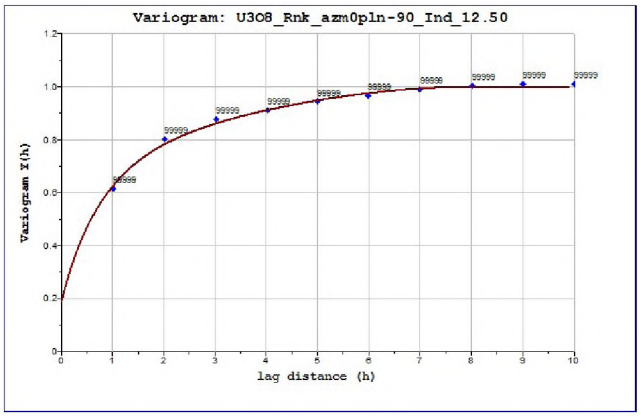

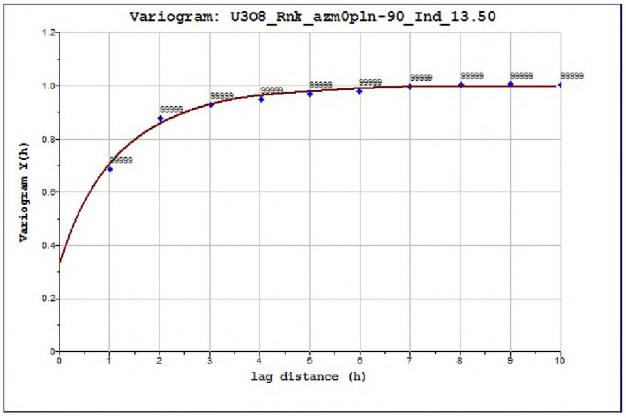

Figure 30: Downhole variography of 4 m x 4 m MIK data

5.4.5 Basic statistics on various estimation methods

Original dataset

Table 15: Statistics on the original unmodified point dataset

		4 m x 4 m x 3 m	12,5m x 12,5m x 3 m	25m x 25m x 3m	50 m x 50 m x 3 m
Number of points used		570 702	87 735	23 101	6 684
Mean	**ppm**	304.2	215.4	204.8	166.7
Coefficient of variation		2.3	2.5	2.5	2.4
Standard deviation		699.6	548.4	515.7	399.9
Q1	**ppm**	11.2	8.1	7.9	7.6
Median		115.1	42.1	36.2	27.3
Q3		347.8	235.7	216.6	163.9
Maximum		32 146.2	32 038.1	14 974.7	13 670.2

Table 15 illustrates the raw dataset of each individual drill spacing for pit G1. It is evident that there is a substantial decrease in data used for the larger block models compared to the blast block data at a 4 m x 4 m spacing. All of the other statistics follow the same trend and, therefore, with the decrease in data availability there is a decrease in subsequent grade which is related to the data support factor. A decrease in the mean grade of about 140 ppm can be observed. The standard deviation decreases by almost 300 ppm throughout. The Q1, Q3 and median values are important indicators as well and show a general decrease in value from the smaller block models towards the larger block models. The maximum values do contain some importance as they indicate the highest grades contained in the dataset. This would signal outlier values which can be interpreted and removed from the cumulative frequency diagrams if need. Removal of outliers or capping outliers is one method of handling outliers in the industry, however this could result in loss of viable data. Another method is domaining, which allows for the control of the affect that these outliers have on the dataset as such. The third method allows for incorporating these outliers into the estimation with certain restrictions on the spatial influence of the dataset (Runge Pincock Minarco Global, 2016). This is especially evident in deposits where the majority of the ore is of lower grade, however, small quantities of the ore is of relatively high grade. Although incorporated, these high grades should be constrained usually by means of improvised search ellipsoids (Runge Pincock Minarco Global, 2016). During this research, capping was used and would therefore eliminate the outliers above a certain grade.

Conditional simulation block model data

Table 16: Statistics of the CS simulated block model

		4 m x 4 m x 3 m block model
Number of points used		570 535
Blocks created		176 769
Mean	**ppm**	291.5
Coefficient of variation		1.1
Standard deviation		319.8
Q1	**ppm**	75.1
Median		195.0
Q3		401.1
Maximum		5 087.3

Table 16 illustrates the statistics obtained from the simulation model. Clearly visible is the decreased number of blocks created by the simulation. This amounts to almost 25 000 difference between the other models. The mean is substantially higher than the other models at this block model dimension. This trend can be observed throughout the statistics where CS does have somewhat higher estimated grades than any other methods. The maximum grade, though, is one of the lowest, with only MIK being lower than 4 000 ppm.

Ordinary kriging block model data

Table 17: Statistics of the OK estimated block models

		4 m x 4 m x 3 m	12,5 m x 12,5 m x 3 m	25 m x 25 m x 3 m	50 m x 50 m x 3 m
Number of points used		570 535	87 735	23 101	6 684
Number of blocks created		200 146	40 315	12 872	4 281
Mean	**Ppm**	242.7	167.1	138.7	109.2
Coefficient of variation		1.5	1.8	1.8	1.6
Standard deviation		366.7	302.2	245.5	178.8
Q1	**ppm**	22.1	13.7	13.3	12.9
Median		125.3	46.5	38.3	32.3
Q3		329.8	200.5	153.9	117.3
Maximum grade		7 130.9	5 591.5	4 350.1	2 237.2

The expected trend of decreasing blocks created with increasing block dimensions can be noted here in Table 17 as is observed in the other methods. This is a function of the decreased data availability and larger block dimensions. There is a rapid decrease in the mean grade which drops

from 242 to 109 ppm at the largest block dimensions. There is a large drop in the standard deviation from about 366 to 179 ppm as the block dimensions increase. The quantile values show the same decreasing trend. A massive decrease in the maximum grade can be seen with a difference of about 5 000 ppm. This is often dependent on the data that was chosen for estimation and therefore is not really dependent on the drill spacing.

IDW^2 block model data

Table 18: Statistics of the IDW^2 estimated block models

		4 m x 4 m x 3 m	12,5 m x 12,5 m x 3 m	25 m x 25 m x 3 m	50 m x 50 m x 3 m
Number of data points used		570 535	87 735	23 101	6 684
Number of blocks created		202 461	44 519	13 968	4 586
Mean	**ppm**	245.0	153.6	130.6	108.1
Coefficient of variation		1.4	1.9	1.9	1.6
Standard deviation		354.4	287.4	251.1	174.0
Q1	**ppm**	23.6	10.9	10.1	11.7
Median		135.8	39.2	30.9	31.2
Q3		336.2	182.7	140.0	122.5
Maximum grade		7 267.4	7 869.6	4 246.3	1 946.4

IDW^3 block model data

Table 19: Statistics of the IDW^{3}estimated block model

		4 m x 4 m x 3 m	12,5 m x 12,5 m x 3 m	25 m x 25 m x 3 m	50 m x 50 m x 3 m
Number of data points used		570 535	87 735	23 101	6 684
Number of blocks created		202 461	44 519	13 968	4 586
Mean	**ppm**	244.4	153.1	129.7	106.7
Coefficient of variation		1.5	2.0	2.1	2.1
Standard deviation		364.7	303.6	267.5	175.6
Q1	**ppm**	22.3	10.2	9.5	11.3
Median		131.0	36.0	27.9	29.2
Q3		331.9	175.7	131.2	118.4
Maximum grade		8 188.3	9 660.9	5 115.0	1 988.2

From Table 18 and Table 19 it can clearly be observed that the results of IDW^2 and IDW^3 are very similar in their outcomes. Interesting to note is the maximum grade obtained. In both cases the 12,5 m x 12,5 m x 3 m block models have increased grades compared to the 4 m x 4 m x 3 m block models. This is unusual as the trend usually decreases in grade with increased block sizes. Both the mean and median have similar values in both methods and exhibit the same trend with decreasing grades of increased block sizes. The mean grade observed decreases from 245 ppm to 108 ppm from the smallest to the largest block model. This is a substantial loss in estimated grade with decreased drilling, although tonnages of lower grades might increase resulting in similar final metal estimates. The standard deviation of IDW^3 is slightly higher than that of IDW^2, but both methods do indicate the same trend which decreases in grade from the smaller to the larger block models.

MIK block model data

Table 20: Statistics of the MIK estimated block models

		4 m x 4 m x 3 m	12,5m x 12,5m x 3 m	25m x 25m x 3 m	50m x 50m x 3 m
Number of points used		570 535	87 735	23 101	6 684
Number of blocks created		217 510	40 955	12 817	3 461
Mean	**ppm**	247.1	175.7	149.8	133.4
Coefficient of variation		1.4	1.5	1.6	1.5
Standard deviation		337.9	268.0	234.2	197.7
Q1	**ppm**	48.4	28.3	22.8	21.5
Median		135.9	68.5	55.5	49.7
Q3		323.0	210.6	170.9	161.0
Maximum grade		4 953.3	2 769.0	2 467.4	1 935.1

Table 20 provides the univariate statistics from the various block models that were constructed during the MIK procedure at different drill spacing. From the 4 m x 4 m x 3 m dataset to the 50 m x 50 m x 3 m dataset there is a drop in the mean grade of about 140 ppm. This a substantial amount of uranium that is gained or lost with drilling. Increased drilling would usually increase the resource grade, whilst less drilling would usually give lower average grades. Also of importance is the maximum grade observed in the block models. Besides the general decrease as observed throughout from the smaller to the larger block models, the maximum grades are lower compared to the other methods.

5.4.6 Rank percentile graphs of various block models

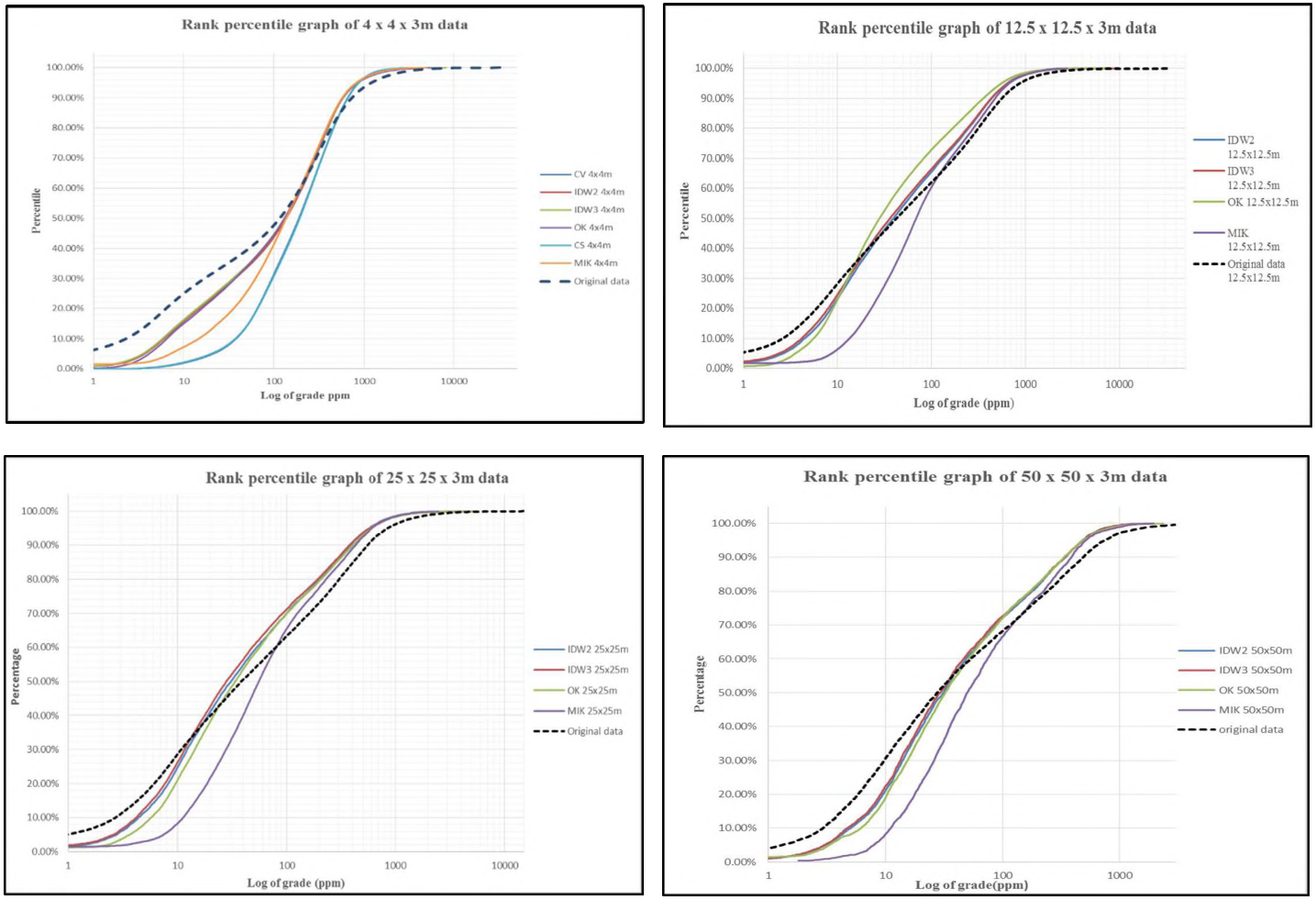

Figure 31: Rank percentile graphs of different estimation methods on different block

The rank percentile graphs illustrated in Figure 31 were used to plot individual estimation methods against the unmodified original data indicated by the black dashed line. These were plotted on different spacing to illustrate the difference between the narrow and wider drill spacing. The aim of the rank percentile graph was to find out the degree of smoothing of the different methods at different drill spacing. This would be illustrated by a deviation of the individual methods from the original data. Noticeable between all methods is the abundance of overestimation of the various methods compared to the original dataset at the specific drill spacing. This is especially visible at the lower grades and can be traced to a frequency of up to 50 %. This is most evident on the 4 m x 4 m and 50 m x 50 m drill spacing.

From a frequency of 50 % or 100 ppm upwards there is a stage in which the estimation methods correspond to the estimation methods at most of the drill spacing. This is only visible for a short time before the estimation methods start to underestimate. The underestimation is much less at the higher-grades than the overestimation at lower grades. This is preferential as the higher-grades determine the profitability of a mine and knowing where these are is of great interest. The greatest range of overestimation is at lower grades which can be observed in the tighter drilling grids. Subsequently the higher-grades follow the original data trend which is preferential. On the broader drill spacing underestimation of higher-grades is more evident.

The methods with highest overestimation compared to the original data are CS and MIK respectively on the tighter drill spacing and only MIK on the broader drilling spacing. CS as mentioned before was not used for modelling the exploration datasets. IDW^2, IDW^3 and OK all follow similar trends at lower grades and resemble the original dataset more closely. The difference can most likely be attributed to the fact that MIK is a non-linear estimation method, whilst both IDW and OK are linear estimations methods. For the high-grades most of the methods follow the trend of the original data. It is observed that only OK underestimates substantially in the 12,5 m x 12,5 m dataset compared to the original dataset. The 25 m x 25 m dataset in general contains the highest underestimation compared to the other datasets. None of the methods stand out in terms of underestimating above average.

Plotted in Figure 32 are the rank percentile graphs of the individual methods used during estimation. Each graph illustrates the method only compared to different drill spacing. Previously the different methods were described on the same drill spacing dataset to see how they deviate from the original data. Here one can observe how the method deviates from the original 4 m x 4

m dataset. From Figure 32 the two IDW methods indicate a very similar trend with no real observable difference between them. At lower grades there is usually some overestimation compared to the original dataset. The larger grid spacing deviates and intersects the original dataset trend between 10 to 100 ppm, whilst the smaller 4 m x 4 m dataset continues overestimating up to just over 100 ppm. The larger drill spacing continues underestimating over most of the higher-grades before converging only after a 1 000 ppm. These grades make up only a small part of the deposit. There is a subtle downsize of underestimation between the 12,5 m x 12,5 m dataset and the larger exploration dataset. The 4 m x 4 m dataset is quite different and follows the original dataset in close proximity. This is expected due to the finer drill spacing and should be representative of reality.

The trend described above is also observed for OK and MIK. For the OK diagram the only observed difference would be the 12,5 m x 12,5 m dataset that is performing similarly to the exploration drilling dataset for grades higher than 10 ppm. MIK however does show differences from the other methods. It overestimates more for the lower grades and drags on for longer well above 10 ppm before the exploration (broader spaced) dataset starts converging towards the original dataset trend. This happens roughly between 10 and 100 ppm. The 4 m x 4 m dataset follows the same general trend as the previous methods, however it continues overestimating for longer. Another observable aspect is the underestimation of the higher-grades from about 75 ppm and higher. The larger grid datasets follow the original dataset's trend closer than the other methods. The 12,5 m x 12,5 m dataset does observably better than in any other methods.

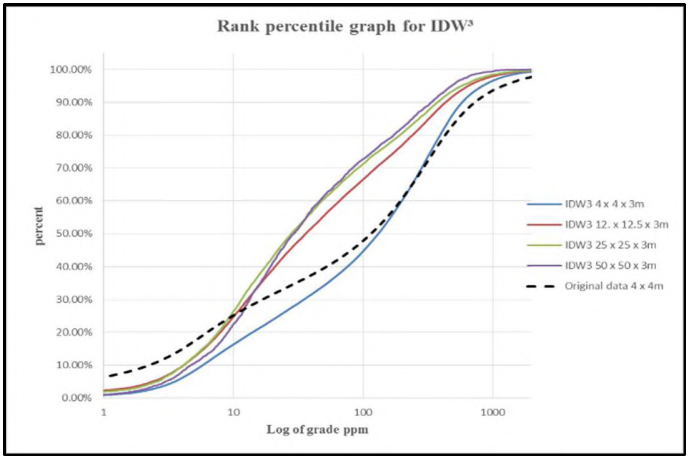

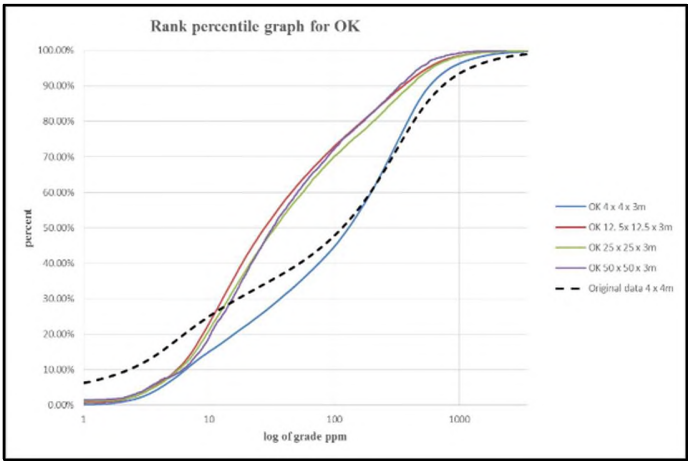

Figure 32: Rank percentile graphs of various methods

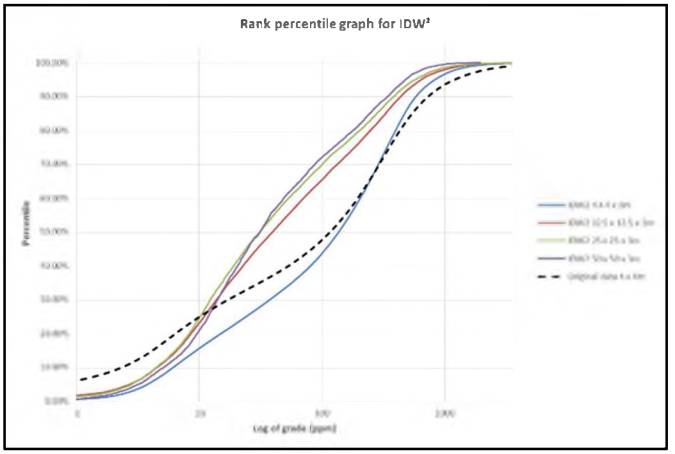
Rank percentile graph for IDW²
Percentile
Log of grade (ppm)

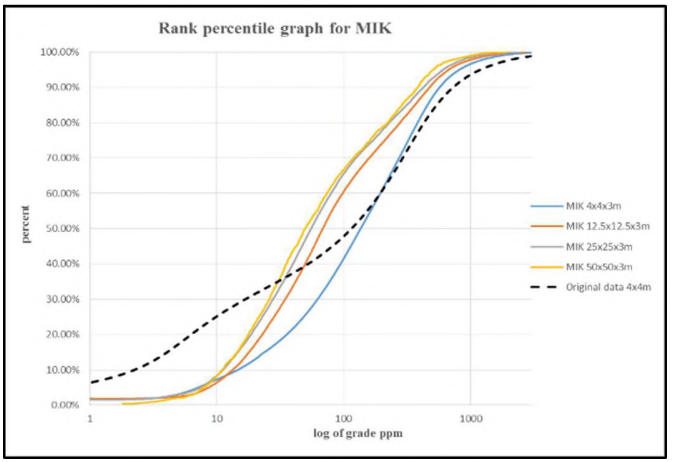
Rank percentile graph for MIK
100.00%
90.00%
80.00%
70.00%
60.00%
50.00%
40.00%
30.00%
20.00%
10.00%
0.00%
percent
1
10
100
1000
log of grade ppm
MIK 4x4x3m
MIK 12.5x12.5x3m
MIK 25x25x3m
MIK 50x50x3m
Original data 4x4m

5.5 Block model report

Table 21: Final block model report on various geostatistical methods and different block dimensions indicating total tonnages including waste

	IDW² (t)	IDW³ (t)	OK (t)	MIK (t)	CS (t)	Mined tonnes	Wireframe estimated tonnes
4 m x 4 m x 3 m	16 498 820	16 495 327	16 597 522	16 816 768	16 019 042	16 228 887	17 126 265
12,5 m x 12,5 m x 3 m	16 980 581	16 971 851	17 015 660	17 025 986	-		
25 m x 25 m x 3 m	17 004 113	17 003 282	17 033 791	17 056 563	-		
50 m x 50 m x 3 m	17 062 275	17 062 275	17 074 372	17 002 554	-		

The bar graph (Figure 33) illustrates the total tonnages from Table 21 that were estimated by the various methods on the different drill spacing. These can now be compared to each other and to the true mined tonnages, which is illustrated as a green bar. Also illustrated is the estimated tonnage contained within the final wireframe of the mined out pit. These three figures can be compared to each other and see whether the methods have overestimated or underestimated. The actual mined tonnes would be a representation of reality. This figure is subject to various errors that do occur in any mining procedure. The Wireframe (WF) mined tonnage should be a good representation of the actual mined tonnage that was removed from the in situ rock. From the pit shell and the surface collar co-ordinates a volume can be calculated from which a tonnage could be determined by using a density of 2,4g/cm³.

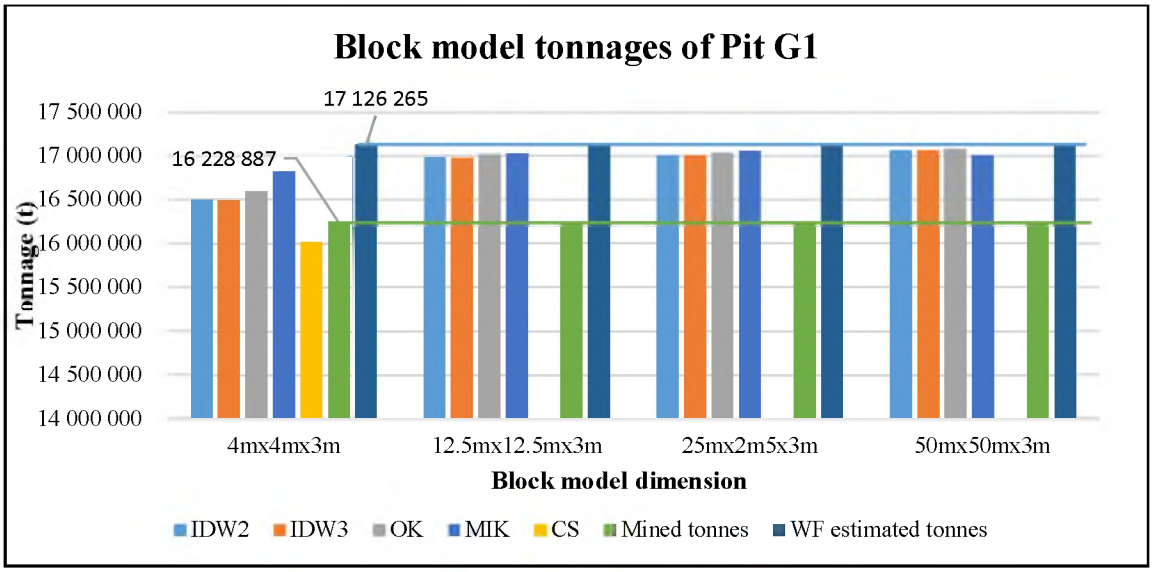

Figure 33: Estimated tonnage vs. mined tonnage vs. final wireframe tonnage

From Figure 34 it can be observed that the mined tonnage is 897 378 t less than what the WF estimated or 5%. This is usually an accepted standard for reporting measured resources. Most of the estimates used during this research fall somewhere between these two ranges, which is a good indication. With focus on the smaller drill spacing of 4 m x 4 m it can be clearly observed that the most variation is found within this category. CS was by far the most conservative method with a total estimation of just over 16 Mt, whilst MIK boasts over 16,8 Mt. OK and IDW all fall in the range of 16,5 Mt, which is close to the actual mined tonnage. All of the tonnages created from the 12,5 m x 12,5 m x 3 m, 25 m x 25 m x 3 m and 50 m x 50 m x 3 m models are remarkably similar and are around 17 Mt. There is a slight increase in tonnages as the drill spacing increases, which is minimal compared to the total tonnages.

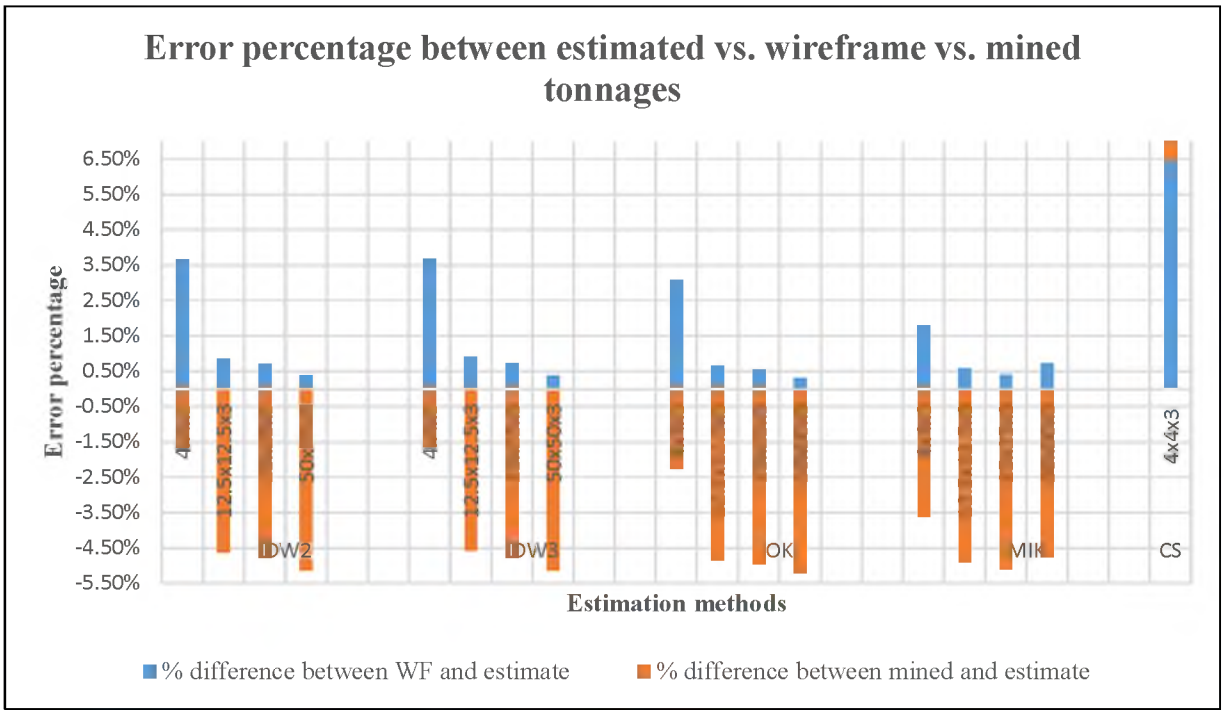

Figure 34: Error percentage between estimates and mined tonnage, and estimated tonnage vs. wireframe tonnage

The graph illustrated in Figure 34 is a representation of the percentage error between the WF tonnage estimation and the difference between the estimated tonnages. Also shown is the difference between the mined tonnages and the estimated tonnages. The difference in tonnages between the various methods and the WF is generally below 4 %. Only CS has an error difference of just over 6%. The lowest is MIK at less than 2 %. It can clearly be observed that the 4 m x 4 m x 3 m block models have the highest error margin, which as stated previously is just less than 4 %. The larger block models have errors of 1 % and less, which is a good indication that most of the

tonnages or volume from the representative pit have been included in the estimate. The error margins between the actual mined figure and the estimated tonnage are usually negative, hence indicating that the methods do overestimate somewhat. This is especially noticeable in the larger block models, where the estimated error does not exceed -6 % on average.

Table 22: Block model report at various grade categories

	Block model dimensions (m)	0-250 ppm Tonnage	Average grade (ppm)	250-400 ppm Tonnage	Average grade (ppm)	400-650 ppm Tonnage	Average grade (ppm)	650-900 ppm Tonnage	Average grade (ppm)	900+ ppm Tonnage	Average grade (ppm)
IDW²	4 x 4 x 3	10 180 664	79.5	2 621 411	319.5	2 125 059	500.3	727 960	757.5	843 726	1499.1
	12,5 x 12,5 x 3	9 445 411	79.8	2 904 165	321.3	2 533 518	506.9	973 849	755.6	1 123 637	1440.9
	25 x 25 x 3	9 397 882	81.8	3 009 346	319.7	2 490 781	497.8	1 056 713	752.1	1 049 392	1374.9
	50 x 50 x 3	9 415 448	87.5	3 330 418	325.8	2 929 660	502.3	908 272	751.4	478 477	1117.7
IDW³	4 x 4 x 3	10 245 124	78.4	2 594 539	319.4	2 084 131	501.3	708 956	756.8	862 576	1524.6
	12,5 x 12,5 x 3	9 590 956	79.0	2 873 038	320.9	2 390 523	506.2	980 737	757.1	1 136 596	1500.2
	25 x 25 x 3	9 645 473	80.6	2 941 183	320.4	2 286 919	499.7	1 027 069	752.6	1 102 637	1447.9
	50 x 50 x 3	9 545 729	88.2	3 187 738	326.4	2 914 722	503.4	874 457	746.9	539 627	1113.1
OK	4 x 4 x 3	10 318 120	74.6	2 535 054	320.0	2 100 591	501.8	752 817	756.9	890 939	1532.2
	12,5 x 12,5 x 3	9 529 217	74.2	2 636 999	319.7	2 621 476	505.7	1 064 875	755.4	1 064 875	1476.3
	25 x 25 x 3	9 481 661	77.5	2 732 399	322.9	2 710 076	501.2	1 111 615	756.5	998 041	1347.9
	50 x 50 x 3	9 745 292	83.1	3 039 831	320.2	2 869 657	496.9	899 983	734.7	899 983	1203.0
MIK	4 x 4 x 3	10 437 232	87.7	2 576 298	320.3	2 122 432	502.0	884 347	757.4	936 209	1498.7
	12,5 x 12,5 x 3	9 383 065	82.8	2 598 589	323.1	2 792 159	505.3	1 070 627	754.5	1 181 545	1350.1
	25 x 25 x 3	9 389 346	84.7	2 675 929	325.3	2 792 210	504.9	1 147 068	760.3	1 052 009	1269.5
	50 x 50 x 3	9 688 794	87.7	2 995 903	324.5	2 881 470	491.7	656 023	755.9	780 363	1158.4
CS	4 x 4 x 3	8 698 970	101.4	2 761 375	319.5	2 595 090	509.6	1 085 921	756.6	877 686	1321.4
Mined		**9 456 698**	**115.3**	**2 624 985**	**357.7**	**2 304 857**	**470.8**	**1 844 347**		**905.0**	

Table 22 illustrates the grade categories of waste, low, medium, high and super high-grade of various estimation methods. The average grade within the category is also specified within the different subdivisions. The waste category contains tonnages between 9,3 Mt and up to 10,4 Mt. Most of the different methods as well as the resultant block models at different spacing fall within this range, except CS which estimated a value below 9 Mt. One distinguishing realization is that the smaller block models estimate the highest waste tonnages typically around 10 Mt. It is however not observed that the larger block models estimate the lowest waste tonnages as would be expected. Grades within the waste category usually average between 75 and 87 ppm. The low-grade category

usually obtained estimates between 2,5 - 3,1 Mt at grades of about 320 ppm. Here it can be observed that the mined low-grade was 30 ppm higher. Medium-grade estimates, as well as the mined tonnages, are mostly consistent at around 2,3 - 2,9 Mt. The mined tonnage falls perfectly into this bracket at 2,5 Mt. The average grade herein is around 505 ppm. The high and super high-grade trends are somewhat different. It can clearly be observed that the 4 m x 4 m x 3 m and 50 m x 50 m x 3 m block models estimated the lowest tonnages compared to the two intermediate block models. The grades however are very similar at about 755 ppm for high-grade and fluctuating between 1 150 and 1 500 ppm for super high-grade. The mined tonnage is calculated as a high-grade category only. It reflects the averages that the 4 m x 4 m x 3 m and 50 m x 50 m x 3 m block models estimated and suggests that the two intermediate block models might have overestimated.

5.5.1 Estimated or simulated tonnage versus mined tonnage variances

Table 23: 4 m x 4 m x 3 m estimated tonnage and mined tonnage

Estimation method	Estimated Waste (t)	Tonnage difference (Mine vs. estimate) %	Estimated LG (t)	Tonnage difference (Mine vs. estimate) %	Estimated MG (t)	Tonnage difference (Mine vs. estimate) %	Estimated HG (t)	Tonnage difference (Mine vs. estimate) %
IDW^2	10 180 664	-7.1	2 621 411	0.1	2 125 059	8.5	1 571 686	17.3
IDW^3	10 245 124	-7.7	2 594 539	1.2	2 084 131	10.6	1 571 532	17.4
OK	10 318 120	-8.3	2 535 054	3.5	2 100 591	9.7	1 643 756	12.2
MIK	10 437 232	-9.4	2 576 298	1.9	2 122 432	8.6	1 820 556	1.3
CS	8 698 970	8.7	2 761 375	-4.9	2 595 090	-11.2	1 963 607	-6.1
Average (t)	**9 976 022**	**-5.2**	**2 617 735**	**0.3**	**2 205 461**	**4.5**	**1 714 227**	**7.6**
Mined tonnage	**9 456 698**		**2 624 985**		**2 304 857**		**1 844 347**	

Table 24: 12,5 m x 12,5 m x 3 m estimated tonnage and mined tonnage

Estimation method	Estimated Waste (t)	Tonnage difference (Mine vs. estimate) %	Estimated LG (t)	Tonnage difference (Mine vs. estimate) %	Estimated MG (t)	Tonnage difference (Mine vs. estimate) %	Estimated HG (t)	Tonnage difference (Mine vs. estimate) %
IDW^2	9 445 411	0.1	2 904 165	-9.6	2 533 518	-9.0	2 097 486	-12.1
IDW^3	9 590 956	-1.4	2 873 038	-8.6	2 390 523	-3.6	2 117 333	-12.9
OK	9 529 217	-0.8	2 636 999	-0.5	2 621 476	-12.1	2 129 720	-13.4
MIK	9 383 065	0.8	2 598 589	1.0	2 792 159	-17.5	2 252 172	-18.1
Average (t)	**9 487 162**	**-0.3**	**2 753 198**	**-4.7**	**2 584 419**	**-10.8**	**2 149 178**	**-14.2**
Mined tonnage	**9 456 698**		**2 624 985**		**2 304 857**		**1 844 347**	

Table 25: 25 m x 25 m x 3 m estimated tonnage and mined tonnage

Estimation method	Estimated Waste (t)	Tonnage difference (Mine vs. estimate) %	Estimated LG (t)	Tonnage difference (Mine vs. estimate) %	Estimated MG (t)	Tonnage difference (Mine vs. estimate) %	Estimated HG (t)	Tonnage difference (Mine vs. estimate) %
IDW²	9 397 882	0.6	3 009 346	-12.8	2 490 781	-7.5	2 106 105	-12.4
IDW³	9 645 473	-2.0	2 941 183	-10.8	2 286 919	0.8	2 129 706	-13.4
OK	9 481 661	-0.3	2 732 399	-3.9	2 710 076	-15.0	2 109 656	-12.6
MIK	9 389 346	0.7	2 675 929	-1.9	2 792 210	-17.5	2 199 077	-16.1
Average (t)	**9 478 591**	**-0.2**	**2 839 714**	**-7.6**	**2 569 997**	**-10.3**	**2 136 136**	**-13.7**
Mined tonnage	**9 456 698**		**2 624 985**		**2 304 857**		**1 844 347**	

Table 26: 50 m x 50 m x 3 m estimated tonnage and mined tonnage

Estimation method	Estimated Waste (t)	Tonnage difference (Mine vs. estimate) %	Estimated LG (t)	Tonnage difference (Mine vs. estimate) %	Estimated MG (t)	Tonnage difference (Mine vs. estimate) %	Estimated HG (t)	Tonnage difference (Mine vs. estimate) %
IDW²	9 415 448	0.4	3 330 418	-21.2	2 929 660	-21.3	1 386 749	33.0
IDW³	9 545 729	-0.9	3 187 738	-17.7	2 914 722	-20.9	1 414 084	30.4
OK	9 745 292	-3.0	3 039 831	-13.6	2 869 657	-19.7	1 799 966	2.5
MIK	9 688 794	-2.4	2 995 903	-12.4	2 881 470	-20.0	1 436 386	28.4
Average (t)	**9 598 816**	**-1.5**	**3 138 473**	**-16.4**	**2 898 877**	**-20.5**	**1 509 296**	**22.2**
Mined tonnage	**9 456 698**		**2 624 985**		**2 304 857**		**1 844 347**	

Table 27: Average percentage variance between estimated and mined tonnage

Block model dimension	Average variance % (mined vs. estimated)			
	W	LG	MG	HG
4 m x 4 m x 3 m	-5.2	0.3	4.5	7.6
12,5 m x 12,5 m x 3 m	-0.3	-4.7	-10.8	-14.2
25 m x 25 m x 3 m	-0.2	-7.6	-10.3	-13.7
50 m x 50 m x 3 m	-1.5	-16.4	-20.5	22.2

The tables above (23-27) illustrate the estimated tonnages of the various estimation and simulation methods. These have been placed in a table form of various block dimensions that were calculated using Micromine. The total tonnages have been subdivided into various cut off grades and categories as they are usually stockpiled. The mined tonnage of the various grade categories is also displayed. The importance of the tables above is highlighted by the percentage difference between the estimated and mined tonnages. This will be used to distinguish the difference between estimated or simulated tonnages compared to the actual mined tonnages. The methods used during estimation were all constrained using the final pit shell and thereby limiting the estimated tonnages. Estimated tonnages will therefore not be excessively over or underestimated, which could be the case in early resource estimation.

The 4 m x 4 m x 3 m block models in Table 23 resulted in the lowest variation between the estimated and the overall mined tonnage, which would be expected. All methods overestimated, only CS that underestimated by about 9 %. In the waste category the predicted tonnage was overestimated, resulting in decreased mined tonnage of about 5 %. In the low-grade category, the predictions matched that of the mined tonnage almost exactly. CS slightly overestimated by 5 %, whilst the rest of the methods underestimated by less than 3 %. In the medium-grade category, the average predicted tonnage was underestimated by about 4 %. CS overestimated at about 11 %, whilst the other methods all underestimated at about 9 %. In the high-grade category the same trend can be observed. The average predicted grade was 7 % less than the mined tonnage. CS however overestimated by 6 %, whilst the rest of the methods underestimated by about 14 %. MIK matched the mined tonnage with an underestimation of 1 %.

The 12,5 m x 12,5 m x 3 m block models in Table 24 displayed some elevated variances between predicated and mined tonnages. In the waste category, most of the methods were accurate with some under and overestimating. In the low-grade category an average of 5 % overestimation was calculated, with IDW^2 exhibiting the largest overestimation at 11 %. In the medium-grade category the predicated grade was overestimated by 12 %, with IDW^3 registering the lowest overestimation at 4 %. In the high-grade category the predicated grade was overestimated by a 14 % average, the lowest being IDW^2 at 12 %.

The 25 m x 25 m x 3 m block models in Table 25 displayed similar tonnage predications and variation compared to the12,5 m x 12,5 m x 3 m block models. In the waste category as previously mentioned, the predicted tonnage is on target with the mined tonnages. In the low-grade category all methods overestimated by just under 7 % compared to what was mined. MIK was the lowest at just under 2 %. In the medium-grade category the predicated tonnages were overestimated on average by 10 %, the lowest being IDW^3 at 1 %. In the high-grade category the estimated tonnages resulted in an overestimation of just under 14 %, the lowest being IDW^2 at 12 %.

The 50 m x 50 m x 3 m block models in Table 26 displayed the largest variance predictions, compared to the smaller block models. In the waste category the predicted tonnages were overestimated on average just under 2 %, with IDW^2 the closest to the mined value. In the low-grade category the estimated grade was overestimated by 16 %, with MIK being the lowest at 12%. In the medium-grade category the predicted grade was overestimated at an average of 21 %, with all four methods estimating variances close to the average. In the high-grade category the various

methods all underestimated at an average of 22 %, with OK delivering the most accurate prediction at 3 %. Table 27 provides a summary of the various block dimensions and the related variance between the estimated and mined tonnages.

5.5.2 Estimated or simulated grade versus mined grade variances

Table 28: 4 m x 4 m x 3 m estimated grade vs. average mined grade

Estimation method	Estimated grade Waste (ppm)	ppm difference (mined vs. estimated) %	Estimated grade LG (ppm)	ppm difference (mined vs. estimated) %	Estimated grade MG (ppm)	ppm difference (mined vs. estimated) %	Estimated grade HG (ppm)	ppm difference (mined vs. estimated) %
IDW^2	79.5	45.0	319.5	12.0	500.3	-5.9	1 155.6	-21.7
IDW^3	78.4	47.1	319.4	12.0	501.3	-6.1	1 178.2	-23.2
OK	74.6	54.6	320.0	11.8	501.8	-6.2	1 177.1	-23.1
MIK	87.7	31.5	320.3	11.7	502.0	-6.2	1 138.6	-20.5
CS	101.4	13.7	319.5	12.0	509.6	-7.6	1 009.1	-10.3
Average (ppm)	84.0	37.3	319.7	11.9	503.0	-6.4	1 131.7	-20.0
Mined grade (ppm)	**115.3**		**357.7**		**470.8**		**905.0**	

Table 29: 12,5 m x 12,5 m x 3 m estimated grade vs. average mined grade

Estimation method	Estimated grade Waste (ppm)	ppm difference (mined vs. estimated) %	Estimated grade LG (ppm)	ppm difference (mined vs. estimated) %	Estimated grade MG (ppm)	ppm difference (mined vs. estimated) %	Estimated grade HG (ppm)	ppm difference (mined vs. estimated) %
IDW^2	79.8	44.5	321.3	11.3	506.9	-7.1	1 122.7	-19.4
IDW^3	79.0	45.9	320.9	11.5	506.2	-7.0	1 156.0	-21.7
OK	74.2	55.4	319.7	11.9	505.7	-6.9	1 115.9	-18.9
MIK	82.8	39.3	323.1	10.7	505.3	-6.8	1 067.0	-15.2
Average (ppm)	79.0	45.9	321.3	11.3	506.0	-7.0	1 115.4	-18.9
Mined grade (ppm)	**115.3**		**357.7**		**470.8**		**905.0**	

Table 30: 25 m x 25 m x 3 m estimated grade vs. average mined grade

Estimation method	Estimated grade Waste (ppm)	ppm difference (mined vs. estimated) %	Estimated grade LG (ppm)	ppm difference (mined vs. estimated) %	Estimated grade MG (ppm)	ppm difference (mined vs. estimated) %	Estimated grade HG (ppm)	ppm difference (mined vs. estimated) %
IDW²	81.8	41.0	319.7	11.9	497.8	-5.4	1 062.4	-14.8
IDW³	80.6	43.1	320.4	11.6	499.7	-5.8	1 112.6	-18.7
OK	77.5	48.8	322.9	10.8	501.2	-6.1	1 036.3	-12.7
MIK	84.7	36.1	325.3	10.0	504.9	-6.8	1 003.9	-9.9
Average (ppm)	81.2	42.0	322.1	11.1	500.9	-6.0	1 053.8	-14.1
Mined grade (ppm)	**115.3**		**357.7**		**470.8**		**905.0**	

Table 31: 50 m x 50 m x 3 m estimated grade vs. average mined grade

Estimation method	Estimated grade Waste (ppm)	ppm difference (mined vs. estimated) %	Estimated grade LG (ppm)	ppm difference (mined vs. estimated) %	Estimated grade MG (ppm)	ppm difference (mined vs. estimated) %	Estimated grade HG (ppm)	ppm difference (mined vs. estimated) %
IDW²	87.5	31.8	325.8	9.8	502.3	-6.3	877.8	3.1
IDW³	88.2	30.7	326.4	9.6	503.4	-6.5	886.6	2.1
OK	83.1	38.7	320.2	11.7	496.9	-5.3	968.9	-6.6
MIK	87.7	31.5	324.5	10.2	491.7	-4.3	974.6	-7.1
Average (ppm)	86.6	33.1	324.2	10.3	498.6	-5.6	927.0	-2.1
Mined grade (ppm)	**115.3**		**357.7**		**470.8**		**905.0**	

Table 32: Average percentage variance between estimated and mined grade

Block model dimension	Average variance % (mined vs. estimated)			
	W	LG	MG	HG
4 m x 4 m x 3 m	37.3	11.9	-6.4	-20.0
12,5 m x 12,5 m x 3 m	45.9	11.3	-7.0	-18.9
25 m x 25 m x 3 m	42.0	11.1	-6.0	-14.1
50 m x 50 m x 3 m	33.1	10.3	-5.6	-2.1

The 4 m x 4 m x 3 m block models in Table 28 indicate the estimated grade from the smallest drill spacing. The waste category underestimated on average about 37 %, with CS substantially lower at 14 %. In the low-grade category the average grade was underestimated just under 12 %, with all five methods with similar results. In the medium-grade category the predicted grade was overestimated at just under 7 %. The high-grade category indicated an overestimation of over 20 %, however CS only resulted in an overestimation of 10 %. There could be a number of reasons

to this extreme difference. It would seem that with more data availability the higher the estimated grade within the grade category. With mining operations however, various factors such as over or undermining of ore blocks can cause significant downgrading of grades and is therefore the most likely cause of the high error difference. Volume variance would be another factor that could add to the error difference which would cause the estimated grades to average out as less data is available and therefore matching the mined grade.

The 12,5 m x 12,5 m x 3 m block model is indicated in Table 29. In the waste category there was a general underestimation of 46 %, with all methods estimating a value around that average. In the low-grade category the estimated grade was 11 % below the mined grade. In the medium category the predicated grades difference was substantially lower at 7 % above the mined grade. In the high-grade category the predicated grade was overestimated at around 19 %. All of the methods had similar outcomes in their respective estimated versus mined grade comparisons.

In Table 30 the 25 m x 25 m x 3 m block model results are illustrated. In the waste category the methods on average underestimated around 42 %. In the low-grade category the predicated grade was 11% less than the mined grade. In the medium-grade category the predicated grade was 6 % more than the mined grade. The anticipated grade for the high-grade category was 14 % more than the mined grade, with MIK the lowest at 11 %. These results are similar to those of the 12,5 m x 12,5 m x 3 m block models above.

Table 31 illustrates the 50 m x 50 m x 3 m block model grade versus mined values. In the waste grade category, the average grade was estimated at 33 % less than the mined grade. The low-grade category suggested relatively good results and indicated a mined grade of 10 % more than the estimated grades. The block model predicated the most accurate grades in the medium category at just under 6 % more than the mined grade. The high-grade category also performed the best with an average of just over 2 % more than the mined grade. MIK and OK did reasonably well with a mined grade of just 7 % less than the estimated grade. Table 32 provides a conclusive summary between the estimated and actual mined grade.

5.6 Grade-Tonnage (GT) plots of various block models

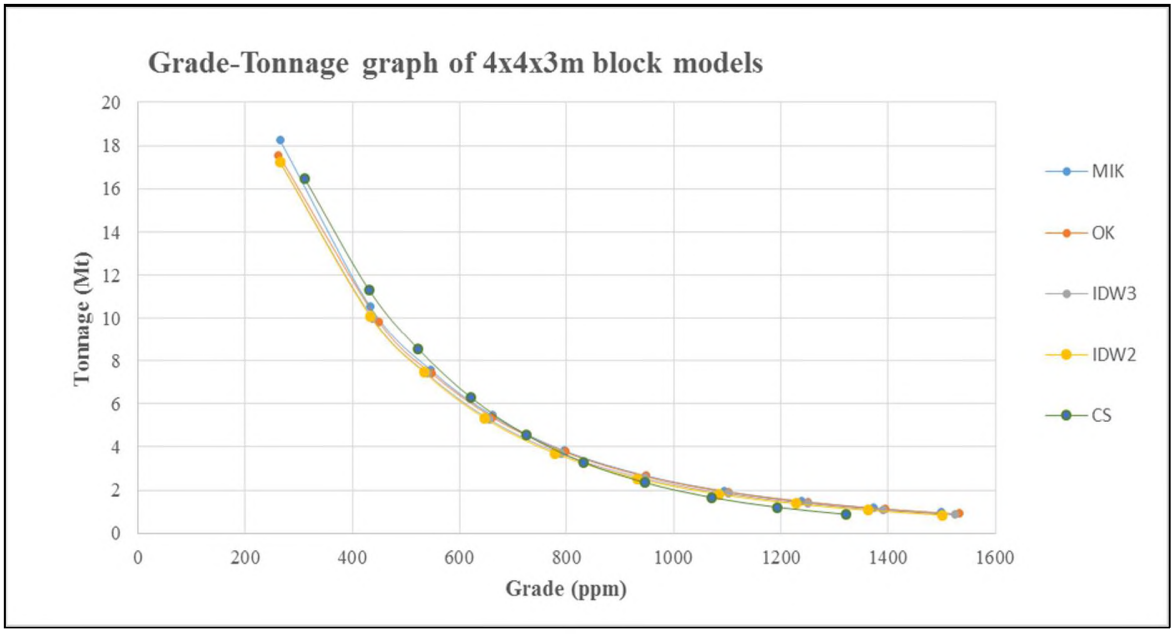

Figure 35: G-T graph of various methods at block dimensions of 4 m x 4 m x 3 m

Figure 35 is represents the G-T graph for the various methods from 4 m x 4 m x 3m data. Between the linear and non-linear kriging methods, not much can be distinguished from the G-T curves. They start at just over 17,5 Mt at an average grade of about 280 ppm and thereafter the gradient follows a steep decline and ends at about 1 Mt at just over 1 500 ppm. CS follows a much more conservative trend and starts at just under 17 Mt at a slightly higher-grade. The graph trend follows the same trend as the other methods, terminating at a lower final grade. Whilst the other methods have grades of 1 500 ppm, CS which is known to provide volume variance issues terminates at just over 1 300 ppm at 1 Mt.

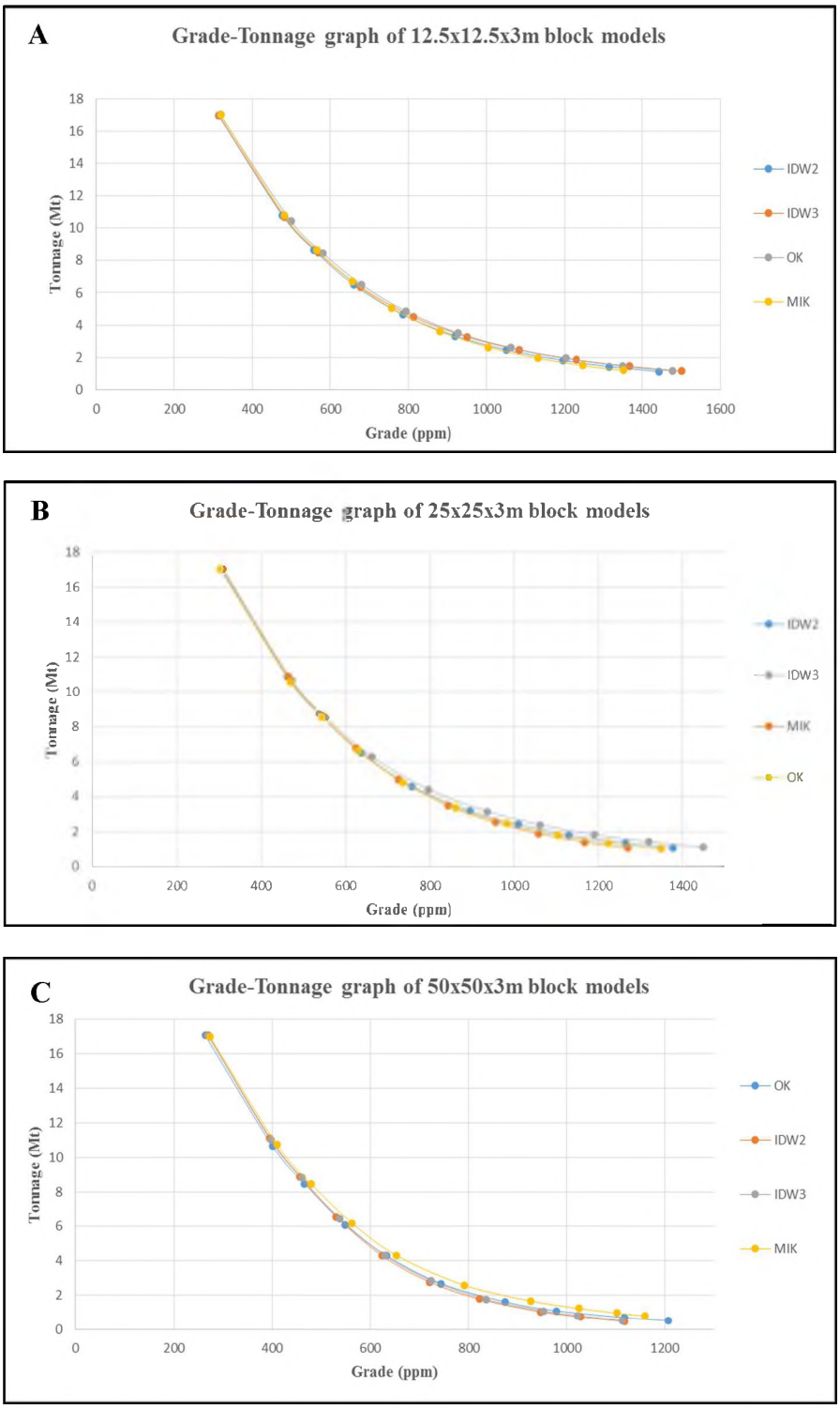

Figure 36: G-T graphs of different estimation methods at various block sizes

Figure 36 illustrates G-T graphs for the larger block models excluding CS. There is no major difference between the individual methods compared to each other and the different block sizes. They all follow the same trend and gradient with no major observable differences. MIK follows the same conservative trend at higher-grades as was observed with CS. The two IDW block models follow identical trends as each other in most block models regardless of grade and tonnage. The most important observation to note from the various G-T graphs is the decrease in elevated grades with larger block spacing. From the 4 m x 4 m x 3 m block models the high-grade drops from about 1 500 ppm to just under 1 200 ppm. This is clear evidence of the volume variance effect which averages out grades with the decrease in data availability. This remarkable decrease is especially present in the 25 m x 25 m x 3 m and 50 m x 50 m x 3 m block models that have lost these high-grades systematically. The 12,5 m x 12,5 m x 3 m block model has retained both the high-grades and tonnages that could be observed in the 4 x 4 x 3m block models.

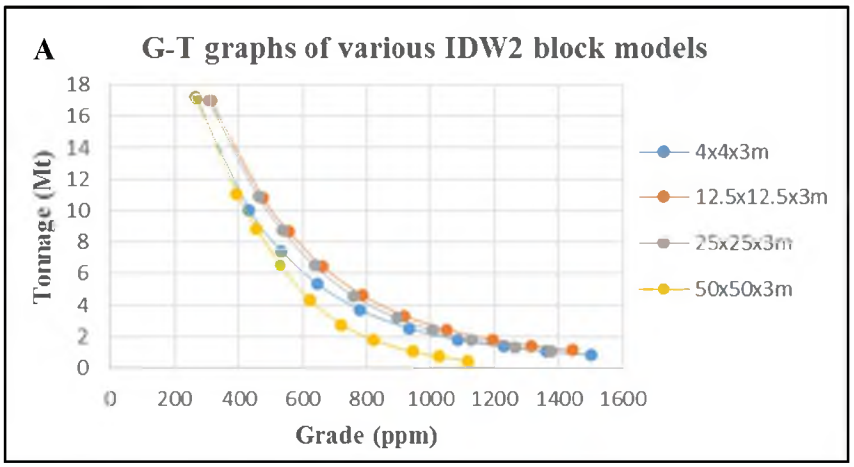

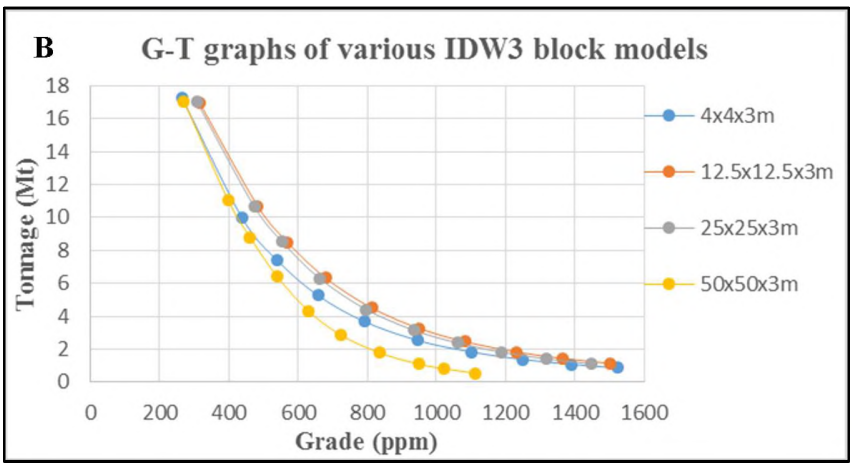

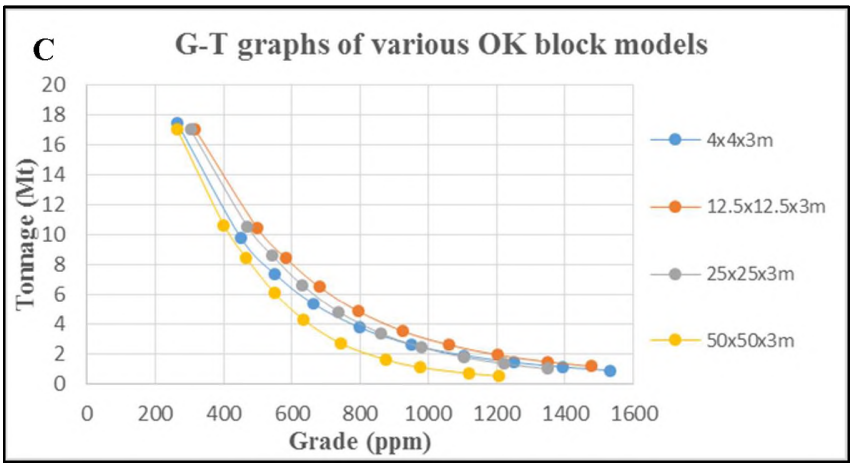

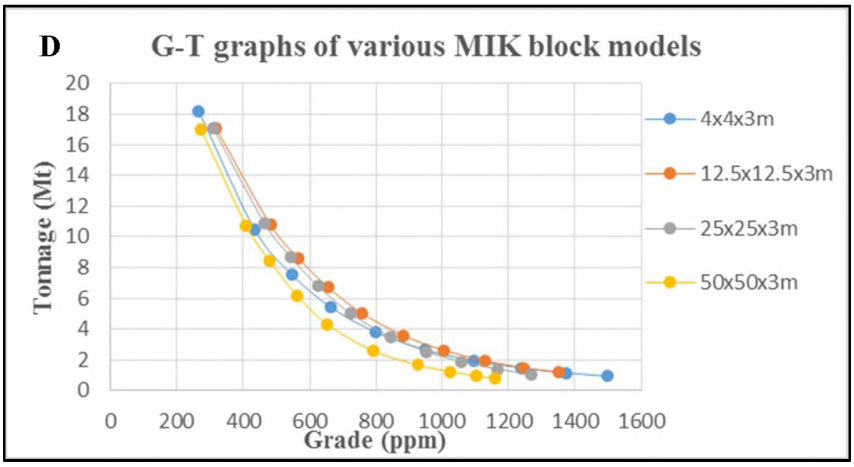

Figure 37: G-T graph of individual methods at various block dimensions

Figure 37 illustrates the four individual estimation methods used during this research and their corresponding G-T graphs from different block model dimensions. The spacing with the highest predicted grade are the 4 m x 4 m x 3 m block models that reach grades of 1 500 ppm at about 1 Mt. The lowest maximum grades are determined from the 50 m x 50 m x 3 m block models that contain a maximum grade between 1 100 and 1 200ppm. The 12,5 m x 12,5 m x 3 m and 25 m x 25 m x 3 m block models fall somewhere in between these two grades mentioned above. It is interesting to observe that there is a relationship in terms of grades between the 4 m x 4 m x 3 m and 50 m x 50 m x 3 m block models. During the initial stages these two lines have somewhat similar trends in grades up to 600 ppm and sometimes more, until the 4 m x 4 m x 3 m line picks up and follows the other two closer spaced block model trends. The 12,5 m x 12,5 m x 3 m and 25 m x 25 m x 3 m block models mimic each other in grade and tonnages with the 12,5 m x 12,5 m x 3 m block indicating maximum grades that are slightly higher.

5.7 Expenditures and cash flow comparisons between various drill spacing

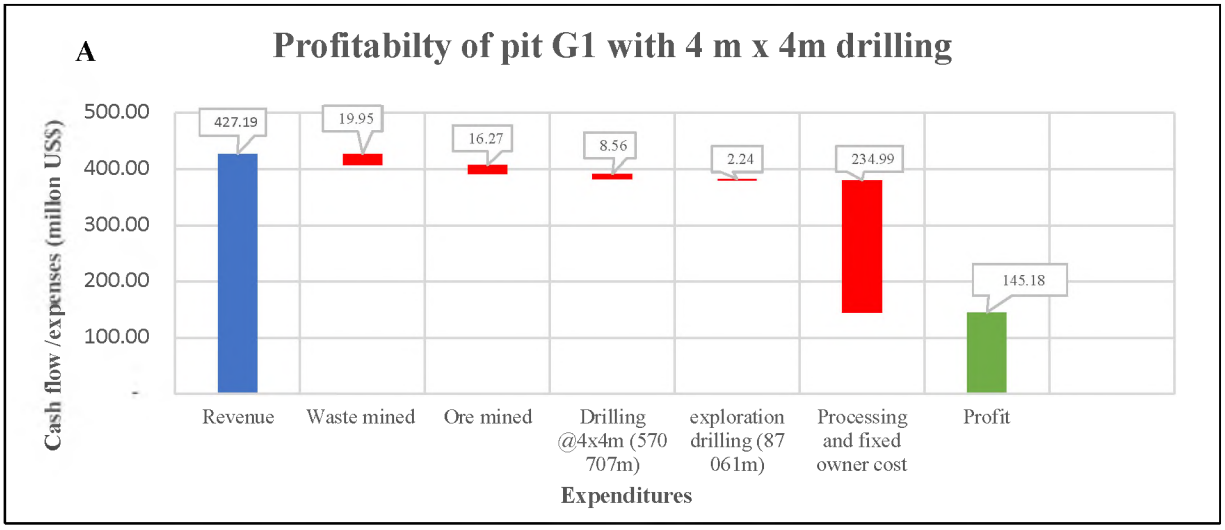

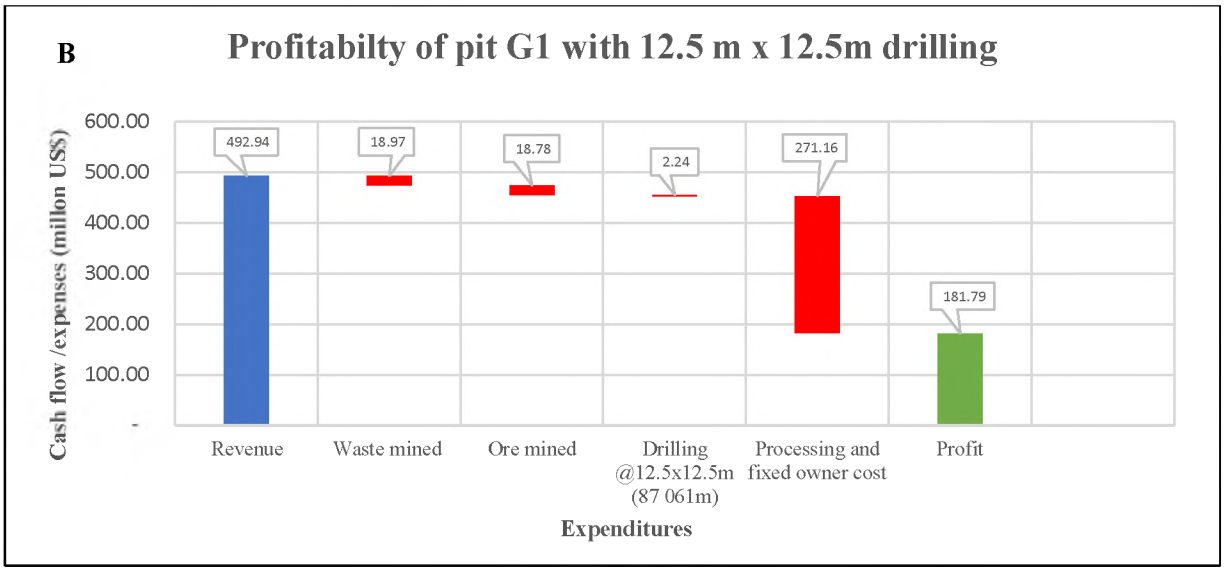

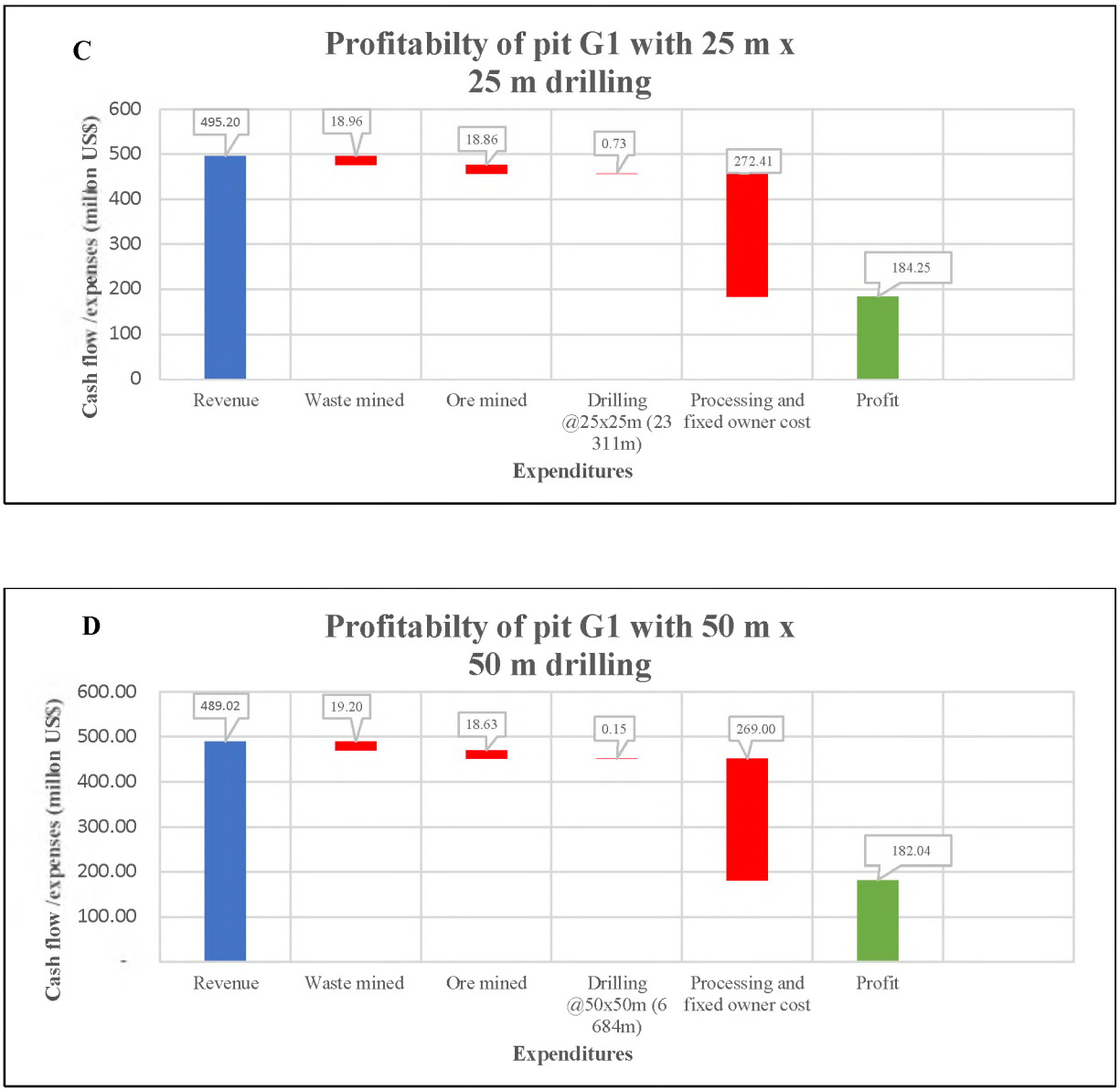

Figure 38: Total cash flow of pit G1 with included drilling costs of various drill spacing

From Figure 38 it can be observed that the revenue created from mining does not fluctuate much between the broader drill spacing, which is usually around USD 490 000 000.00. It is interesting to note that not even the smaller 12,5 m x 12,5 m drilling grid yielded an extremely different revenue value from the much larger 50 m x 50 m drill spacing. There is, however, a substantial drop of about USD 60 000 000.00 between the 4 m x 4 m drilling grid and the broader exploration drilling grids. A different trend is observed in mined tonnages between the exploration and grade

control drill spacing. The larger drilling grids all have similar amounts for waste and ore mined. The narrow 4 m x 4 m drill spacing indicates more waste mined and less total ore mined.

With regards to drilling, the expenditure effect thereof is minimal compared to the total cash flow of the pit. All the exploration drilling for pit G1 accounted for 0,8 % of the total money spent. This includes all drilling up to a grid of 12,5 m x 12,5 m. The 4 m x 4 m drilling is compulsory and is used for blasting and therefore a fixed cost. The optional radiometric logging on the 4 m x 4 m grid gives in detail insight that the exploration data cannot predict. The blast hole drilling although compulsory accounts for about 2,8 % of the total expenditure. It can therefore be concluded that drilling alone accounts for less than 4 % of the total expenditure for pit G1. It is evident that drilling cost increases with more drilling, but the total expenditure thereof dwarfs the knowledge gained from the data obtained.

The waterfall charts in Figure 38 are meant to give a representative idea of the cash flow and expenditures of mining and processing. The differences in cash flow observed are mainly due to differences in estimated tonnages and drilled metres on the different drill spacing. It must be noted that the currency used here is in USD and processing values used were given at the end of 2014. The uranium price has somewhat dropped and operating costs have decreased since then. The drilling costs at various drill grids and the estimation at those drill spacing are the focus point of this exercise. Waste and mined tonnages were calculated using the average of the various estimation methods at the specific drill spacing illustrated in the charts.

CHAPTER 6. RESULTS AND DATA ANALYSIS OF PIT H1

Pit H1 as mentioned before was used in this research as a comparative dataset towards the larger dataset of pit G1. It forms part of the main palaeo channel and is situated downstream in the deeper parts of the palaeo channel towards the west as indicated in Figure 39. Here ore is situated somewhat deeper than in pit G1 and therefore the waste to ore strip ratio is also higher. Ore is situated in finer, wetter and clayey to sandy calcareous rock. Ore in pit G1 is situated in a combination of harder, drier calcareous sand near the surface and sandy clayey calcareous rock at the bottom. Pit H1 is mined as part of a large continuation of pits that are merged together and follow the main direction of the Langer Heinrich palaeo channel. It is mined in the general east-west direction of the old river channel and becomes deeper with regards to ore deposition towards the west. During the modelling all the waste from the upper elevation of about 620 to 600 m was not included in the modelling exercise. It was removed because there was no need to do radiometric logging on a 4 m x 4 m grid of the grade control holes. Radiometric logging was only started at an elevation of about 600 m where ore presents itself.

As in pit G1 two different representative elevations were chosen for display purposes of ore blocks and grade distribution throughout the palaeo channel. These two elevations were taken at 573,5 m and 564,5 m respectively. They should be representative of the ore and waste distribution at the upper elevations and somewhat lower near the unmineralised basement rock (ore body shape and distribution). The high-grade lenses as in pit G1's observation will be used as the main visible markers, because these are the easiest to identify. Other characteristics like grade distribution will also be considered between different block model dimensions and different methods.

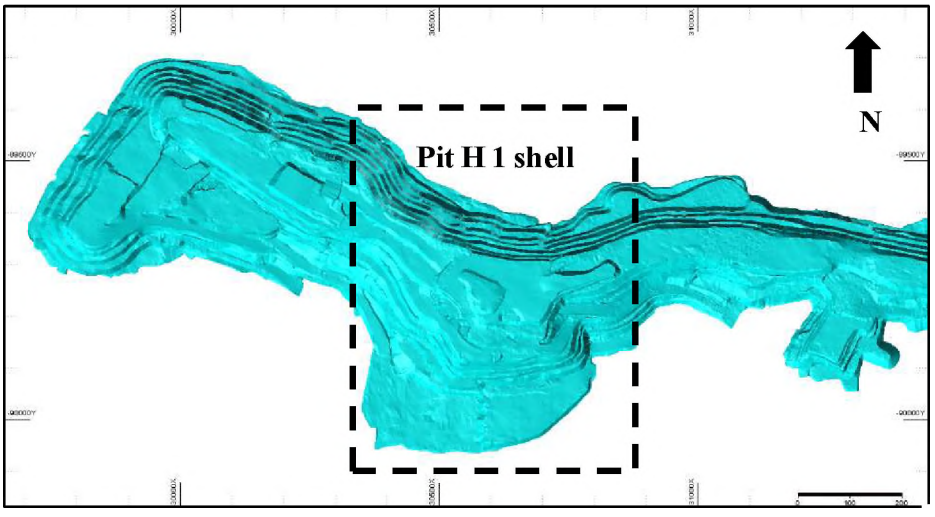

Figure 39: Location of Pit H1 with regards to main palaeo channel

6.1 Conditional simulation block models at 4 m x 4 m x 3 m and resulting CV model

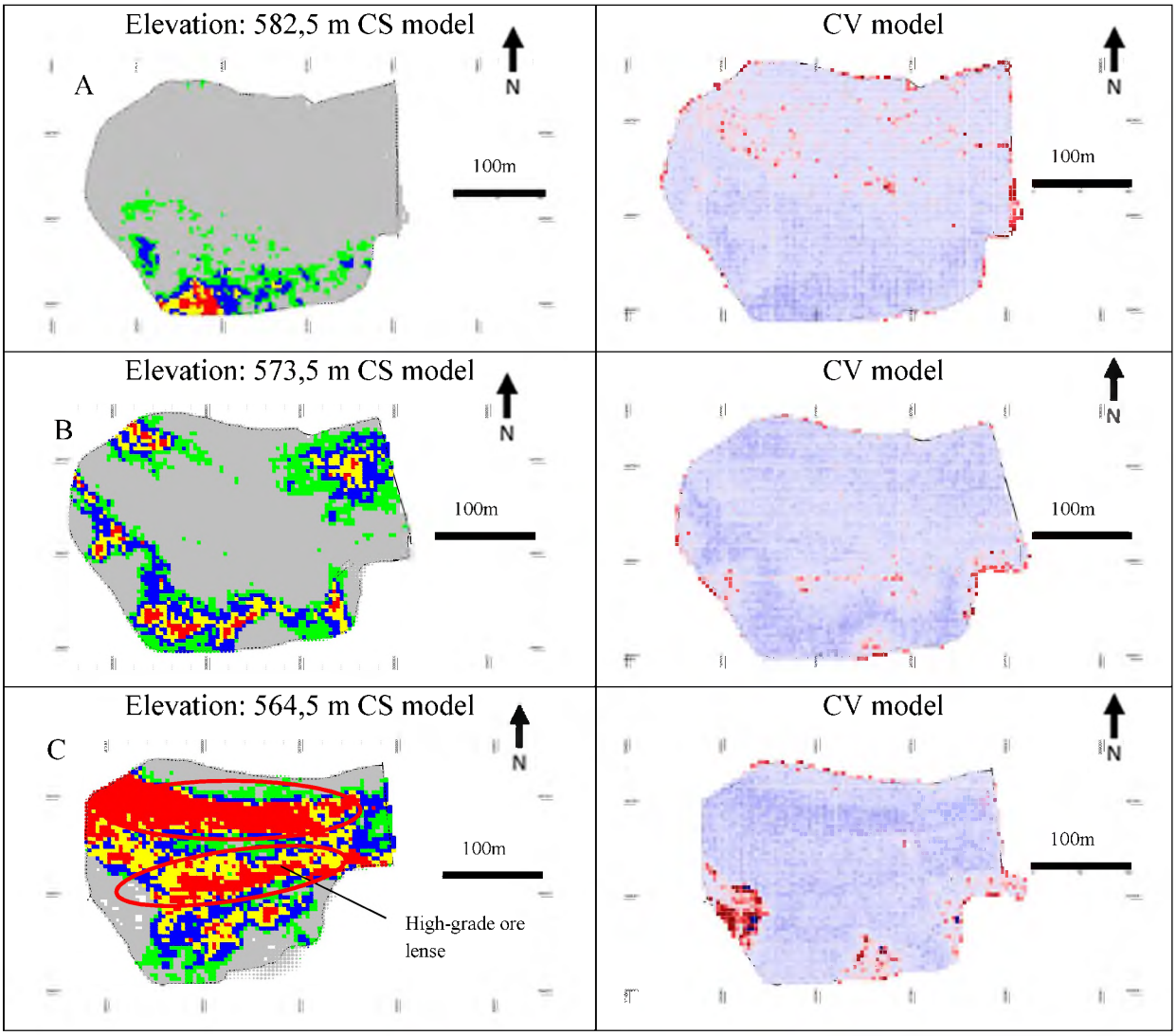

Figure 40: CS and resultant CV model of three selected elevations to illustrate ore distribution in pit H1

Grade (ppm)	Colour
Waste 0-250	
Low-grade 250-400	
Medium-grade 400-650	
High-grade 650-900	
Super high-grade 900+	

Value	Label
	< -0.11
-0.11	-0.11 to 0.14
0.14	0.14 to 0.22
0.22	0.22 to 0.30
0.30	0.30 to 0.45
0.45	0.45 to 0.62
0.62	0.62 to 0.70
0.70	0.70 to 0.86
0.86	0.86 to 0.93
0.93	0.93 to 1.02
1.02	1.02 to 1.22
1.22	1.22 to 1.34
1.34	>= 1.34

Table 33: Grades and associated colour representation on block models (left) and colours of various coefficient of variation of the CV models

The same parameters regarding the CS modelling were used here as in pit G1. The block dimensions are therefore 4 m x 4 m x 3 m and are displayed on the two elevations that are displayed in Figure 40 with the addition of another near surface elevation. Their related coefficient of variation CV model at the same elevation are used as previously mentioned to confirm precision of data estimations. The various CV cut-offs and colour coding are displayed in Table 33. No basement high is observed in pit H1 as was seen in G1. Elevation 582,5 m (A) is only displayed in this model and illustrates the upper levels or starting elevation where ore makes an appearance after about 20 m of waste stripping. At elevation 573,5 m (B), it is clear that the start of the ore body is revealed. This should represent the upper section of the main ore body that follows below. At this elevation there appears to be two small high-grade lenses in the north and some smaller dispersed yet connected high-grade lenses in the south. These are connected by low-grade and medium-grade. It can also be observed that grades in most cases fade slowly from higher-grades into lower grades and then waste.

At elevation 564,5 m (C), ore has clustered in the centre of the palaeo channel. This is relatively close to the impermeable basement rock which would allow for groundwater ponding and therefore ideal conditions for mineralisation. The two different ore bodies from the previous elevation have fused or concentrated into one larger ore body. A large rectangular super high-grade lens makes up most of the northern part of the pit. It is separated by an area of lower grades before fusing together again with a rectangular high-grade lens in the centre of the pit. There is a slight indication of the main ore body splitting in the southern section of the pit at this elevation. There are, however, no super high-grade lenses in the southern parts of the pit, which is mostly made up of medium and low-grade.

The CV model in Figure 40 as mentioned before represents data certainty. Low confidence data is represented by lighter shades of blue and red, whilst higher certainty is indicated by darker shades of blue. Red colors would indicate areas where not much data is available and is usually around the pit edges. It is clear from the CV models that the darker shades of blue indicate areas of importance in which ore is illustrated. It mimics the CS model in terms of ore distribution. Areas that have been estimated as waste have turned out in lighter shades of blue on the CV model.

6.2 Block models of other estimation methods at elevation 573,5 m

6.2.1 4 m x 4 m x 3 m block models

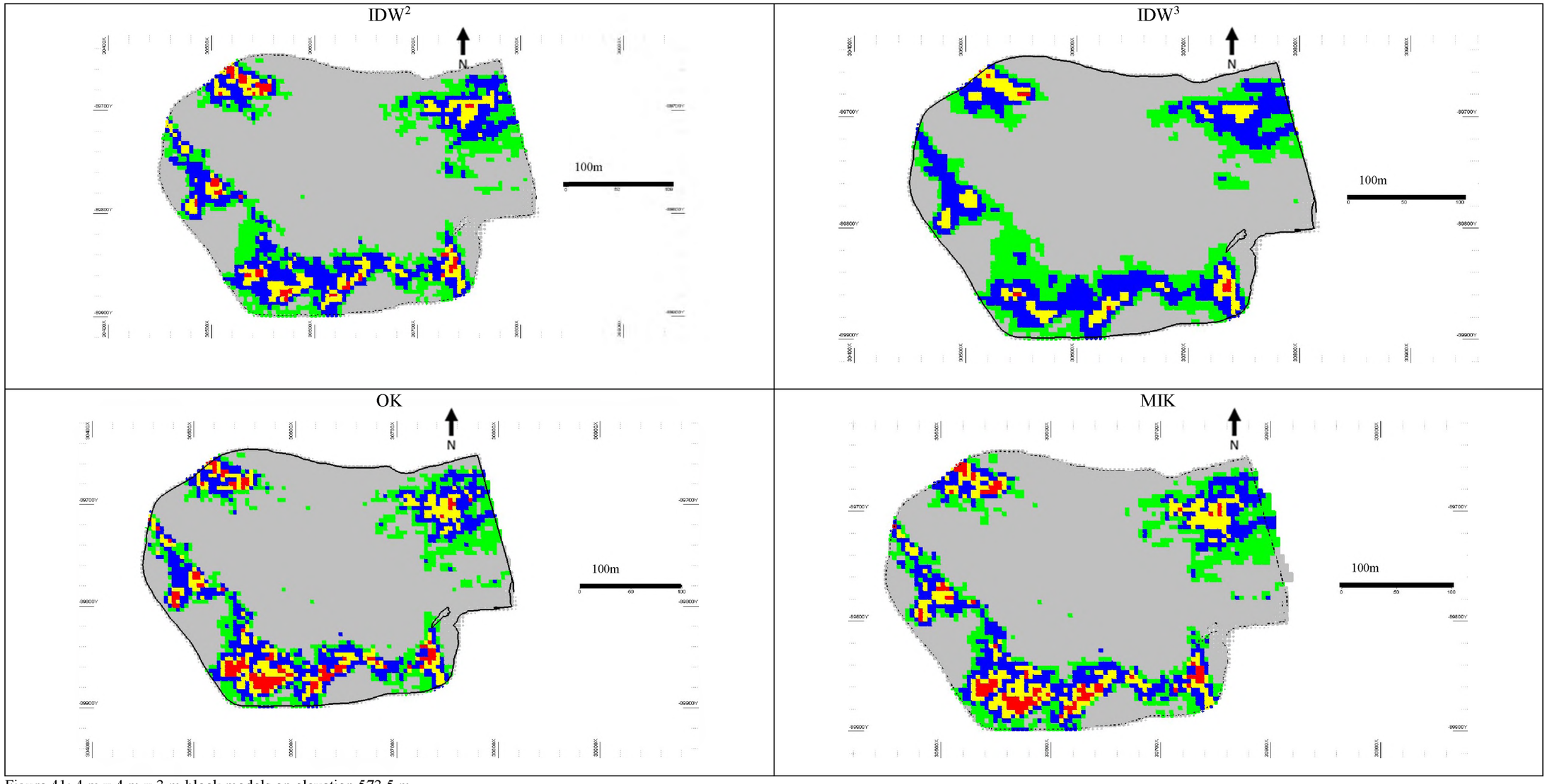

Figure 41: 4 m x 4 m x 3 m block models on elevation 573,5 m

Grade (ppm)	Colour
Waste 0-250	
Low-grade 250-400	
Medium-grade 400-650	
High-grade 650-900	
Super high-grade 900+	

General observations

The most important markers in Figure 41 at this elevation are two smaller high-grade lenses in the northern parts of the pit, one in the eastern and one in the western corner. These are separated by mostly waste between each other and the ore in the south. In the southern parts of the pit there are numerous smaller high ore bodies within a larger continuous low-grade ore body.

Block model observations

Throughout the various block models created in pit G1, not much variation between IDW^2 and IDW^3 was observed in Figure 41. Here there are some noticeable differences between the two models. The two high-grade lenses in the north show differences in both grade and size of ore distribution. IDW^2 has more super high-grade indicated in red. The ore body in the northeastern section of the pit in the IDW^3 model is visibly smaller than all of the other models. In the southern sections, both models show lower amounts of high-grade than the other models, with IDW^3 containing the lowest amounts of high-grade. Not much difference in super high-grade is observed although there is evidently more high-grade in IDW^2.

Both MIK and OK models are representatively similar in ore distribution. The two northern ore lenses contain more super high-grade compared to the IDW models. The continuous southern ore body looks similar in shape and grade distribution. Both models contain more super high-grade than IDW models, which seems to have the least super high-grade in the southern ore body. IDW^3 seems to have the least overall high-grade present.

6.2.2 12,5 m x 12,5 m x 3 m block models

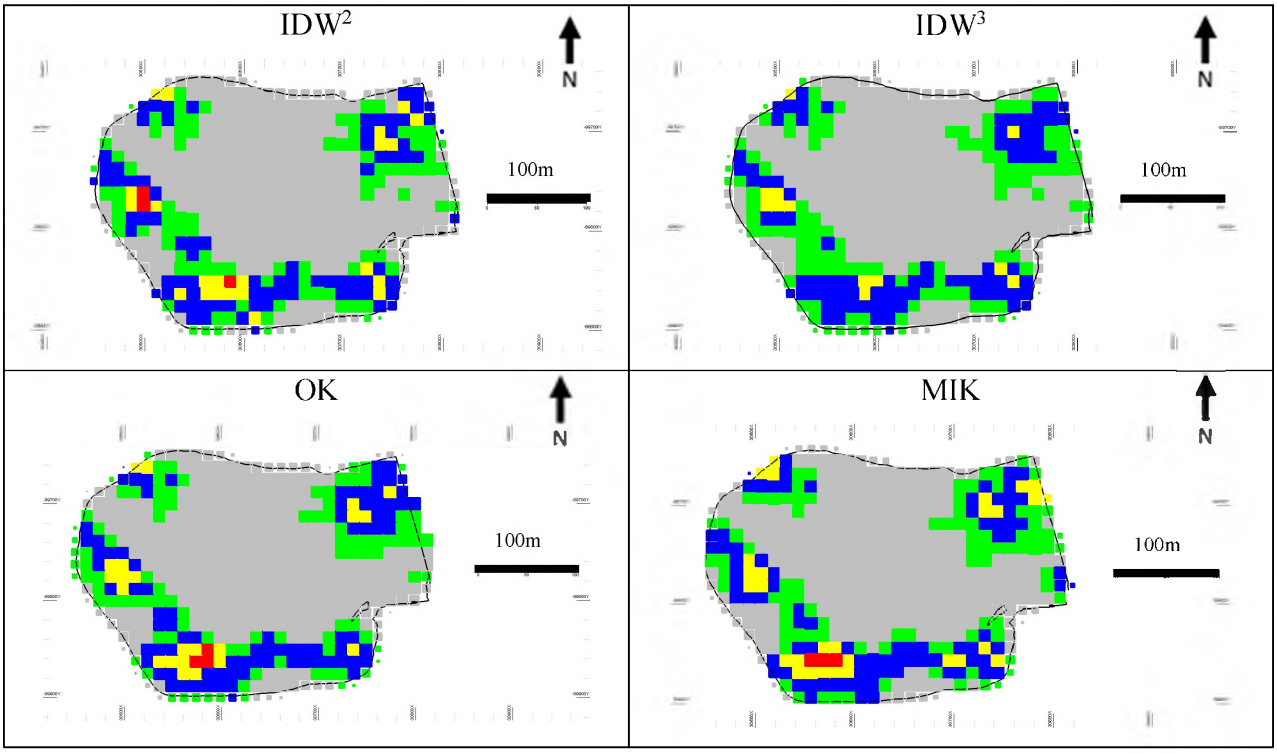

Figure 42: 12,5 m x 12,5 m x 3m block models on elevation 573,5 m

The same ore markers that were described in the 4 m x 4 m x 3 m block models can be observed in Figure 42. The two ore lenses on the northern side of the pit are still eminent in all four models. They all contain a high-grade nucleus and sometimes on the edges of the pit, with the absence of super high-grade. In the southern ore body the general continuation remains present as well as its grade distribution. The high-grade lenses have become more isolated though and almost all super high-grade has been diluted. IDW^3 indicates the lowest amount of high-grades, with the total absence of super high-grade.

6.2.3 25 m x 25 m x 3 m block models

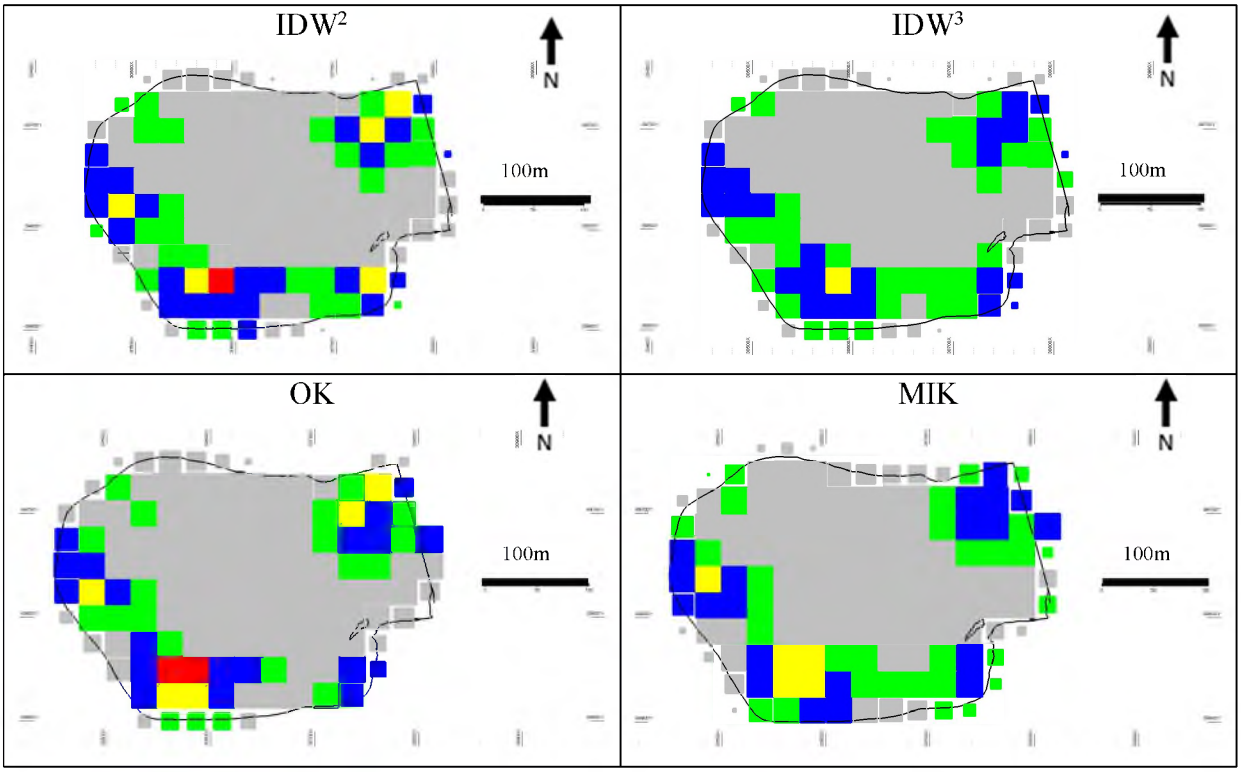

Figure 43: 25 m x 25 m x 3 m block models on elevation 573,5 m

The 25 m x 25 m x 3 m block models in Figure 43 indicate that some of the ore lenses that were previously visible before have now been diluted into lower grades. The ore lenses in the north-western parts of the pit, although visible, have almost disappeared completely in all block models. Only IDW^2 and OK have retained some of their high-grade blocks in the north-eastern ore body. The southern ore bodies are more bulky and continuous in the IDW models, whilst the OK and MIK model have diluted some of its lower grades to waste. The OK model has maintained some the super high-grade which is also present in the IDW^2 model but absent in the MIK and IDW^3 model.

6.2.4 50 m x 50 m x 3 m block models

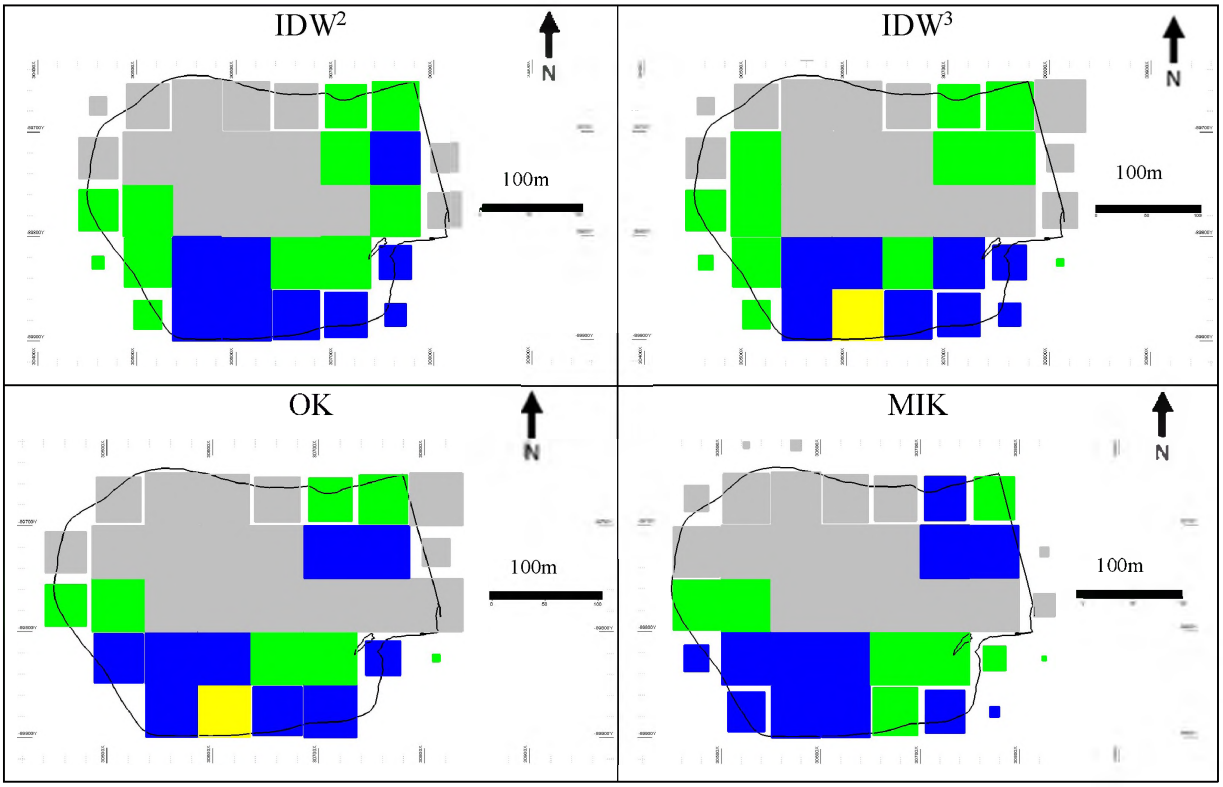

Figure 44: 50 m x 50 m x 3 m block models on elevation 573,5m

On the 50 m x 50 m x 3 m block dimensions as shown in Figure 44, a lot of the data has been fused with lower grades and ore blocks have been diluted. All models have lost the ore lens in the north-western corner of the pit. IDW^3 shows a potential of a remnant ore body in the north-western part of the pit. The ore body in the north-eastern corner of the pit in all models has diluted their high-grade ore blocks and has been downgraded to medium and low-grade. The ore body in southern parts of the pit has retained its general shape in all models. The MIK and IDW^2 models are the only models that have downgraded all of their high-grade lenses into lower grades. All of the models indicate similar block model grades with minor differences between each other. This is especially clear in the larger ore lens in the southern section of the pit.

6.3 Block Models of other estimation methods at elevation 564,5m

6.3.1 4 m x 4 m x 3 m block models

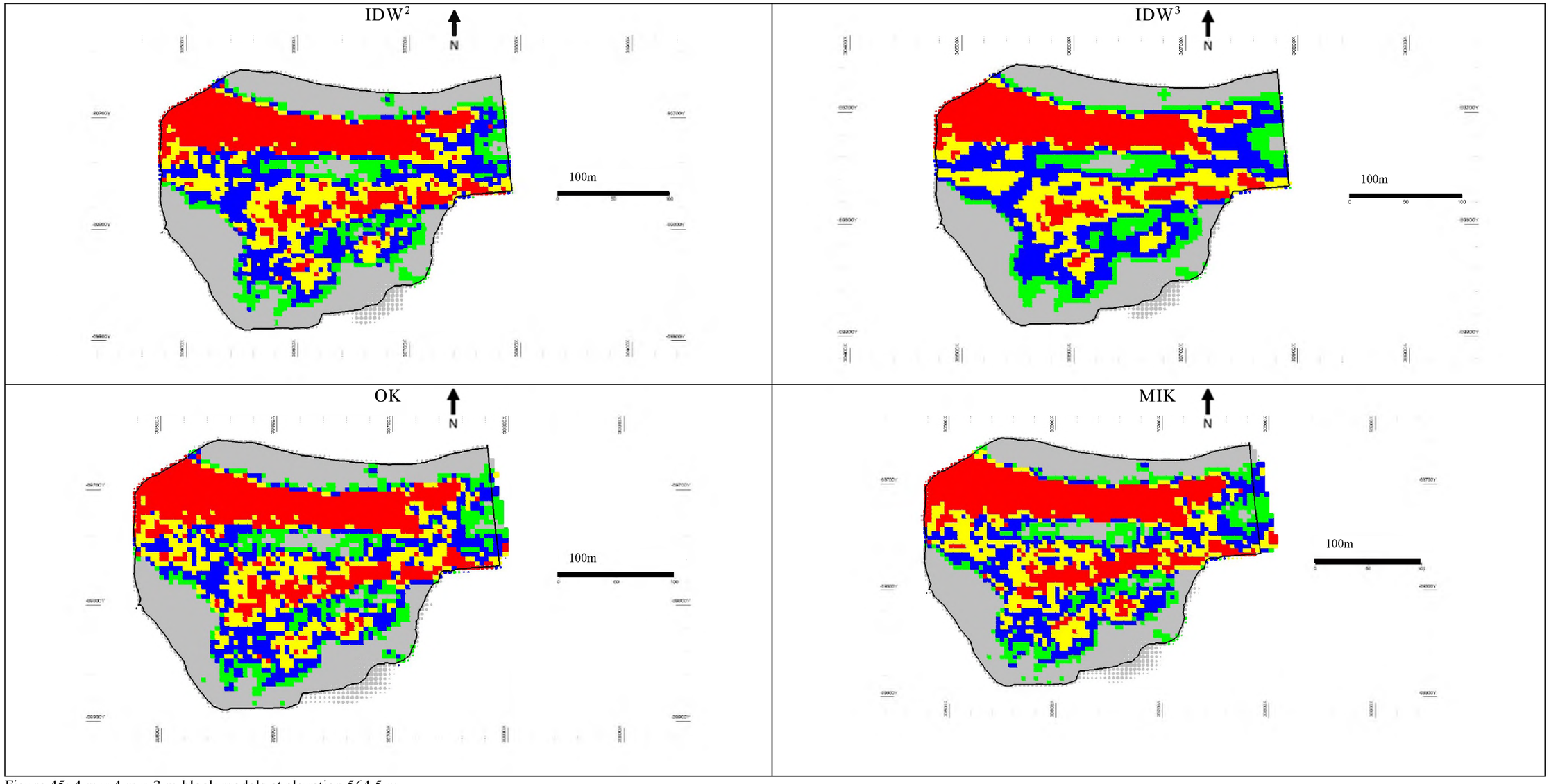

Figure 45: 4 m x 4 m x 3 m block models at elevation 564,5 m

Grade (ppm)	Colour
Waste 0-250	
Low-grade 250-400	
Medium-grade 400-650	
High-grade 650-900	
Super high-grade 900+	

General observations

This elevation represents the ore distribution of the lower part of the ore body in the main palaeo channel. This shows a totally different picture in grade and associated distribution compared to the previous elevation. Ore is generally distributed as massive and homogenous elongated body with no real separation between north and south. This was not observed in the previous elevation where ore was found to be more scattered towards the northern parts of the pit and a second larger ore lens in the south. The most distinguishing feature at this elevation is the east-west trending super high-grade lens towards the northern edge of the pit. This elongated lens is separated towards the central south by a patch of waste and low-grade. The central patch of waste seems to be an unmineralised island in the center of the palaeo channel almost indicating a split in groundwater flow.

Block model descriptions

No large-scale differences can be observed from the print screens in Figure 45. The focus lies on the super high-grade lens in the northern section of the pit. Both shape and grade distribution is fairly homogenous throughout the various models. It can be observed that IDW^3 has somewhat less super high-grade towards the eastern part of the large elongated lens. The super high-grade in all models is fairly homogenous without any internal irregularities in grade. Towards the north of the pit, the super high-grade fades abruptly into low-grade and then waste. This forms the rectangular non-mineralised island in the middle of the pit which is likely attributed to groundwater movement. Towards the southern parts of the pit lies another irregularly shaped high-grade lens separated by a patch of waste. The OK and IDW^3 block models contain less super high-grade within this high-grade ore body. The high-grade lens, unlike the one in north, is surrounded by mainly medium-grade that fades slowly into the surrounding waste. IDW^3 seems to visibly contain the highest amount of medium-grade within this area and is indicative of homogenization of total grade distribution.

6.3.2 12,5 m x 12,5 m x 3 m block models

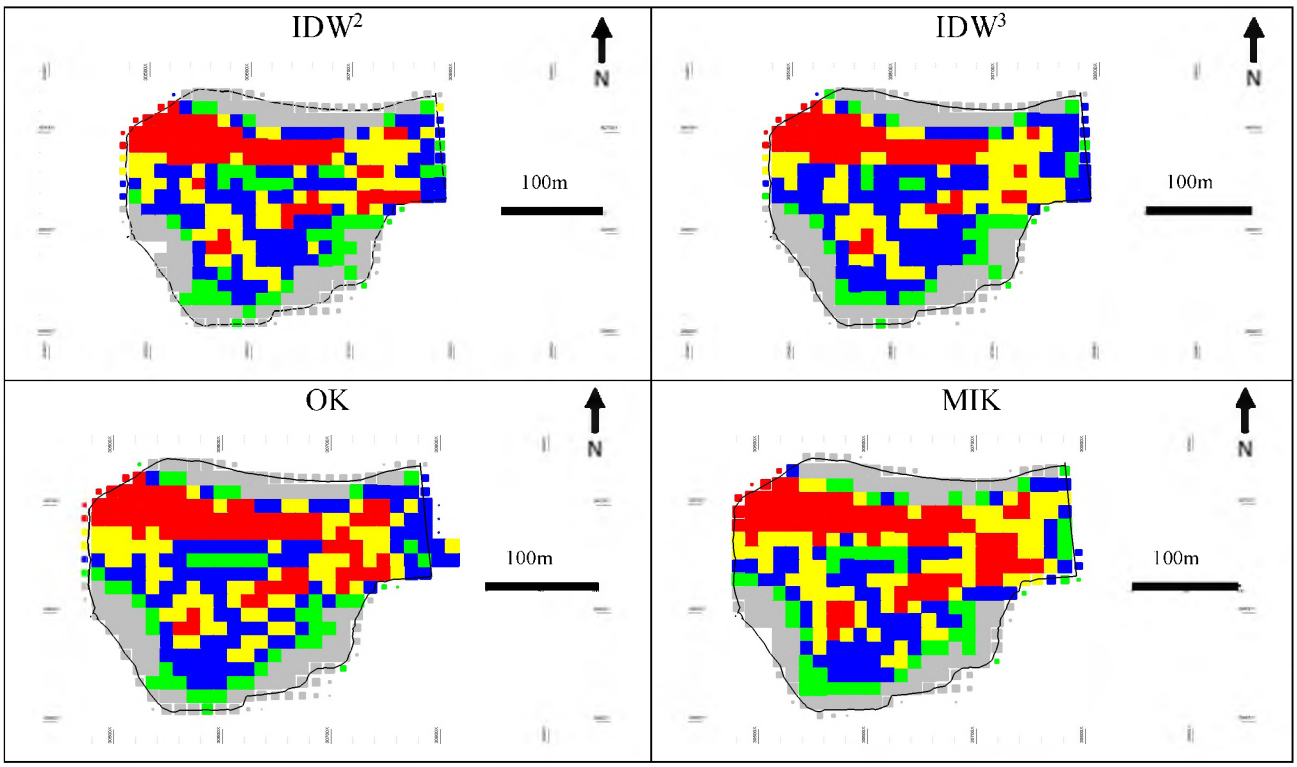

Figure 46: 12,5 m x 12,5 m x 3 m block models on elevation 564,5 m

With reference to Figure 46, not much in terms of general ore block distribution is lost in these models compared to the smaller block models observed in Figure 45. The larger elongated super high-grade ore body in the northern sections is clearly present, however somewhat more irregular or distorted in grade distribution with regards to high-grade. IDW^2 and IDW^3 seem to have the least super high-grade therein. The patch of central waste has been upgraded to low and medium-grade within all block models. This is again evidence of volume variance, which is actively present in all the block models with less data availability. The high-grade ore body in the southern section of the pit is highly irregular and patchy.

6.3.3 25 m x 25 m x 3 m block models

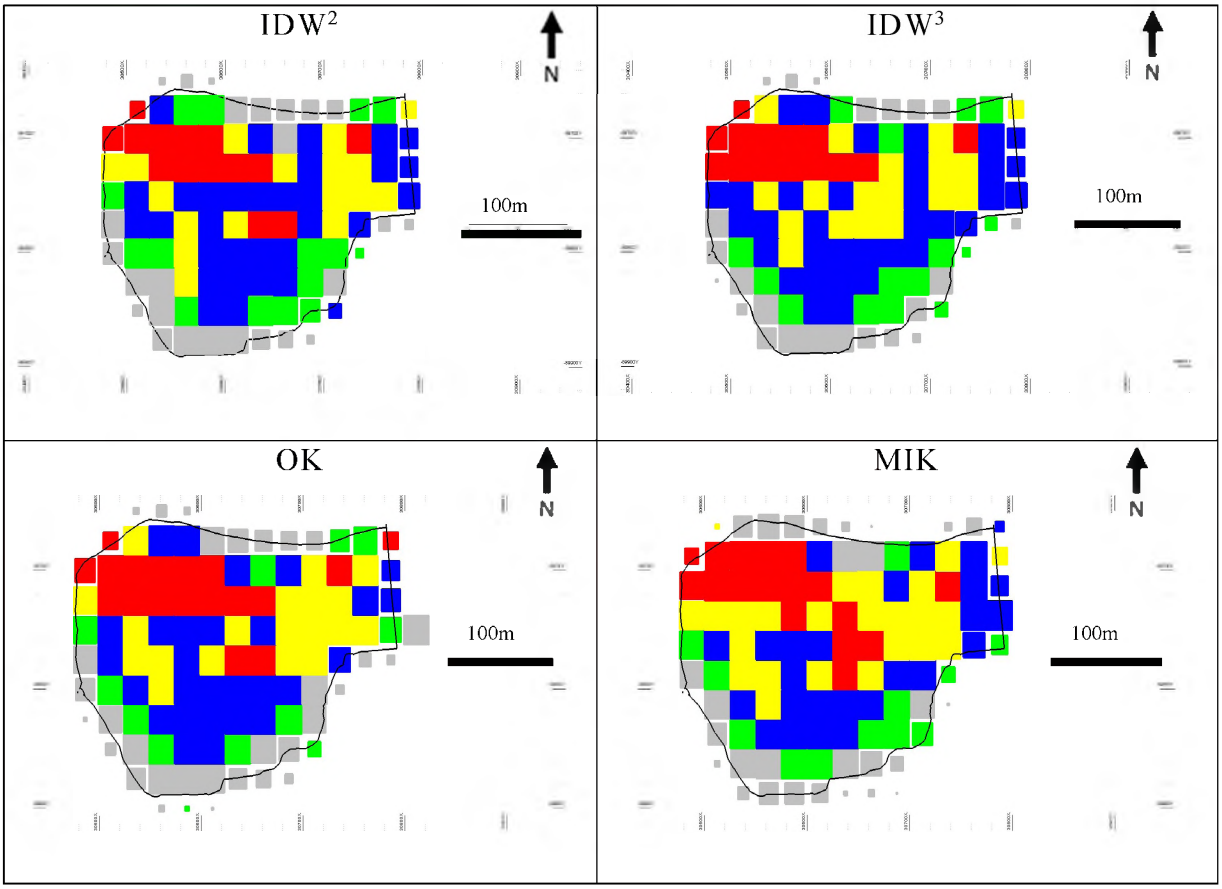

Figure 47: 25 m x 25 m x 3 m block model on elevation 564,5 m

With regards to Figure 47, no real distinction between a northern and smaller southern high-grade lens can be determined in these block models. The smaller high-grade lens in the south has been diluted to medium-grade. All four block models have remnants of the elongated super high-grade lens, which is mostly visible in the north-western section of the pit. The eastern section has been downgraded into normal high-grade and even medium-grade. The former irregular shaped high-grade lens in the southern section of the pit has partly fused with the high-grade lens in the north. The southern high-grade lens consists primarily of normal high-grade and more medium-grade. IDW^3 contains the least high-grade in the southern sections of the pit.

5.3.4 50 m x 50 m x 3 m block models

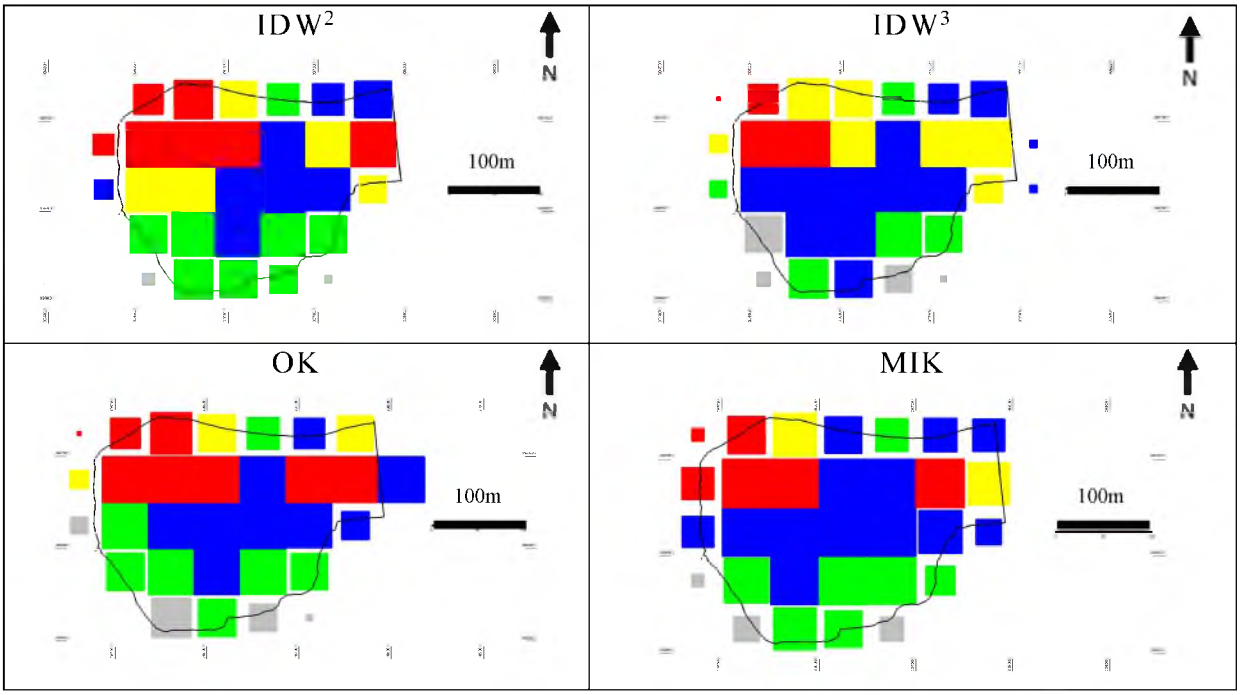

Figure 48: 50 m x 50 m x 3 m block models on elevation 564,5 m

The wide-spaced exploration data displayed in Figure 48 provides the results of less data availability. The general structure of grade distribution is nevertheless maintained. Most models indicate the large elongated super high-grade lens in the northern parts of the pit. More super high-grade is observed than in the previous 25 m x 25 m x 3 m block models. Minor low and medium-grade is visible in the super high-grade lens. The southern high-grade lens has completely been downgraded or diluted to medium-grade. This is especially visible in the OK and MIK model, whilst the IDW^2 model has a much larger zone of normal high-grade just south of the northern super high-grade ore body.

6.4 Block model setup, variography and statistical representation

6.4.1 Conditional simulation data preparation

Across-strike Variogram

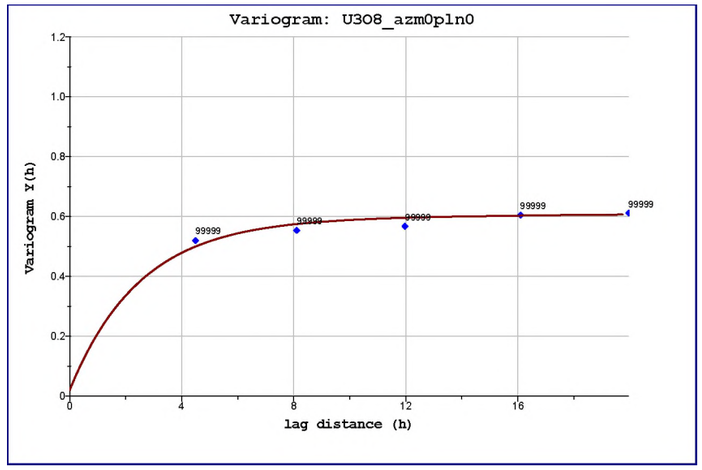

Along-strike Variogram

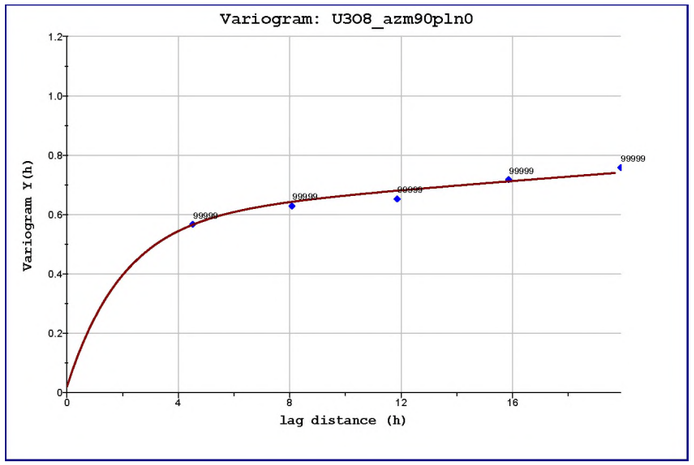

Down-hole variogram

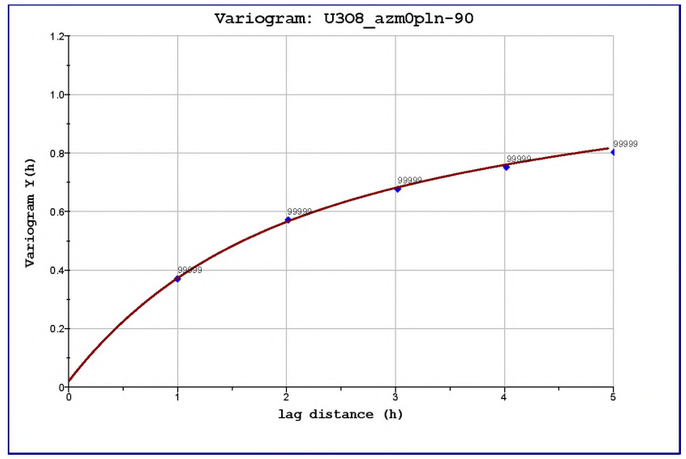

Variogram map

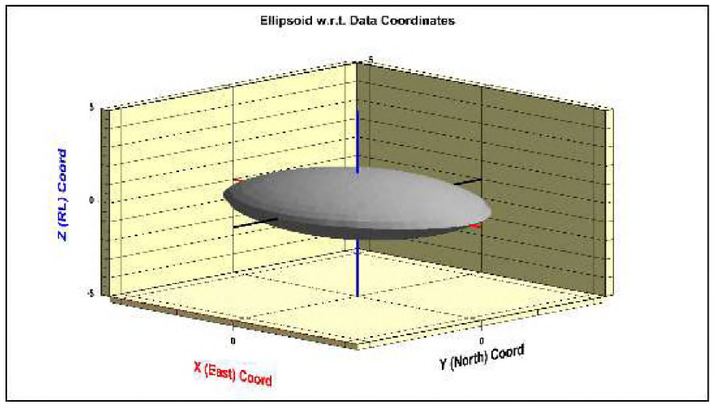

Cumulative histogram

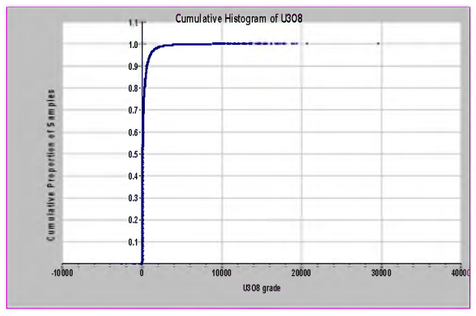

Univariate Statistics

Variable:	U3O8
Weighted by:	no weight
Mean:	242.289
Variance:	365708.250
CV:	2.496
Minimum:	-2621.246
Q1:	11.466
Median:	59.869
Q3:	225.474
Maximum:	29637.436
IQR:	214.008
No. Data:	244602

(Data set at full limits)

Q-Q plot

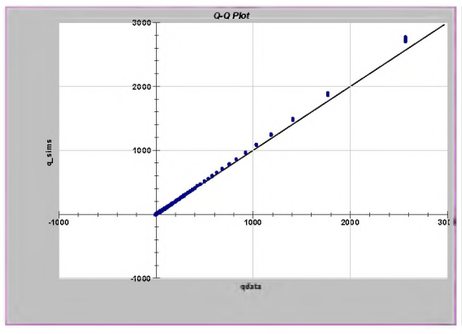

Data Statistics

Variable: qdata	q_sims
Weight by: --	--
Mean: 212.801	219.756
Variance: 153681.719	172507.609
CV: 1.842	1.890
Minimum: -4.867	-3.286
Q1: 11.465	10.634
Median: 59.855	56.957
Q3: 225.323	227.327
Maximum: 2564.139	2770.794
IQR: 213.858	216.693
Covariance: 162808.078	
Pearson: 1.000	
Spearman: 1.000	
No. of Data: 9900	

(Data set at full limits)

Figure 49: Variograms, cumulative frequency graph and Q-Q plot used during CS

6.4.2 Ordinary kriging data preparation

4 m x 4 m x 3 m data setup

Across-strike Variogram

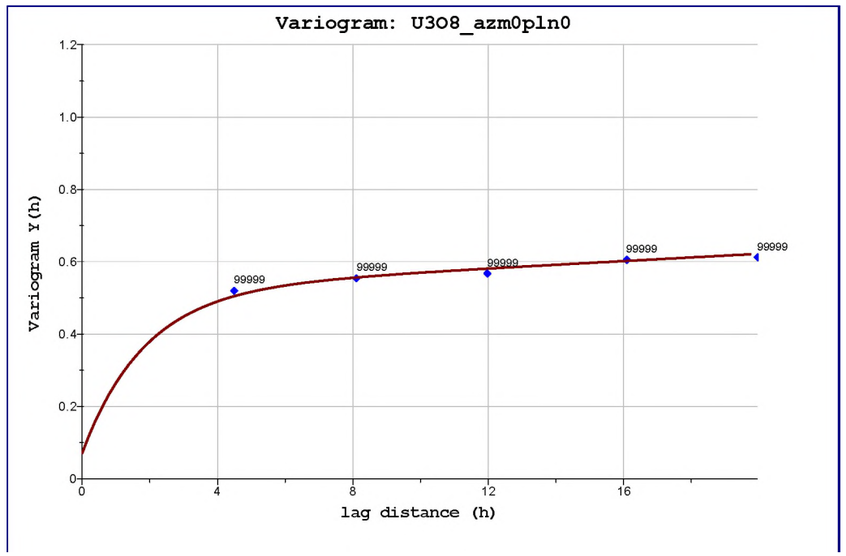

Along-strike Variogram

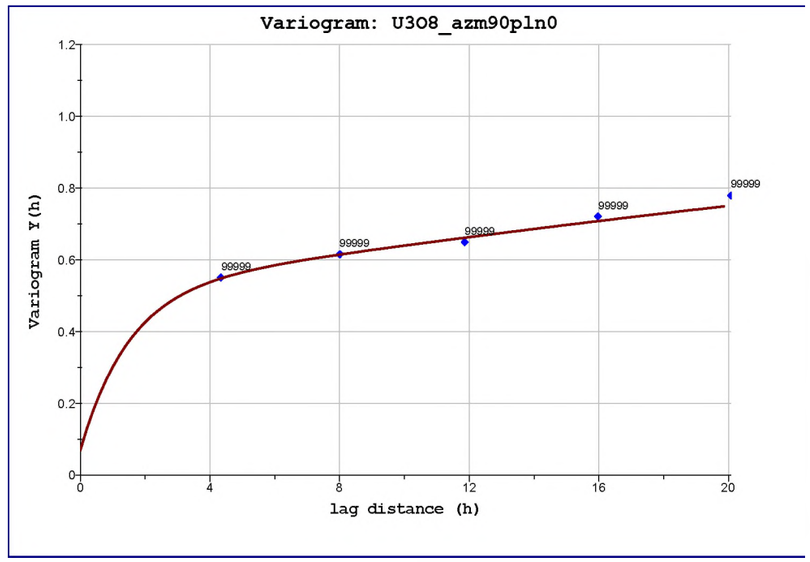

Down-hole variogram

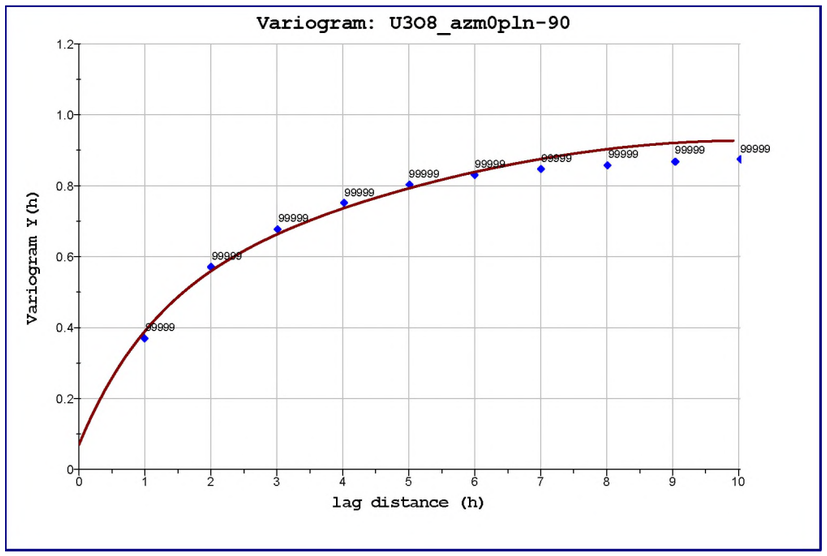

Variogram map

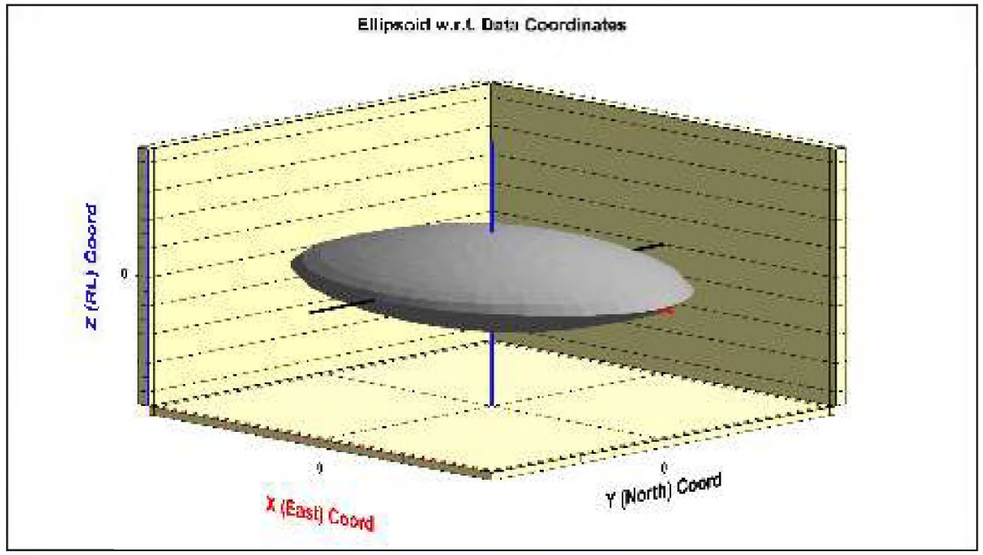

Figure 50: Variography of OK of 4 m x 4 m x 3 m block model

12,5 m x 12,5 m x 3 m data setup

Across-strike Variogram

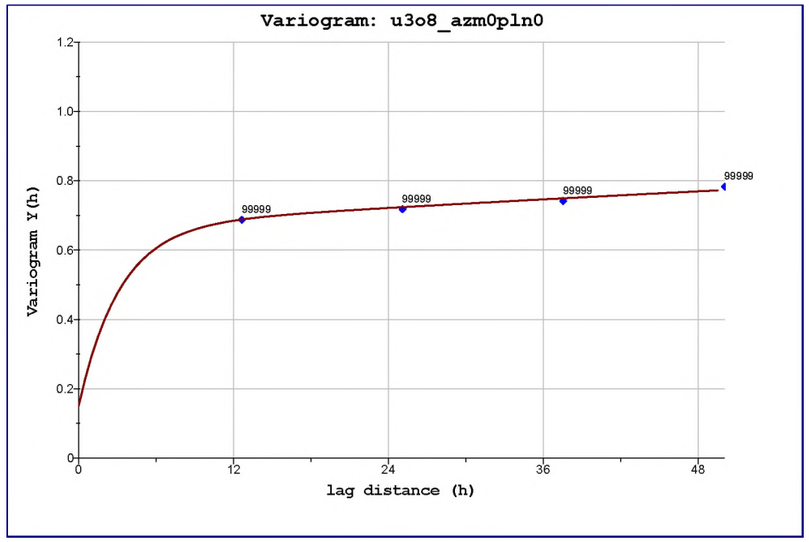

Along-strike Variogram

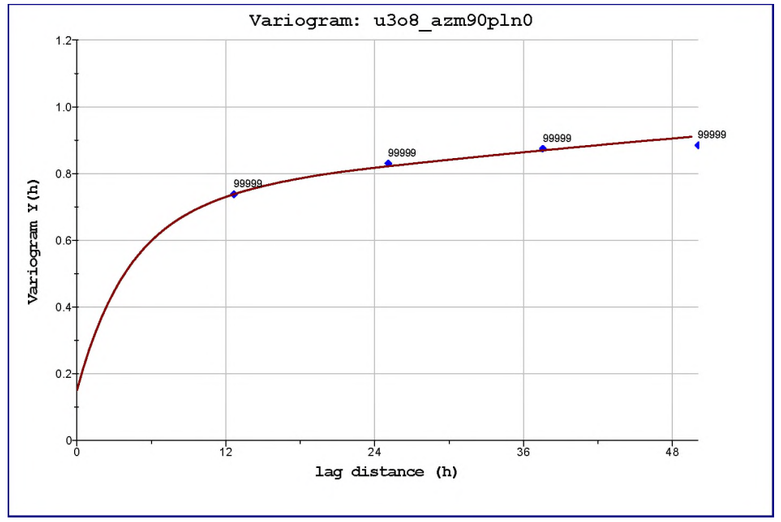

Down-hole variogram

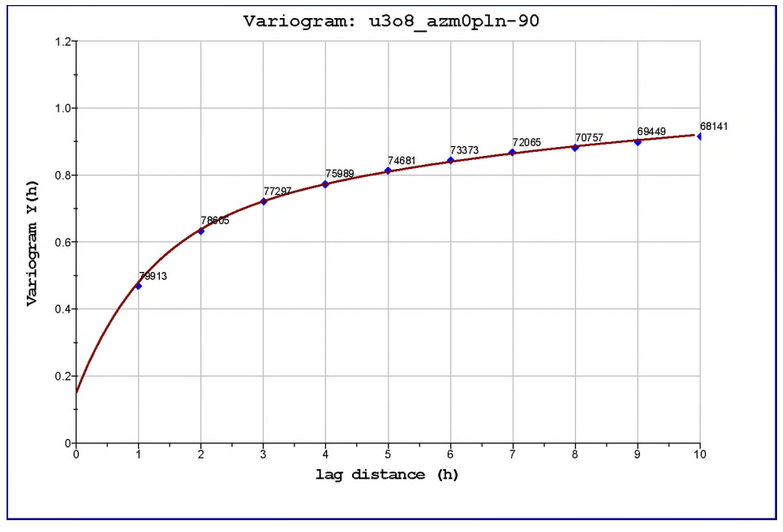

Variogram map

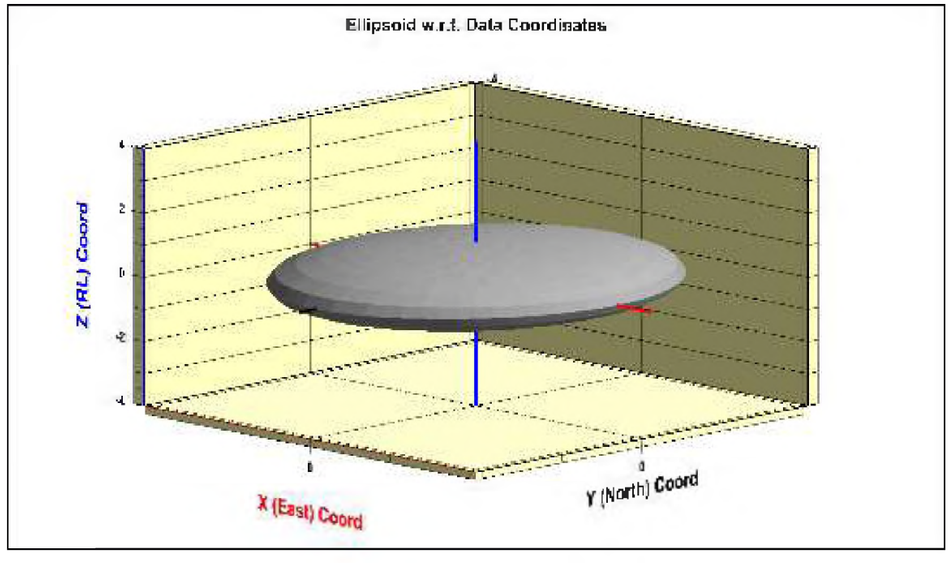

Figure 51: Variography of OK of 12,5 m x 12,5 m x 3 m block model

25 m x 25 m x 3 m data setup

Across-strike Variogram

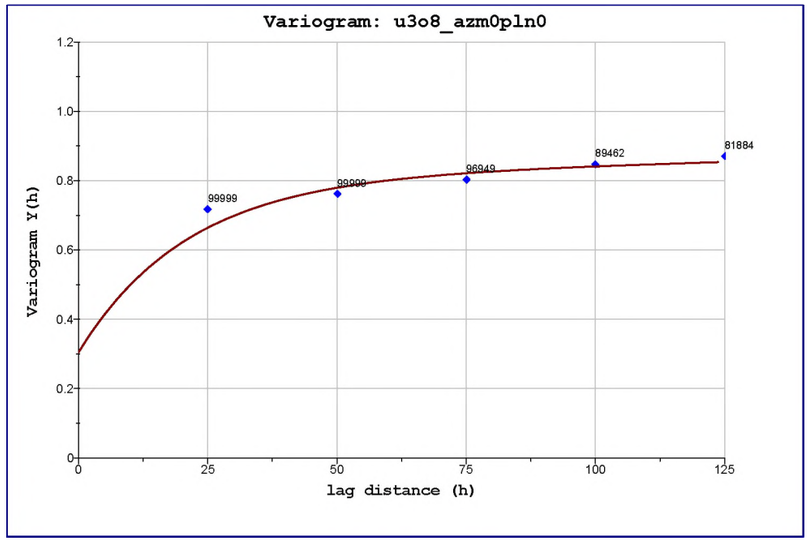

Along-strike Variogram

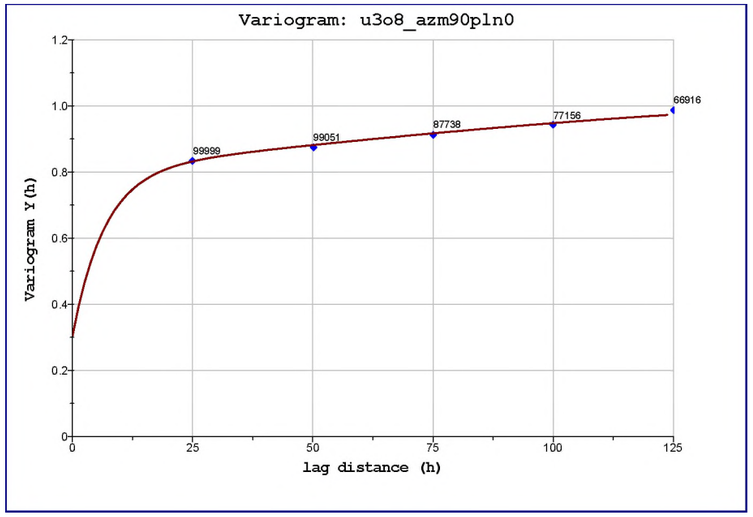

Down-hole variogram

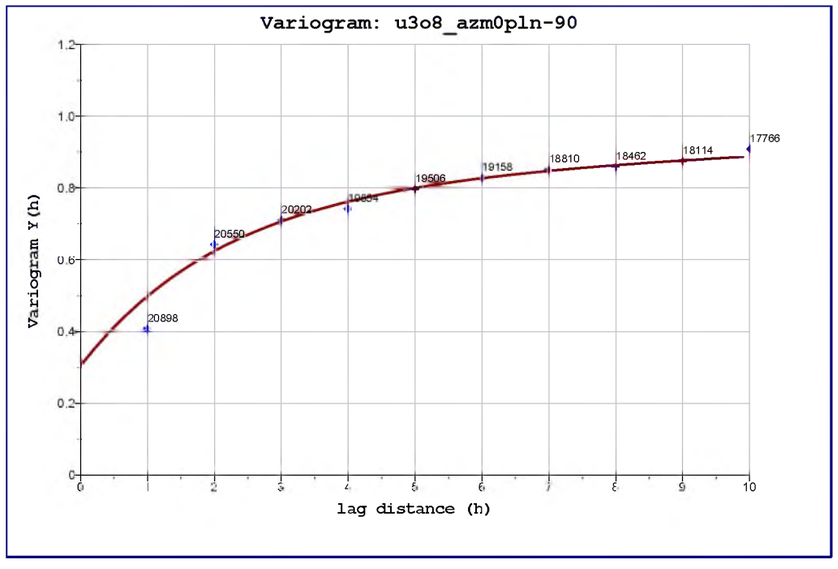

Variogram map

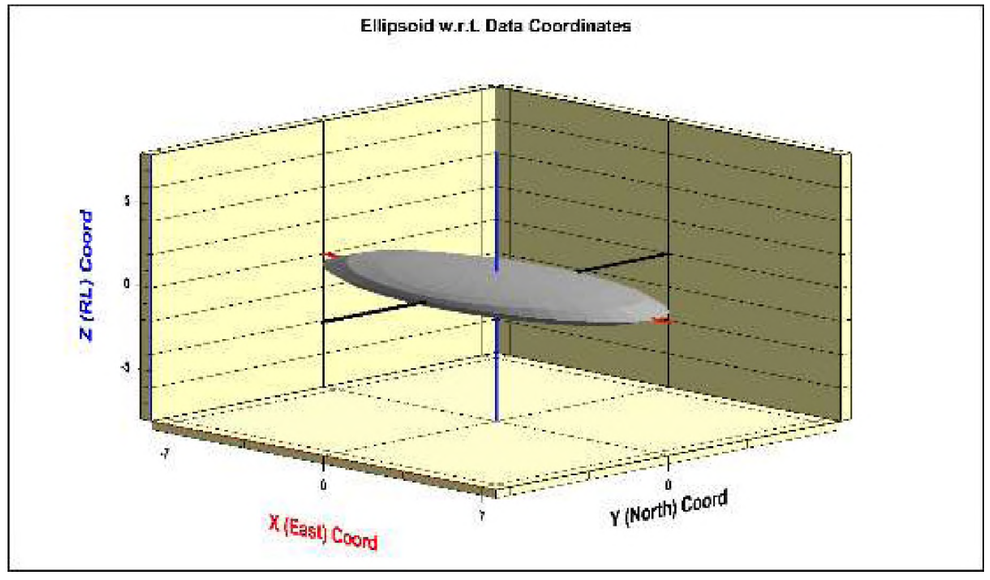

Figure 52: Variography of OK of 25 m x 25 m x 3 m block model

50 m x 50 m x 3 m data setup

Across-strike Variogram

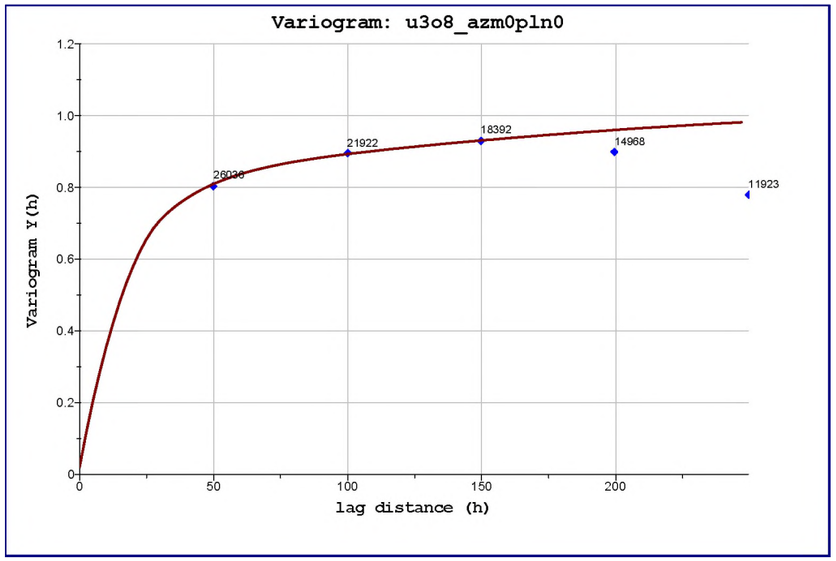

Along-strike Variogram

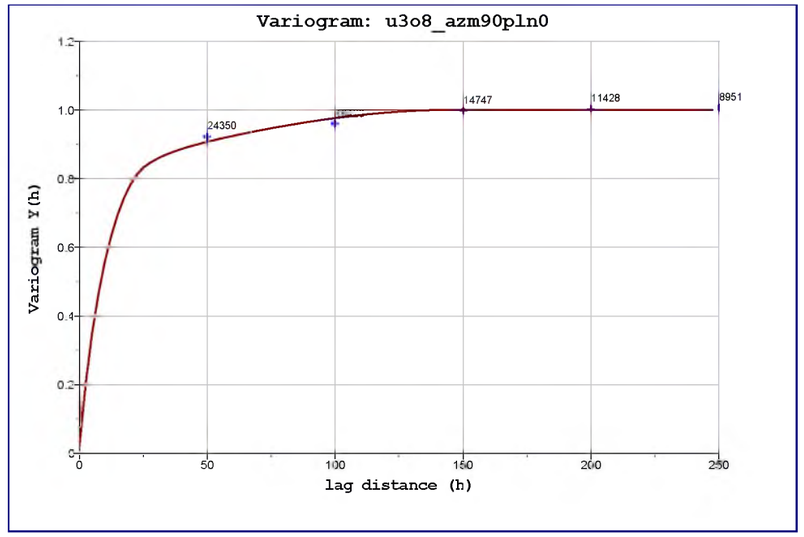

Down-hole variogram

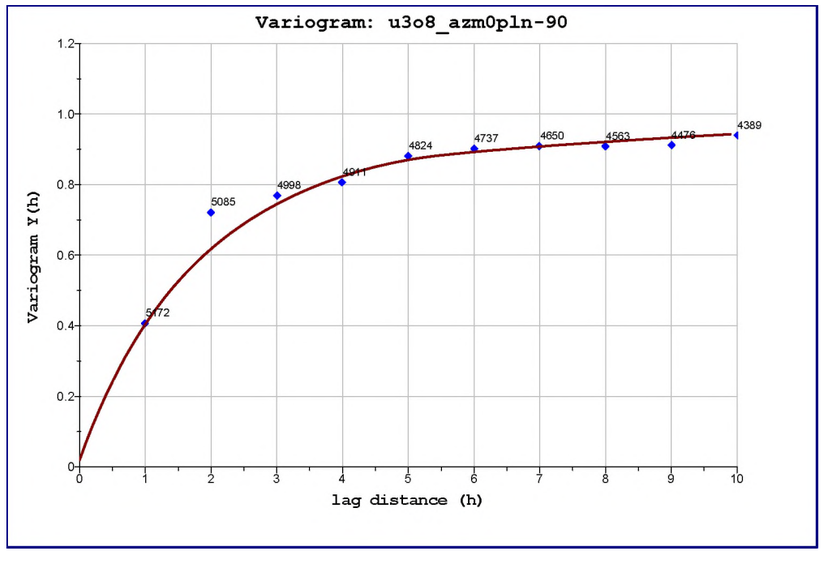

Variogram map

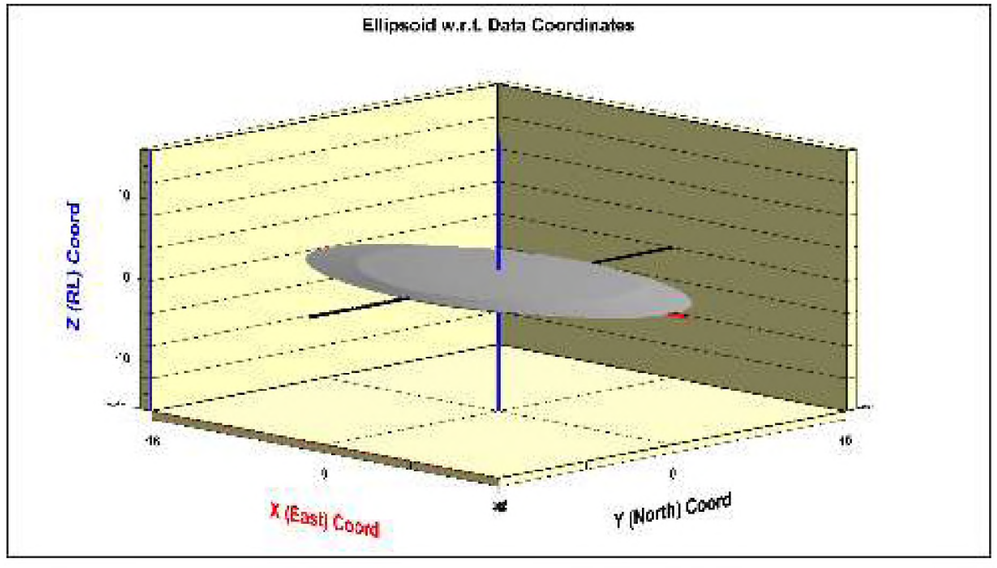

Figure 53: Variography of OK of 50 m x 50 m x 3 m block model

The same variogram parameters were used during CS and OK estimations in both pit H1 and G1. There are no significant changes with regards to mineralisation downstream from the Pit G1 area and therefore the parameters remained the same. The dataset used in H1 was substantially smaller than that of pit G1 and therefore there was no need to split the data into sections during the estimations. The along strike and downhole variograms from CS in Figure 49 all indicated zonal anisotropy as they did not flatten out. The across strike variogram indicates geometrical anisotropy as it seems to be leveling out. The variograms represent those created from exponential variogram modelling, which is indicated by the steep start of the variograms followed by a shallow longer second structure. The downhole variogram is more gradual than the other two variograms. The cumulative histogram used to find the cut off values and identify the outliers is consistent to about 19 000 ppm or just under 20 000 ppm. There are no major outlier groupings up to this interval, which only follow after 20 000 ppm. The Q-Q plot in Figure 49 indicates a slight overestimation for the CS block model in general. This is indicated by points falling just over the X-Y line, especially visible in the higher grades. The actual mean of the original unmodified dataset is around 213 ppm whilst the simulated mean is around 220 ppm.

The variograms created from OK in Figure 50 to Figure 53 all start off with a short steep structure followed by a longer shallow second structure. This is typical of a zonal anisotropic variogram shape. The sill seems to be reached at 1,0 and the nugget effect is usually between 0,2 and 0,4. The slope of the end of these variograms is, however, shallower and seems to flatten out. The downhole variograms have the best fit as is the case in all variography throughout this deposit.

6.4.3 Multiple indicator kriging data preparation
4 x 4 m x 3 m data setup

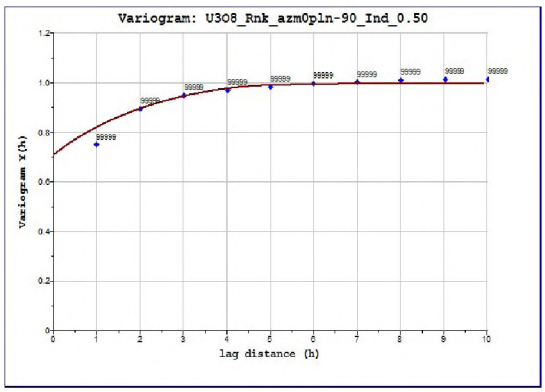

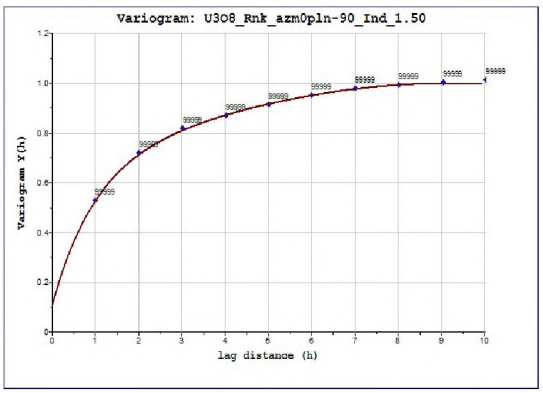

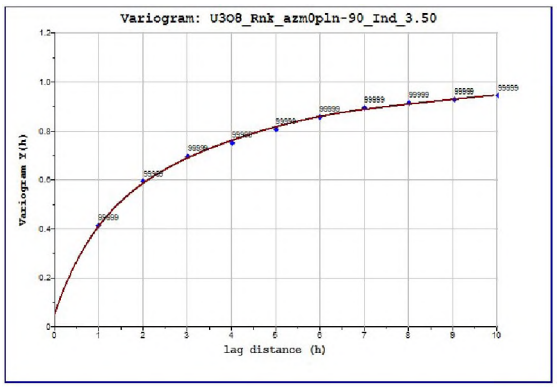

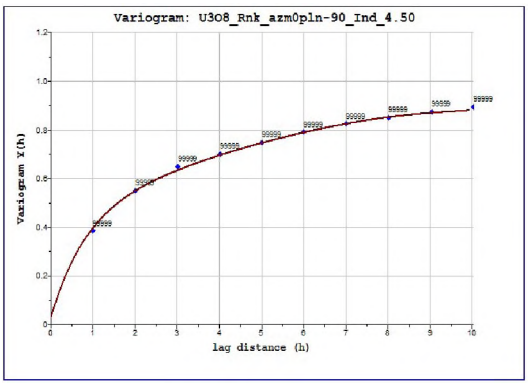

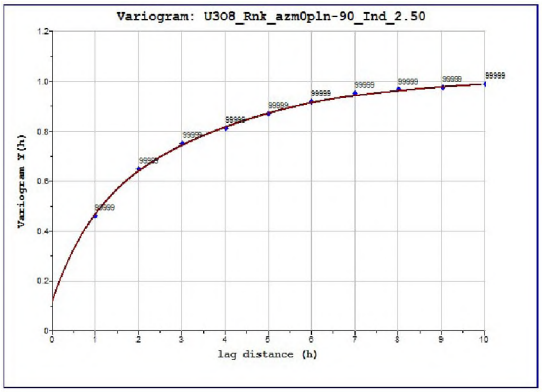

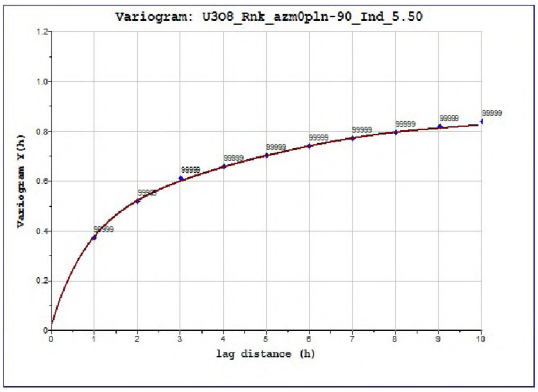

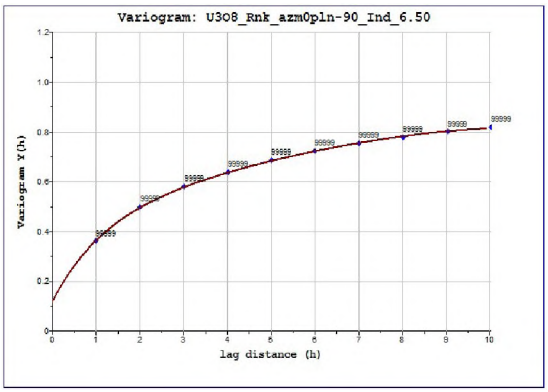
Variogram: U308_Rnk_azm0pln-90_Ind_6.50
Variogram Y(h)
lag distance (h)

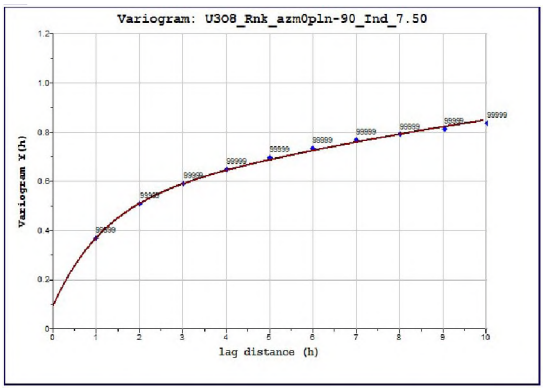
Variogram: U308_Rnk_azm0pln-90_Ind_7.50
Variogram Y(h)
lag distance (h)

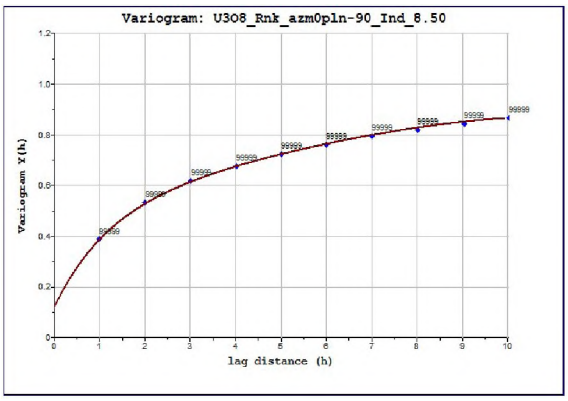
Variogram: U308_Rnk_azm0pln-90_Ind_8.50
Variogram Y(h)
lag distance (h)

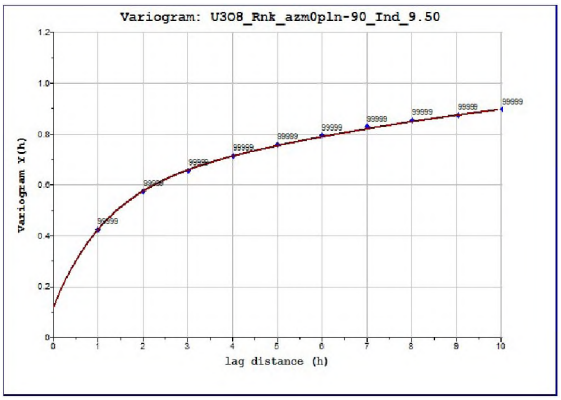
Variogram: U308_Rnk_azm0pln-90_Ind_9.50
Variogram Y(h)
lag distance (h)

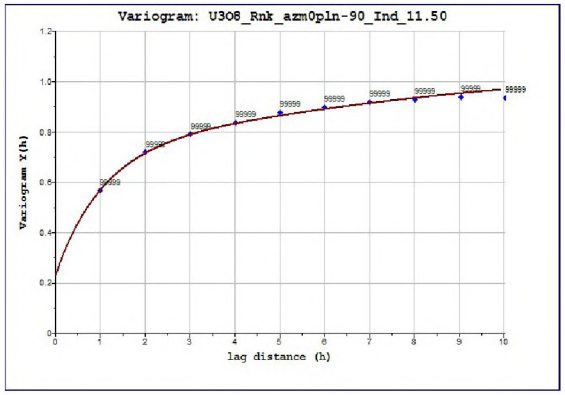
Variogram: U308_Rnk_azm0pln-90_Ind_11.50
Variogram Y(h)
lag distance (h)

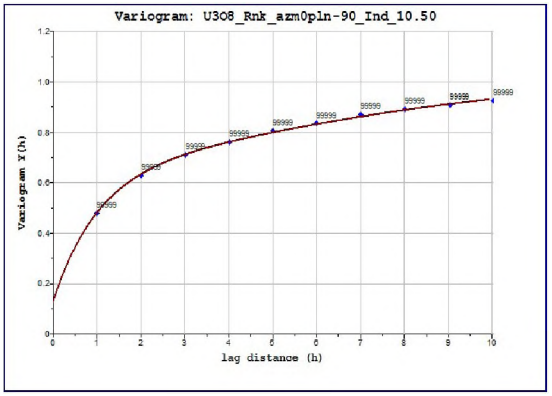
Variogram: U308_Rnk_azm0pln-90_Ind_10.50
Variogram Y(h)
lag distance (h)

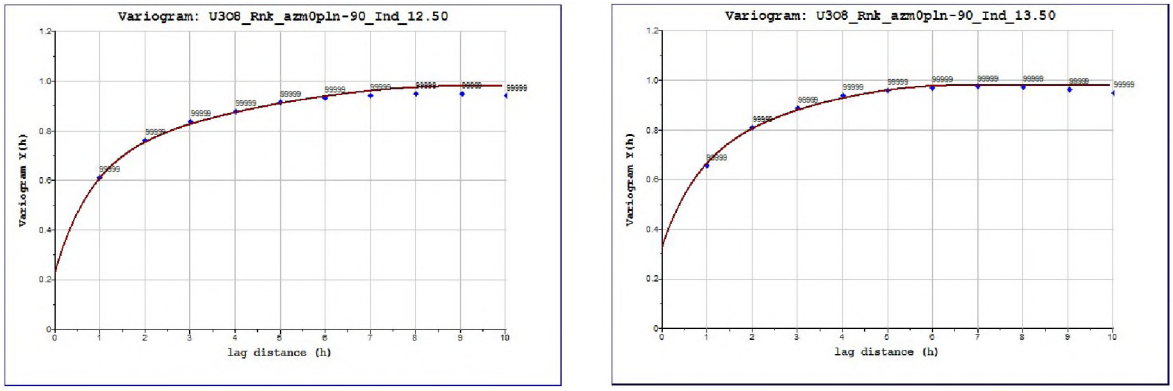

Figure 54: Downhole variography of 4 m x 4 m x 3 m MIK data

The same procedures and parameters were used here in relation to pit G1. 14 Different variograms were constructed and therefore 14 different cut-off values were selected. Displayed in Figure 54 are the 14 selected downhole variograms constructed during the MIK procedure. Along with these another 24 variograms were created, 12 along and 12 across strike. These variograms are harder to fit as there is less data available laterally than vertically. Therefore, the downhole variograms were much easier to fit and display. These variograms usually have a nugget effect around 0,2 and would flatten out towards a sill of 1,0. Only the first variogram (0.50) has a nugget value of 0,7. This is somewhat higher, although similar to the variogram seen in the pit G1 MIK variogram and most likely has to do with the low grade cut-off value below 100ppm. The variograms, as do the others, consist of a steep initial short structure followed by a longer gentle dipping structure. The variograms show zonal anisotropy and were modelled using the exponential model.

6.4.4 Basic statistics on various methods

Original dataset

Table 34: Statistics on the original unmodified dataset

		4 m x 4 m x 3 m	12,5 m x 12,5 x 3 m	25 m x 25 m x 3 m	50 m x 50 m x 3 m
Number of points used		244 602	81 221	21 246	5 259
Mean	**ppm**	242.3	146.8	147.3	155.9
Coefficient of variation		2.5	2.9	2.9	3.7
Standard deviation		715.0	421.5	433.9	572.6
Q1		11.5	12.8	12.4	12.2
Median		59.9	40.8	39.9	38.7
Q3	**ppm**	225.5	115.9	114.5	114.3
Maximum grade		29 637.4	37 903.5	23 269.4	23 269.4

The mean grade as seen in the pit G1 dataset would be the best statistic in terms of trend settings which would reflect the volume variance effect. As in pit G1 there is the clear indication that grade decreases with the decrease of data availability which is a factor of volume variance and can be observed in Table 34. The mean grade on the smallest block dimension displayed in Table 34 is almost 100 ppm more than the larger block model spacing. The 12,5 m x 12,5 m and 25 m x 25 m block models have similar mean grades, whilst the largest block models shows an increase of about 8ppm. This is unusual and differs from the usual trend of decreased grades with less data availability. The Q1 grades remain roughly the same throughout the block models, but both the median value as well as the Q3 value show the usual trend that decreases with less data availability. The maximum grades of the smallest block models is somewhat lower by 8 000 ppm compared to the 12,5 m x 12,5 m block model. It is higher, though, than the other larger block models by about 6 000 ppm.

The cumulative frequency charts observed in Figure 55 were used to decide which grades in the various sized block models would be capped. The capping grades used during simulations and estimations were as followed: The 4 m x 4 m block models were capped at 18 000 ppm, the 12,5 m x 12,5 m blocks were capped at 12 000 ppm, the 25 m x 25 m block models were capped 6 500 ppm and the 50 m x 50 m block models were capped at 5 000 ppm. This is a clear factor of data availability and therefore volume variance.

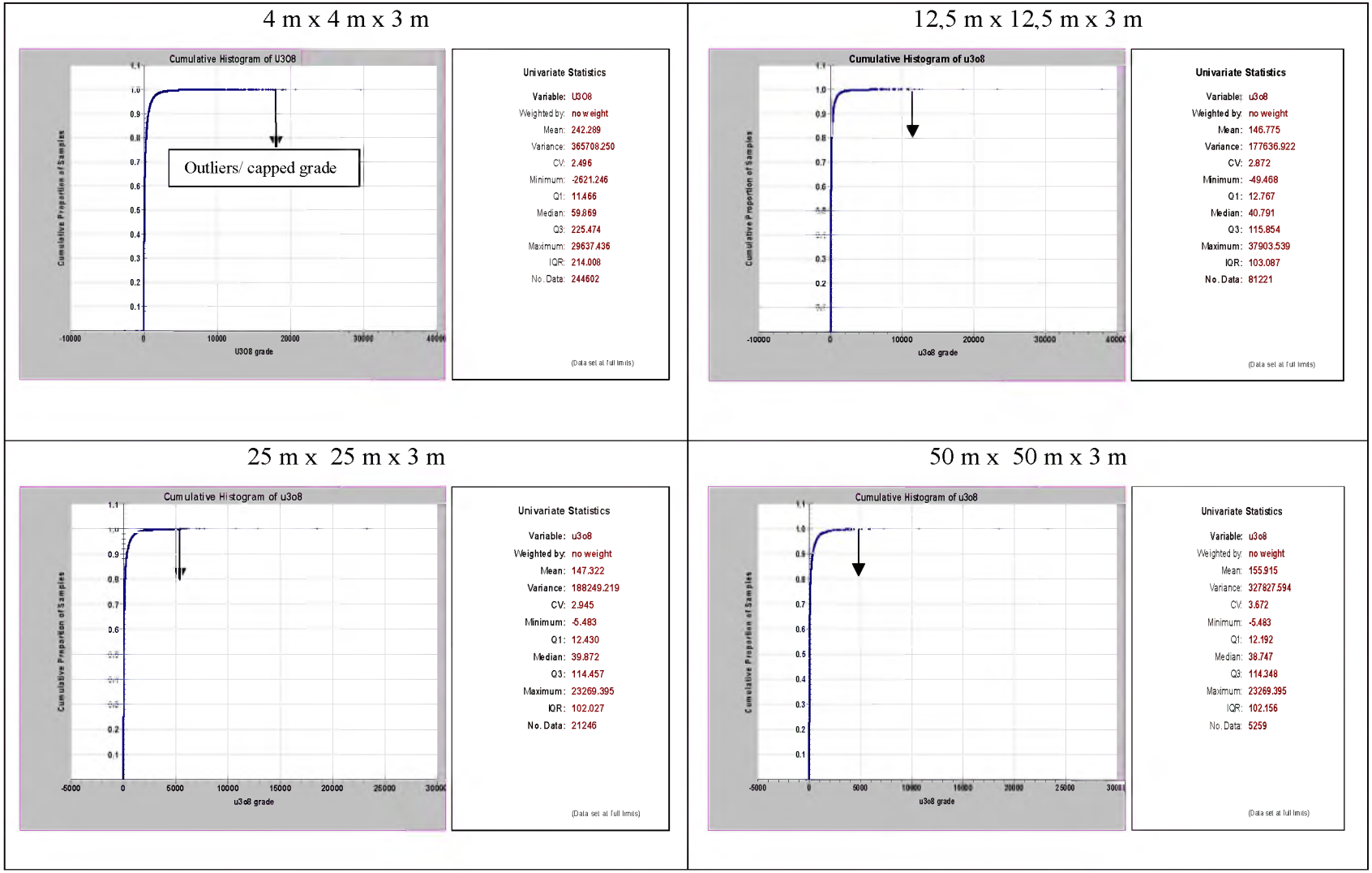

Figure 55: Cumulative frequency diagrams of original data

Conditional Simulation block model data

Table 35: Statistics of the CS simulated block model

		4 m x 4 m x 3 m
Number of points used		244 602
Blocks created		82 042
Mean	**ppm**	249.2
Coefficient of variation		1.4
Standard deviation		359.1
Q1	**ppm**	47.2
Median		124.7
Q3		302.6
Maximum grade		7 817.8

The blocks created by CS from the available data are presented in Table 35 is as in pit G1 less than any of the other methods. This trend was also observed in the pit G1 dataset. The mean is somewhat lower or rather average and close to the original dataset. The standard deviation is lower than the other methods. The Q1 and median (and therefore the average) of the lower grades are lower than any of the other block models, whilst the Q3 value is similar to the other methods. The maximum grade created from the CS model is low and somewhat conservative compared to the other methods.

Ordinary kriging block model data

Table 36: Statistics of the OK estimated block models

		4m x 4 m x 3m	12,5 m x 12,5 m x 3m	25 m x 25 m x 3m	50 m x 50 m x 3m
Number of points used		244 602	81 221	21 246	5 259
Blocks created		87 751	34 451	10 050	3 010
Mean	**ppm**	244.3	129.7	130.1	134.3
Coefficient of variation		1.9	1.7	1.9	1.7
Standard deviation		464.5	226.9	243.6	224.5
Q1	**ppm**	30.5	20.0	19.1	20.0
Median		89.6	53.5	52.1	58.1
Q3		273.6	129.7	130.4	149.1
Maximum grade		12 235.7	5 230.8	7 190.1	3 490.6

The blocks created from available data in Table 36 resembles that of IDW compared to the other methods. The mean for the smallest block model is similar to that of CS at about 245 ppm. The mean of the larger block models remains nearly the same around 130 ppm, which is lower than the original dataset and similar to that of the 12,5 m x 12,5 m and 25 m x 25 m block models of IDW. The standard deviation is relatively low compared to the original data and the IDW block models.

The Q1, median and Q3 values are similar to that of IDW but higher than the original dataset. The maximum grade, although higher than the CS block model, is lower than the IDW block models and much lower than that of the original dataset.

Inverse Distance Weighted ^{2} block model data

Table 37: Statistics of the IDW^2 estimated block models

		4 m x 4 m x 3 m	12,5 m x 12,5 m x 3m	25 m x 25 m x 3 m	50 m x 50 m x 3m
Number of points used		244 602	81 221	21 246	5 259
Blocks created		101 742	33 799	9 408	2 691
Mean	**ppm**	261.1	128.3	129.9	149.7
Coefficient of variation		1.9	1.8	1.8	1.7
Standard deviation		486.3	227.2	232.3	240.1
Q1	**ppm**	30.3	18.2	18.2	18.8
Median		91.7	51.7	53.6	59.7
Q3		284.8	126.8	133.5	163.0
Maximum grade		18 044.1	6 026.2	6 087.5	2 982.1

Inverse Distance Weighted ^{3} block model data

Table 38: Statistics of the IDW^3 estimated block models

		4 m x 4 x 3 m	12,5 m x 12,5 m x 3 m	25 m x 25 m x 3 m	50 m x 50 m x 3m
Number of points used		244 602	81 221	21 246	5 259
Blocks created		110 308	38 356	11 011	2 847
Mean	**ppm**	252.4	116.1	119.2	138.6
Coefficient of variation		1.9	1.7	1.7	1.7
Standard deviation		473.2	199.9	199.9	240.7
Q1	**ppm**	33.6	17.3	17.2	16.5
Median		94.3	46.6	48.9	54.1
Q3		281.0	116.7	126.6	147.9
Maximum grade		15 146.9	5 055.8	3 820.4	3 063.9

The IDW block models as observed in the pit G1 dataset (Table 37 and Table 38) do not differentiate much from each other. The blocks created from the 4 m x 4 m block models are substantially higher than any of the other methods. The blocks created from the larger models are similar to that of the other methods, whilst the smaller block models created more blocks. The standard deviation follows the same trend in which the grade difference is elevated in the 4 m x 4

m block models, whilst the others resemble a similar grade to the other methods. The Q1, median and Q3 grades are similar to those of the other methods. The maximum grades are higher than all of the other methods but lower than the original dataset.

Multiple indicator kriging block model data

Table 39: Statistics of the MIK estimated block models

		4 m x 4 m x 3 m	12,5 m x 12,5 m x 3 m	25 m x 25 m x 3 m	50 m x 50 m x 3 m
Number of points used		244 602	81 221	21 246	5 259
Blocks created		97 403	34 221	9 332	2 607
Mean	**ppm**	246.9	133.2	136.7	137.3
Coefficient of variation		1.6	1.6	1.5	1.5
Standard deviation		391.4	211.8	207.9	188.3
Q1		51.1	23.3	25.6	26.0
Median	**ppm**	99.2	56.3	58.4	61.7
Q3		271.8	136.3	149.6	164.5
Maximum grade		4 419.9	2 423.2	2 422.9	1 288.6

MIK data as seen in Table 39 and in the grade tonnage plots below is the most conservative method in terms of grades. The maximum grade obtained is much lower than the other methods, although the mean grade is representative in comparison to the other methods. Most of the other statistics are similar to that of MIK displayed below, although the grade tonnage graphs clarify that MIK is somewhat more conservative compared to the other methods. There are no major differences between the Q1, median and Q3 figures, although there is always a large jump between the 4 m x 4 m x 3 m block models and the rest.

6.4.5 Rank percentile graphs of block models

The rank percentile graphs presented in Figure 56 and Figure 57 should provide evidence on the degree of smoothing of various estimations. Tested here is the degree of smoothing among different estimation methods on the same block dimensions and degree of smoothing of the same methods, but at different block dimensions. The dashed line indicates the original unmodified dataset drilled at 4 m x 4 m as a realistic comparison to reality. From Figure 56 it is clear that the largest variation between individual lines is displayed in the 4 m x 4 m x 3 m block modelled data. In the rank percentile graph it can be observed that there is a high degree of over-smoothing within the various methods in the lower grades. This becomes increasingly less from about 100 ppm upwards and follows the same trend as the original dataset for the higher-grades. This is optimal as these grades are economically viable and are therefore of interest. From the individual methods it can be observed that OK and IDW indicate the lowest degree of over-smoothing for the lower grades, whilst MIK and CS show similar trends and a higher degree of over-smoothing. The rank percentile graphs of the larger block models all have a similar shape and structure. There is less over-smoothing in the lower grades of the larger block models than the 4 m x 4 m x 3 m data. The 25 m x 25 m and 50 m x 50 m x 3 m rank percentile graphs all indicate a degree of over-smoothing much higher than 100 ppm, which was the limit in the 4 m x 4 m x 3 m graphs. These larger block dimensions indicate a percentile of more than 80 %, whilst the smaller block dimensions indicate a smoothing trend less than that compared to the original dataset.

The rank percentile graphs illustrated Figure 57 have been plotted to see how the individual methods perform on different drill spacing in relationship to the original dataset obtained from a 4 m x 4 m drill spacing. Of interest is the degree of smoothing of the various estimation methods at higher-grades, hence above 250 ppm which would be regarded as ore. All of the graphs above show similar trends in terms of their display. Two differences in line positioning compared to the original dataset can be observed. There is a large degree in smoothing difference between the smaller 4 m x 4 m x 3 m block model estimations and the larger block model estimation. This can be seen in their relative position compared to the original dataset. The 4 m x 4 m x 3 m estimation in all methods shows a higher degree of over-smoothing in lower grades below 100 ppm. It is also observed that over-smoothing continues to slightly higher-grades than the broader spaced estimations. The broader spaced estimations usually decrease in their degree of smoothing just after 10 ppm, and intersect the original dataset steeply to continue undersmoothing for the high-grades, most likely due to the volume variance effect. This is seen throughout all the various methods used. The undersmoothing continues up to roughly 1 000 ppm where it stabilises and follows the original dataset. This represents only 5 % that follows the original dataset. The 12,5 m

x 12,5 m x 3 m estimation slightly differs from the broader spaced estimations, however there is a major difference between it and the 4 m x 4 m x 3 m estimation. This is primarily due to the amount of data used for the estimations. The 4 m x 4 m x 3 m estimation indicates as mentioned before the highest degree of over-smoothing, especially visible in grades below 100 ppm. Between 10 and 100 ppm the degree of over-smoothing decreases steeply cutting the original dataset projection at about 100 ppm and between 50 and 60 %. After this intersection the estimation honours the original dataset onwards for the higher-grades which is preferable and expected.

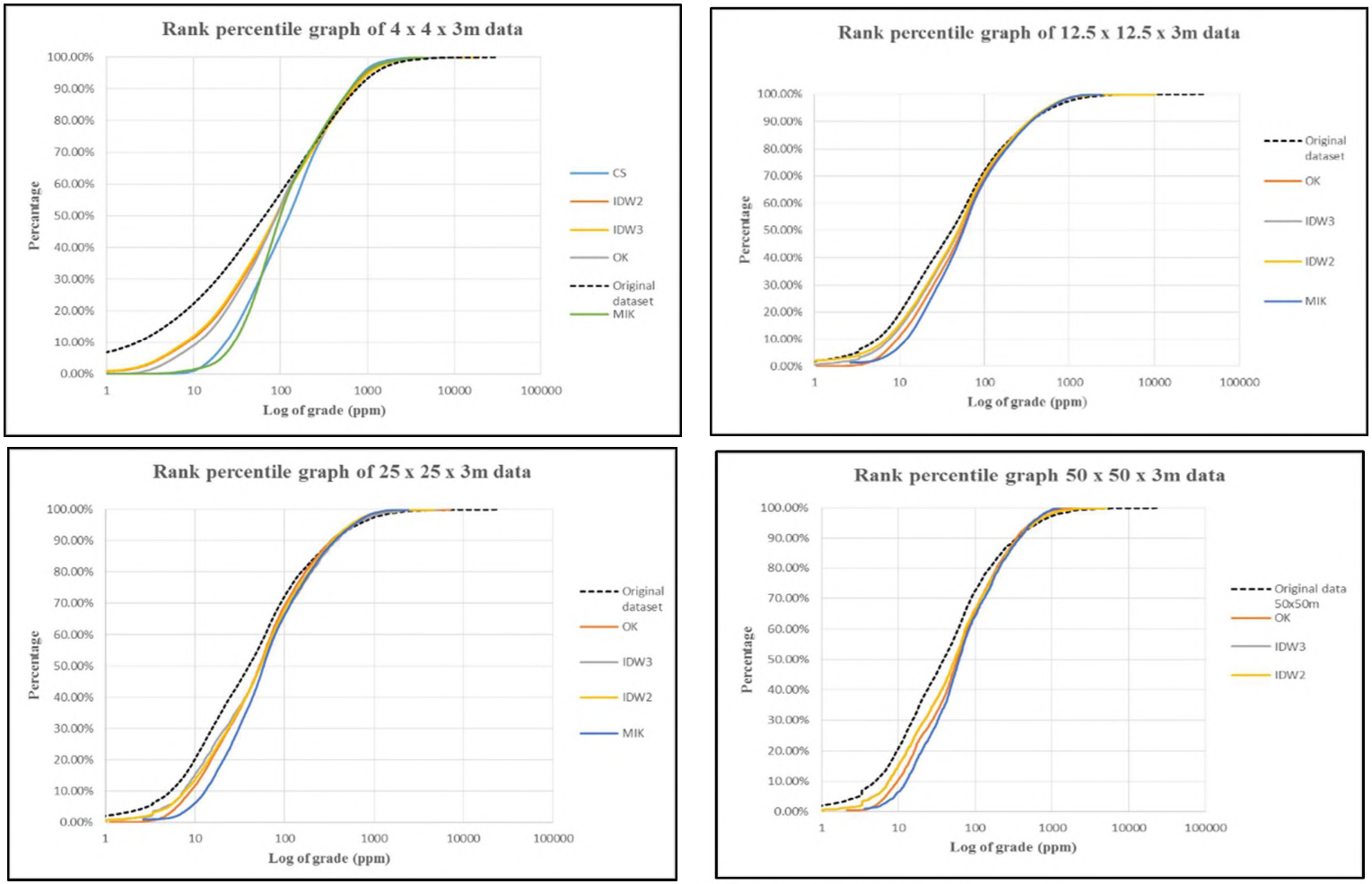

Figure 56: Rank percentile graphs of the same block dimensions using various estimation methods

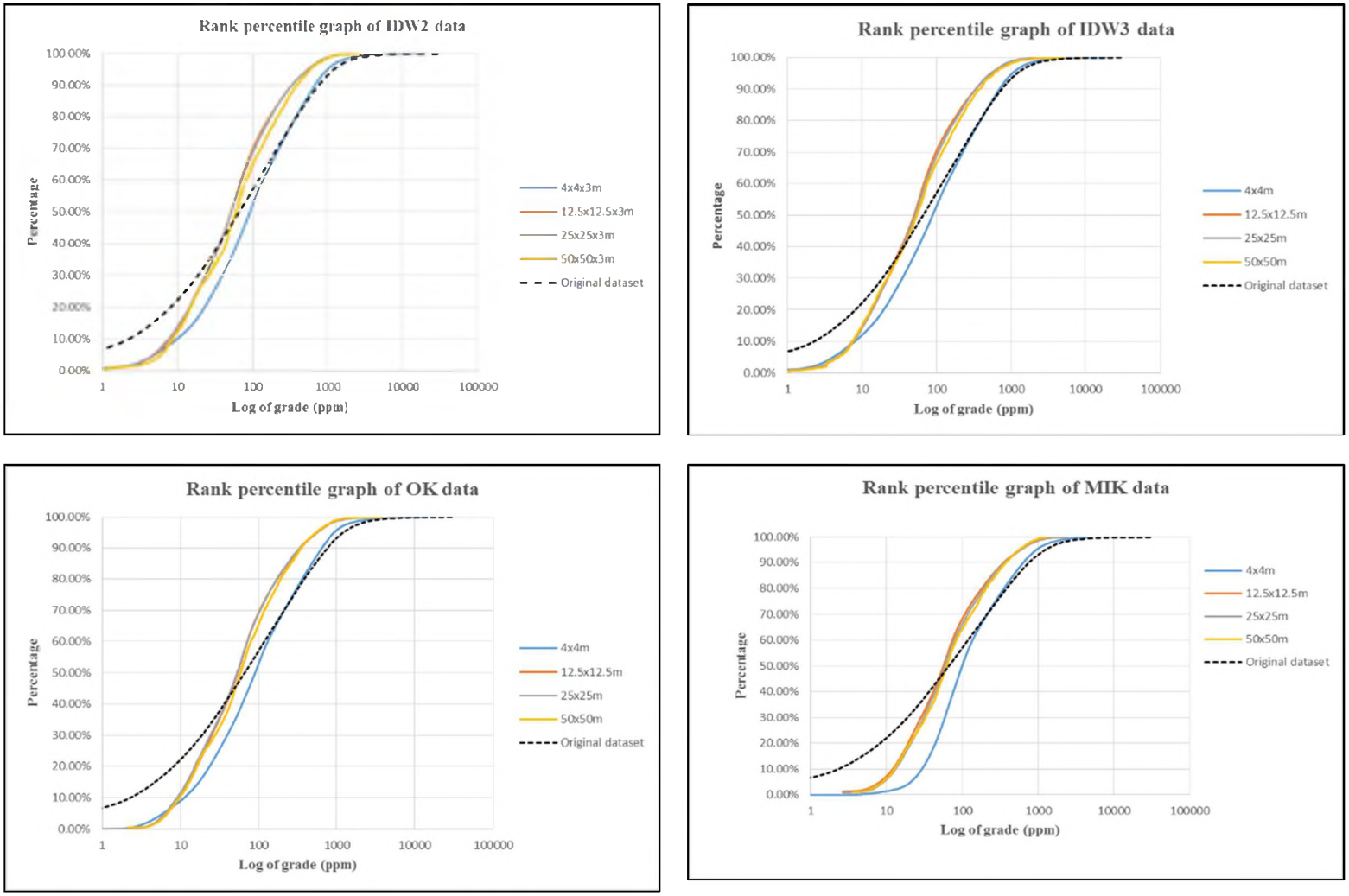

Figure 57: Rank percentile graphs of different block dimensions using the same estimation method

6.5 Block model report

Table 40: Final block model report on various geostatistical methods and different block dimensions

Block model dimension	IDW² (t)	IDW³ (t)	OK (t)	MIK (t)	CS (t)	Mined tonnes (t)	WF estimated tonnes (t)
4 m x 4 m x 3m	8 054 803	8 073 451	8 039 354	8 075 300	7 962 837	8 256 112	8 294 997
12,5 m x 12,5 m x 3m	8 085 940	8 090 232	8 088 660	8 082 013	-		
25 m x 25 m x 3m	8 090 111	8 090 232	8 090 232	8 088 569	-		
50 m x 50 m x 3m	8 090 232	8 090 232	8 090 232	8 090 232	-		

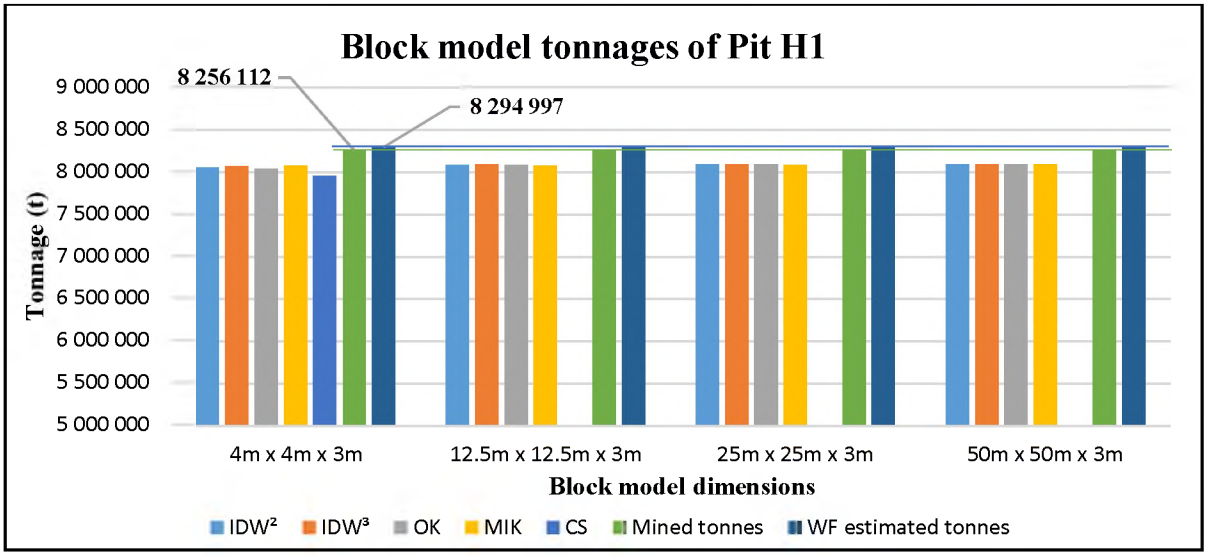

Figure 58: Estimated tonnage versus mined tonnage versus final wireframe tonnage

Table 40 and Figure 58 illustrate the final tonnages that were mined and estimated from various geostatistical methods. The final mined tonnage of pit H1 was about 8 256 112 t, which is approximately half of that of pit G1 and therefore substantially less. The WF or wireframe tonnage resulted in 8 294 997 t and is therefore about 39 000 t more than the final mined figure. All of the methods used were limited to the pit shell of the wireframe and therefore accurately represents the tonnage thereof. The various estimates are usually very similar or less than the WF tonnage. It can be observed that with decreasing block sizes used during estimation, there is increase in variance of the WF tonnage. Therefore the smallest block sizes have the lowest comparative tonnage and therefore the highest variance. Of the various methods, CS has the highest variance and is less than 8 000 000 t in total. This is more than 294 000 t less than the restrictive WF used during estimation.

Figure 59 presents the error variance between the mined tonnage and various estimation methods. It can clearly be observed that the actual mined tonnage was roughly 0,5 % less than the WF and comparative estimations. Also visible is that the 4 m x 4 m x 3 m block models have a higher variance between both mined and WF tonnage. This gradually decrease with the increase in the block sizes and data availability. Both linear and non-linear estimation methods produced similar results. CS produced estimation with the highest variances which ranged between 3-4 %.

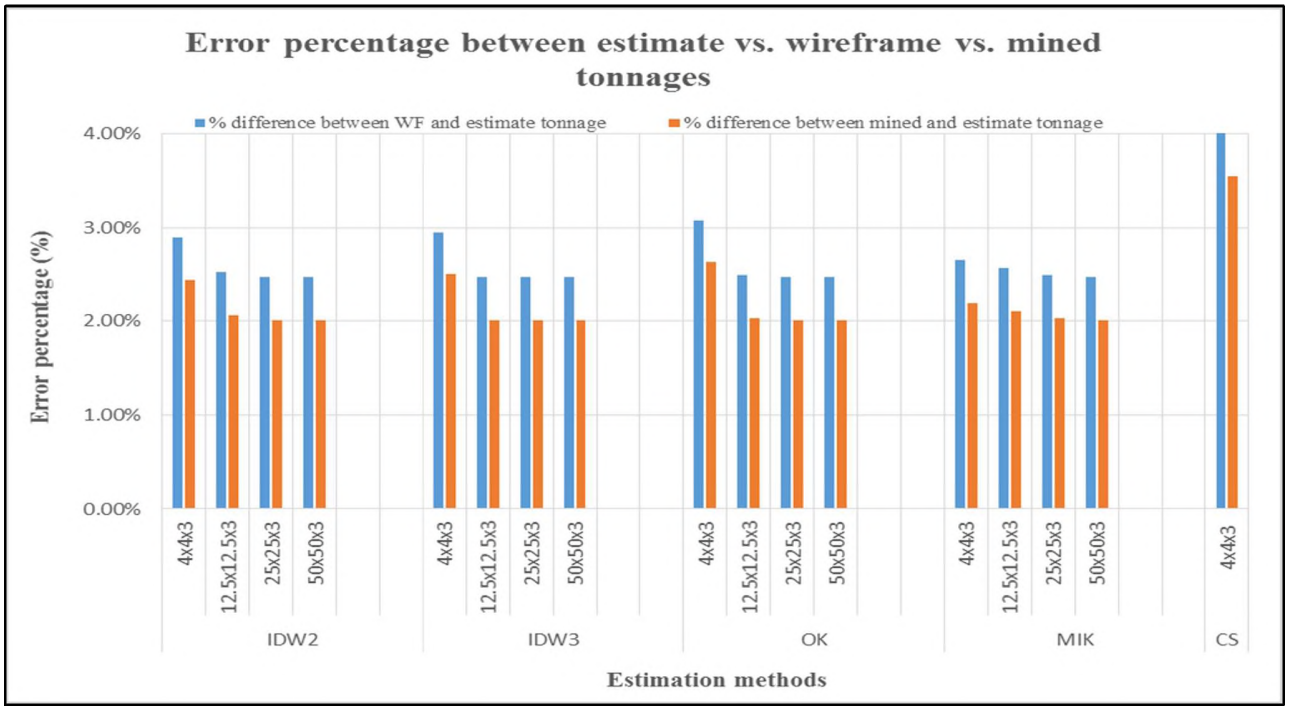

Figure 59: Error percentage between estimates and mined tonnage, and estimated tonnage vs. wireframe tonnage

Table 41: Block model report at various grade categories

	Block model dimension (m)	Waste 0-250 ppm (Tonnage)	Average grade (ppm)	Low-grade 250-400 ppm (Tonnage)	Average grade (ppm)	Medium-grade 400-650 ppm (Tonnage)	Average grade (ppm)	High-grade 650-900 ppm (Tonnage)	Average grade (ppm)	Super high-grade 900+ ppm (Tonnage)	Average grade (ppm)
IDW²	4 x 4 x 3	5 570 878	76.9	798 893	318.3	793 893	513.6	423 517	759.1	467 946	1 652.6
	12,5 x 12,5 x 3	5 390 044	94.3	937 903	316.4	933 622	514.5	462 148	755.0	362 222	1 345.8
	25 x 25 x 3	5 313 661	95.8	1 027 042	320.8	980 057	514.5	456 514	757.9	312 838	1 456.3
	50 x 50 x 3	4 913 828	98.3	1 180 529	314.2	1 085 489	524.4	398 721	742.5	511 665	1 321.2
IDW³	4 x 4 x 3	5 515 804	81.0	834 598	317.4	853 535	513.9	429 247	759.2	440 266	1 589.1
	12,5 x 12,5 x 3	5 330 546	99.2	973 539	317.5	1 018 352	517.1	469 776	755.8	298 020	1 274.6
	25 x 25 x 3	5 137 053	99.9	1 159 693	318.2	1 094 521	514.2	456 929	748.2	242 035	1 280.0
	50 x 50 x 3	4 996 947	100.4	1 117 025	321.8	1 170 052	524.1	463 103	777.2	343 105	1 435.4
OK	4 x 4 x 3	5 601 644	73.9	776 863	318.7	765 495	512.4	412 740	760.5	482 611	1 656.2
	12,5 x 12,5 x 3	5 359 274	92.0	974 472	319.4	942 519	514.7	462 670	754.7	349 825	1 353.2
	25 x 25 x 3	5 341 031	93.0	993 500	313.1	945 712	510.3	498 997	745.6	310 993	1 504.3
	50 x 50 x 3	4 987 043	95.8	1 191 181	322.7	1 068 286	513.0	444 100	764.7	399 623	1 407.7
MIK	4 x 4 x 3	5 561 166	84.5	798 881	319.0	770 016	514.5	437 551	761.6	506 686	1 515.2
	12,5 x 12,5 x 3	5 315 394	93.4	960 396	318.1	916 297	512.6	508 289	758.0	381 638	1 187.3
	25 x 25 x 3	5 190 089	97.6	1 013 316	319.7	1 029 360	520.7	562 696	750.9	293 107	1 165.9
	50 x 50 x 3	4 958 594	99.0	1 041 990	324.3	1 262 655	500.9	507 079	751.2	319 914	1055.4
CS	4 x 4 x 3	5 415 156	89.8	874 509	318.8	813 779	512.1	433 339	759.6	426 054	1 421.9
Mined		5 772 889	89.6	847 827	325.8	747 613	515.0	887 783		1 162.9	

Table 41 provides an illustration of the various estimated grades and tonnages along with their representative estimation method at different block dimensions. The total mined waste was 5 772 889 t at 90ppm, whilst the total ore mined was 2 483 223 t. With regards to waste, the estimated grade was around 80-100 ppm for the larger drill spacing, whilst about 10-20 ppm lower for the smaller drill spacing between the various estimation methods. This also represents a similar average grade that was mined. The waste tonnage mined indicates that with increasing grade there is a decrease in tonnage. In the low-grade category the average grade is around 320 ppm, with not much variation between the different block sizes and methods. The average low grade mined had a grade of 326 ppm, slightly higher than the estimated grades. The highest tonnages within the categories are observed in the larger block models which are observed in OK and MIK, whilst IDW has much lower tonnages.

In the medium-grade category the grades are usually around 515 ppm with tonnage variations between 740 000 and 1 260 000 t. The general trend in tonnage estimation indicates that the lowest

tonnages are observed in the 4 m x 4 m x 3 m block models whilst the highest tonnages are observed in the larger block models. The average grade for normal high-grade is around 755 ppm which corresponds to the average grade mined at 761 ppm. Tonnages vary from about 420 000 to a little over 500 000 t. the grade however is higher here than in the larger block models, which is most likely a factor of volume variation. In the super-high category, the average grades have increased variability. These grades vary from 1 050 to 1 700 ppm and tonnages from 290 000 to 500 000 t. Generally the highest tonnages are observed in the smallest block models and also the highest corresponding grades. This trend is clearly observed in the MIK and OK methods, whilst IDW deviates in a way that the largest block models have similar grades and tonnages to that of the 4 m x 4 m x 3 m block models.

6.5.1 Estimated or simulated tonnage versus mined tonnage variances

Table 42: 4 m x 4 m x 3 m estimated tonnage and mined tonnage

Estimation method	Estimated Waste (t)	Difference (%)	Estimated LG (t)	Difference (%)	Estimated MG (t)	Difference (%)	Estimated HG (t)	Difference (%)
IDW^2	5 570 878	3.6	798 893	6.1	793 893	-5.8	891 463	-0.4
IDW^3	5 515 804	4.7	834 598	1.6	853 535	-12.4	869 513	2.1
OK	5 601 644	3.1	776 863	9.1	765 495	-2.3	895 351	-0.8
MIK	5 561 166	3.8	798 881	6.1	770 016	-2.9	944 237	-6.0
CS	5 415 156	6.6	874 509	-3.1	813 779	-8.1	859 393	3.3
Average (t)	5 532 930	4.3	816 749	3.8	799 344	-6.5	891 991	-0.5
Mined tonnage (t)	5 772 889		847 827		747 613		887 783	

Table 43: 12,5 m x 12,5 m x 3 m estimated tonnage and mined tonnage

Estimation method	Estimated Waste (t)	Difference (%)	Estimated LG (t)	Difference (%)	Estimated MG (t)	Difference (%)	Estimated HG (t)	Difference (%)
IDW^2	5 390 044	7.1	937 903	-9.6	933 622	-19.9	824 370	7.7
IDW^3	5 330 546	8.3	973 539	-12.9	1 018 352	-26.6	767 796	15.6
OK	5 359 274	7.7	974 472	-13.0	942 519	-20.7	812 495	9.3
MIK	5 315 394	8.6	960 396	-11.7	916 297	-18.4	889 927	-0.2
Average (t)	5 348 815	7.9	961 578	-11.8	952 698	-21.5	823 647	7.8
Mined tonnage (t)	5 772 889		847 827		747 613		887 783	

Table 44: 25 m x 25 m x 3 m estimated tonnage and mined tonnage

Estimation method	Estimated Waste (t)	Difference (%)	Estimated LG (t)	Difference (%)	Estimated MG (t)	Difference (%)	Estimated HG (t)	Difference (%)
IDW^2	5 313 661	8.6	1 027 042	-17.4	980 057	-23.7	769 352	15.4
IDW^3	5 137 053	12.4	1 159 693	-26.9	1 094 521	-31.7	698 964	27.0
OK	5 341 031	8.1	993 500	-14.7	945 712	-20.9	809 990	9.6
MIK	5 190 089	11.2	1 013 316	-16.3	1 029 360	-27.4	855 803	3.7
Average (t)	5 245 459	10.1	1 048 388	-19.1	1 012 412	-26.2	783 527	13.3
Mined tonnage (t)	5 772 889		847 827		747 613		887 783	

Table 45: 50 m x 50 m x 3 m estimated tonnage and mined tonnage

Estimation method	Estimated Waste (t)	Difference (%)	Estimated LG (t)	Difference (%)	Estimated MG (t)	Difference (%)	Estimated HG (t)	Difference (%)
IDW^2	4 913 828	17.5	1 180 529	-28.2	1 085 489	-31.1	910 386	-2.5
IDW^3	4 996 947	15.5	1 117 025	-24.1	1 170 052	-36.1	806 208	10.1
OK	4 987 043	15.8	1 191 181	-28.8	1 068 286	-30.0	843 723	5.2
MIK	4 958 594	16.4	1 041 990	-18.6	1 262 655	-40.8	826 993	7.4
Average (t)	4 964 103	16.3	1 132 681	-25.1	1 146 621	-34.8	846 828	4.8
Mined tonnage (t)	5 772 889		847 827		747 613		887 783	

Table 46: Average percentage variance between estimated and mined tonnage

Block model dimension	Average variance % (mined vs. estimated)			
	W	LG	MG	HG
4 m x 4 m x 3 m	4.3	3.8	-6.5	-0.5
12,5 m x 12,5 m x 3 m	7.9	-11.8	-21.5	7.8
25 m x 25 m x 3 m	10.1	-19.1	-26.2	13.3
50 m x 50 m x 3 m	16.3	-25.1	-34.8	4.8

In the waste category in Table 42, the average mined tonnage was 4 % more than the average estimated tonnage. In the low-grade category the mined tonnage was on average just under 4 % more than the estimated tonnages. IDW^3 estimated the lowest variance with an underestimation of just under 2 %. In the medium-grade category most estimations were now overestimated. The mined tonnage on average was about 7 % less than the estimated tonnage. Both OK and MIK has the lowest overestimations at under 3 %. In the high-grade category there were increased differences between various estimation methods. The mined tonnage was 0,5 % less than the average estimated tonnage, and variances observed varied from 6 % overestimation up to 3 % underestimations. Both IDW^2 and OK resulted in reasonably good estimates.

Table 43 illustrates the estimated and mined tonnage calculated from the 12,5 m x 12,5 m x 3 m data. The waste category on average contained estimates that were 8 % less than the mined tonnage.

In the low-grade category all methods overestimated by about 12 % compared to the mined tonnage. All methods estimated similar tonnages, with IDW^2 being the lowest at under 10 % difference. In the medium-grade category slightly increased overestimations are observed. The average estimation yielded a difference of 22 % higher tonnages than what was mined. In the high-grade category a variety of estimation results are observed, the average being 8 % less than what was mined. MIK yielded the best tonnage estimate, which has less than 1 % variance.

Table 44 illustrates the results of the 25 m x 25 m x 3 m block models. In the waste category the mined tonnage was 10 % more than estimated tonnages. In the low-grade category as mentioned before, the estimated tonnage was on average 19% more than the mined tonnage. OK performed the best with an overestimation of 15 %. In the medium-grade category the average estimation method overestimated by 26 %, with IDW^2 being the lowest at 24 %. In the high-grade category 13 % was mined more compared to estimated tonnages. MIK resulted in the best estimation with an underestimation of just under 4 %.

In Table 45 the estimation results are presented from the 50 m x 50 x 3 m block models. In the waste category 10 % was mined more than the estimations predicted. In the low-grade category on average the estimations resulted in a 25 % overestimation. In the medium-grade category all methods overestimated substantially. In total the methods overestimated by approximately 34 % compared to what was mined, with all methods estimating similar tonnages except for IDW^3. In the high-grade category the average estimation was 5 % less than what was mined. Some variances in tonnage predications can be observed with IDW^2 being the lowest at 3 % overestimation. Table 46 provides a summary of the various block dimensions and the related variance between the estimated and mined tonnages.

6.5.2 Estimated or simulated grade versus mined grade variances

Table 47: 4 m x 4 m x 3 m estimated grade vs. average mined grade

Estimation method	Estimated grade Waste (ppm)	ppm difference (mined vs. estimated) %	Estimated grade LG (ppm)	ppm difference (mined vs. estimated) %	Estimated grade MG (ppm)	ppm difference (mined vs. estimated) %	Estimated grade HG (ppm)	ppm difference (mined vs. estimated) %
IDW^2	76.9	16.5	318.3	2.4	513.6	0.3	1 228.1	-5.3
IDW^3	81.0	10.6	317.4	2.6	513.9	0.2	1 179.4	-1.4
OK	73.9	21.2	318.7	2.2	512.4	0.5	1 243.3	-6.5
MIK	84.5	6.0	319.0	2.1	514.5	0.1	1 166.0	-0.3
CS	89.8	-0.2	318.8	2.2	512.1	0.6	1 087.9	6.9
Average (ppm)	**81.2**	**10.3**	**318.4**	**2.3**	**513.6**	**0.3**	**1 181.0**	**-1.5**
Mined grade (ppm)	**89.6**		**325.8**		**515.0**		**1 162.9**	

Table 48: 12,5 m x 12,5 m x 3 m estimated grade vs. average mined grade

Estimation method	Estimated grade Waste (ppm)	ppm difference (mined vs. estimated) %	Estimated grade LG (ppm)	ppm difference (mined vs. estimated) %	Estimated grade MG (ppm)	ppm difference (mined vs. estimated) %	Estimated grade HG (ppm)	ppm difference (mined vs. estimated) %
IDW^2	94.3	-5.0	316.4	3.0	514.5	0.1	1 014.6	14.6
IDW^3	99.2	-9.7	317.5	2.6	517.1	-0.4	957.2	21.5
OK	92.0	-2.6	319.4	2.0	514.7	0.1	1 012.4	14.9
MIK	93.4	-4.1	318.1	2.4	512.6	0.5	942.1	23.4
Average (ppm)	**94.7**	**-5.4**	**317.9**	**2.5**	**514.7**	**0.1**	**981.6**	**18.5**
Mined grade (ppm)	**89.6**		**325.8**		**515.0**		**1 162.9**	

Table 49: 25 m x 25 m x 3 m estimated grade vs. average mined grade

Estimation method	Estimated grade Waste (ppm)	ppm difference (mined vs. estimated) %	Estimated grade LG (ppm)	ppm difference (mined vs. estimated) %	Estimated grade MG (ppm)	ppm difference (mined vs. estimated) %	Estimated grade HG (ppm)	ppm difference (mined vs. estimated) %
IDW^2	95.8	-6.5	320.8	1.6	514.5	0.1	1 041.9	11.6
IDW^3	99.9	-10.3	318.2	2.4	514.2	0.2	932.3	24.7
OK	93.0	-3.7	313.1	4.1	510.3	0.9	1 036.9	12.2
MIK	97.6	-8.2	319.7	1.9	520.7	-1.1	893.0	30.2
Average (ppm)	**96.6**	**-7.2**	**318.0**	**2.5**	**514.9**	**0.0**	**976.0**	**19.1**
Mined grade (ppm)	**89.6**		**325.8**		**515.0**		**1 162.9**	

Table 50: 50 m x 50 m x 3 m estimated grade vs. average mined grade

Estimation method	Estimated grade Waste (ppm)	ppm difference (mined vs. estimated) %	Estimated grade LG (ppm)	ppm difference (mined vs. estimated) %	Estimated grade MG (ppm)	ppm difference (mined vs. estimated) %	Estimated grade HG (ppm)	ppm difference (mined vs. estimated) %
IDW^2	98.3	-8.9	314.2	3.7	524.4	-1.8	1 067.7	8.9
IDW^3	100.4	-10.8	321.8	1.2	524.1	-1.7	1 057.3	10.0
OK	95.8	-6.5	322.7	1.0	513.0	0.4	1 069.3	8.8
MIK	99.0	-9.5	324.3	0.5	500.9	2.8	868.9	33.8
Average (ppm)	**98.4**	**-8.9**	**320.8**	**1.6**	**515.6**	**-0.1**	**1 015.8**	**15.4**
Mined grade (ppm)	**89.6**		**325.8**		**515.0**		**1 162.9**	

Table 51: Average percentage variance between estimated and mined grade

Block model dimension	Average variance % (mined vs. estimated)			
	W	LG	MG	HG
4 m x 4 m x 3 m	10.3	2.3	0.3	-1.5
12,5 m x 12,5 m x 3 m	-5.4	2.5	0.1	18.5
25 m x 25 m x 3 m	-7.2	2.5	0.0	19.1
50 m x 50 m x 3 m	-8.9	1.6	-0.1	15.4

In Table 47 the predicted grades of the 4 m x 4 m drill data are compared to the actual mined data. In the waste category the predetermined estimated grades were about 10 % less than the mined grade, with high variances among various methods. In the low-grade category the average estimated grade was 2 % less than the mined grade. In the medium-grade all methods were on target with the mined grade. In the high-grade category, all methods except for CS overestimated by less than 7 %. CS in comparison underestimated by 7 %. The average estimated grade was therefore overestimated by just under 2 %.

In Table 48 the predicated versus actual mined grades are indicated which were obtained from 12,5 m x 12,5 m drill data. In the waste category, the estimated grades were 5 % more than the mined grades. In the low-grade category the mined grade was 3 % more than the estimated grades, with OK being the lowest at 2 %. In the medium-grade category all methods reported average grades in the range of 515 ppm similar to the mined grade. In the high-grade category estimated grade was somewhat lower than the mined grade. The average variance was underestimated at just under 19 %, with both IDW^2 and OK doing better at just under 15 %.

In Table 49 the estimated grades are compared to the mined grades using 25 m x 25 m drill data. In the waste category the estimated grades were on average 7 % higher than the mined grade. In the low-grade category the estimated grades were on average 3 % lower than the mined grade. The medium-grade as in previous instances was on target with no reasonable variances. In the high-grade category the estimates were on the conservative side averaging 19 % less than the mined grade. OK estimated more accurately at 12 % less than mined grade.

In Table 50 the results of the predicated grades versus the mined tonnages are represented using the 50 m x 50 m data. In the waste category, the average estimated grade was 9 % more than the mined grade. In the low-grade category the mined grade was higher by just under 2 % compared to the estimated grade. In the medium-grade category the results mimicked that of previous drill spacing and no major variance can be recorded. OK performed best and estimated a grade matching that of the mined grade. In the high-grade category the average estimated grade was 15 % less than the mined grade. MIK performed the worst by underestimating by more than 30 %. This is unusual as MIK is used in deposits to deal with unusually high and erratic grades. Table 51 provides a conclusive summary between the estimated and actual mined grade.

6.6 Grade tonnage plots of various block models

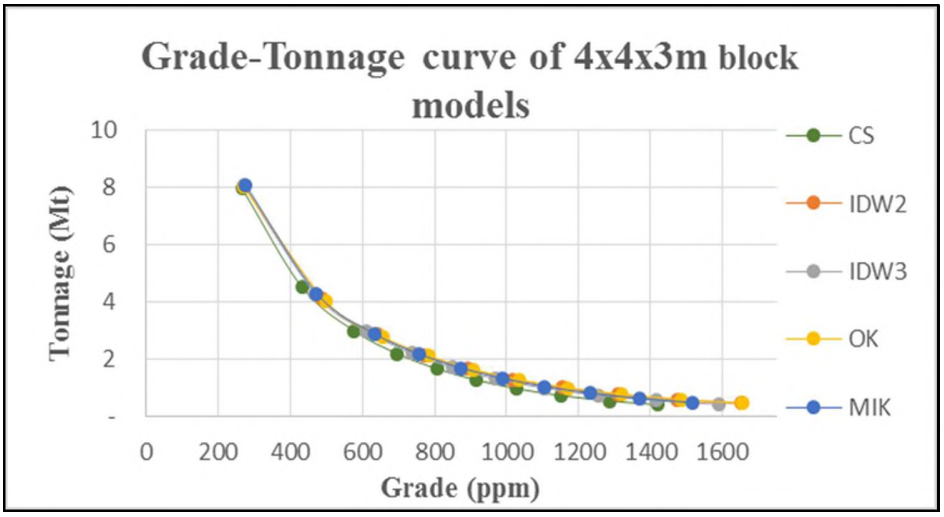

Figure 60: G-T graph of various methods at block dimensions of 4 m x 4 m x 3 m.

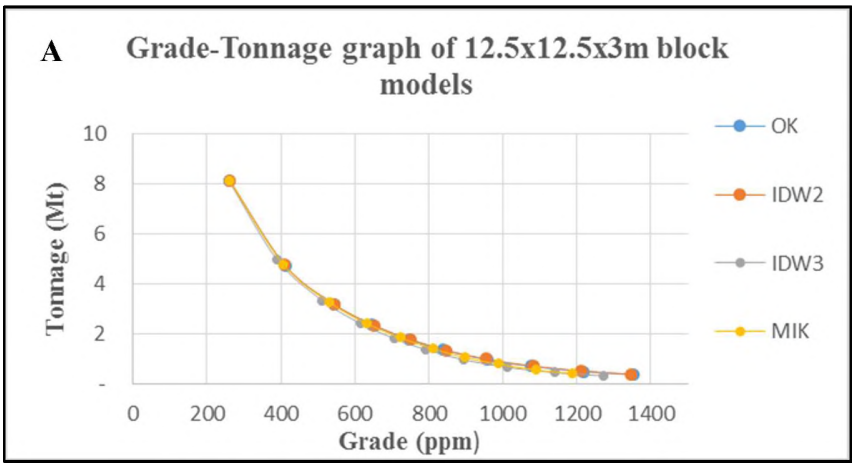

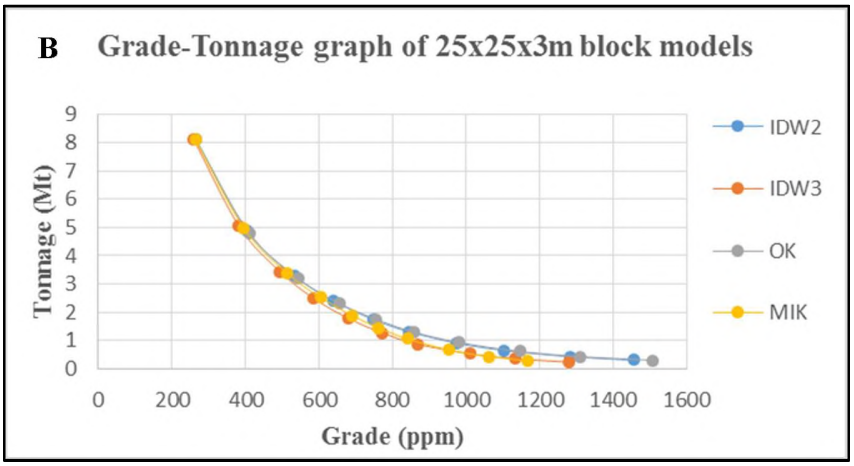

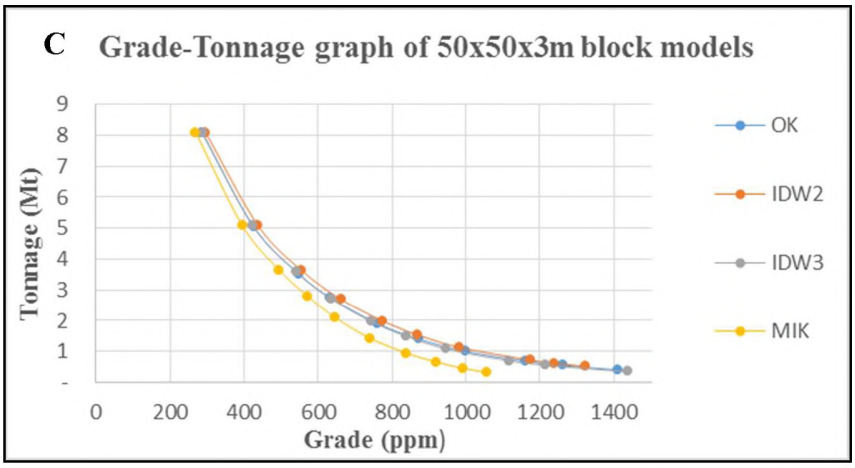

Figure 61: G-T graphs of different estimation methods at various block sizes

Between the various estimation methods not much can be distinguished in the general trend illustrated in Figure 60. All plots start off at a grade around 300 ppm and a tonnage of about 8 Mt. The trend then steeply decreases to around 400-500 ppm and about 4,0 - 4,4 Mt. Thereafter the trend dip starts to decrease more gently, slowly decreasing in tonnage and increasing in grade. There are some differences in high-grades among the various methods. The non-linear method seems to be somewhat more conservative, of which CS has the lowest high-grade. The most conservative method is CS at around 1 400 ppm, followed by MIK at around 1 500 ppm. The linear methods of both IDW and OK all have higher-grades reaching a maximum of around 1 600 – 1 700 ppm.

The three grade tonnage graphs in Figure 61 give an idea of grade and tonnage of the larger spaced block model estimation, excluding CS. Graph A illustrates the G-T estimation of the 12,5 m x 12,5 m x 3 m block models. Not much is lost in terms of tonnage compared to the smaller previous block model, however there is a significant decrease in the higher-grades. None of the methods contained maximum grades above 1 400 ppm, whilst in the smaller block models, grades of well over 1 600 ppm were observed. MIK remains the most conservative method with maximum grades just under 1 200 ppm and around 300 000 t. OK and IDW both reach grades just under 1 400 ppm with the same tonnage.

In graph B the 25 m x 25 m x 3 m grade tonnage graphs are displayed. Not much has changed in terms of tonnage difference, however minor changes in grades especially visible in the high-grades have taken place. MIK has retained a minimum grade at just under 1 200 ppm at about 300 000 t. IDW^2 has increased in its maximum grade to about 1 500 ppm, whilst IDW^3 has retained a maximum grade of 1 300 ppm. OK on the other hand has increased the maximum grade to about 1 500 ppm. Graph C illustrates the G-T estimation of the largest block models. No large visible changes in tonnages are present on the graph, but high-grade variations have increased. MIK indicates the most visible difference in terms of it higher-grades. Its lowest grade is just under 1 100 ppm and roughly 400 000 t. OK retained its grade at 1 400 ppm with IDW having maximum grades that represent those of the 4 m x 4 m x 3 m block models. At 1 400 ppm and 500 000 t respectively, IDW has estimated the highest grades and tonnages.

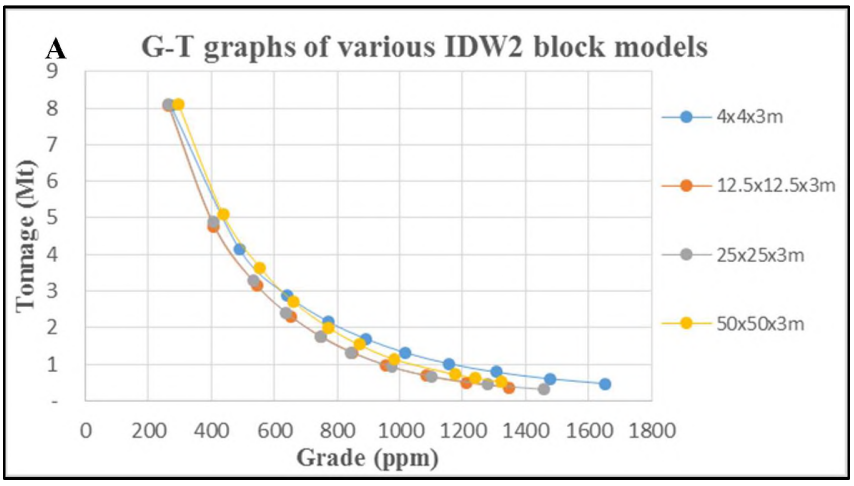
A
G-T graphs of various IDW2 block models
Tonnage (Mt)
Grade (ppm)
4x4x3m
12.5x12.5x3m
25x25x3m
50x50x3m

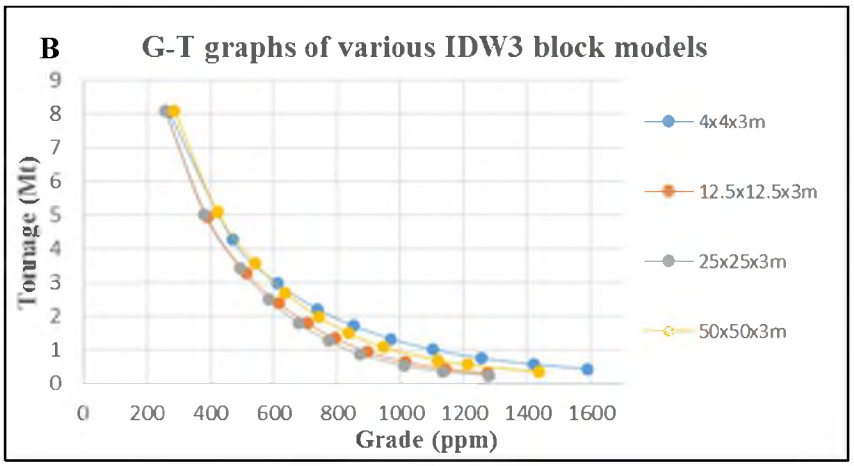
B
G-T graphs of various IDW3 block models
Tonnage (Mt)
Grade (ppm)
4x4x3m
12.5x12.5x3m
25x25x3m
50x50x3m

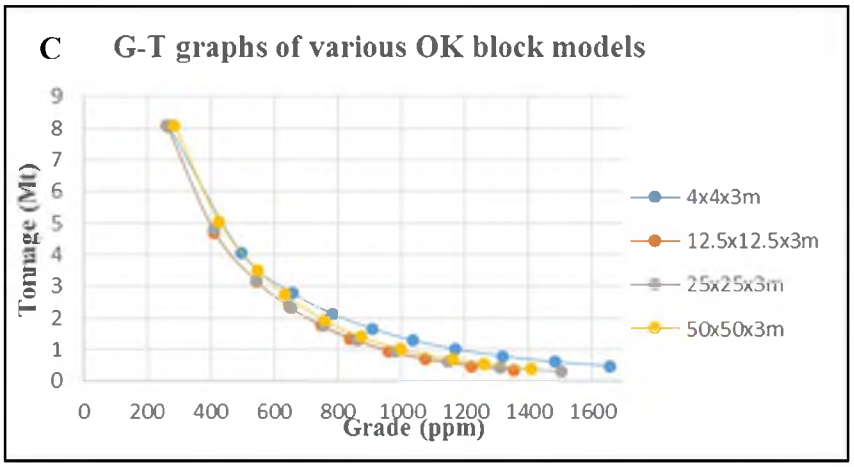
C
G-T graphs of various OK block models
Tonnage (Mt)
Grade (ppm)
4x4x3m
12.5x12.5x3m
25x25x3m
50x50x3m

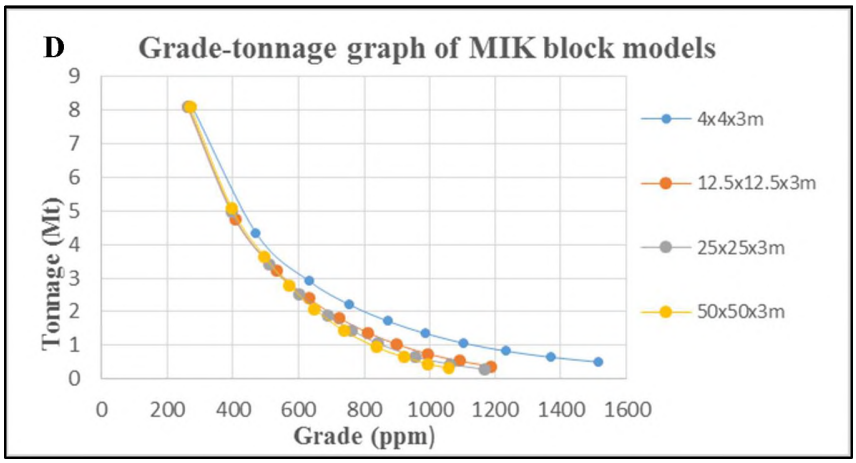

Figure 62: G-T graph of individual methods at various block dimensions

The G-T graphs in Figure 62 illustrate various grades and tonnages of the estimation methods used for pit H1. The highest grades are observed in IDW^2 and OK with grades of 1 700 ppm obtained from the 4 m x 4 m x 3 m block models. The lowest grades are observed in the MIK model at 1 100 ppm, which was created from the 50 m x 50 m x 3 m model. The IDW^2 block model illustrates the highest grades are created from the 4 m x 4 m x 3 m block model at just under 1 700 ppm, followed by the 25 m x 25 m x 3 m and then only the 12,5 m and 50 m x 50 m x 3 m block models at just under 1 400 ppm. The IDW^3 block model again created the highest grades at 1 600 ppm from the 4 m x 4 m x 3 m block model, followed by the 50 m x 50 m x 3 m block model and with lesser grades the 12,5 m and 25 m block models at around 1 300 ppm. The OK block models has similar grades and tonnages to that of the IDW^2 block model. The MIK block model is by far the most conservative in terms of grades. The 4 m x 4 m x 3 m block models contains the highest grades at 1 500 ppm. This is followed by the 12,5 m, 25 m and 50 m block models at 1 200 ppm and less. This creates a difference of about 300 ppm less between the wider spaced block models and the finer spaced block model. This is a function of volume variance which is dependent on the available drill data.

6.7 Expenditures and cash flow comparisons between various block models

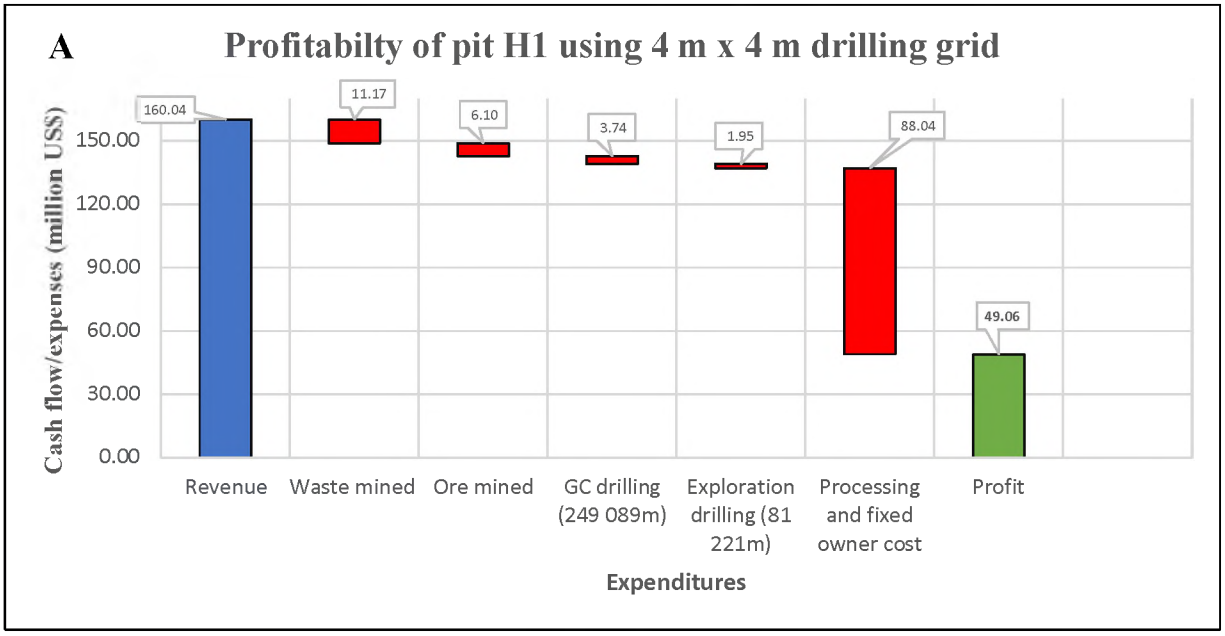

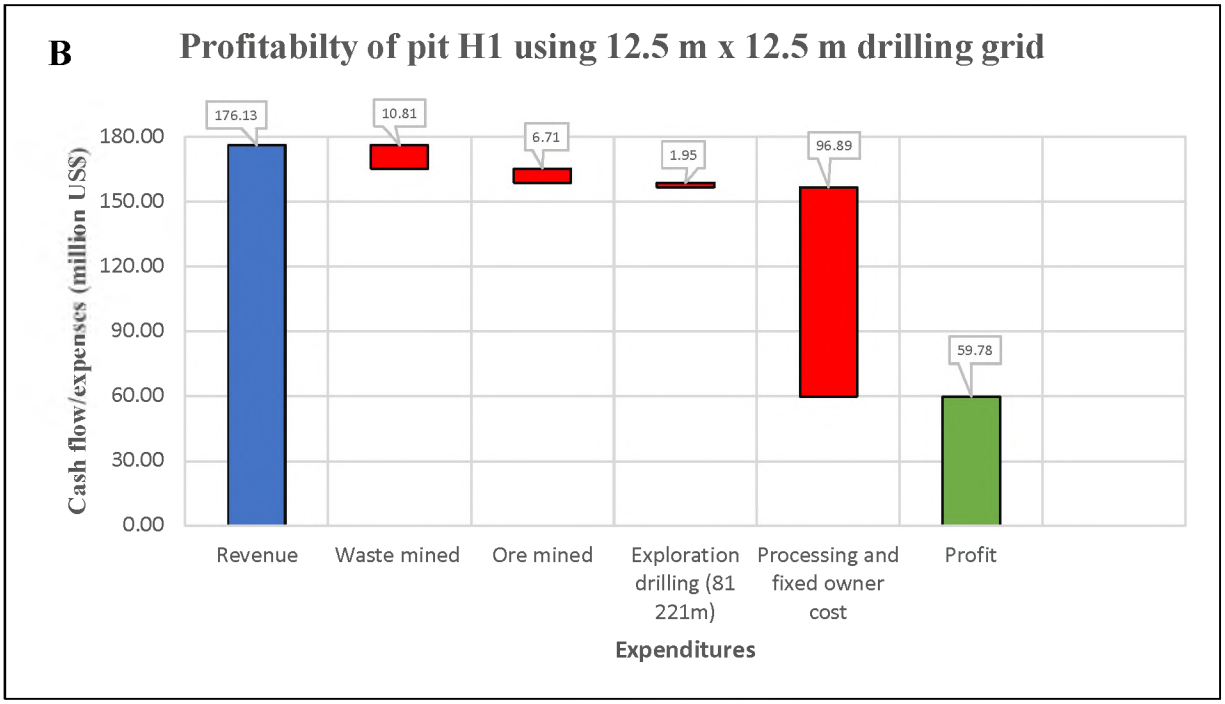

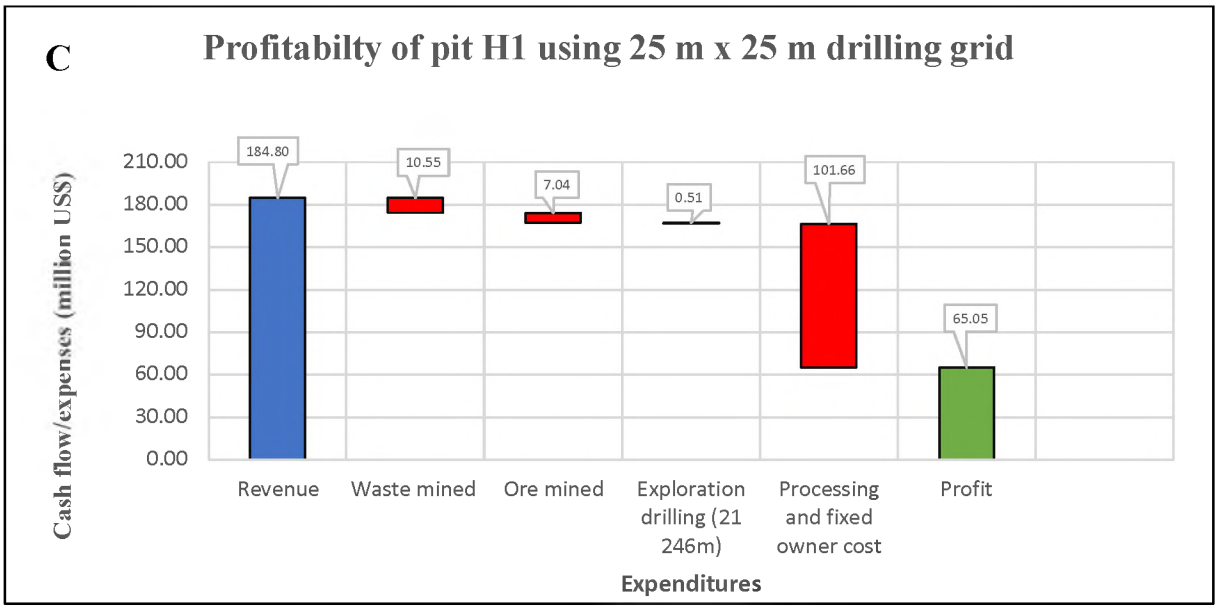

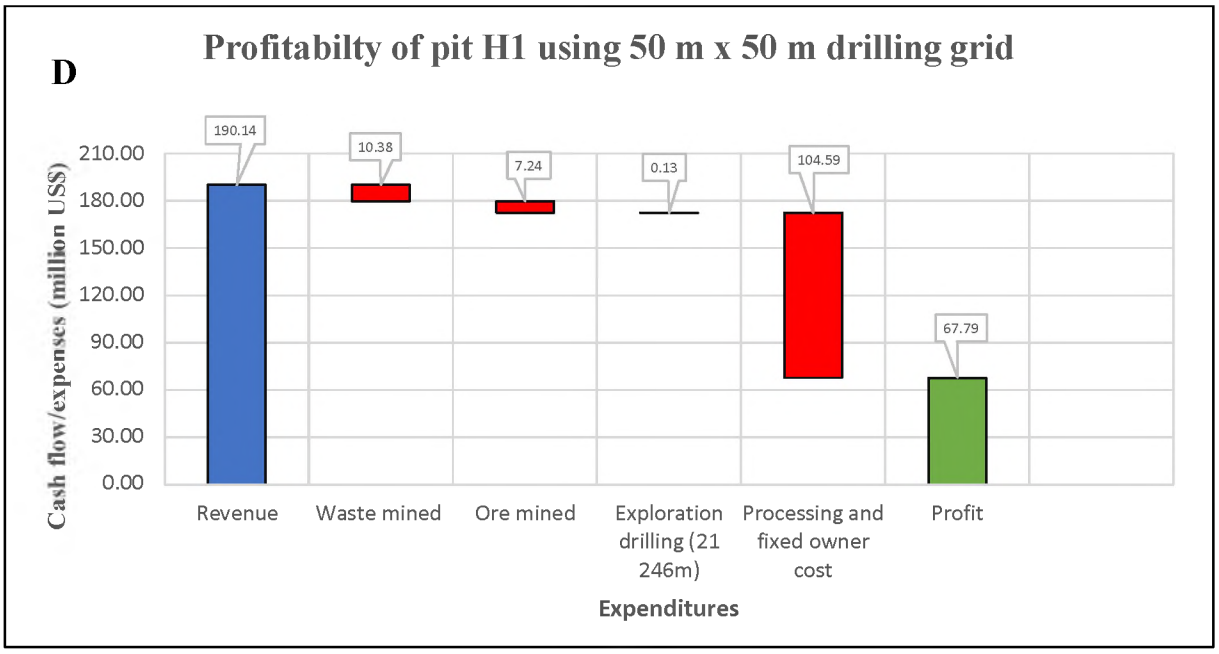

Figure 63: Total cash flow of pit G1 with included drilling costs of various drill spacing

The most visible difference in Figure 63 in terms of cash flow of the waterfall charts is the profit figures. It can be seen that the profit amount increases systematically with the larger drill spacing. The smallest drill spacing includes both the blast hole drilling and the added total exploration drilling and is therefore about US$ 18 700 000.00 less than the largest drill spacing in profit value. Total revenue increases systematically with the larger grid spacing. It is logical that drilling costs increase with the smaller grid spacing with the benefit of obtaining more detailed data. The general assumption suggests that with less availability of data, hence larger drill spacing, less ore is predicted and the more waste is estimated and therefore mined. Thus it is evident that the smallest drill spacing estimates an average of 11,2 Mt of waste and only 6,1 Mt of ore to be mined, whilst the 50 m x 50 m drill spacing estimates that 10,4 Mt of waste and 7,25 Mt of ore to be mined. The rest of the drill spacing predict something in between. This is approximately 1 Mt difference between the largest and smallest drill spacing and could yield big differences as seen in the total profit figures.

With regards to drilling, the expenditure effect thereof is minimal compared to the total cash flow of the pit. For exploration drilling the percentage of total expenditure is between 0,1 and 1,7 %. For grade control drilling the total expenditure of drilling only used for blasting would be about 3,4 % and about 5,1 % for the total drilling undergone on the pit. This still not much compared to other expenses of which processing and fixed costs are by far the highest. It has to be stated that drilling no matter at what grid spacing has to amount to a lesser expenditure than the waste that would have been mined if drilling would not have been sufficient. Hence, there has to be a balance between drilling expenses and the cost saved in terms of later mining that is based on those drilling results. It has to be mentioned that drilling on a 4 m x 4 m grid is mandatory for blasting and therefore part of the fixed capital. Any extra work performed on the blast holes is part of the operational cost that can fluctuate depending on saving strategies.

CHAPTER 7. DISCUSSION

7.1 Introduction

A relatively large number of surficial calcrete-hosted uranium deposits are known throughout the world that are very similar to the numerous deposits that occur in Namibia. Well known deposits occur in Australia (Yeelirrie, Lake Maitland, Lake Austin), Tanzania, Botswana, Mauritania, Canada, Somalia and the USA (IAEA, 1984). There are few deposit types where resource estimation is a straight forward process. In most cases a large degree of experience as well as trial and error throughout the mining period are required. Often reconciliation projects similar to this one have to be carried out during and after mining operations, to enhance future resource estimation efficiencies of that specific deposit as well as improving current mining operations. Numerous deposit types in nature exhibit a high degree of grade variation throughout the deposit, which makes grade prediction a subjective matter and somewhat problematic. Gold (coarse) deposits are probably the most well-known deposit types with a high nugget effect and extreme grade variation (Rossi & Deutsch, 2014). Various geostatistical resource estimation methods can be tested throughout the mining operation as reconciliation projects to determine the optimal method and even the efficiency of past drill spacing and their input. This was the case during this research exercise where the drill spacing and resource estimation methods were tested on depleted pits with real-time data available.

7.2 The bigger picture and significance of the grade control model research

The Langer Heinrich Uranium Deposit, as with many other calcrete-hosted uranium deposits, provides complex issues in resource estimation. Grade concentrations, distribution and continuity variations are the contributing factors that make resource estimation difficult. Large-scale grade variations or erratic mineralisation distribution are known to occur over short distances both laterally and vertically. Resource estimation procedures have to be closely considered due to the grade complexity along with geological interpretations that could influence the estimations. The various geostatistical resource estimation techniques considered all have positive and negative attributes described in Table 9. There was no need for de-clustering data as the area selected for this research was situated in the main palaeo channel where grades are ideal and were drilled at regular intervals. IDW and OK both have long been used in the mining industry and have been adopted in various other science sectors as well. These often form some part of the parent algorithm from which hybrid or a combination of geostatistical methods develop. Indicator kriging along with sequential Gaussian conditional simulation are somewhat newer and are preferred in some

deposits, especially those with high grade variations. Deposits such as these include gold, uranium, platinum group elements and some base metal deposits.

Figure 64 should be a fair representation of variable grade changes over short distances in pit G1.It is clear from Figure 64 that grade variation in these cross sections occur predominantly and more abruptly in a vertical direction relative to lateral variations. There are, however, abrupt grade variations in a lateral direction as well as variations that gradually change over greater distances. These lateral variations have been described throughout the literature and essentially occur as sporadic lenses within the palaeo channel (Hambleton-Jones, 1976). The sporadic high-grade lenses tend to occur predominantly in the eastern part of the palaeo channel of which a prime example is pit G1 used in this research. These high-grade pits are linked by somewhat lower grades that follow the morphology of the palaeo channel. Other small high-grade ore lenses included pit G2A, G3 and G3B in the eastern area of the mine licence area. These lateral grade variations of these abovementioned pits are evident in the variograms that have been modelled in a horizontal section. The variograms modelled in vertical section such as those of Figure 30 and Figure 54 prove that the variogram has a better fit to the sampled points. Pit H1is used as a comparative case study, and forms part of the much larger continuous orebody that is situated in the central parts of the deeper palaeo channel in the western area of the mining licence. Grade changes laterally and vertically are more subtle in the deeper palaeo channel compared to the shallow near surface lenses in the eastern part of the licence area. It is thought that mineralisation in parts of the eastern palaeo channel has been subject to erosion. This complexity in mineralisation and predictions thereof formed the base of this research. Through the various geostatistical approaches mentioned above, four different drill grids at regular spacing and the presence of a realistic mined out dataset makes this study a reasonable reconciliation project.

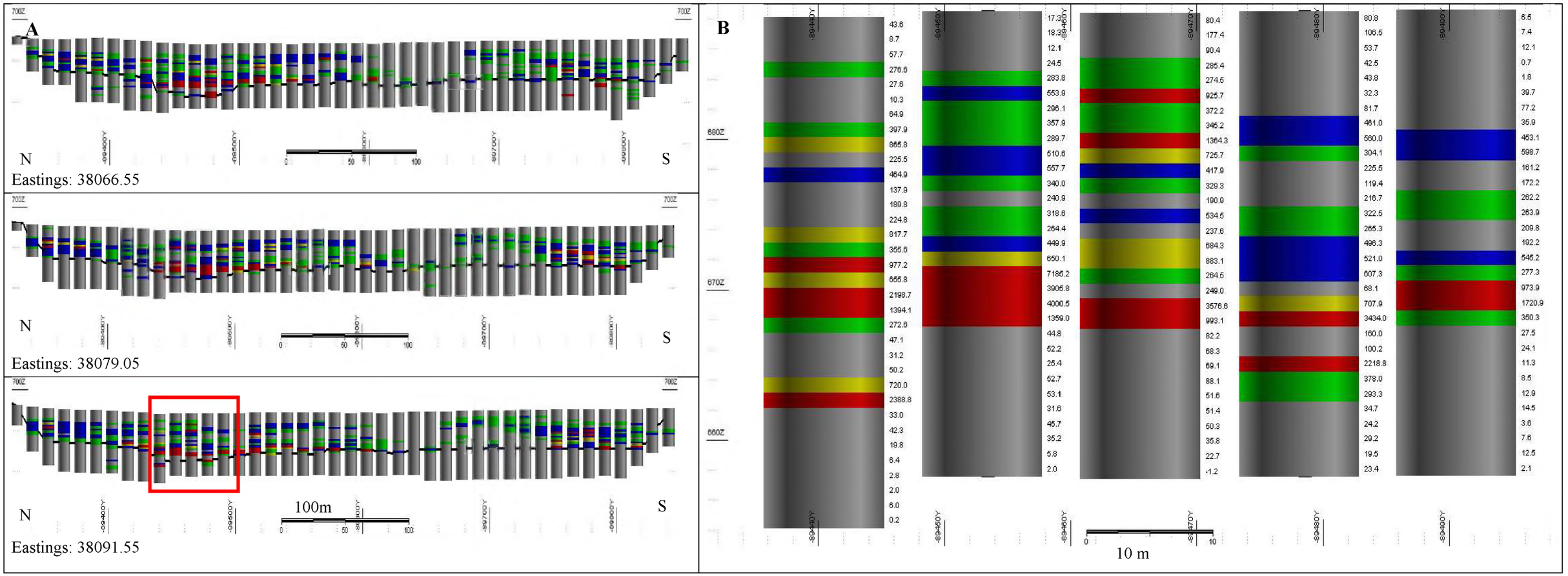

Grade	*U3O8 ppm*	*Colour*
Waste	0-250	
Low-grade	250-400	
Medium-grade	400-650	
High-grade	650-900	
High-grade (concentrated high-grade)	>900	

Figure 64: **A:** Three lateral N-S drill lines at 12,5 m x 12,5 m drill spacing cross-cutting the palaeo channel in pit G1. **B:** Illustrates a close-up indicated by the red square in figure A and provides the grade variation vertically of 5 adjacent drill holes. Each band illustrates a grade composite of 1m in ppm.

7.3 Ore block grade control estimation reconciliation outcome: 12,5 m x 12,5m versus 4 m x 4 m drill patterns

The purpose of this research (based on chapter 4) was to investigate whether mining operations can function efficiently by modelling ore blocks using data from pit delineation drilling on a 12,5 m x 12,5 m drilling grid. Although blast blocks are all drilled on an approximate 4 m x 4 m drilling grid and therefore are quantified under fixed costs, there are extra costs involved in radiometrically logging each of those holes. The additional radiometric logging of the 4 m x 4m drill holes can be classified under variable costs. These can be improvised during improved economic times. The proposal has, therefore, already been implemented in a trial form to mine blocks that have been designed or estimated using only 12,5 m x 12,5 m drill data. These can now be compared to the mined out blocks that have been designed from the 4 m x 4 m drill data. The resulting data of the 10 blast blocks selected and mined on each drill spacing yielded remarkably similar results as illustrated in Table 11 and Table 12 of Chapter 4.

The results in general indicated the significant impact that under mining and over mining contributes to ore dilution. In both cases ore blocks have either been upgraded or downgraded in their presumed ore category, due to the expense of either under or over mining. These practices, if not controlled, often result in mining ore that is higher or lower in grade than the surrounding ore blocks and consequently cause positive or negative ore dilution. It is therefore important that mining personnel take considerable care of the mining operations. Other factors that contribute to ore dilution include ore movement during blasting (lateral and vertical), dozing material during mining in an uncontrolled manner and further down the line misclassification of mined material. This could include malfunction of radiometric truck scanner and pit control destination misclassifications. Geo-technician operators as well as mining geologist are responsible for the grade control procedures and therefore need close 24 hour supervision to make sure various other parties involved follow their training.

From the results it can be noted that much more accuracy with regards to mining practices is accounted for when loading high-grade ore blocks. This is partially due to the high feed grade above 600 ppm U_3O_8 and the current low market prices of uranium. Planned over mining of high-grade ore blocks is also a common practice and can be of substantial importance for blast blocks that are situated near the bottom of the ore body. As mentioned before, carnotite is known to be found within fractures in the schist basement at depths of up to 2m. This material is usually highly weathered and can be mined by simple rip and doze methods. It has to be mentioned, however,

that over mining of high-grade ore blocks can contribute to downgrading of the high-grade ore into lower grade categories. This could be seen in blast block F-653-001, ore block HG1 in Table 13, where the estimated grade of 887 ppm was downgraded to an average mined grade of 422 ppm. This is highly likely due to substantial over mining of the ore block. Low-grade and medium-grade mining operations performed very similarly and more preference has to be appointed to medium-grade mining operations in the future.

Larger blast blocks are more likely to contain blocks that have been over mined compared to smaller blast blocks. With regards to grades in terms of estimated versus mined grades, only a few ore blocks could be easily identified where the estimation method has either over or underestimated. In the 4 m x 4 m drill data approximately 10 ore blocks could clearly be identified where conditional simulation has been used to over or underestimate. In the 12,5 m x 12,5 m mined data, a total of three ore blocks could be identified where kriging either over or underestimated. This leads to a conclusion that the estimation or simulation methods did not have a significant impact or influence on ore misclassification and dilution. It could furthermore be seen that conditional simulation does in cases overestimate at grades higher than 1 000 ppm.

In general a positive relationship between the two different drill spacing data can be concluded. The estimated total tonnage mined for the 4 m x 4 m data was 2,8 % more than the mined tonnage, whilst the total mined tonnage for the 12,5 m x 12,5 m drilled data was only 4,0 % more. With regards to the mined grades, the mined grade for the 4 m x 4 m drill data was 1,8 % more than the estimated grade, whilst the mined grade for the 12,5 m x 12,5 m drill data was 4,4 % less than the estimated grade. This leads to a conclusion that drill data from the brownfield exploration programme at a drill spacing of 12,5 m x 12,5 m could yield data that can be used for estimation and later mining operations. Due to the low differences between mined and estimated tonnages and grades, the 12,5 m x 12,5 m data could yield a good alternative to make the operation more cost efficient. This way of mining would be preferable during times when the market price is low and cost saving is a priority. However, the 4 m x 4 m drill data did provide the most accurate solutions and is preferable in times when operations can afford to use radiometric logging on this drill spacing. This operation, although more costly and time consuming, does indicate the promoting benefits of a larger denser dataset. A compromise could be suggested where additional data is radiometrically logged on a 4 m x 4 m drill spacing. This would add infill data of the larger 12,5 m x 12,5 m drill spacing and therefore adding data confidence without significantly increasing costs. Alternative estimating methods like co-located co-kriging amongst others could also be used.

7.4 Optimal drill spacing for deposit

Drilling on site has been an ongoing process since the 1970s and substantial drill metres have been added since delineating the uranium mineralisation in the palaeo channel. Six reverse circulation drills (RC dual tube) have operated and drilled up to 200 m per day per rig since 2013. Drill hole depths vary between 4 and 120 m in the deepest parts of the palaeo channel. Drill holes cut through Cenozoic unconsolidated topsoil, various calcareous horizons, and into a predominantly unmineralised calc-silicate schist basement. All of the drill spacing throughout the licence area have taken place on a regular grid pattern. The aim thereof is to create a representative dataset for the entire area of investigation. This would decrease the potential bias created from target drilling or irregular spaced drilling. Another benefit of the regular spaced drill programme is that advanced infill or pit optimisation drilling can be undertaken within the larger regular grid and thereby saving resources. This was the case at the Langer Heinrich Mine, where exploration was undertaken at a regular 50 m x 50 m grid. Infill drilling was undertaken at a 25 m x 25 m drill spacing to increase both grades and resources. A final infill grid at 12,5 m x 12,5 m was proposed and undertaken from the previous larger drill spacing of 25 m x 25 m. The smallest infill drilling fits into the spacing of the previous larger drilling programmes and therefore increases data accuracy and provides or maintains a regular drilling grid. The smallest infill drilling of 12,5 m x 12,5 m increases the data amount. It has to be said that the drill costs are proportional to this and becomes resource intensive at about N$ 240.00/m.

With regards to the optimal drill spacing, various important factors have to be considered. Figure 65 provides an illustration of data availability with various drilling grids. Data availability increases substantially with refined or smaller drilling grids. There has to be a relationship between the drilling cost and the amount of waste that can be excluded from mining from the refined or improved pit design of the smaller drilling grid. The width of the palaeo channel varies from 250-700 m. The length is about 8 km and covers the entire mining licence area and extends further westwards. The 50 m x 50 m grid would therefore be sufficient in outlining the main palaeo channel and the boundaries thereof. Pockets or lenses of high-grade as well as the general grade distribution can be outlined, but detailed grades and tonnages will only be broadly estimated.

Figure 65: Various drill spacing in pit G1, hence data availability. Red: 50 m x 50 m Green: 25 m x 25 m Blue: 12,5 m x 12,5 m

With regards to tonnage estimations and comparison, Table 27 and Table 46 summarise the average variance between the estimated tonnages and mined tonnages. Table 27 highlights the results of pit G1 and Table 46 shows the results of pit H1. It has to be mentioned that the final mined out pit wireframe was used as an estimation limiting factor. Although data points or drill holes might have extended beyond the pit wireframe, these were not included in the final estimation results as they are situated outside the pit shell. This would limit tonnage and grade estimation, that would not be available during past exploration programmes to determine the in-situ resources.

The 50 m x 50 m x 3 m block model, as would be assumed, resulted in the highest tonnage variation between the predicted grade categories and what was actually mined. This was the case in both pit G1 and H1. The waste category therein had the lowest variance with regards to the mined tonnages. The LG and MG categories all overestimated between 16-35 % compared to the final mined figures. The HG category in pit G1 underestimated by 22 % compared to the mined tonnage. However, the estimated tonnage for HG in pit H1 was below 5 %. A likely explanation of LG and MG

overestimations can be explained by grade overestimation by the various methods used and ore dilution during mining. The availability of data from the wide spaced drilling will be the most likely cause of the larger over and underestimations. This is a well-known aspect in resource estimation and is clearly proven by less data availability. It has to be mentioned that the pit H1 dataset was much smaller compared to the G1 dataset and therefore relatively small tonnage and grade discrepancies can have a larger influence on the percentage variance. Volume variance has an obvious effect on the dataset from the larger and finer drill data.

The 25 m x 25 m and 12,5 m x 12,5 m drill data estimations are very similar in predicting tonnages. This is observed in Table 27 of the pit G1 dataset, which displayed minor discrepancies between the two drill spacings. In the waste category the estimated tonnage is similar to that of the mined tonnage. In the LG category the 12,5 m x 12,5 m drill spacing performed slightly better with an overestimation of 5 %. The 25 m x 25 m drill spacing had an increased overestimation of 8 %. Towards the higher-grade categories of MG and HG, the two drill spacings had resulting overestimations between 10-11 % and 13-14 % respectively. These grades are critical to the viability of the deposit and accurate delineation of these is therefore of vital importance. Pit H1, however, as seen in Table 46, gave rise to the prediction that with increased data comes more certainty. There are substantial differences between the two drill spacings and their tonnage estimations. The 12,5 m x 12,5 m drill data provided measurably more certainty through all grade category predictions. In the LG, MG and HG category, the 12,5 m x 12,5 m drill data performed better with improved predictions between 5-8 % compared to the estimations of the 25 m x 25 m drill data. This provides comfort in the thought that, with increased drilling and therefore more data availability, comes increased estimation certainty. The loss of ore from the mined figures, could be attributed to overestimation by the various geostatistical methods or rather by ore dilution during mining and earlier blasting. Dilution during mining and blasting is a general mining operation issue that cannot be eliminated, only minimised by making operations more efficient.

A comparative argument between the 12,5 m x 12,5 m and 25 m x 25 m drill spacing would be a reasonable talking point due to the small variance in tonnage predictions. The aim of the tighter drill spacing is to decrease waste mining or stripping, which would have been more cost intensive than spending on the 25 m x 25 m drilling. Due to their similarity and low error variance as seen from the pit G1 dataset, the obvious assumption would be to proceed with the 25 m x 25 m drill spacing and thereby limit operational costs. This should be dependent on the market relationship of the commodity and therefore in challenging market conditions a 25 m x 25 m drill spacing would be efficient to promote further brownfields exploration. However, the 12,5 m x 12,5 m

provides more than twice as much data to create a more sufficient delineation model for pit optimization and waste mining limitations. This promotes the idea of the information effect that takes into account that the decision on the final pit designs are constructed using the finest drill spacing. This is a factor of the increased abundance of data availability that the 12,5 m x 12,5 m drill grid has to offer. The results of increased data availability were proven by the estimation of the pit H1 dataset. This however comes at a far larger cost. Drilling costs between 50 m x 50 m and 12,5 m x 12,5 m increase by more than 6 times and more than twice between the 25 x 25m and 12,5 m x 12,5 m. This is however proportional to data obtained from the extra drilling and has been the determining factor at the mine due to high grade variations.

A compromise between the 12,5 m x 12,5 m and 25 x 25m drill spacings would be a 12,5 m x 25 m drill spacing, although this drill spacing does not form a regular interval grid and therefore might incorporate some biasness. However, it provides a meaningful alternative. The mineralisation as seen in Figure 64 indicates that the mineralisation is laterally extensive along the palaeo channel and less erratic. Therefore, grades tend to fade out over longer distances laterally. Vertically grades are far less predictive. This drill spacing, although not as extensive and regular as the 12,5 m x 12,5 m drill spacing, would still focus on the lateral extent of the deposit and provide reasonable details for pit optimization and resource estimation. There are other factors to consider that does make this drill spacing viable. The first is that it is not as cost intensive as the 12,5 m x 12,5 m drill spacing. It provides twice as much data as the larger 25 m x 25 m drill spacing, whilst the 12,5 m x 12,5 m provides more data.

The 4 m x 4 m x 3 m block models created from the grade control drilling resulted in the most accurate tonnage predictions in both pit G1 and H1 which would be expected. Their error variance compared to the actually mined figures are displayed in both Table 27 and Table 46. This drill spacing should represent the most accurate predictions compared to the mining results. Unlike the other drill spacing, the 4 m x 4 m in most cases was more conservative in tonnage predictions. Most of the grade categories resulted in underestimation compared to the other drill spacing that usually overestimated. It is only in the MG and HG category of pit H1 that the methods overestimated by an average between 1 and 6 %. It has to be emphasised that grade control drilling is a necessary procedure to enable blasting; however, the work, time and costs going into radiometric down-hole logging each hole promotes the investigation of finding an alternative drill spacing to do estimations.

7.5 Optimal geostatistical method for deposit

The methods used during estimation in this research were all constrained using the final pit shell and thereby limiting the estimated tonnages and grade influences further outside the final pit. Estimated tonnages will therefore not be excessively over or underestimated as could be the case in exploration campaigns with limited data. The grades, however, are related to the actual methodology of the various estimations or simulation technique used. The criteria used during ore estimations have been discussed in chapters 5 and 6. It should therefore be stated that these methods can, with experience as well as with trial and error, be fine-tuned into providing more optimal ore estimations.

It has to be mentioned that the grades for the waste categories do contain a significant measure of uncertainty within this research. Waste grades are preliminarily calculated using the various estimation or simulation techniques from drill data available. However, unlike low, medium and high-grade (pay loads), waste is only passed through the scanner if there is a suspicion of ore presence. This usually occurs along boundaries of ore outlines on the blast block and where the handheld Radeye picks up elevated readings on daily monitoring exercises. Usually, if waste blocks are mined, the grade assigned to the truck will be the average pre-calculated or estimated grade of the ore block. Therefore, in the waste category no preferred estimation method can be accounted for, although it is interesting to note the variances in grade predictions between the various pits. Pit G1 was radiometrically logged on a 4 m x 4 m drill spacing from the surface. Pit H1 on the other hand was only radiometrically logged on a 4 m x 4 m drill grid when ore started at an elevation of 599 m. This could be a reason for the general high variance in the waste category between the two pits.

The low-grade mined grades also carry some minor uncertainties. Due to the presence of 24 Mt of low-grade stockpiles and decreasing uranium spot prices since the Fukushima disaster in 2011, various cost saving practices regarding low-grade ore movement from the pit were implemented. With an average plant feed grade of 720 ppm U_3O_8 (2015-2016), no low-grade is blended into the mill. Due to the presence of the large low-grade stockpiles, low-grade ore is sometimes not scanned with the mobile radiometric scanners. Low-grade ore blocks often receive the average estimated ore grade when hauling material. There are two radiometric truck scanners on site, of which only one is partially mobile. Depending on the prevalent mining location within the paleo channel and the distance of the truck scanner, the mobile scanner will be located as close as possible in order to reduced haulage costs. This promotes another low-grade cost saving practice, whereby every 5th truck of low-grade is scanned. The rest of the trucks that follow in succession are all assigned the

grade of that 5th scanned truck. This procedure reduces haulage costs if the mobile radiometric truck scanner is located at further distances. This does create some bias in the grade comparisons, but it has to be noted that this procedure allows for cost efficient mining at times when the spot price of uranium is depressed.

Table 52: Average percentage variance between mined tonnages and grades compared to estimated tonnages and grades of pit G1

Block model dimension	Average variance % (mined vs. estimated grade)				Average variance % (mined vs. estimated tonnage)			
IDW²								
	W	**LG**	**MG**	**HG**	**W**	**LG**	**MG**	**HG**
4 m x 4 m x 3 m	45.0	12.0	-5.9	-21.7	-7.1	0.1	8.5	17.3
12,5 m x 12,5 m x 3 m	44.5	11.3	-7.1	-19.4	0.1	-9.6	-9.0	-12.1
25 m x 25 m x 3 m	41.0	11.9	-5.4	-14.8	0.6	-12.8	-7.5	-12.4
50 m x 50 m x 3 m	31.8	9.8	-6.3	3.1	0.4	-21.2	-21.3	33.0
IDW³								
4 m x 4 m x 3 m	47.1	12.0	-6.1	-23.2	-7.7	0.1	8.5	17.3
12,5 m x 12,5 m x 3 m	45.9	11.5	-7.0	-21.7	-1.4	-8.6	-3.6	-12.9
25 m x 25 m x 3 m	43.1	11.6	-5.8	-18.7	-2.0	-10.8	0.8	-13.4
50 m x 50 m x 3 m	30.7	9.6	-6.5	2.1	-0.9	-17.7	-20.9	30.4
OK								
4 m x 4 m x 3 m	54.6	11.8	-6.2	-23.1	-8.3	3.5	9.7	12.2
12,5 m x 12,5 m x 3 m	55.4	11.9	-6.9	-18.9	-0.8	-0.5	-12.1	-13.4
25 m x 25 m x 3 m	48.8	10.8	-6.1	-12.7	-0.3	-3.9	-15.0	-12.6
50 m x 50 m x 3 m	38.7	11.7	-5.3	-6.6	-3.0	-13.6	-19.7	2.5
MIK								
4 m x 4 m x 3 m	31.5	11.7	-6.2	-20.5	-9.4	1.9	8.6	1.3
12,5 m x 12,5 m x 3 m	39.3	10.7	-6.8	-15.2	0.8	1.0	-17.5	-18.1
25 m x 25 m x 3 m	36.1	10.0	-6.8	-9.9	0.7	-1.9	-17.5	-16.1
50 m x 50 m x 3 m	31.5	10.2	-4.3	-7.1	-2.4	-12.4	-20.0	28.4
CS								
4 m x 4 m x 3 m	13.7	12.0	-7.6	-10.3	8.7	-4.9	-11.2	-6.1

Table 53: Average percentage variance between mined tonnages and grades compared to estimated tonnages and grades of pit H1

Block model dimension	Average variance % (mined vs. estimated grade)				Average variance % (mined vs. estimated tonnage)			
IDW²								
	W	**LG**	**MG**	**HG**	**W**	**LG**	**MG**	**HG**
4 m x 4 m x 3 m	16.5	2.4	0.3	-5.3	3.6	6.1	-5.8	-0.4
12,5 m x 12,5 m x 3 m	-5.0	3.0	0.1	14.6	7.1	-9.6	-19.9	7.7
25 m x 25 m x 3 m	-6.5	1.6	0.1	11.6	8.6	-17.4	-23.7	15.4
50 m x 50 m x 3 m	-8.9	3.7	-1.8	8.9	17.5	-28.2	-31.1	-2.5
IDW³								
4 m x 4 m x 3 m	10.6	2.6	0.2	-1.4	4.7	1.6	-12.4	2.1
12,5 m x 12,5 m x 3 m	-9.7	2.6	-0.4	21.5	8.3	-12.9	-26.6	15.6
25 m x 25 m x 3 m	-10.3	2.4	0.2	24.7	12.4	-26.9	-31.7	27.0
50 m x 50 m x 3 m	-10.8	1.2	-1.7	10.0	15.5	-24.1	-36.1	10.1
OK								
4 m x 4 m x 3 m	21.2	2.2	0.2	-6.5	3.1	9.1	-2.3	-0.8
12,5 m x 12,5 m x 3 m	-2.6	2.0	0.1	14.9	7.7	-13.0	-20.7	9.3
25 m x 25 m x 3 m	-3.7	4.1	0.9	12.2	8.1	-14.7	-20.9	9.6
50 m x 50 m x 3 m	-6.5	1.0	0.4	8.8	15.8	-28.8	-30.0	5.2
MIK								
4 m x 4 m x 3 m	6.0	2.1	0.1	-0.3	3.8	6.1	-2.9	-6.0
12,5 m x 12,5 m x 3 m	-4.1	2.4	0.5	23.4	8.6	-11.7	-18.4	-0.2
25 m x 25 m x 3 m	-8.2	1.9	-1.1	30.2	11.2	-16.3	-27.4	3.7
50 m x 50 m x 3 m	-9.5	0.5	2.8	33.8	16.4	-18.6	-40.8	7.4
CS								
4 m x 4 m x 3 m	-0.2	2.2	0.6	6.9	6.6	-3.1	-8.1	3.3

Table 52 and Table 53 provide a summary of the percentage variance between the mined tonnages and grade compared to estimated tonnages and grades of the various geostatistical methods used. The two datasets are from two different mined-out pits to provide a reasonable comparative analysis. With regards to grades in pit G1 on a 4 m x 4 m x 3 m block dimension, CS performed the best results followed by MIK. In pit H1 MIK proved to be the best method followed by IDW^3. In the 12,5 m x 12,5 m x 3 m block models, MIK performed slightly better than the other methods in pit G1. Most of the methods had fairly similar results. In pit H1 OK yielded the most accurate results, followed by IDW^2. In the 25 m x 25 m x 3 m block models of pit G1, MIK outperformed the rest of the methods. OK and IDW^2 however proved to be the more accurate methods in pit H1.

In the 50 m x 50 m x 3 m block models, IDW in general proved slightly better than the other methods in pit G1. OK proved to be the most accurate method followed by IDW^2 in pit H1.

With regards to tonnage estimations in the 4 m x 4 m x 3 m block models MIK proved to be the best method in pit G1, followed by CS. In pit H1, however, OK provided the most accurate predictions followed by MIK and IDW^2 that had similar results. In the 12,5 m x 12,5 m x 3 m block models OK or IDW^3 would be the preferable method in pit G1 which indicated the lowest variances compared to the mined tonnage. In pit H1 MIK provided the most accurate estimations followed by IDW^2. In the 25 m x 25 m x 3 m block models IDW^3 performed the best estimations followed by MIK in pit G1. In pit H1, IDW^2 followed by OK proved to most closely represent the mining figures. In the 50 m x 50 m x 3 m block models OK performed by far better than any of the other estimation methods in pit G1. In pit H1 both OK and MIK performed best in tonnage estimations.

Going forward, it can be suggested from the two preceding paragraphs that MIK in general would be the ideal geostatistical resource estimation method for the Langer Heinrich deposit. It proved to be the most efficient method in both grade and tonnage estimations; however, it was observed in some cases that either OK or IDW did perform better. MIK can perhaps be recommended for the use of early resource estimations in other calcrete-hosted secondary uranium deposits. This has been tested by the company Deep Yellow Limited from Australia in their Tumas and Tubas deposits in Namibia. MIK being a non-linear estimation method uses kriging methods at various cut-offs. This involves selecting the appropriate number of cut-offs, in this case 14, and applying variography to each of them. MIK is known to be able to handle high skewed data, which makes it applicable to the highly positively skewed Langer Heinrich dataset. The method is known to handle data with extreme grade variations and high-grade outliers (Vann et al., 2000). This is common at the Langer Heinrich deposit where grades are known to change from one extreme to another over relatively short distances.

CS or MIK proved to be the best simulation or estimation methods on narrow spaced drill data. This was evident in the 4 m x 4 m x 3 m blocks where the linear estimators OK and IDW performed worse than CS and MIK. CS is the current grade control estimation method used for estimating and constructing ore mark outs for blast blocks prior to blasting. It is preferred over MIK because the data amount is relatively small and therefore up to 100 simulations can be prepared without taking excessive time. It is also not as complex and involves only one stage of variography,

compared to MIK that involves multiple cut-off grades and variography. CS is not a preferred method of estimation on larger drill spacing, but it proved very efficient on narrow data samples. Domaining or the assumption of stationarity was not used during CS as the mineralisation or grade is not related to any specific geological domain. OK in some cases proved measurably similar to the outcomes of MIK and should be a viable option as well. Being a linear method and somewhat biased by incorporating a degree of smoothing, this method does yield potential. It is still widely used in the industry which is proven by the fact that numerous other uranium exploration companies are using OK during early phase exploration. OK was used in the comparative surficial deposits of the Wiluna deposits in Australia, the Trekkopje deposit in Namibia and the Laguna Salada deposit in Argentina.

IDW proved to be the method that is least favoured, although in minor cases it did marginally prove the best grade or tonnage estimation. IDW^2 did prove to be more beneficial than IDW^3 which was especially visible in the grade estimation figures. With regards to the methods used during this research, CS and MIK are the preferred methods used during mining and hence grade control estimation where narrow spaced data is available. MIK is however time consuming and requires experience in the resource sector. Therefore, during time limited mining operations CS might prove to be the better option. MIK provided the most accurate results with the wide spaced exploration data and is followed by OK. Both of these techniques are used currently by various exploration companies and can therefore be suggested as the preferred resource estimation methods.

7.6 Geology and mineralisation

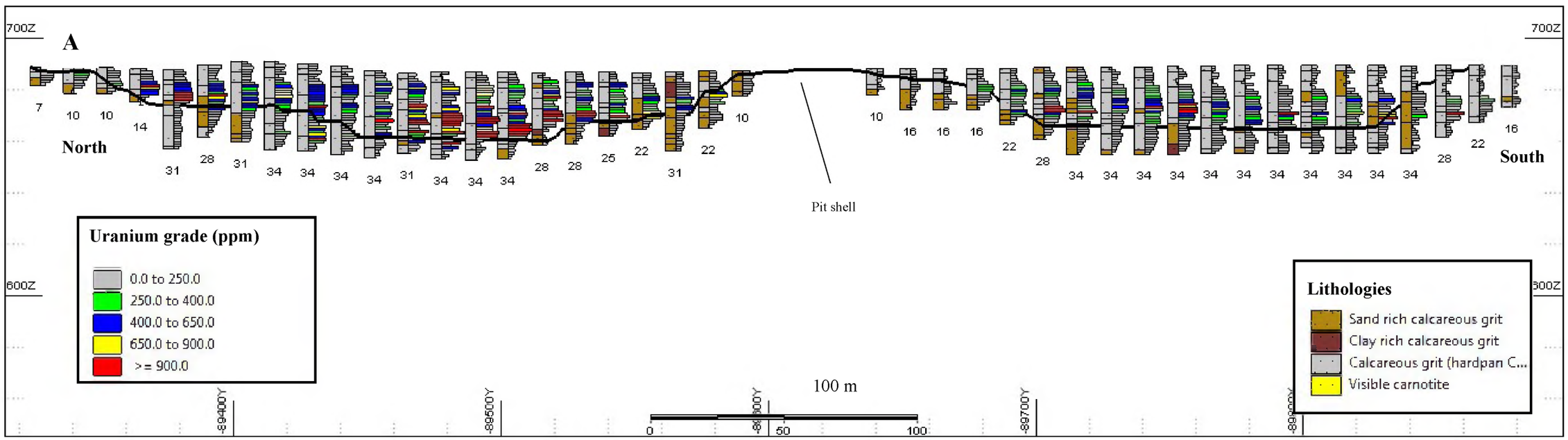

Figure 66: **A** and **B**: Cross section of palaeo channel of pit G1 and H1 respectively with pit shell indicated as a black string. The related composite grades and geology of the 12,5 m x 12,5 m drill holes are displayed.

Indicated in Figure 66 are cross sections through the two pits that have been used in this research. The cross-section cuts the pits in a north-south direction and illustrates drill holes at 12,5 m x 12,5 m spacing. The various lithologies are indicated in different colours on the left side of the drill hole, whilst the one metre grade composites are displayed on the right in ppm. Figure 66 A represents a cross sections through pit G1 and Figure 66 B represent a cross sections through pit H1.

Clearly visible are differences in the shape of the two pit shells and therefore the shape of the palaeo channel. Pit G1 is by far shallower indicated by the depths of the exploration drill holes. The depth varies typically between 7 and 34 m in depth and should be followed by about 3 m of unmineralised basement rock. Most of the mineralisation is situated in the central parts or deeper areas of the pits in both pit G1 and H1. The mineralisation in pit G1 is more extensive in a vertical aspect and occurs nearer to the surface compared to mineralisation in H1. Mineralisation in pit G1 can start from 4 m downwards. Mineralisation in H1 is situated deeper at around 35 m downwards. This has large economic implications as large volumes of waste have to be stripped in order to reach high-grades that are economic for mining (reducing stripping ratios). These deep seated high-grade ore zones have to make up in grade, tonnage and metal content for the waste stripping and are therefore dependent on uranium market prices. Pit G1 is therefore a decent example of a small-scale so-called rat hole mining operation where mining targeted shallow-seated high-grade ore lenses. Although smaller and less laterally extensive than the deeper-seated uranium grades in H1, these small pits are more economically viable during current uranium market conditions.

Geological lithologies and mineralisation are somewhat difficult to distinguish. It has been noted that mineralisation occurs predominantly throughout the palaeo channel as disseminations throughout the calcareous sediments and clast coatings. Mineralisation can also be observed in fractures of the unmineralised basement (Becker & Kärner, 2009). This can be observed in Figure 7 under the mineralogy section. Carnotite mineralisation occurs predominantly throughout the matrix in a disseminated form and is not related to any specific rock types of which calcareous grits (sandstones) and conglomerates predominate. Prior studies (Hartleb, 1988) along with the most recent studies from Becker and Kärner (2009) have suggested that ponding of uranium pregnant groundwaters have resulted in the most dominant method of mineralisation, although most likely a mixture of factors mentioned in chapter 2 was involved in the carnotite mineralisation.

Figure 66 indicates that mineralisation can be confined to specific calcareous grits within certain parts of the palaeo channel. In pit G1 mineralisation is mostly contained within calcrete rich

calcareous grit and sands also known as hardpan calcrete. This lithology usually appears in different shades of grey and white. The hardpan calcrete is known to be very competent and hard, compared to other calcareous lithologies within the palaeo channel. These hard calcrete rich calcareous grits are illustrated in the stratigraphic logs of Figure 66 in a grey colour. Most of pit G1 is made up of these calcareous grits and are followed by more clayey and sand rich calcareous sediments towards the bottom of the palaeo channel. These clay and sand rich grits comprise a smaller unit of the palaeo channel sediments in pit G1 compared to the thicker sediments in pit H1.

Mineralisation in pit H1 is somewhat different which can be attributed to the position of the pit approximately 8 km downstream. As mentioned before, the palaeo channel is much deeper here and can reach depths of 90 m and more. The sediments appear to be more mature, thicker and well defined. In Figure 66 B it can be seen that the upper sections of the pit consist of about 40 m of thick competent hardpan calcareous grit. The upper 20 m may consist of a younger light brown calcareous grit that forms part of the Gawib Flat Unit and upper parts of the Langer Heinrich formation (Trittschack, 2008). The lower light grey hardpan calcrete forms the dominant part of the Langer Heinrich formation. As seen in Figure 66 B mineralisation predominantly occurs in the lower parts of the channel from about 35 m downwards. These calcareous sediments reveal a higher clay and moisture contents, with lower calcite concentrations. The softer clay rich calcareous sediments allow for wider grade control drill spacing and a decreased powder factor for blasting, which results in far less dilution of ore blocks after blasting and therefore increased recovery rates.

CHAPTER 8. CONCLUSION

The Langer Heinrich uranium deposit is probably one of the most well-known presently mined surficial calcrete-hosted uranium deposits in the world. The secondary uranium mineral carnotite occurs in a variety of mineralisation forms which include clast coatings, disseminations within the calcrete matrix and within fractures in the weathered calc-silicate schist basement rock. The complexity of grade distribution within the Langer Heinrich palaeo channel sparked the interest in this research. The four resource estimations methods (IDW, OK, MIK and CS) that were tested, provide the basic principles used in linear, non-linear kriging as well as simulation practices within the mineral resource industry. These four resource estimation techniques were applied to two mined out pits using actual mining data for comparison purposes.

With regards to finding the best performing resource estimation method, various factors play a role in selecting a preferential method. OK is the most widely used method in surficial uranium deposits globally. During this study MIK revealed the most favourable grade and tonnage predictions compared to the actual mined tonnage and grades. OK did however, perform reasonably well and due to its simplicity might be suitable for exploration purposes. MIK, although time consuming and adequate experience needed in performing the estimation successfully, would yield beneficial results in resource estimation as well as later infill drilling phases. CS remains the preferential estimation method on narrow drill spaces such as the 4 m x 4 m drill spacing used at Langer Heinrich during grade control. This is mainly due to the fact that CS is less time consuming than MIK and provides similar results.

Determining the ideal drill spacing remains a somewhat subjective matter and often relates to the resources available. In the case of exploration and ore delineation drilling at the Langer Heinrich Mine, there have been three major phases of wider spaced drilling. This included the first phase 50 m x 50 m grid, followed by two phases of infill drilling of 25 m x 25 m and 12,5 m x 12,5 m. Minimal waste mining strategies are a crucial factor in mining operations and reducing waste stripping without overspending on costs prior to mining should be a priority before mining commences. The 50 m x 50 m wide spaced exploration drilling grid using conventional RC drilling is the optimal exploration method. This spacing allows for outlining the majority of the palaeo channel in addition to providing reasonable insight into the uranium grades. If resources are limited, a 50 m x 100 m or 100 m x 100 m grid would be acceptable in obtaining a reasonable resource estimate. With regards to infill drilling, resources available is again a major factor to consider. The 12,5 m x 12,5 m and 25 m x 25 m drill spacing yielded similar results and it can therefore be recommended that in times of low asset availability a 25 m x 25 m or perhaps 25 m x 12,5 m drill

grid would be sufficient. The 12,5 m x 12,5 m drill does however, indicate a measurable indication of decreasing waste tonnages in the final pit designs at the cost of increased drilling and increased data availability. This drill spacing has also provided a reasonable beneficial dataset that can be used for estimations of ore blocks during mining at later stages.

The additional small-scale study investigating the estimation results of the usual 4 m x 4 m drill spacing compared to the larger 12,5 m x 12,5 m using 10 mined ore blast blocks yielded interesting results. This study did not test the estimation method efficiency, rather the estimation results regarding the effect of data availability with consideration of resources availability. From the results it is clear that there is only a minor difference between the 4 m x 4 m and 12,5 m x 12,5 m estimations. It can therefore be concluded that the 12,5 m x 12,5 m drill data estimation is a suitable substitute to save on costs and produces acceptable grade and tonnage predictions for mining activities. Data availability may be increased by treating some of the 4 m x 4 m drill holes, which is a fixed cost, as infill logging holes and thereby increasing the estimation accuracy. This exercise has also given insight into a measure of quantification of the degree of over and under mining at the Langer Heinrich Mine. Future mining operations can be improved by coherent teamwork and efficient ore extraction procedures.

Focusing on the final recommendation, drilling on a 12,5 m x 12,5 m spacing with a sufficient budget would yield the best estimation results using MIK as the preferred method. With a limited budget for exploration, the 12,5 m x 25 m or even 25 m x 25 m drill spacing would also yield reliable results. During mining operations, the 4 m x 4 m blast pattern only marginally performed better than the estimations provided from the 12,5 m x 12,5 m drill data. As a compromise, using additional data from the 4 m x 4 m drill data would probably yield reasonably accurate estimations using CS or MIK as preferred estimation methods.

LIST OF REFERENCES

Armstrong, M., & Boufassa, A. (1988). Comparing the Robustness of Ordinary Kriging and lognormal kriging: outlier resistance. Mathematical Geology, 20(4), pp. 447- 457.

Babish, G. (2006). Geostatistics without tears: A practical guide to surface interpolation, geostatistics, variograms and kriging (3rd Ed.). Ecological Research Division: Saskatchewan, Canada, pp. 116.

Barrett, D.M. (2008). Basic Radioactivity Theory and Measurement. Paladin Energy In-House notes. pp. 1-41

Baufeldt, S. (2012). Lateral continuity of geological facies and associated grade distribution of uranium and vanadium at the Langer Heinrich Mine, Namibia. University of Stellenbosch, South Africa. Unpublished Honours Thesis. pp. 25-27.

Becker, E., & Kärner, K. (2009). Geological setting of the Langer Heinrich uranium mine, Namibia. International Atomic Energy Agency (IAEA). Vienna, Austria. 41, pp. 1-10.

BME (2016). Bulk emulsions. Retrieved November 21, 2016 from http://www.bme.co.za.

Bowell, R., Barnes, A., Grogan, J., & Dey, M. (2009). Geochemical Controls On Uranium Precipitation In Calcrete Palaeochannel Deposits Of Namibia. SRK Technical Report. pp. 1-4.

Boyle, D. (1984). Surficial Uranium Deposits: The Genesis of surficial uranium deposits. International Atomic Energy Agency (IAEA), Vienna, Austria. pp. 45-52.

CAMECO. (2015). Cigar Lake reserves and resources. Retrieved November 10, 2016, from https://www.cameco.com/businesses/uranium-operations/canada/cigar-lake/reserves-resources.

Carlisle, D. (1980). Possible variations on the calcrete-gypcrete uranium model. University of California and Bendix Field Engineering Corporation. United States Department of Energy, USA. pp. 8-29.

Cross, A., Jaireth, S., Rapp, R., & Armstrong, R. (2011). Reconnaissance-style EPMA chemical U–Th–Pb dating of uraninite. Australian Journal of Earth Sciences, 58, pp. 675-683.

De Vitry, C., Vann, J., & Arvidson, H. (2007). A guide to selecting the optimal method of resource estimation for multivariate iron ore deposits. Iron Ore Conference. Perth, Australia. pp. 1-12.

Deep Yellow Limited. (2014). Tubas Sand Project- Resource Update. Retrieved November 10, 2016, from http://www.deepyellow.com.au/projects/tubas-sand-project.html.

Deep yellow Limited. (2016). Project Locality Map. Retrieved November 10, 2016, from http://www.deepyellow.com.au/projects/locality-map.html.

Deep Yellow Limited. (2016). Tumas Mineral Resource Estimate. Retrieved November 10, 2016, from http://www.deepyellow.com.au/projects/namibia-development-tumas-project.html.

Gilchrist, A. R., Kooi, H., & Beaumont, C. (1994). Post-Gondwana geomorphic evolution of southwestern Africa: Implications for the controls on landscape development from observations and numerical experiments. Journal of Geophysical Research, 99(B6), pp. 12211-12228.

Glacken, I., & Blackney, P. (1998). A practitioner's implementation of indicator kriging. Beyond Ordinary Kriging: Non-linear geostatistical methods in practise. Geostatistical Association of Australia Perth, WA. pp. 26-39.

Hambleton-Jones, B. (1976). The geology and geochemistry of some epigenetic uranium deposits near the Swakop River, South West Africa. University of Pretoria, South Africa. Unpublished PhD thesis. pp. 306.

Hambleton-Jones, B. B. (1984). Surficial uranium deposits in Namibia. International Atomic Energy Agency. Vienna, Austria. IAEA-TECDOC-322. pp. 205-216.

Hableton-Jones, B., Levin, M., & Waegner, G. (1986). Uraniferous surficial deposits in Southern Africa. In C. Anhaeusser, & S. Maske, Mineral Deposits of Southern Africa II .Geological Society of South Africa. pp. 2269-2287.

Hartleb, J.W.O. (1988). The Langer Heinrich Uranium Deposit: Southwest Africa, Namibia. Ore Geology Reviews, 3, pp. 277-287.

International Atomic Energy Agency (IAEA). (1984). Surficial uranium deposits. Vienna, Austria. Technical Document 322, pp. 1-236.

International Atomic Energy Agency (IAEA). (2016). IAEA. Retrieved November 8, 2016, from https://infcis.iaea.org/UDEPO/UDEPOMain.asp?Order=1&RPage=1&Page=1&RightP=Summary

Isaaks, E. H., & Srivastava, R. M. (1989). An Introduction to applied geostatistics. Oxford University Press, New York. 1, pp. 289.

Kinnaird, J., Nex, A. (2016). Uranium in Africa. Episodes, 37(2), pp. 335-359.

Larrondo, P., Deutsch, C.V. (2004). Accounting for geological boundaries in geostatistical modelling of multiple rock types. Seventh International Congress. Quantitative Geology and Geostatistics. pp. 3-12.

Lipton, I., Gaze, R., Horton, J., & Khosrowshahi, S. (1998). Practical application of multiple indicator kriging and conditional simulation to recoverable resource estimation for the Halley's lateritic nickel deposit. Symposium on beyond ordinary kriging. Mining and Resource Technology, Perth, WA. pp. 88-105.

Mann, A.W., & Deutscher, R.L. (1978). Hydrogeochemistry of a calcrete-containing aquifer near Lake Way, Western Australia. Journal of Hydrology, 38 (3-4), pp. 357-377.

Mann, A.W., & Horwitz, R. (1979). Groundwater calcrete deposits in Australia some observations from Western Australia. Geological Society of Australia, 26, pp. 293-303.

MEGA Uranium LTD. (2009). Lake Maitland National Instrument 43-101 Technical Report. Retrieved from http://www.megauranium.com/_resources/Technical-report-maitland-2009.pdf pp.1-164

Mendelsohn, J., Jarvis, A., Roberts, C., & Robertson, T. (2010). Atlas of Namibia. A portrait of the land and its people. Cape Town, South Africa: Sunbird Publishers. pp. 200.

Miller, R. (2008). The Geology of Namibia - Volume 2: Neoproterozoic to lower Palaeozoic. Geological Survey of Namibia, Windhoek. pp. 13-1 - 13-4.

Miller, R. (2008). The Geology of Namibia - Volume 3: Palaeozoic to Cenozoic. Geological Survey of Namibia, Windhoek. pp. 25-1 – 25-66.

Netterberg, F. (1976). Some road making properties of South African calcretes. Proceedings of the 4th Regional Conference of African Soil Mechanical Foundations and Engineering 1, Cape Town. pp. 77-81.

Otton, J. (1984). Surficial Uranium Deposits: Summary and Conclusions. Technical Document NI 43-101. International Atomic Energy Agency, Vienna. pp. 243-247.

Paladin Energy PTY Ltd. (2015). Annual Report. Perth, Australia. Retrieved from http://www.paladinenergy.com.au/financial-reports/2015

Ravenscroft, P.J. (1994) Conditional simulation for mining: Practical implementation in an industrial environment. Proceedings of the Geostatistical Simulation Workshop, Fontainebleau, France. pp. 79-87.

Robb, L. (2005). Introduction to ore-forming processes (1 Ed.). Blackwell Publishing. Oxford, UK. pp 374.

Roesener, H., & Schreuder, C. (1998). Uranium. In The Mineral Resources of Namibia. Ministry of Mines and Energy, Geological Survey Namibia. pp. 7.1-42-7.1-43.

Rossi, E., & Deutsch, C. E. (2014). Mineral Resource Estimation (1st Ed.). Springer, New York. pp. 332.

Runge Pincock Minarco Global. (2016, February). Runge Pincock Minarco Global Company. Retrieved from www.rpmglobal.com/newsletter

Shi, B., Bloom, L. M., & Mueller, U. A. (2000). Applications of conditional simulation to a positively skewed platinum mineralization. Natural Resources Research, 9(1), pp. 65-76.

Tankard, A. J., Jackson, M. P., Eriksson, K. A., Hunter, D. R., Hobday, D. K., & Minter, W. E. (1982). Crustal evolution of Southern Africa: 3.8 billion years earth history (1st Ed.). New York: Springer-Verlag. pp. 523.

Toro Energy Limited. (2015). 20% increase in mineral resources at Wiluna's Centipede/ Millipede deposits. ASX release document. Retrieved from https://www.toroenergy.com.au/wp-content/uploads/2016/03/151009-Resource-Upgrade_Board-copy-6.pdf. pp. 1-43.

Trittschack, R. (2008). Geological identification and Mineralogical characterisation of the palaeo surfaces and channel fills at the Langer Heinrich Uranium deposit-Namibia. Martin-Luther University, Germany: Unpublished MSc Thesis. pp. 1-155.

U3O8 Corporation. (2011). Laguna Salada Project, Chubut Province, Argentina: NI 43-101 Technical Report Laguna Salada Initial Resource Estimate. Prepared by Coffey mining. Retrieved from: http://www.u3o8corp.com. pp. 1-164.

Uramin Inc. (2007). Trekkopje Uranium Project Swakopmund and Karibib Districts, Erongo Region, Namibia. Technical Report NI 43-101. Retrieved from https://www.sedar.com. pp. 1-187.

Vann, J., Guibal, D., & Harley, M. (2000). Multiple indicator kriging- is it suited to my deposit? 4th International Mining Geology Conference. Queensland, Australia. pp. 187-192

Wilkinson, M. J. (1991). Palaeo-environments in the Namib Desert: The lower Tumas Basin in the Late Cenozoic (1 Ed.). Chicago, USA. University of Chicago Geography Research paper no. 231. pp.75.

Wong, D., & Lu, G. Y. (2008). An adaptive inverse distance weighting spatial interpolation technique. Computers & Geosciences, 34, pp. 1044-1055.

World-Nuclear Association. (2015). World uranium mining production. Retrieved November 08, 2016, from http://www.world-nuclear.org/information-library/nuclear-fuel-cycle/mining-of-uranium/world-uranium-mining-production.aspx

Wright, V. & Maurice, M., 1991. Calcretes. International Association of Sedimentologists Reprint Series, 2. Blackwell Scientific Publications, London, UK. pp 1-22.

Yi, H., Choi, Y., & Park, H. D. (2014). Application of multiple indicator Kriging for RMR value estimation in areas of new drift excavation during mine site redevelopment. Environment Earth Science, 71, pp. 4379-4386.

Yunsel, T. (2012, March). A practical application of geostatistical methods to quality and mineral reserve modelling of cement raw materials. The Journal of the Southern African Institute of Mining and Metallurgy, 112, pp. 239-249.